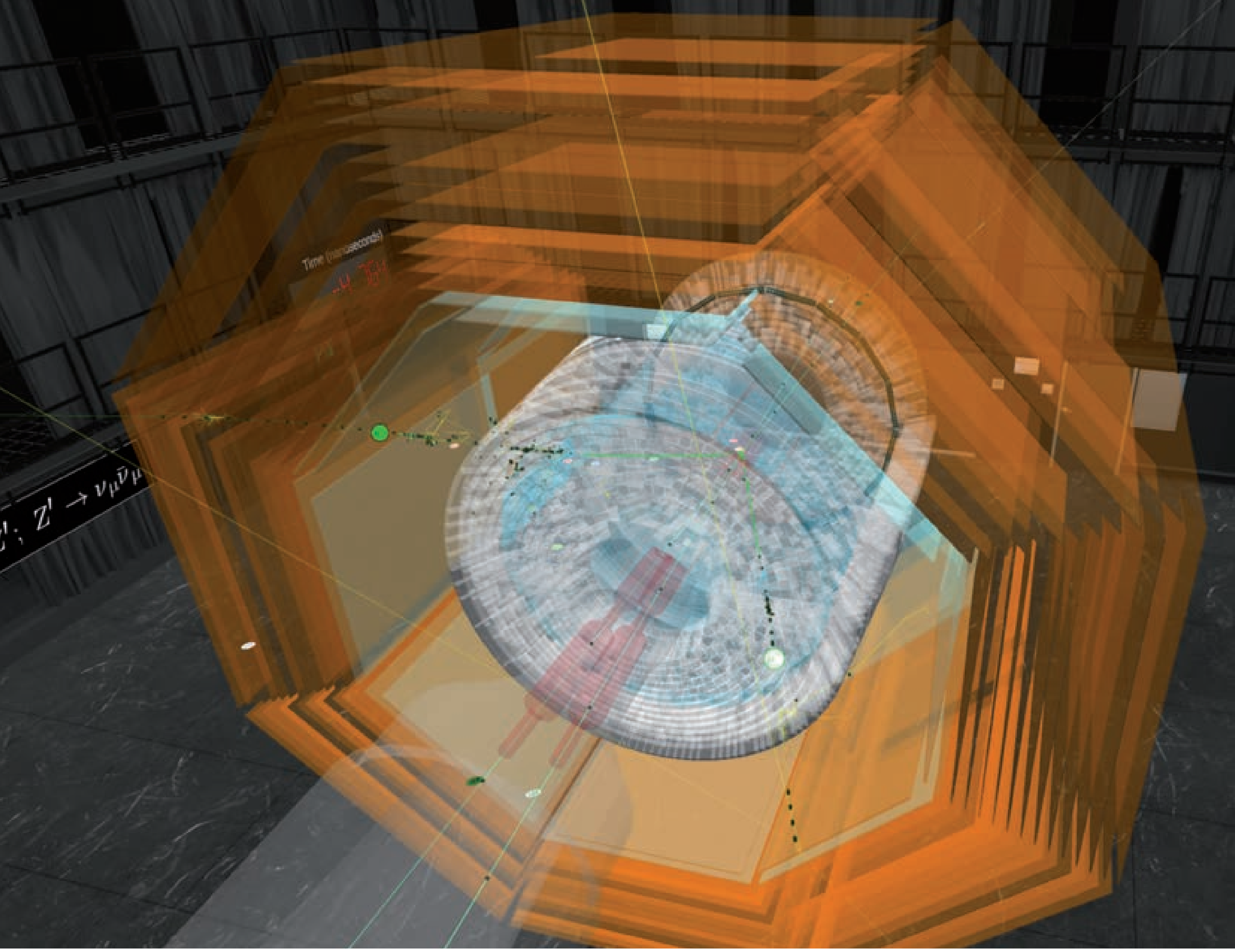

PARTICLE PHYSICS 2020.

Highlights and Annual Report

Deutsches Elektronen-Synchrotron DESY
A Research Centre of the Helmholtz Association

Cover

Event © Leo Piilonen

Rendering of a 3D virtual-reality display of a simulated $e^+e^- \rightarrow \mu^+\mu^- + Z'$ event in the Belle II detector. The operation of the SuperKEKB collider and the Belle II experiment at KEK in Japan in 2020 was very successful. In June, the team of SuperKEKB accelerator physicists achieved a new world record in instantaneous luminosity. By the end of the year, the Belle II collaboration had accumulated data corresponding to an integrated luminosity of almost 90 fb^{-1}.

PARTICLE PHYSICS 2020.

Highlights and Annual Report

Contents

The year 2020 at DESY

Chairman’s foreword

Dear Colleagues and Friends of DESY,

2020 was a truly unusual year for the global society. In March, the coronavirus brought our accustomed everyday life to a standstill and mercilessly exposed the vulnerability of our modern society to such crisis. We will have to put many of our habits, which have finally proven to be unsustainable, to test and find new ways forward. We have already learned a great deal in recent months, most importantly that our society can rely on science and on decision makers who listen to scientists.

We at DESY reacted quickly and very cautiously to the pandemic and moved the research centre into a safe mode that kept the laboratories and our research largely in operation while protecting all staff from infection as efficiently as possible.

These measures were critical with respect to the user operation of our large-scale research facilities PETRA III and FLASH. Especially the unique analysis capabilities at PETRA III have proven to be most important for the fight against the COVID-19 coronavirus. We have to ensure that these technologies will be even more targeted to molecular drug research and even more crisis-proven in the future. To this end, we have drawn up a major proposal for the establishment of a National Analysis Center for Molecular Infection Research, in which new digital and technical concepts, like artificial intelligence, remote control and robotics, are to be incorporated. “Digital DESY” has become a new building block in our DESY strategy, in response to the challenges of the current pandemic and of future crisis

Figure 1

Part of the DESY staff in Hamburg hold up the DESY-60 logo.

Figure 2
Senate reception for the 60th anniversary of DESY in Hamburg: with forward-looking, cutting-edge research into the new decade.

situations. We will also pay even greater attention to sustainable concepts in all our activities and future projects.

DESY is well on its way into this future. The priority project is PETRA IV, which has now entered the technical design phase. We are very pleased that with Riccardo Bartolini, who joined DESY in April 2020, we have been able to attract an internationally renowned accelerator physicist for this future project. In the next few years, the task will be to prepare all the logistical and personnel prerequisites for the upgrade of the synchrotron radiation source PETRA III and to raise the necessary financial resources for this complex project. Nearly all areas of DESY will be involved here in the upcoming decade.

In 2020, we have made good progress in various projects, such as in the development of the Centre for Molecular Water Science (CMWS), the commissioning of the Detector Assembly Facility (DAF) and the construction of the Bahrenfeld Start-Up Labs, as well as in the Centre for X-ray and Nano Science (CXNS), which will open in 2021. An active innovation culture that interlinks basic research and fast transfer of innovative concepts to the market will remain an integral part of DESY's future strategy.

In the coming years, further projects are on the agenda: Major new construction measures include the DESYUM visitor centre, the building for the accelerator division, the TECHNICUM for technical groups, the DESY Innovation Factory and the Wolfgang Pauli Centre (WPC) for theoretical physics.

Important research and upgrade projects, such as the upgrade of the free-electron laser FLASH to FLASH2020+, the KALDERA-ATHENA project for future accelerator technologies, the Any Light Particle Search experiment ALPS II, the telescope in search of dark-matter particles BabyIAXO as well as the Cherenkov Telescope Array (CTA) and its Data Centre, will be implemented.

Promoting our top scientists and our young talents is an essential component of the DESY strategy. The new Helmholtz graduate school DASHH has been well established in 2020. The aim of the school is to educate the future generation of data scientists who can efficiently analyse measured data using e.g. artificial intelligence or machine learning. In 2020, we have implemented the COAST programme, which will assist our postdocs in shaping their individual career pathways. Our HR department has done a remarkable job in this respect. Over the coming months, we must and will develop concepts to offer our top academic performers new career paths within the research centre.

DESY celebrated its 60th anniversary in the Hamburg city hall at the beginning of 2020. Many congratulations came from the global science community and honoured DESY as a world-leading centre in the exploration of matter. We are well prepared for the coming decades to continue the legacy of DESY.

Even in these challenging times, the extraordinary commitment of the DESY staff and all our users and partners, national and international, made research possible at DESY – I would like to thank all those who contributed to the joint efforts!

Helmut Dosch
Chairman of the DESY Board of Directors

Particle physics at DESY

Introduction

Dear Colleagues and Friends of DESY,

2020 was in many ways a very special year. It had a bright start, with a highly successful review of DESY and its research programme; it then quickly became very challenging with the COVID-19 crisis; and it ended with the unexpected call for Joachim Mnich, DESY Director in charge of Particle Physics, to become research director at CERN.

Together with the other areas in the Helmholtz research field "Matter" – photon science, astroparticle physics as well as nuclear and hadron physics – the particle physics division at DESY started the year with a review of its activities for the next programme-oriented funding period (PoF IV) of the Helmholtz Association. We defended our programme in front of a high-profile international review board, and we came out of this evaluation with flying colours: Our vision for the future of DESY and particle physics was extremely well received. Our proposal of a top-class programme at the world's major collider experiments combined with a very ambitious set of local experiments plus an intense technology R&D programme found greatest support, thus providing convincing confirmation of our overall strategy. The "outstanding" marks received for the topic of fundamental particles and forces allow us to look with confidence to the future.

Shortly after the PoF evaluation, in March 2020, the COVID-19 pandemic cast its shadow over Europe and also over DESY. The pandemic changed everything. Many of us are still working from home today or under much more restricted conditions than we would have ever thought possible. We all miss the personal encounters and the direct exchange with colleagues, and we are all tired of yet another video conference. But we managed to maintain stable and safe operations of DESY, and we continued to make remarkable progress in all our activities, thanks to the immense effort and dedication of all the DESY staff members. Many thanks to all of you for making this possible!

Here are a few examples of the achievements we made in 2020: Work on the on-site experiment ALPS II to search for weakly interacting slim particles continued. Commissioning of the experiment will be finished in 2021, and we are confident that we will see the first data by the end of the same year. In addition, we made significant progress in the development of other on-site projects, with BabyIAXO, MADMAX and LUXE in the pipeline. The setup of the Detector Assembly Facility (DAF) was optimised, and the facility is now gearing up to start production of the tracker end-caps for the upgrades of the ATLAS and CMS experiments at the Large Hadron Collider (LHC) at CERN near Geneva, Switzerland. The flagship experiments ATLAS and CMS as well as Belle II at the SuperKEKB collider at KEK in Japan delivered numerous high-impact results, with key contributions by DESY scientists.

The DESY II Test Beam Facility managed to provide user service for most of the year, enabling challenging detector development projects under very demanding conditions. Even in these difficult times, it was possible to host the Beamline for Schools (BL4S) competition at the DESY test beam, an educational activity in cooperation with CERN.

A new initiative that has received a lot of attention is "Digital DESY" – the vision of a more digitised campus and work environment. "Digital DESY" comprises six work packages, to most of which the particle physics division can make significant contributions: We will further develop our portfolio in "digital matters" in the coming years. One important topic in this context is the quickly evolving quantum technologies, which we are pursuing in three different pillars: quantum computing application, materials for quantum computers, and quantum sensors. Pilot projects have progressed encouragingly and will be complemented by research on quantum machine learning.

In summer 2020, the CERN Council acknowledged the update of the European Strategy for Particle Physics. The update is the result of an intense discussion process lasting more than two years, to which DESY scientists contributed in many places. The new strategy sets the stage for future developments in our field. Besides a clear focus on the successful completion of the High-Luminosity LHC

Figure 1

Joachim Mnich will join the CERN Directorate on 1 January 2021.

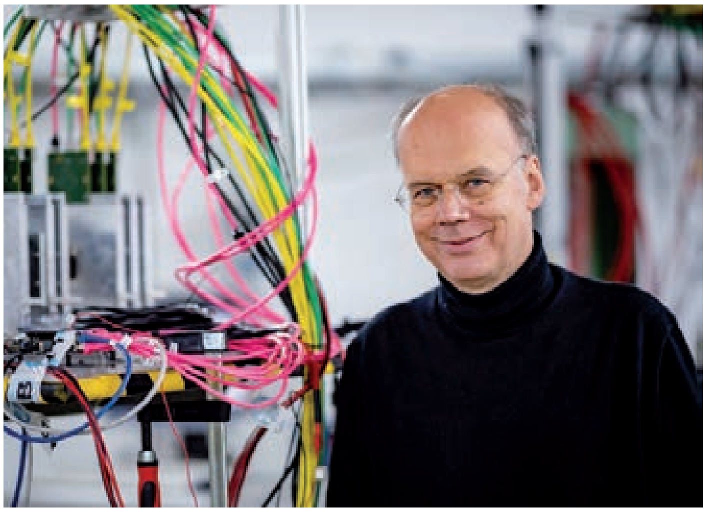

Figure 2

Ties Behnke takes over as the interim Director in charge of Particle Physics.

(HL-LHC) programme, it emphasises the importance of technologies – accelerators, detectors and computing – and presents a clear vision for a “Higgs factory” as the next big collider project in the field. The feasibility of a large hadron collider, to follow after the LHC, should be investigated. All in all, the new European strategy matches our strategic planning, as documented in the DESY 2030 strategy, extremely well. With our backbone engagement in the LHC experiments and in Belle II, with our efforts in the physics and technology for future colliders, with our growing on-site experimental programme and with our world-class theory group, we can confidently look forward to remaining an important voice in the European and global particle physics landscape.

At the end of 2020, Joachim Mnich left the helm of the DESY particle physics division and took on the responsibility of Director for Research and Computing at CERN, succeeding Eckhard Elsen. Joachim Mnich had been the DESY Director in charge of Particle Physics for 12 years, and under his leadership, the particle physics division flourished. His term in office saw many remarkable events and achievements, among them the firm establishment of the DESY ATLAS and CMS groups at the LHC and the commitment to the LHC Phase 2 upgrade projects, the participation in the Belle II experiment and the construction of the Belle II pixel vertex detector, the progress of the ALPS II experiment and the extension of the on-site experimental programme, the erection of the DAF as well as the participation of the particle physics division in DESY’s FLASHForward plasma wakefield acceleration facility. While a successor for Joachim Mnich is being searched for, Ties Behnke has stepped in as interim Director in charge of Particle Physics until the new director is appointed later in 2021.

In summary, 2021 also promises to be an exciting year, and we are looking forward to mastering the upcoming challenges together with all of you!

Joachim Mnich
Director in charge of Particle Physics

Ties Behnke
Interim Director in charge of Particle Physics

News and events

A busy year 2020

January

Senate reception to celebrate DESY's 60th anniversary

On 16 January, about 500 guests attended the Senate reception in celebration of DESY's 60th anniversary in the Hamburg city hall. On the occasion, Katharina Fegebank, Hamburg's Second Mayor and Senator for Science, Research and Equality, paid tribute to the achievements of DESY: "As a world-class research centre, DESY has played a major role in shaping Hamburg as a centre of science in the past – and, as a driver of innovation and a fundamental component of the Science City Hamburg Bahrenfeld, it will continue to play an important role in Hamburg's progress in the future. Like our city, DESY stands for cosmopolitanism, courage and innovative ideas for the world of tomorrow."

About 500 guests attended the Senate reception in the Hamburg city hall.

Wolf-Dieter Lukas, State Secretary at the German Federal Ministry of Education and Research (BMBF), attributed another far-reaching significance to DESY's accomplishments: "Basic research is not only the basis for innovation, it is above all an indispensable foundation of a democratic society and of knowledge-based debate in politics. We need research centres like DESY as 'scientific fact guarantors' in order to jointly find solutions for urgent challenges of the 21st century, which pose enormous tasks for society and politics, economy and science."

Katharina Fegebank, Hamburg's Second Mayor and Senator for Science, Research and Equality, acknowledged the achievements of DESY.

Otmar Wiestler, President of the Helmholtz Association, appreciated DESY's innovative drive: "DESY has evolved into a centre with enormous international appeal, especially with its new generation of research infrastructures. It thus makes an essential contribution to solving major societal challenges in line with the Helmholtz mission."

Current and former DESY Directors with State Secretary Wolf-Dieter Lukas (front, centre) and Helmholtz President Otmar Wiestler (middle row, second from right)

"From the experience of the last 60 years, I am convinced that the centre is well positioned for the future," summarised DESY Director Helmut Dosch. "We are constantly questioning and developing ourselves. But the original mission, to decipher the structure of matter – from the big bang to DNA – this remains."

City of Hamburg funds three new projects with DESY participation

The City of Hamburg is funding two new research clusters – called Hamburg X projects – and a research network with DESY participation. With the federal-state funding, which can be applied for by local universities, Hamburg aims to create top-class research projects and networks within the city, strengthen the networking of universities with other research institutions and promote links to local business and industry.

In the Hamburg X project "Center for Data and Computing in Natural Science (CDCS)", a cooperation of Universität Hamburg, TU Hamburg and DESY, an interdisciplinary centre is being created to develop methods for the optimal evaluation of the drastically growing amounts of data generated in natural-science experiments. The natural sciences, applied mathematics and computer science are to be interlinked to improve the acquisition and analysis of large and complex data sets, the automation of experimental research as well as digitisation and methods for simulations. In addition, DESY is involved in the Hamburg X project "CIMMS – Center for Integrated Multiscale Materials Systems" and in the research network "Control of the special properties of water in nanopores".

In total, in the current third round of the federal-state research funding, the City of Hamburg is funding 18 new research projects and four Hamburg X projects. Together, the Hamburg X projects will receive 12 million euros by 2022, while the research networks are to get a maximum of 1.8 million euros each over a period of 3.5 years.

Virtual view of the planned Science City Hamburg Bahrenfeld, which is to become a beacon for interdisciplinary research

February

New German–Swedish graduate school

The new “Helmholtz–Lund International Graduate School” (HELIOS), which combines the expertise of DESY, Universität Hamburg and the University of Lund in Sweden, aims to prepare doctoral students for a new era in the study of matter. The rapidly growing amounts of data and increasingly complex instruments in this field and other natural sciences require new approaches in instrumentation, data acquisition and analysis. Based on an interdisciplinary approach bringing together fields such as molecular physics, particle physics, nanoscience and photon science, HELIOS will provide students at both locations with the skills needed to plan, conduct and evaluate complex experiments and develop new methods. In addition to funding for their research projects, the students will benefit from an extensive qualification programme and a stay of at least three months in the respective partner country.

HELIOS will run for a total of 22 doctoral positions over two three-year periods. The international school is funded by the three partner institutions, the Helmholtz Association and the Hamburg Ministry of Science, Research and Equality (BWFG) with around 8 million euros. The project is also intended to further advance the scientific cooperation between Hamburg and Lund in general.

HELIOS
Helmholtz-Lund International Graduate School

March

Corona pandemic: DESY operates in reduced mode

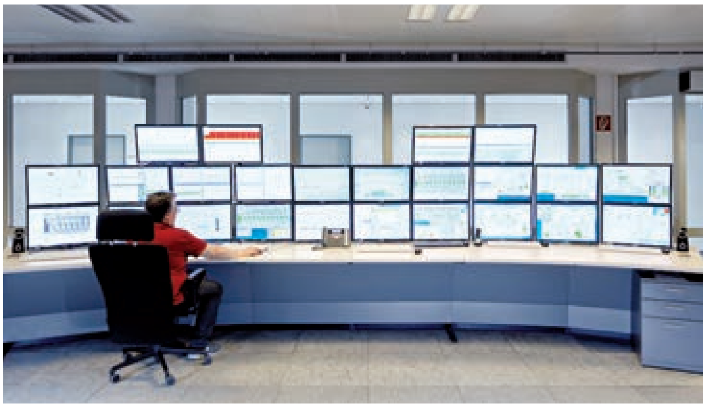

To contain the spread of the SARS-CoV-2 virus, the DESY accelerator control room was operated with reduced staff.

As a measure against the further spread of the SARS-CoV-2 virus, DESY entered a reduced operating mode on 16 March. Although the DESY sites in Hamburg and Zeuthen remained open, staff were asked to work from home as much as possible, so that staff presence on campus was reduced to what was absolutely necessary. Where possible, the particle accelerators and other facilities were put in “safe mode”, and user operation at the X-ray sources PETRA III and FLASH and at the test beam was suspended until further notice. PETRA III was powered up only for SARS-CoV-2-relevant measurements. To help fight the pandemic, DESY set up a fast-track access mode for corresponding research projects. The reduced operating mode was maintained until May for PETRA III and August for FLASH, after which user operation resumed with strict measures to minimise the risk of infection.

April

In search of the *Z’* boson: Belle II delivers first results

Almost exactly one year after the Belle II detector went into operation at the SuperKEKB collider at KEK in Japan, the international Belle II collaboration published the first results obtained with the detector. The publication in *Physical Review Letters* outlines the properties of the *Z’* boson, a hypothetic new particle related to the mysterious dark matter, which, according to current knowledge, is more than five times more abundant in the universe than the matter we are familiar with.

The Belle II detector started physics data taking in March 2019. Both the SuperKEKB particle accelerator and Belle II had been upgraded over several years to achieve a 40 times higher data rate than their respective predecessors.

May

A solar telescope in search of dark matter

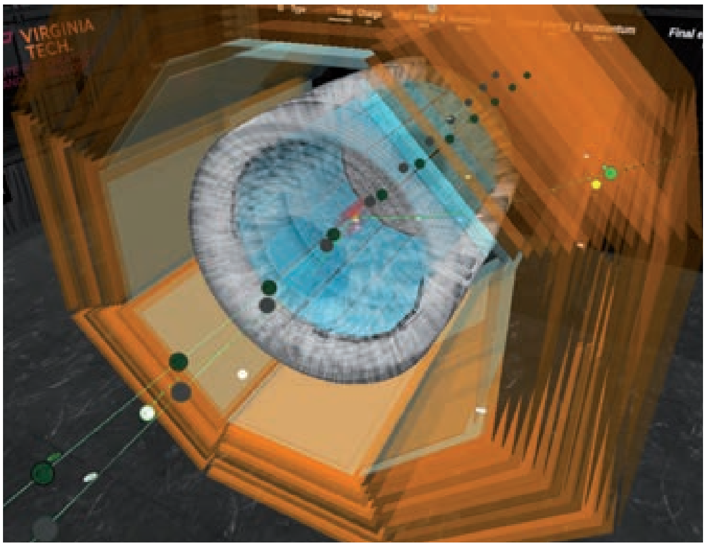

Impression of a collision in the Belle II detector

At the top of physicists' most-wanted list is dark matter, which scientists all over the world are tracking down using various approaches, experiments and methods. DESY too will soon run several experiments looking for dark-matter particles. One of them is BabyIAXO, which is being built in an underground hall of DESY's former HERA accelerator and for which first components were delivered in May.

First components for the BabyIAXO helioscope arrived at DESY.

Using Belle II, scientists are searching for traces of new physics that could explain, for example, the asymmetry between matter and antimatter in the universe or the enigmatic dark matter. One of the so far undiscovered particles that the Belle II detector is looking for is the *Z*' boson – a variant of the photon (particle of light) that, unlike the photon, has mass. The *Z*' boson could help us to understand the behaviour of dark matter. In addition, its discovery could explain other results of precision measurements that are not consistent with the Standard Model, the fundamental theory of particle physics.

While the Belle II data have not yet provided any indication of the *Z*' boson, the new data can be used to limit its mass and coupling strengths with a previously unattainable level of precision. The Belle II collaboration will need to evaluate many more collision data before the *Z*' becomes visible – or is ruled out as an explanation for the mysterious precision measurements.

BabyIAXO is both a telescope in search of dark-matter particles emitted by the sun and a prototype for the even larger and more powerful International Axion Observatory (IAXO). The telescope is directed at the centre of the sun, from which, according to theory, axions should rain down on Earth all the time. Setting up the experiment requires several technological advances, first of all a strong, long magnet with a large aperture, which is developed at CERN. BabyIAXO will be about four times more powerful than the previous experiment CAST at CERN. The sensitivity of the large proposed follow-up experiment IAXO would be another five times higher.

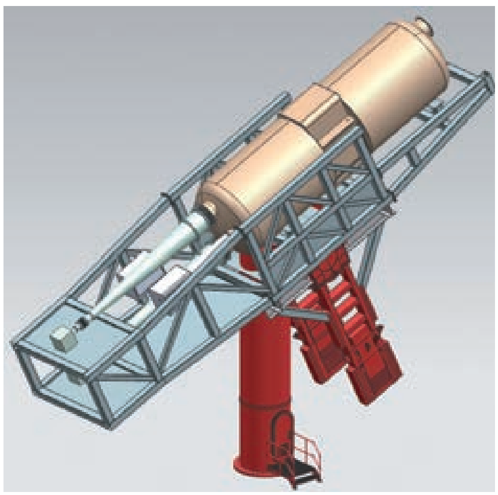

CAD drawing of BabyIAXO in its final form

DESY produces face shields for Hamburg doctors and nursing facilities

Beate Heinemann from DESY (left) handed over a box of face shields to Stefanie Schäfer (KVH).

DESY handed over more than 2000 face shields for protection against the SARS-CoV-2 virus to the Hamburg Association of Statutory Health Insurance Physicians (KVH) and the Federal Association of Private Providers of Social Services (bpa). The shields were produced and assembled at DESY with 3D printers and in the research centre's workshops. They were to be delivered to particularly vulnerable practices, nursing homes, infectious-disease practices or COVID-19 consultations.

Face shield assembly line in a DESY seminar room

The mastermind of face shield manufacturing at DESY is Beate Heinemann, leading scientist in the DESY ATLAS group and a professor at the University of Freiburg, Germany. As a member of the "CERN against COVID" task force, she learned about the various ways to build protective equipment. After a doctor friend of hers confirmed the urgent need for such protective equipment for medical personnel in Hamburg, a team of physicists, engineers and technicians from the high-energy physics community got together to plan how DESY could help. In the central workshop, aluminium brackets were produced using a large water cutting machine and bent. The shields were then assembled in the ATLAS seminar room. More than 30 volunteers – from students to group leaders – worked in shifts of up to three people each. Some 100 in-house design shields were produced every day.

Computers against corona: DESY IT supports COVID-19 research

A substantial part of research on the SARS-CoV-2 coronavirus is carried out digitally, by simulating the interactions of different active substances with the proteins of the virus. This requires a lot of computing power. There are even projects, such as Rosetta@home and Folding@home, that you can support with your own computer. These projects have in common that a large, complex problem, such as the decoding of proteins, is broken down into small subtasks, which are then distributed independently to the participating computers.

DESY is also involved in these activities. In 2020, Rosetta@home and Folding@home, for instance, ran on the large computer systems at DESY in Hamburg and Zeuthen, contributing about 3.5 million CPU hours in April 2020 – equivalent to the performance of about 1200 laptops computing day and night for an entire month.

The DESY computer centre

The DESY IT groups in Hamburg and Zeuthen operate powerful computer systems that are part of the worldwide computing infrastructure for the LHC experiments ATLAS and CMS. In agreement with the DESY ATLAS and CMS groups, part of the computing power provided for this purpose was made available to the Folding@home project. Another high-performance computer operated by DESY, the Maxwell cluster in Hamburg, also plays a special role in the fight against the coronavirus, as it has been running the data analysis of the COVID-19-related experiments conducted at the X-ray source PETRA III. Users received prioritised access for these computing tasks.

June

Theoretical physicist Roberto Peccei died

On 1 June, the Italian theoretical physicist Roberto Peccei died at the age of 78 in his home city of Los Angeles, USA. Peccei, who led the DESY theory group from 1984 to 1989, gained great fame for his work especially on the Peccei–Quinn symmetry, which he developed together with his colleague Helen Quinn. The symmetry explained an important problem in quantum chromodynamics, the theory behind the strong force. It predicted a new, light elementary particle, the axion, which is today the subject of research around the world.

Roberto Peccei

Using big data to help predict immunity

Armed with his experience in using advanced statistical models that can handle large data sets and multiparametric analyses, DESY theorist Ayan Paul took part in the COVID-19 Challenge hackathon organized by the Massachusetts Institute of Technology (MIT) in April, which rallied more than 1500 participants from all over the world. Paul's team including six other participants was selected as one of the winning teams. They had proposed the development of an intelligent algorithm to track immunity development and reduce clinical burden.

Ayan Paul from the DESY theory group

This marked the beginning of Paul's research related to COVID-19. At that time, problems in manual tracing made several tech giants and governments propose the use of automated contact tracing through mobile devices. With his knowledge of basic statistical analysis, it seemed to Paul that the advocates of automated contact tracing were being too optimistic. Together with Hyunju Kim from the Beyond Center for Fundamental Sciences at Arizona State University, USA, Ayan showed that the disease characteristics must be well understood and connected with the transmission parameters to properly understand the efficacies of contact tracing.

In the meantime, Ayan and his team won the second round of the MIT COVID-19 Challenge and founded the company CoVis. Combining knowledge of contact tracing and immunity development in individuals, their aim was to build a risk and immunity probability assessment platform for mobile devices, intended to support healthcare providers, businesses and public institutions in creating plans and policies related to the pandemic. It combines information from the medical literature, extensive data sets on local disease spread and individual user information to make a statement abut how high a person's risk of infection is and how likely they are to have become immune from an unrecognised COVID-19 infection.

September

Valery Rubakov wins Hamburg Prize for Theoretical Physics 2020

In recent years, research teams around the world have gained important insights into the origin of the universe. To do so, they often relied on the work of Valery Rubakov, one of the most recognised Russian theoretical physicists. A leading scientist at the Institute for Nuclear Research of the Russian Academy of Sciences in Moscow and a professor at M.V. Lomonosov Moscow State University, Rubakov is an expert in quantum field theory, elementary particle physics and cosmology. In recognition of his work, he won the 2020 Hamburg Prize for Theoretical Physics, which is endowed with 137 036 euros – an allusion to Sommerfeld's fine structure constant, which plays an important role in theoretical physics.

Valery Rubakov will spend several research visits in Hamburg.

The Hamburg Prize for Theoretical Physics is one of the highest-endowed awards for physics in Germany. It is awarded by the Joachim Herz Foundation in cooperation with the Wolfgang Pauli Centre, DESY and the two clusters of excellence of Universität Hamburg "CUI: Advanced Imaging of Matter" and "Quantum Universe".

His Majesty the King's Gold Medal for Carl Lindstrøm

DESY scientist Carl Andreas Lindstrøm was awarded the Gold Medal of His Majesty the Norwegian King Harald V for outstanding young researchers from the University of Oslo. The Norwegian scientist, who works at DESY on future linear accelerators, was honoured for his doctoral thesis on innovative particle accelerator concepts. Among other things, he discovered an innovative plasma lens for focusing particle beams and investigated the acceleration of positrons in a hollow plasma channel.

For electrons, plasma wakefield acceleration achieves the properties needed to build the next generation of accelerators: Electrons can be accelerated as a tightly focused particle bunch in the plasma wake, they are accelerated quickly and beam quality is maintained. Positron bunches, in contrast, tend to lose their compact shape and their focus in the plasma environment. At SLAC in the USA, Lindstrøm and his colleagues therefore investigated the options of accelerating positrons in a hollow plasma channel, in which the positrons stayed tightly focused as they flew through.

Carl Andreas Lindstrøm at the award ceremony in Oslo

Beamline for Schools teams experiment at the DESY test beam

Kick-off for the Beamline for Schools competition, with the two winning teams arriving at CERN and DESY

While two international groups of students were supposed to meet and perform their experiments at DESY, only one team actually made it to Hamburg: eight students from the Werner-von-Siemens-Gymnasium in Berlin, taking part in the Beamline for Schools competition as team ChDR Cheese. Their fellow winners – the six-member team Nations' Flying Foxes from the International School of Geneva – had to supervise their experiment from Switzerland because of travel restrictions due to the COVID-19 pandemic. The team was connected to all lectures and control rooms through a dedicated live stream, allowing them to conduct their experiment in Hamburg virtually.

Beamline for Schools is an international competition, organised by CERN, open to all secondary-school students worldwide. Student teams devise an experiment that can be carried out using a particle beam and write a short research proposal. Applications are then evaluated by researchers from CERN and DESY, and two winning teams are selected. These are invited to conduct their experiments at a test beam together with scientists from CERN and DESY. As the particle accelerators at CERN were still shut down in 2020, the competition took place at DESY for the second year in a row.

Beamline for Schools is an education and outreach project funded by the CERN & Society Foundation and supported by individual donors, foundations and companies. For 2020, the project was partly supported by the Wilhelm and Else Heraeus Foundation with additional contributions from the Arconic Foundation, Amgen Switzerland AG and the Ernest Solvay Fund, which is managed by the King Baudouin Foundation.

Joachim Mnich to join CERN management

Joachim Mnich, DESY Director in charge of Particle Physics for the last 12 years, will move to CERN on 1 January 2021 to become Director for Research and Computing there. When Mnich took office as DESY research director in 2009, DESY had just switched off its large particle collider HERA. During Mnich's term of office, the DESY particle physicists joined the experiments at the LHC. By now, the DESY groups not only form the largest German LHC user groups, but also play leading roles in the upgrade of the LHC detectors for the high-luminosity phase, due to begin in a few years. DESY's participation in the Belle experiment in Japan and the establishment of a programme to search for dark matter on the DESY campus, in which CERN is also involved, also fall within Mnich's term of office.

Joachim Mnich, DESY Director in charge of Particle Physics, will join the CERN Directorate on 1 January 2021.

The next years will be decisive for the future of international particle physics, and CERN plays a central role in the planning and decision-making process. In spring 2020, the European community of particle physicists defined the direction for the research field in a strategy process, and now, it is up to Joachim Mnich, among others, to implement the community's recommendations in projects in consultation with the CERN member states. Moreover, he will oversee the upgrade of the LHC, a challenging international undertaking.

October

All ALPS magnets installed in the tunnel

DESY's "light shining through the wall" experiment ALPS II is taking shape. ALPS, short for Any Light Particle Search, is being installed in a tunnel section of DESY's former HERA accelerator. The international ALPS team will search for dark matter using 24 modified HERA magnets, laser light and a highly sensitive detector. The last of these superconducting magnets was installed in October.

Installation of one of the last superconducting magnets for ALPS II

Almost exactly one year ago, the ALPS II team celebrated the installation of the first magnet in the tunnel. If all goes according to plan, data taking could begin in another year. The use of the tunnel, the changes to the superconducting magnets, the complicated laser system, the highly sensitive detector – all this seemed impossible at first and is now becoming reality. This has been achieved thanks to the great commitment of many "old" DESY staff members, who still know the secrets of HERA, and to the involvement of all the collaboration partners, whose know-how enables state-of-the-art technologies to move into the HERA tunnel once again. The next steps for ALPS II are the precise alignment of the magnets and the completion of three cleanrooms in which the complex and highly sensitive optics will be set up.

The last two magnets of ALPS II, between which light is supposed to "shine through the wall" when ALPS II will go into operation

November

EU innovation funds for five DESY projects

Research projects under DESY coordination or with DESY involvement will receive more than 48 million euros from the European Commission over the next four years. These European projects range from driving innovation in synchrotrons and free-electron lasers to nanotechnologies and showcase DESY's diverse fields of expertise, its drive for innovation and its close ties to industry.

In particle physics, detector development got a boost: The AIDAinnova project builds on the success of its predecessors AIDA and AIDA-2020, both of which improved infrastructure at research centres for the development of new detector technologies. The successor project AIDAinnova, coordinated by CERN, will receive 10 million euros in EC funding over four years and now includes 46 international partners, 12 of them from industry. This direct involvement of industrial companies in detector development is a first, enabling faster turnaround times and more innovation for both research and industry. The scientific coordinator of the project is DESY scientist Felix Sefkow.

From Horizon 2020 to Horizon Europe: funding for innovative EU projects

PhD Thesis Prize 2020

The 2020 PhD Thesis Prize of the Association of the Friends and Supporters of DESY (VFFD) was awarded in equal parts to Valeria Botta for her thesis entitled "Measurement of the coupling strength of the Higgs boson to τ leptons with the CMS experiment at the LHC" and to Gregor Loisch for his thesis entitled "Demonstrating high transformer ratio beam-driven plasma wakefield acceleration".

Valeria Botta

Gregor Loisch

Valeria Botta joined the DESY CMS group in 2015, working on Higgs physics with data from LHC Run 2. Her Higgs-into-tau analysis is an important milestone in Higgs physics. In 2017, a new pixel detector, to which DESY also contributed, was installed in CMS. Valeria Botta played a key role in the alignment of the detector, thanks to which she became tracker alignment convener. Gregor Loisch worked at DESY in Zeuthen as a student of Universität Hamburg. The aim of his work on beam-driven plasma wakefield acceleration of electrons was to provide experimental proof that the transformer ratio in a plasma accelerator can be greater than two.

DESY theorist Frank Tackmann wins ERC Consolidator Grant

Frank Tackmann from the DESY theory group won one of the prestigious ERC Consolidator Grants awarded annually by the European Research Council (ERC). The 2 million euro grant will begin in summer 2021 and run for five years. With the funding, Tackmann will set up a team of theorists to make precise predictions of a certain type of collision at the LHC. These will be particularly useful for the coming LHC upgrade, after which the LHC will generate a much higher number of collisions, thus providing the opportunity to study physics phenomena much more precisely.

When protons collide in the LHC, many particles are created. These interact with each other or decay, producing yet more particles, all within tiny fractions of a second, until they cannot decay any further. This is then called their "final state". Together with three postdocs and three doctoral students, Tackmann will look at a particular "colour-free" type of final state. While theoretical predictions for these collisions exist, the group aims to significantly reduce their theoretical uncertainty. Experimental physicists can then exploit these predictions to make even more precise measurements at the LHC, enabling them to check for deviations that might hint at processes beyond the currently known particles and interactions.

ERC Consolidator Grants are awarded to outstanding researchers with at least seven and up to twelve years of experience after their PhD. The funding of up to 2 million euros per grant is provided for up to five years and covers mostly the employment of researchers and doctoral students.

DESY theorist Frank Tackmann

Ties Behnke takes over as director

Dr. Ties Behnke has taken over as Director in charge of Particle Physics (interim) from 1 January 2021. He will hold this position until a successor for Joachim Mnich, who left for CERN, has been found. The DESY Foundation Council confirmed this arrangement in its session in December 2020. Ties Behnke has been a leading scientist in particle physics at DESY since 1998, focusing on electron–positron colliders and detector development. He is also the spokesperson of the Helmholtz program "Matter and Technologies".

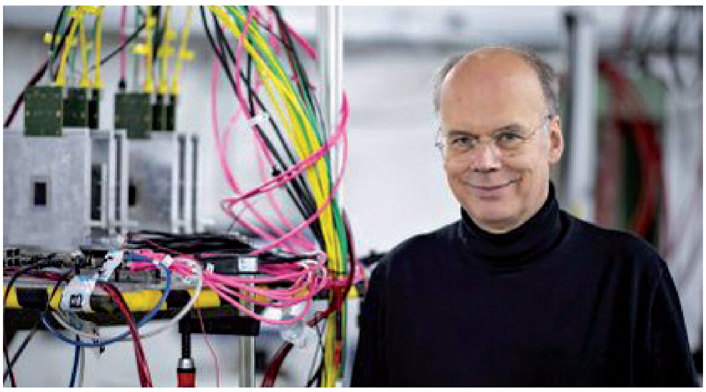

Ties Behnke, interim director of the DESY particle physics division

Experimental particle physics

Physics with protons has been at the heart of DESY's particle physics activities since the start-up of its former electron–proton collider HERA in 1992. Today, the cornerstones of DESY's proton physics programme are its ATLAS and CMS groups, which are involved in a large variety of developments at the Large Hadron Collider (LHC) at CERN, from hardware design to data analysis.

Since its discovery, the Higgs boson has been an important focus of research. Unravelling its precise properties constitutes one of the main activities at the LHC experiments. This includes studying its properties under charge–parity (CP) conjugation (p. 24), investigating complex scalar sectors (p. 35) and exploring its implementation in an effective field theory approach (p. 26).

Another focus of the LHC is the heaviest particle of the Standard Model, the top quark. Here, first evidence of four-top-quark events was observed (p. 30), a new professorship was established (p. 34), and the possible connection to dark-matter processes was analysed (p. 28). Other studies explored the structure of the proton (p. 20) and further probes of the electroweak sector (p. 27 and 31).

At the same time, the DESY LHC groups are preparing for the future LHC upgrades – in particular, the high-luminosity upgrade (HL-LHC) foreseen for the years after LHC Run 2. Activities at DESY for these upgrades include the development of new detectors (p. 32) and tracker technology (p. 22). Another highlight in recent years has been the knowledge transfer to medical imaging (p. 25).

Physics with lepton beams – and the R&D work for the necessary accelerators and detectors – constitutes the second pillar of DESY's particle physics activities. The focus here is on future linear colliders, particularly the International Linear Collider (ILC), and on the upgraded SuperKEKB accelerator with the Belle II experiment at the Japanese national particle physics laboratory KEK. In 2020, SuperKEKB has been breaking luminosity records (p. 42), paving the way for new experimental avenues, such as searches for axion-like particles (p. 44). Regarding a future electron–positron linear collider, the two main activities at DESY in 2020 have been to explore the physics case of a Higgs factory (p. 38) and improve shower simulations for this kind of accelerator experiment (p. 40). Finally, FLASHForward has reached new milestones in plasma acceleration (p. 36).

DESY has also broadened its activities in the field of axion-like particles (p. 45). The construction of the ALPS II experiment is proceeding as foreseen, while preparations started for two new experiments, IAXO and MADMAX.

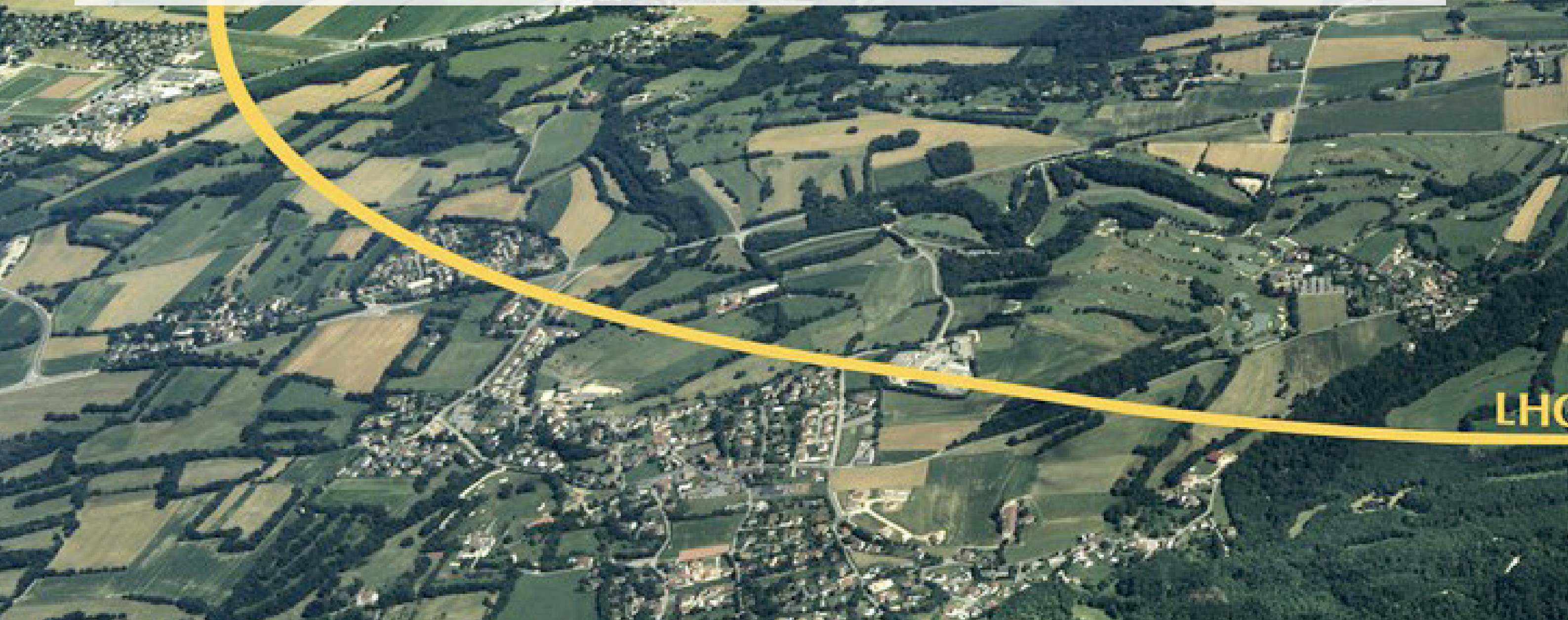


LHCb
ATLAS
CERN Meyrin
CERN Prévessin
27 km

3D model of hadrons

Mapping the 3D structure of the proton

Quarks and gluons are the fundamental constituents of the proton. Mapping their three-dimensional structure in the proton is crucial for our understanding of quantum chromodynamics (QCD) and of matter in general. The 3D quark and gluon content in momentum space is encoded in the so-called transverse-momentum-dependent parton densities (TMDs). A very promising approach to access these distributions is the parton branching method. The DESY CMS group has extracted quark, gluon and even photon TMDs from the experimental data in this framework and successfully applied them to collider observables in a wide range of centre-of-mass energies.

Proton 3D imaging

In hadronic collisions, the interacting proton constituents (partons) receive transverse-momentum contributions from the partonic medium in the proton. As the interaction between the partons occurs, they also emit partonic radiation in a similar way to how an electrically charged particle emits bremsstrahlung in a magnetic field. Understanding the 3D structure of the proton, which results from the transverse-momentum contributions to the interacting partons, and the longitudinal component of the momentum that the partons inherit from the parent proton can be important to systematically improve calculations of hadronic collisions.

The parton branching (PB) method aims at a consistent description of hadronic collisions that includes the transverse-momentum contributions to the interacting partons from both the radiation of further partons and the proton medium. This method has been successfully applied to describe data from inclusive deep-inelastic scattering (DIS) measured at the former HERA experiments at DESY as well as Drell–Yan (DY) measurements from the LHC [1–3] and can be further used to obtain consistent predictions for future collider experiments.

DY production at the LHC

The production of Z bosons (DY) in proton–proton collisions is one of the most precisely measured processes. To describe some of these measurements, understanding the partonic transverse-momentum contributions is crucial. For instance, when the transverse momentum (p_T) of the Z boson is small, measurements are sensitive to the contributions from the proton medium, whereas if the Z-boson p_T is large, an accurate description of partonic radiation is necessary. On the other hand, it is a much bigger challenge to simultaneously describe the Z-boson p_T spectrum across different centre-of-mass energies of the proton–proton system. With the PB approach, the DESY CMS group has been able to accurately predict this observable.

Low-mass, low-energy DY production

At lower mass m_{DY}, the DY process is experimentally challenging, especially at the LHC. At lower centre-of-mass energies, DY measurements covering the low-p_T region exist from the experiments PHENIX at BNL, R209 at CERN and NuSea at Fermilab. Predictions for DY production at low mass and low centre-of-mass energies are obtained, including TMDs through the PB approach (PB-TMDs) and higher-order correction calculations. These low-energy

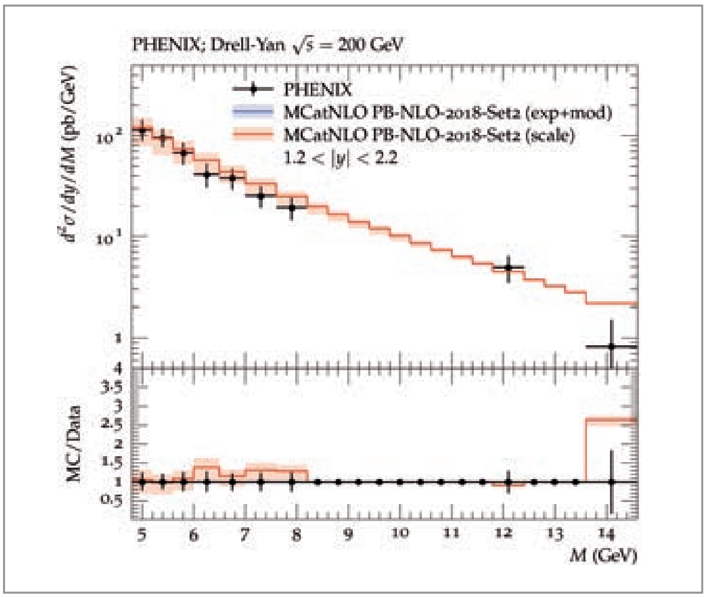

Figure 1

DY mass distribution production measured by PHENIX compared to predictions at NLO using PB-TMDs

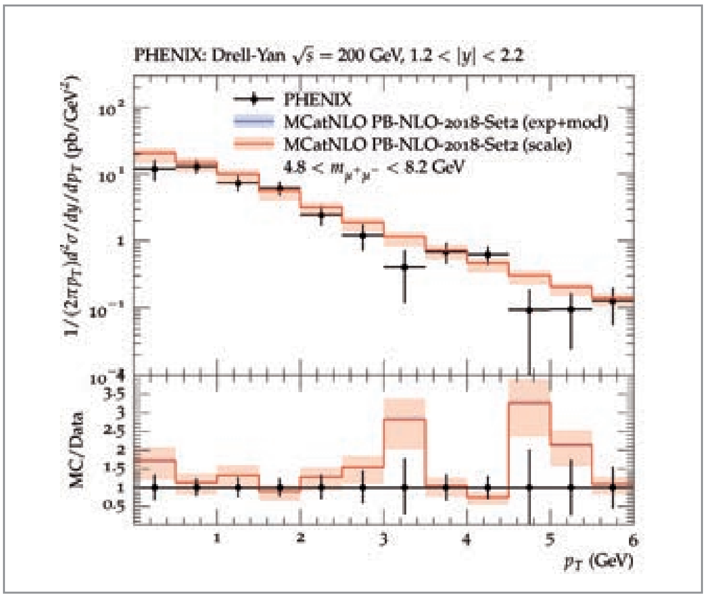

Figure 2

DY transverse-momentum distribution production measured by PHENIX compared to predictions at NLO using PB-TMDs

measurements are very well described in the whole range of p_T/m_{DY} [3].

In Figs. 1 and 2, the DY mass and transverse-momentum predictions obtained with PB-TMDs are compared with experimental measurements from PHENIX. The inclusion of soft parton emissions in the PB-TMDs is essential to describe the low-p_T/m_{DY} regions at low energies.

High-mass, high-energy DY production

The PB method has been also applied to predict very-high-mass DY production. At these high masses, contributions from photon–photon scattering into lepton pairs plays a role. Our group has calculated the photon parton density of the proton by applying the PB method [4]. As shown in Fig. 3, the next-to-leading order (NLO) PB quantum electrodynamics (QED) parton distribution functions describe well the measured dilepton mass spectrum at LHC centre-of-mass energies [5]. The small contribution from photon-initiated (PI) lepton production ($\gamma\gamma \rightarrow l^+l^-$, with $l = e, \mu$) is also calculated.

For the first time, the transverse-momentum distribution of photons inside the proton has been calculated. These photon TMDs have been used to predict the transverse-momentum spectrum of DY lepton pairs at very high masses (Fig. 4).

In recent investigations, our group has been exploring the possibility of using the recent TMD calculations [1, 2, 3] obtained through the PB method [7] together with the MLM merging algorithm [8] in order to combine precise parton-level computations with calculations that include TMD parton radiation.

We have also developed a new merging algorithm that takes into account the contributions to the transverse momentum

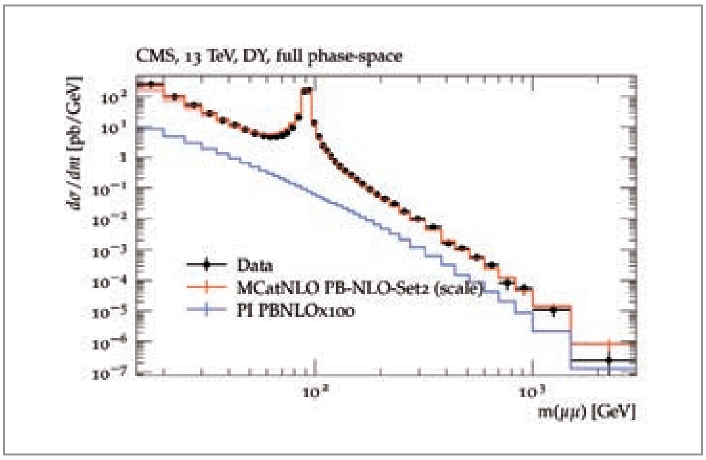

Figure 3

Dilepton high-mass distribution production compared to predictions of QCD+QED using PB-TMDs in the full phase space. The scaled photon-induced contribution is also shown.

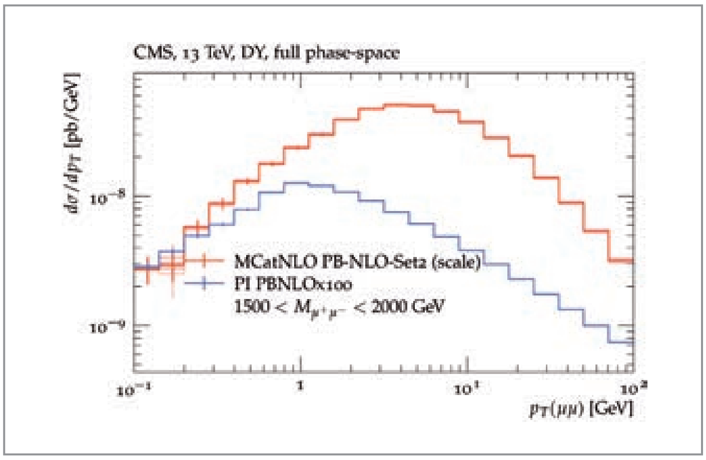

Figure 4

Standard DY and photon-induced transverse-momentum spectra based on collinear and PB-TMD-QED (Set2) in different high-mass regions

of the interacting partons both from the proton medium and from parton radiation. In addition, the algorithm allows us to improve the description of very hard partonic emissions. The preliminary results are promising, extending the good description achieved for the low transverse momentum using the PB-TMD calculation [2, 3] to values at the TeV scale for pure QCD and Z+jets exclusive observables.

Contact:

Sara Taheri Monfared, sara.taheri.monfared@desy.de
Armando Bermudez Martinez, armando.bermudez.martinez@desy.de

References:

[1] A. Bermudez Martinez et al., Phys. Rev. D 99, 074008 (2019)
[2] A. Bermudez Martinez et al., Phys. Rev. D 100, 074027 (2019)
[3] A. Bermudez Martinez et al., Eur. Phys. J. C 80 7, 598 (2020)
[4] H. Jung, S. T. Monfared and T. Wening, arXiv:2102.01494 [hep-ph]
[5] CMS Collaboration, JHEP 12, 059 (2019)
[6] R. Angeles-Martinez et al., Acta Phys. Polon. B 46, 2501 (2015)
[7] F. Hautmann et al., JHEP 1801, 070 (2018)
[8] M. L. Mangano et al., Nucl. Phys. B 632, 343 (2002)

CMS tracker upgrade for the HL-LHC

Science meets industry to deliver the next generation of tracking detectors

The high-luminosity phase of the LHC (HL-LHC) will start in 2027. The CMS collaboration is preparing an upgrade of the CMS detector systems to enhance their performance and meet the HL-LHC demands. For this upgrade, the DESY CMS group will build one of the two end-caps for the outer tracker detector. This process involves the construction of silicon sensor modules and mechanical support parts, followed by the assembly of the whole system into the end-cap. All these steps will be performed on the DESY Hamburg site in the cleanrooms of the Detector Assembly Facility (DAF), which were successfully commissioned and fitted with high-grade equipment in previous years.

Assembly of silicon sensor modules

The upgraded CMS outer tracker will be equipped with several thousand silicon sensor modules of two types: modules with a pixel sensor and a strip sensor (PS) and modules with two strip sensors (2S). The correlated signals from both sensors will allow an instantaneous decision to be made as to whether a collision event should be further reconstructed or rejected, a feature that will eventually enable the CMS experiment to record larger amounts of interesting collision data. For this innovative functionality to work, the two sensors must be aligned with remarkable precision. For example, their rotational misalignment is required not to exceed 45 (22) millidegrees for the PS (2S) modules. Dedicated fiducial markers are engraved onto the corners of the sensors to control the alignment.

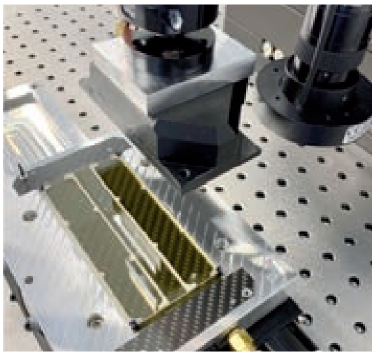

Figure 1

Latest glass-based PS module prototype, together with the pickup tool and the camera equipped with a ring light

The DESY CMS group has pledged to assemble about 1250 PS modules and established a robot-assisted (automated) procedure for this purpose. The procedure employs an integrated motion and vision system, comprising a motion stage equipped with a pickup tool and a high-resolution camera, all controlled by a single software application. Images from the camera are used to identify the fiducial markers of the sensor by means of pattern recognition. The real-time position of the sensor is then derived. Next, the sensor is lifted by the pickup tool, which can move in the *x*, *y* and *z* direction with high precision, and placed in the desired location for gluing with other module components. This assembly method has been designed and

Figure 2

First functional 2S module built at DESY

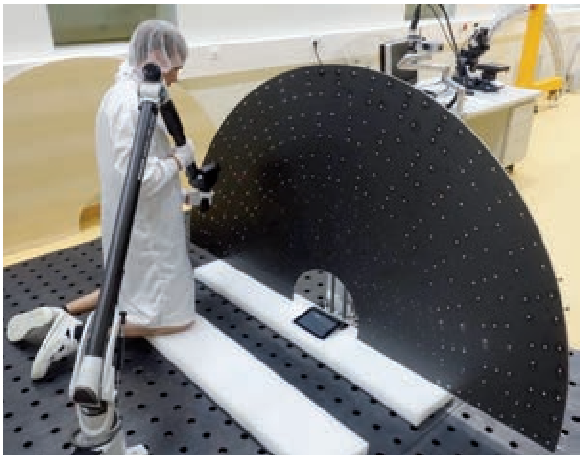

Figure 3

Laser scan of the prototype Dee

continuously developed at DESY, and adopted by the CMS groups at Fermilab and Brown University in the USA.

The year 2020 started with the assembly of the first mechanical prototype of a PS module using dummy silicon parts at DESY. Furthermore, a member of the DESY CMS group played a leading role in redesigning the PS module spacers – components used for the spatial separation of the two layers of sensors – and carried out the relevant finite element analysis (FEA) performance simulations. Afterwards, among numerous improvements, the automated assembly setup was equipped with a new assembly platform compatible with the new spacer design and with a ring light around the camera for reproducible illumination of the fiducial markers. Figure 1 showcases the recently assembled glass-based PS module prototype with the new type of spacers. The production of the first functional PS module at DESY is due in 2021 as part of preparations for the engineering design review within the CMS collaboration.

Another major highlight of 2020 in the CMS upgrade effort at DESY was the assembly of the first functional 2S module (Fig. 2) and its test beam campaign, whose data is currently being analysed. The module was assembled manually using dedicated jigs. Considering the similarity between the 2S and PS module designs, this exercise served as an excellent opportunity to gain experience in handling the new components and materials before moving on to the serial production of the PS modules.

Development and testing of the mechanical support structure

The outer-tracker end-cap is comprised of five double disks with a diameter of 2.2 m. Each double disk is designed in such a way that it detects a charged particle at least once, by equipping each disk on both sides with overlapping modules. One disk consists of two half disks, the so-called Dees, which are the main mechanical elements for precisely positioning the modules and providing them with cooling power. A Dee is built as a carbon fibre sandwich with a foam core and has six wedge-shaped cooling sectors embedded inside. A prototype Dee was built together with industry partners and thoroughly studied for its mechanical and thermal properties.

Figure 3 shows the prototype Dee being laser-scanned with a coordinate measurement arm to evaluate the flatness of the structure. This was followed by a measurement of the position of the inserts that will later be used to attach the detector modules. These inserts need to be at very precise locations to ensure that the detector modules, which are produced with tight tolerances, fit the structure and that the modules are at their intended positions.

Figure 4 shows a sketch of the Dee where the arrows indicate the deviation of the measured insert positions. The length of the arrows indicates the magnitude of the deviation at a scale of 1:1000.

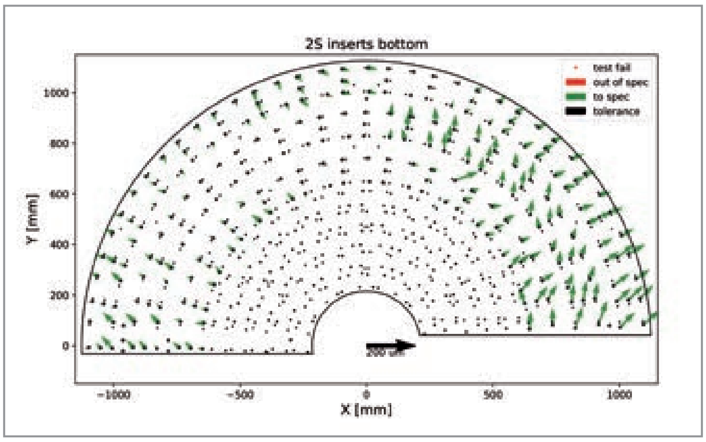

Figure 4

Metrology results of the 2S detector mounting inserts, indicating the deviation of the position from the ideal location

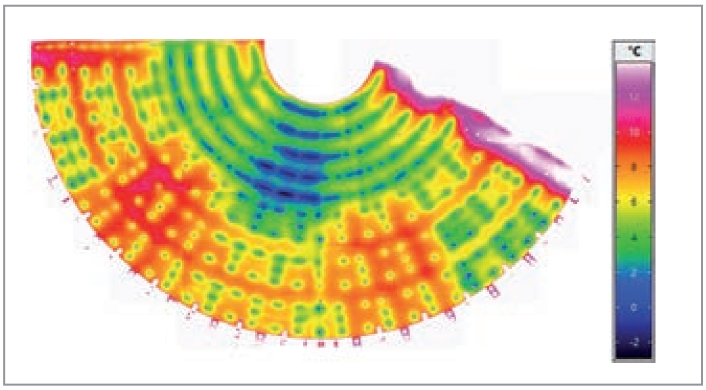

Figure 5

Infrared picture of the Dee while being cooled at -8°C. The upper right cooling sector was not connected to the cooling circuit.

To verify the thermal performance needed to efficiently extract the heat produced by the detectors, pictures with an infrared camera were taken. Figure 5 shows the surface temperature of the Dee while running a cooling fluid through the embedded cooling pipes at a temperature of -8°C at the inlet. The five inner rings of cold surfaces can clearly be seen. These are needed for the large-area cooling contact required to efficiently cool the PS modules.

Both verification methods – the metrology measurement and the infrared pictures – will be the main qualification procedures to evaluate all final Dees after production at industry partners. The Dee prototype production run has provided invaluable feedback on the design and the production process. The tools and techniques to qualify the Dees were commissioned and improved, and preparation of the preproduction with many design improvements has started.

Contact:
Moritz Guthoff, moritz.guthoff@desy.de
Oskar Reichelt, oskar.reichelt@desy.de
Mykola Savitskyi, mykola.savitskyi@desy.de

The Higgs through the looking glass.

CP mirror on the wall, is the Higgs even or odd?

Using the full LHC Run 2 data set collected by the CMS experiment at a centre-of-mass energy of 13 TeV, the DESY CMS group, in collaboration with other institutes, has investigated the CP properties of the Higgs boson in its decays to tau leptons. Results of the study marked the first measurement of the CP mixing in the Higgs-to-tau Yukawa coupling.

A priority for the LHC physics programme is to measure the Higgs-boson properties, as a way to search for hints of new physics. In particular, it is important to address what the Higgs boson looks like under charge–parity (CP) conjugation – a “CP mirror” (Fig. 1) that flips spatial coordinates and swaps particles and antiparticles. The Higgs-boson predicted in the Standard Model (SM) is a pure CP-even state, with couplings to the SM particles that are invariant under CP conjugation. The observation of the Higgs-boson decays to vector bosons, $H \rightarrow WW/ZZ$, has already excluded a pure CP-odd Higgs. However, the Higgs could also appear in a CP-mixed state, as predicted in theories beyond the Standard Model to explain the observed matter–antimatter asymmetry in the universe.

In $H \rightarrow \tau\tau$ decays, the amount of CP mixing in the Yukawa coupling can be expressed in terms of the CP mixing angle $\phi_{\tau\tau}$, defined so that $\phi_{\tau\tau} = 0$, $\pi/2$ and $\pi/4$ correspond to a pure CP-even, pure CP-odd and maximal CP-mixed case, respectively. $\phi_{\tau\tau}$ can be inferred by measuring the acoplanarity angle ϕ_{CP} between the planes spanned by the visible τ decay products.

The production of the Higgs boson in proton–proton collisions is a rare process, overwhelmed by a large background. To efficiently separate signal from background, a state-of-the-art neural network algorithm was deployed. Measuring ϕ_{CP} also required sophisticated analysis techniques, like an improved τ decay mode identification, and methods to measure its decay length to the level of 20 µm, i.e. half the width of a human hair!

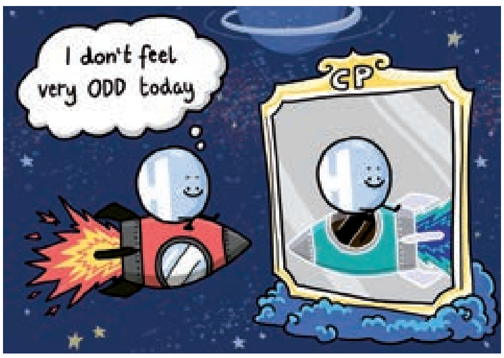

Figure 1
Drawing showing the Higgs boson reflected in the CP mirror [1]

The DESY CMS group made one of the leading contributions to the measurement of the ϕ_{CP} distribution, which shows a clear preference for the CP-even hypothesis (Fig. 2). The measured value of the CP mixing angle, $\phi_{\tau\tau} = (4 \pm 17)°$, is consistent within a confidence level of 68% with the SM prediction, $\phi_{\tau\tau} = 0°$, and excludes a pure CP-odd hypothesis with a confidence level of over 99% (more precisely, 3.2 σ).

The uncertainty is largely of statistical nature, meaning that collecting more data will allow us to see the Higgs boson reflection in the CP mirror with increased clarity.

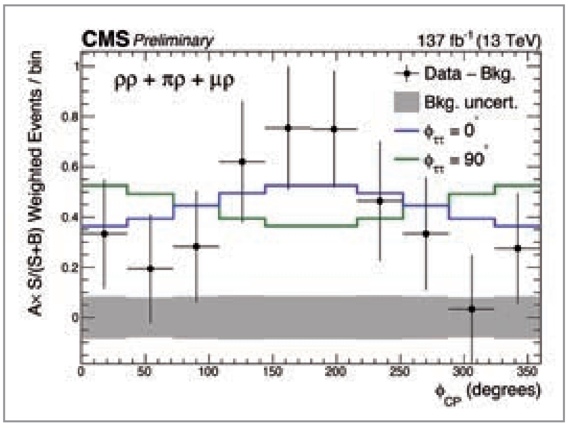

Figure 1
Weighted acoplanarity angle distribution for the most sensitive channels [2]

Contact:
Alexei Raspereza, alexei.raspereza@desy.de
Andrea Cardini, andrea.cardini@desy.de

References:

[1] Credits for the image: Designdoppel GbR – Anna Penkner and Renate Pommerening: www.designdoppel.de
[2] CMS Collaboration, CMS-PAS HIG-20-006

Electron vision

Towards a new medical imaging modality

Medical imaging is a source of civil radiation exposure, and its annual dose in the population is – on average – comparable to the natural dose. The DESY CMS group is involved in translating particle physics know-how into a novel imaging modality that has the potential to minimise civil radiation exposure from medical diagnostics such as X-ray computed tomography (CT). The new technique is based on measuring the deflection angles of electrons in the 200 MeV/c momentum range, which are able to traverse a patient, allowing the reconstruction of the material density of the illuminated area. Owing to the low energy loss of electrons in this energy range, the technique has the potential to reduce the imaging dose while providing equal or better image quality.

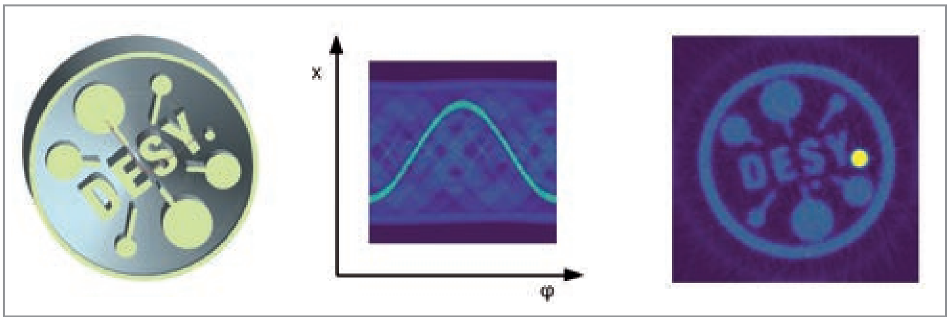

Figure 1

Left: Cross section of a 3D-printed phantom with the DESY logo. The gaps were filled with air, and the “dot” was replaced by an iron rod. Centre: Sinogram of one data row. Right: Tomographic reconstruction of the cross section.

Building on research carried out over the last years, in 2020, a team from the DESY CMS group studied multiple Coulomb scattering of electrons with a momentum of around 200 MeV/c. Making use of the DESY II Test Beam Facility and its beam telescopes – a set of six silicon pixel detectors placed one after another – the team was able to reconstruct the trajectories of electrons traversing a sample placed in the middle of the six sensors and thereby measure the electrons’ incidence position and scattering angle. This allowed an image of the illuminated sample to be created using electrons instead of optical light or X-rays. (Note that the image is not simply “taken” by a sensor behind the object, but is generated using the reconstructed track information of the scattered electrons.)

At a momentum of around 200 MeV/c, a “sweet spot” is reached, as the electrons are energetic enough to traverse e.g. a human head, but leave only a small portion of their energy in the traversed sample, possibly leading to a low-dose, non-destructive imaging modality.

For illustrative purposes, a 3D-printed plastic cylinder with the DESY logo extruded along the cross section was produced and studied (Fig. 1, left). The plastic used (polylactic acid) had a similar density to biological tissue. The dot in the DESY logo was replaced by an iron rod, leading to an increase in scattering. The electrons traversed the sample in the plane of the cross section, and the variance of the scattering angle grew continuously along their path. Various 2D images (“projections”) were taken at different rotation angles of the sample. The sinogram (Fig. 1, centre) represents the scattering data for one image row of the sample at various rotation angles. Finally, a simultaneous iterative reconstruction technique was used to create a tomographic image of the object (Fig. 1, right).

With electron accelerators growing smaller and smaller, this imaging technique, along with compact electron sources, has the potential to be integrated into hospitals and serve as an imaging modality in the context of cancer treatment.

Contact:

Daiki Hayakawa, daiki.hayakawa@desy.de
Hendrik Jansen, hendrik.jansen@desy.de
Paul Schütze, paul.schuetze@desy.de

Reference:

[1] H. Jansen, P. Schütze, Appl. Phys. Lett. 112, 144101 (2018)

Measuring the Higgs boson – effectively

Interpreting ATLAS Higgs measurements using effective field theory

Ever since the discovery of the Higgs boson, physicists at DESY and elsewhere have studied its properties as precisely as possible. Deviations from the predictions of the Standard Model could indicate the need for a new theory. However, how can you search for signs of a new theory if you do not know what to look for exactly? One answer to this age-old question, at least in the context of particle physics, is provided by effective field theories (EFTs), which the DESY ATLAS group used to hunt for effects beyond the Standard Model (BSM) in Higgs-boson measurements.

At the LHC, the Standard Model EFT formulation can be used to describe phenomena that occur at very high energies and cannot be directly found in proton–proton collisions, for example particles with extremely large masses. Almost all such phenomena would give rise to new interactions, with different models leaving different EFT signatures in the low-energy regime. The strengths of these interactions are determined by the Wilson coefficients, which are free parameters of the theory, as well as by the energy scale of the new physics.

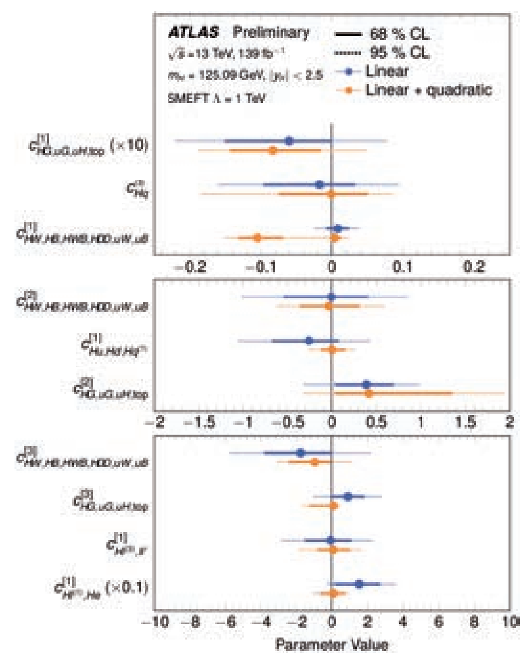

Figure 1

Allowed ranges for the coupling coefficients of new EFT interactions in the rotated Warsaw basis. The coefficient $c^{(3)}_{Hq}$, for example, describes the strength of an effective four-particle interaction between two quarks, a gauge boson and the Higgs boson – which is not present in the Standard Model. The other coefficients, $c^{[i]}_{X}$, correspond to the *i*-th most sensitive direction in the subspace composed of the operators *X*. The Standard Model prediction for all of these coefficients is zero.

Using the full LHC Run 2 data set of 139 fb^{-1} collected with the ATLAS detector in the years 2015–2018, a combined Higgs-boson production measurement was performed based on Higgs-boson decays to pairs of photons, *Z* bosons or bottom quarks. Combining different channels allows multiple Wilson coefficients to be constrained simultaneously. In order to make the best use of the data, a rotation to the most sensitive direction in EFT space was performed. Two sets of results were presented, reflecting different orders in perturbation theory: a “linear” model including only leading-order BSM effects and a “linear+quadratic” model including higher-order effects where possible. The results are more generic and easier to reinterpret than studying one coefficient at a time.

Figure 1 shows the allowed ranges for the Wilson coefficients of new EFT interactions to which the combined ATLAS Higgs analysis is sensitive. The Standard Model predicts all these coefficients to be zero, as their corresponding interactions are not present. Significant positive or negative deviations would indicate new phenomena. All measurements are compatible with the Standard Model, indicating that – if there is physics beyond the Standard Model – it is either at energy scales much larger than 1 TeV, or manifests itself in interactions to which the available measurements are not (yet) sensitive.

Contact:

Carsten Burgard, carsten.burgard@desy.de
Sarah Heim, sarah.heim@desy.de

References:

[1] ATLAS-CONF-2020-027
[2] ATLAS-CONF-2020-053

Flavour tagging at ATLAS

Algorithms for classifying the origin of jets

Identification of particle jets containing *b* hadrons (*b* jets) is a powerful tool in many ATLAS searches and measurements. To identify these *b* jets, the distinct properties of *b* hadron decays are exploited using advanced machine learning techniques. The DESY ATLAS group is involved in both the development and calibration of these jet classification algorithms used for analyses at ATLAS.

Algorithm development

Due to the complex nature of jets, many different inputs are used to distinguish (through “flavour tagging”) *b* jets from jets containing *c* hadrons (*c* jets) or from those initiated by light quarks. These inputs are mainly the jets kinematic properties as well as the tracks and reconstructed vertices associated to them. This information is then combined into powerful discriminants, each one targeting a distinct property of the *b* jets with respect to lighter-quark jets. In particular, one of the important algorithms uses a recurrent neural network (RNN) [1], which examines the tracks that are associated with the jet and capitalises on their kinematic properties and correlations to identify *b* jets.

The currently recommended flavour tagger for ATLAS analyses is DL1r, which combines the output of the RNN with jet properties and further preclassification algorithms inside a deep neural network to create a powerful final classification algorithm.

The improvements resulting from the latest developments compared to previous flavour taggers (DL1, MV2) are shown in Fig. 1.

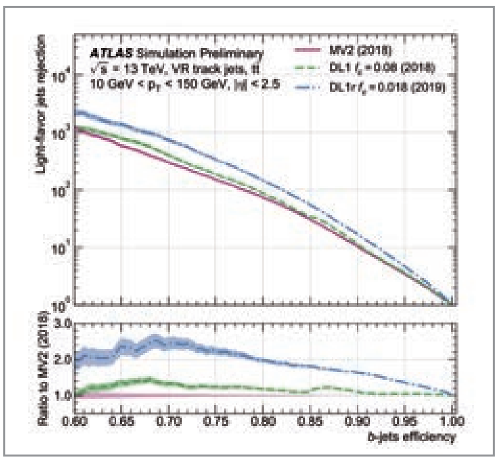

Figure 1
Light-flavour jet rejection rates for the latest *b* tagger (DL1r) and its predecessors (DL1, MV2) [2]

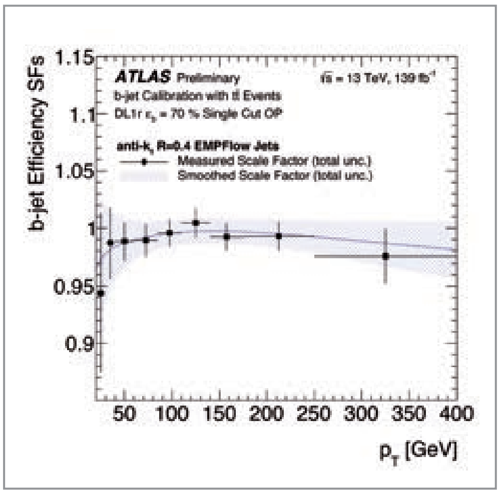

Figure 2
Data-to-simulation scale factors for variable-radius track jets, derived by researchers from DESY [3]

Flavour tagger calibration

Flavour taggers at ATLAS are trained by supervised learning using information about the true nature of each jet, obtained from simulation, to help the neural networks learn the differences between the jets.

However, these simulations do not deliver a perfect description of nature, which leads to the neural networks possibly learning wrong correlations, thus limiting their performance. This needs to be corrected, which is done by measuring the flavour tagging efficiency in data events and comparing it to the efficiency in simulation. The resulting ratios of these efficiencies are the so-called scale factors (SFs), which are displayed in Fig. 2.

The DESY ATLAS group played a significant role in the development and calibration of the described taggers, which are an important tool to fully exploit the LHC Run 2 physics programme.

Contact:
Janik von Ahnen, janik.von.ahnen@desy.de; Alvaro Lopez, alvaro.lopez@desy.de
Krisztian Peters, krisztian.peters@desy.de

References:

[1] ATLAS Collaboration, ATL-PHYS-PUB-2017-003
[2] ATLAS Collaboration, ATLAS-PLOTS-FTAG-2019-005
[3] ATLAS Collaboration, ATLAS-PLOTS-FTAG-2021-001

The hunt for dark matter

Top quarks as a gateway to the dark universe

The existence of dark matter is by now well established by astrophysical observations, yet its exact origin remains one of the unsolved mysteries of modern particle physics. Several theories involving physics beyond the Standard Model exist, predicting new signatures that could be visible at the LHC. Various efforts are ongoing at DESY using data collected by the ATLAS experiment at the LHC in order to probe these theories and find dark matter. Several new results highlight the wide variety of models and analyses employed and conducted by scientists of the DESY ATLAS group.

Introduction

A wide range of astrophysical and cosmological observations suggests the existence of a non-baryonic and non-luminous matter component of the universe, called dark matter (DM). Of the many types of DM candidates proposed, weakly interacting massive particles (WIMPs) are among the most compelling from a theoretical perspective, assuming they are consistent with the expected DM density. If WIMPs are the manifestation of DM in nature, then it may be possible to produce them directly at the LHC – and we are eager to find them.

The hunt for these particles proceeds in dedicated searches, using as guidance models with a minimum set of expected new particles as well as more complete theories.

The DESY ATLAS group is leading efforts focusing on DM particles produced through the decay of a spin-0 mediator (scalar or pseudoscalar) particle produced in association with top-quark pairs or single top quarks (Fig. 1). This production of DM in association with top quarks is expected to be enhanced with respect to that of the other Standard Model (SM) quarks, under the assumption of a coupling between the SM quark and the mediator that is proportional to the SM quark's mass.

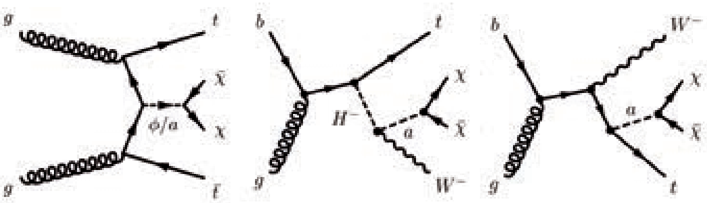

Figure 1

Feynman diagrams of the important processes considered, involving top quarks, a new scalar or pseudoscalar mediator and dark matter. The left diagram is referred to as DM$t\bar{t}$, whereas the two diagrams in the middle and right are labelled DM*t*.

Top-quark pairs and dark matter

The DESY ATLAS group investigated models that include a pair of top quarks using different final-state signatures following the possible decay ways of the two top quarks: All hadronic, semi-leptonic and dileptonic final states were tested [1–4]. Figure 2 shows the results of the dilepton final-state analysis, which was found to have the best sensitivity for these models [1]. This important result was obtained, first of all, by exploiting the largest data set available to date, corresponding to 139 fb^{-1} of proton–proton collision data collected by the ATLAS experiment during LHC Run 2 (2015–2018) at a centre-of-mass energy of $\sqrt{s}$ = 13 TeV, and by using a new discriminating variable, called the "object-based missing transverse energy (E_T^{miss}) significance" [2]. Finally, to improve the sensitivity to those models, events were separated according to single lepton flavours, different-flavour leptons or same-flavour leptons in 12 totally exclusive signal regions.

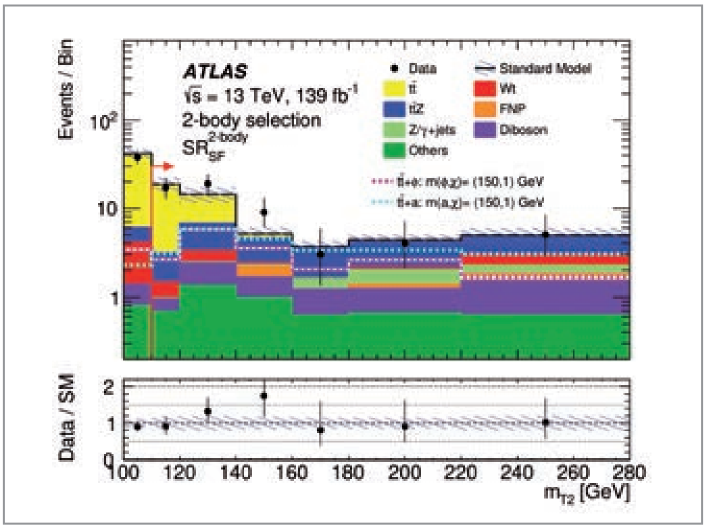

Figure 2

Distribution of the transverse mass m_{T2} in the same-flavour signal region [1]. Reference dark-matter signal models (DM$t\bar{t}$) are overlaid for comparison.

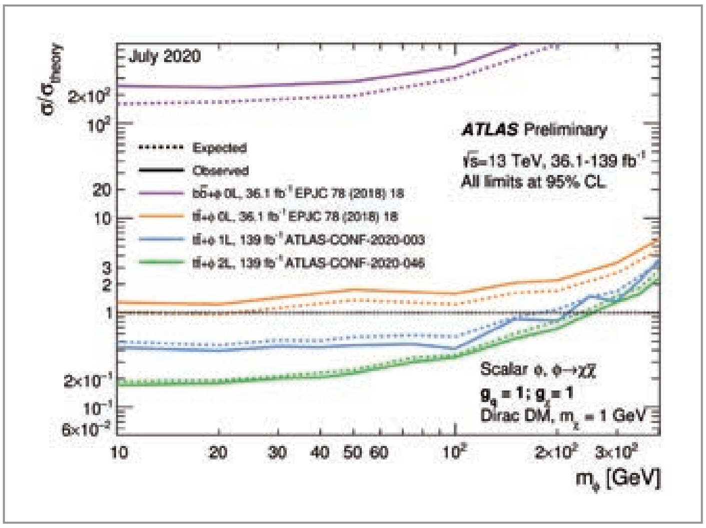

Figure 3

Exclusion limits for colour-neutral scalar-mediator dark-matter models (DM$t\bar{t}$) as a function of the mediator mass m_ϕ for a dark-matter mass m_χ of 1 GeV [1, 3, 4]

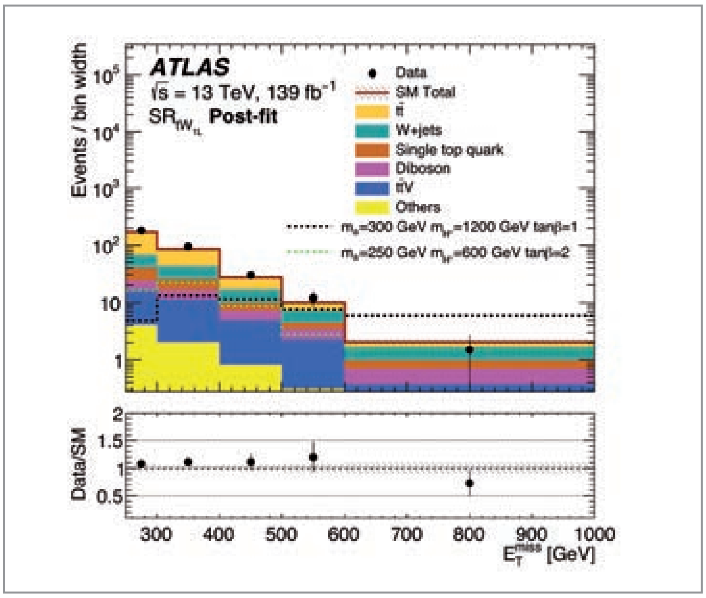

Figure 4

Distribution of the missing transverse energy spectrum of the one-lepton search [6]. The distributions of two possible DMt signal scenarios are shown as well for comparison.

Figure 3 presents the overview results for DM$t\bar{t}$ as a function of the mass of the scalar mediator, with a dark-matter mass fixed at 1 GeV.

Single top quarks and dark matter

While models containing a minimum set of new particles are an excellent tool to explore large parts of possible signatures, sometimes a more complete theory allows final states that would otherwise be missed. One of these examples is provided in the context when DM is mediated by new scalar particles extending the Higgs sector [5]. One particularly interesting aspect, which had not been covered by existing ATLAS searches so far, arises when DM is produced in association with a single top quark. This aspect was the focus of a recently submitted study led by DESY [6], in which the complex theoretical model space of single-top-quark production in association with DM was explored.

The middle and right parts of Fig. 1 show the two main Feynman diagrams that play a leading role in this model. Both diagrams interfere destructively. In particular, the presence of a charged Higgs boson (Fig. 1, middle) provides a unique signature (i.e. higher-energy final-state particles) that would otherwise not be present in a simplified approach (Fig. 1, right). Additionally, the relative importance of the DM$t\bar{t}$ process, depicted on the left side of Fig. 1, as well as other single-top-quark production modes are drastically reduced.

The search was carried out with one or two leptons in the final state. Figure 4 shows the observed data in the missing transverse energy spectrum of the one-lepton search. At the end, several analysis categories were statistically combined. These combinations are an important tool to extend the sensitivity beyond what a single analysis could focus on. This is highlighted in Fig. 5, where several model parameters are varied (i.e. the mass of the charged Higgs boson as well as

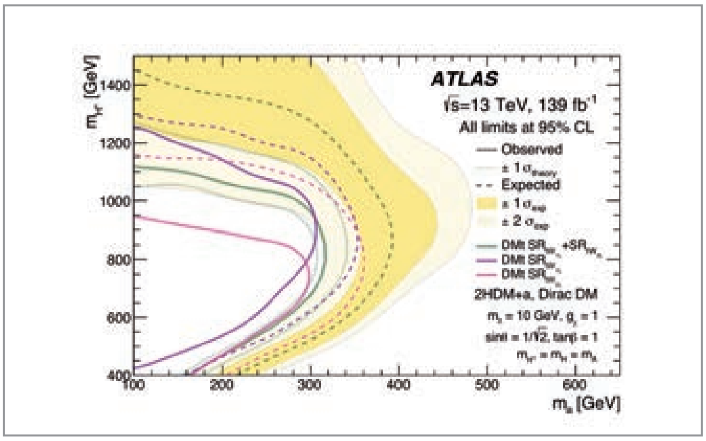

Figure 5

Exclusion limits as a function of the mass of the charged Higgs boson and the mediator mass for the DMt signature [6]

the mediator mass). The expected sensitivity of the combined result is represented by the green dashed line, while the sensitivities of the separate one-lepton and two-lepton searches are depicted by the magenta and pink dashed lines.

All the presented results are pushing the limits on the mass of the new mediator particle into the range of several hundred GeV.

Contact:

Marco Rimoldi, marco.rimoldi@desy.de
Claudia Seitz, claudia.seitz@desy.de

References:

[1] ATLAS Collaboration, arxiv.org/abs/2102.01444
[2] ATLAS Collaboration, ATLAS-CONF-2018-038
[3] ATLAS Collaboration, EPJC 78, 18 (2018)
[4] ATLAS Collaboration, arxiv.org/abs/2012.03799
[5] M. Bauer et al., JHEP 1705, 138 (2017)
[6] ATLAS Collaboration, arxiv.org/abs/1612.00850

Evidence of four-top-quark production with ATLAS

Rare and very energetic processes as a window into new physics

In May 2020, the ATLAS collaboration announced strong evidence of the production of four top quarks – a finding in which the DESY ATLAS group played a leading role. The Standard Model predicts such an event to take place once for every 70 000 top-quark pairs produced at the LHC. The rarity of the process makes it exceptionally challenging to discover.

The top quark is the heaviest fundamental particle in the Standard Model (SM) and, with a threshold energy of about 700 GeV, the production of four top quarks is one of the most massive SM processes at the LHC. This extremely energetic, rare process provides a gateway to the discovery of new physics, as the presence of new heavy particles or yet unknown interactions can enhance the rate at which the process occurs at the LHC. It is also sensitive to the CP nature of the top–Higgs coupling and to the Higgs width. Thus, any deviations from the rate predicted by the SM may reveal long-sought new physics.

The four top quarks produce four *W* bosons and four jets originating from bottom quarks, leaving distinct signatures in the detector. Using 139 fb^{-1} of data collected by the ATLAS detector at $\sqrt{s}$ = 13 TeV, ATLAS physicists studied the process in events with at least one pair of same-charge leptons in the final state. This signature, which contributes to roughly 10% of the four-top decays, is particularly favoured due to the small background in proton–proton collisions.

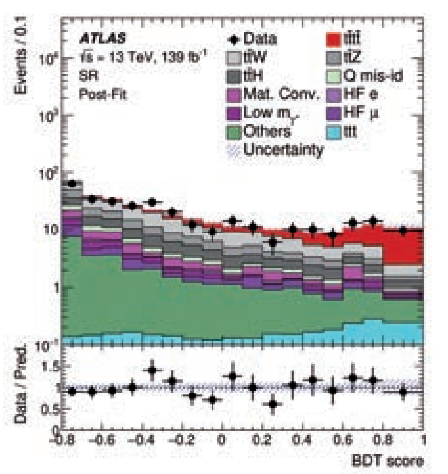

Figure 1

Multivariate discriminant output for the signal region [1]

In order to see the process, the ATLAS physicists, including DESY scientists and collaborators from other German institutes, studied the remaining background carefully and applied novel methods. A multivariate discriminant (Fig. 1) using advanced machine learning techniques was trained to distinguish the signal from background, taking into account the number of (*b*-)jets, the energy of the final-state particles and the angular correlations between them. The analysis of leptons and (*b*-)jets is very important in detecting the signal, and DESY physicists played leading roles in these areas.

The backgrounds with a similar signature to four-top-quark production are dominated by the production of top-quark pairs in association with a *W, Z* or Higgs boson. Each of these processes was estimated by means of simulations using state-of-the-art theoretical predictions. “Fake” leptons might also arise from the semi-leptonic decay of *B* hadrons, photon conversions, or wrong charge assignment. This challenging background was estimated using dedicated control samples to reduce systematic uncertainties and increase the signal sensitivity.

The cross section for four-top-quark production was found to be 24^{+7}_{-6} fb [1], which is in agreement with the SM prediction within 1.7 standard deviations. The observed (expected) signal significance is 4.3 (2.4) standard deviations. This milestone result paves the way to the discovery of this rare process, as the LHC collects more data in the coming years.

Contact:

Xingguo Li, xingguo.li@desy.de
James Ferrando, james.ferrando@desy.de

Reference:

[1] ATLAS Collaboration, Eur. Phys. J. C 80, 1085 (2020)

Making a weak light brighter

Probing the electroweak sector in a new process

In interactions we encounter every day, photons (γ), the particles of light, only interact with charged particles and therefore not with each other. However, as energies increase, this self-interaction becomes possible through charged intermediaries, producing various particles. One such process is the photon-induced production of a pair of *W* bosons, schematically displayed in Fig. 1, which represents a direct interaction of carriers of the electromagnetic and weak force. This rare process was finally observed after a long search by the ATLAS collaboration with a contribution from DESY, marking an important confirmation of the Standard Model.

Collisions at the LHC usually happen between constituent partons of the protons, mostly quarks and gluons. Radiation off these partons and interactions between the proton remnants lead to a large multiplicity of particles detected by the LHC experiments. However, the colliding protons can also emit photons, resulting in a plethora of photon–photon processes. Since the protons stay intact in these processes, such events exhibit a distinctive low particle activity in the detector. This makes it possible to find them among other LHC collisions. In the case of the production of two weak bosons, $\gamma\gamma \rightarrow WW$, the W particles can decay into a pair of charged leptons and neutrinos. Since the neutrinos do not interact with the detector, only the two leptons are detected.

This process was observed for the first time by the ATLAS collaboration [1]. Besides the rather low number of events, the main challenge of the measurement is the presence of a background due to *WW* production with quarks in the initial state, $qq \rightarrow WW$, where the decay products of the W boson pair are accompanied by additional particles. Modelling of the particle activity of this background process is inaccurate, and several corrections had to be derived in order to estimate its contribution precisely.

Figure 2 shows the charged-particle activity around the collision point for the data, the $\gamma\gamma \rightarrow WW$ signal and the background, which is dominated by the $qq \rightarrow WW$ process.

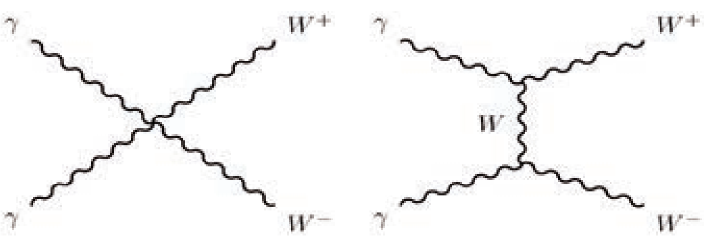

Figure 1

Feynman diagrams showing the interaction of two photons γ and two weak bosons W

The zero-track bin contains most of the signal, while the other bins are used to control the backgrounds. The measurement established the presence of the $\gamma\gamma \rightarrow WW$ process with 8.4 σ significance. The next goal is to measure its properties in more detail and to search for hints of physics beyond the Standard Model.

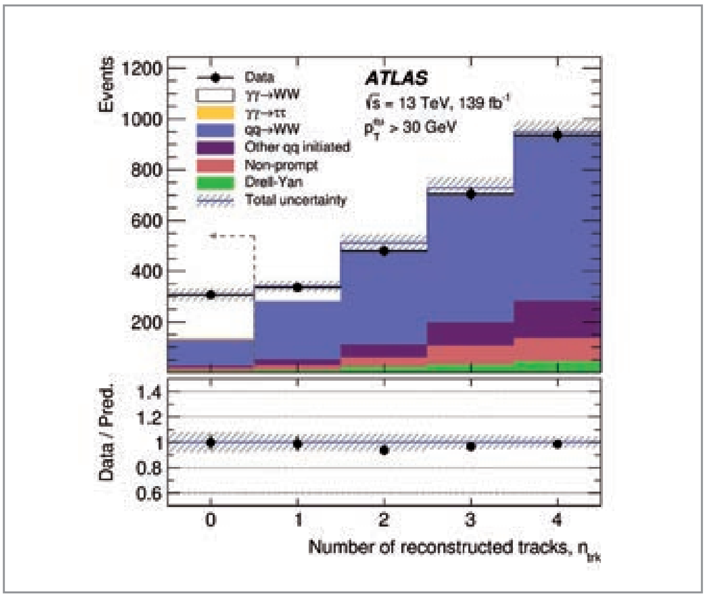

Figure 2

Distribution of the number of reconstructed charged particles (tracks). The $\gamma\gamma \rightarrow WW$ signal region requires zero tracks, as indicated by the arrow.

Contact:

Filip Nechanský, filip.nechansky@desy.de

Reference:

[1] ATLAS Collaboration, arXiv:2010.04019, submitted to Phys. Lett. B

ATLAS ITk strip detector for the HL-LHC

Moving towards production

The ATLAS collaboration is working towards upgrading its detectors for the High-Luminosity LHC (HL-LHC). The DESY ATLAS group is strongly involved in the development, design, construction and installation of the new silicon tracking detectors. The year 2020 brought obvious, marked challenges – nonetheless, progress was still possible despite restrictions due to the COVID-19 pandemic. Preparations for the detector production made up the focus of 2020. This included the further development and commissioning of production tools, the construction of prototype parts and internal CERN reviews.

Working on the next generation of silicon trackers

While work towards the high-luminosity upgrade of the LHC continues at CERN, DESY is getting ready to build a major part of the tracking detectors for the ATLAS experiment. For several years already, the DESY ATLAS group has directed a significant amount of its efforts towards achieving this goal. Among the key milestones of 2020 were the passing of the final design reviews of the ATLAS inner tracker (ITk) strip module and local support designs (with co-lead from DESY) as well as the manufacture and readout of the multimodule structures. The overall speed of the project was heavily hampered by the global pandemic. Still, work could continue globally, at about half the normal speed.

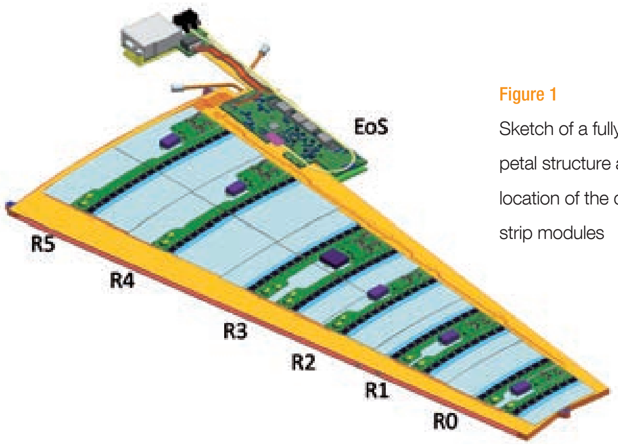

Figure 1

Sketch of a fully loaded petal structure and the location of the different strip modules

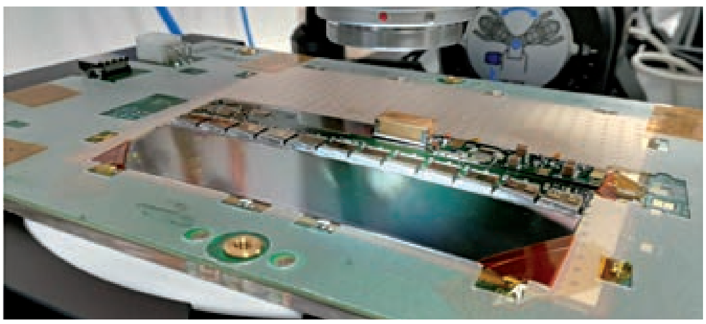

Figure 2

First R2 strip module built at DESY in Hamburg and Zeuthen

The building blocks: modules and petals

The DESY ATLAS group spans the two DESY campuses – detector development, design and construction are performed in close cooperation by group members at both sites. In the cleanrooms in Zeuthen and Hamburg, silicon strip detector modules are being constructed and tested. The modules are composed of a silicon sensor (~5000 n-in-p channels on ~10 x 10 cm^2 of p-bulk silicon), a readout flex board loaded with amplifier application-specific integrated circuits (ASICs) and a power converter board. The module components are precision-glued, wire-bonded (with about 6000 wire bonds per module) and then exposed to stringent quality control tests.

The ITk comprises six different types of strip end-cap modules, depending on their radial position within the local support structures, called petals. The sketch in Fig. 1 shows a petal with its six different modules. The first fully electrical R2 module with the latest chipset was built in 2020 and thoroughly tested at DESY (Fig. 2), along with numerous R0 modules with previous chipset incarnations. Novel techniques were used in the construction of the R2 module, such as the use of a glue-dispensing robot to apply the glue layers between the readout chips and their carrier board, the so-called hybrid, as well as between the hybrid and the silicon sensor. A very precise control of those glue layers (down to the level of tens of micrometres) is of utmost importance, as they strongly contribute to the capacitive coupling (and hence the electronic noise) between the silicon strips and their readout channels. In addition, the glue layers constitute the thermal path for the effective cooling of the electronics through the local supports, which is mandatory for the proper operation of the module.

Another building block of the ITk strip tracker is the local support, i.e. the petal core in the case of the end-cap subdetector. It consists of a "sandwich" composite structure, mostly made of carbon fibre reinforced polymer (CFRP), and embedded titanium cooling pipes, with extremely good thermo-mechanical properties. DESY plays a leading role in the construction of these structures. Two prototypes following the latest approved design were recently manufactured at the DESY mechanical and carbon fibre laboratories and proved to be up to the required specifications through quality control testing at the DESY laboratories. Figure 3 shows one of the two prototypes and, as an example, a thermal image of it obtained by infrared imaging at one of the DESY setups.

In addition, DESY is responsible for the design and test of the data concentrator boards, called EoS boards, which are in charge of the signal and data distribution to and from the local support structures. In 2020, numerous prototype boards were designed, submitted for manufacture and thoroughly tested.

The R2 module and one of the two support structures built at DESY as well as one of the EoS boards designed and tested at DESY became part of the first fully electrical petal built within the ATLAS ITk Strip collaboration (Fig. 4). The full evaluation of this prototype will constitute one of the most important milestones of the preproduction phase of the ATLAS ITk strip tracker.

The DESY ATLAS group is also in charge of developing the procedure for the installation of the petals in the global end-cap structures. Great progress was achieved in 2020, culminating in the construction of the petal insertion tooling at the DESY workshops. Figure 5 shows the crucial components of the insertion tooling, the two types of insertion "hands" that clamp the fully loaded structures and insert them into the structure with micrometric precision.

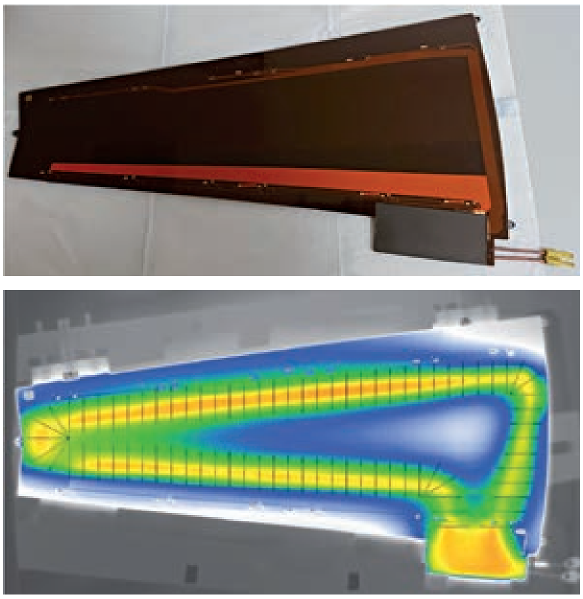

Figure 3

Top: Prototype petal core manufactured at DESY. Bottom: Infrared imaging of the structure while subjected to CO_2 cooling.

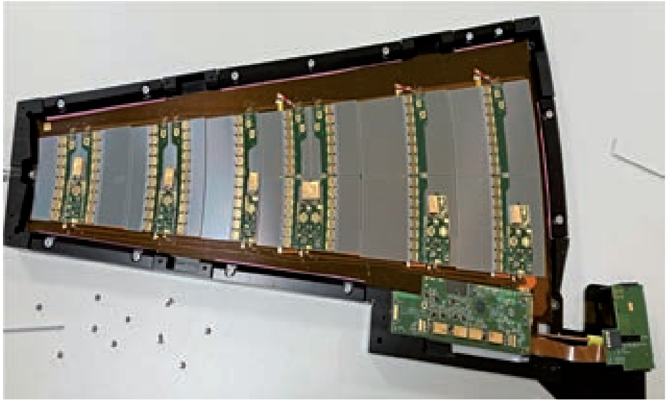

Figure 4

First ITk electrical petal, with numerous components manufactured at DESY

Figure 5

The two types of insertion "hands", designed and manufactured at DESY

Passing reviews – getting ready for production

One of the key steps towards production of the ATLAS ITk tracker consists of the approval of the detector designs and of the manufacturing and quality control procedures in numerous internal CERN reviews, which trigger the beginning of the different preproduction and production phases. In this context, two important final design reviews (FDRs), the ITk strip module FDR and the ITk strip local support FDR, both with strong DESY involvement, were successfully conducted in 2020. These reviews effectively marked the beginning of the preproduction phases of those ITk activities.

Working during the pandemic

The ATLAS ITk group at DESY has been slowed down, but not stopped by the effects of the global COVID-19 pandemic. Significant progress was made in finalising the prototypes of modules, petals and integration tooling as well as many other aspects of the ITk in which DESY is involved. This work was planned and carried out keeping the safety of the DESY workforce a foremost priority, following strict safety regulations.

Contact:
Ingo Bloch, ingo.bloch@desy.de
Sergio Diez Cornell, sergio.diez.cornell@desy.de

Towards new physics through precision

Top-quark mass, strong coupling and constraints on new physics at the LHC

The modern understanding of matter is encoded in the Standard Model of particle physics. In spite of its remarkable success in describing observed phenomena, the model is know to be still incomplete. Stringent tests of the Standard Model and of its extensions demand knowledge of its parameters, masses and couplings, at a new level of precision. A new group established in the context of the Helmholtz W2/W3 professorship programme at the University of Wuppertal and DESY will use the LHC data to improve the precision of the measurements of the strong coupling and of the mass of the top quark, simultaneously imposing constraints on the couplings of possible interactions beyond the Standard Model.

Hundred years ago, the observation of a continuous spectrum in β decays indicated the exchange of a W boson, a particle with a mass much larger than the energy that was actually available in the experiment. This observation established the electroweak interaction, which is meanwhile encompassed in the Standard Model. Similarly, today, the proton–proton collisions at the LHC might unveil fundamentally new interactions happening at energies beyond those available in the collisions. The hints at this "new" physics might appear as deviations of the measured quantities from the Standard Model expectation, and their interpretation is driven by the precision of both the measurement and the prediction.

The new Helmholtz group focuses on investigations of the production of top quarks and hadron jets in proton–proton collisions at the LHC. These are closely linked to each other through their sensitivity to the strong coupling constant α_S, to the top-quark mass m_t and to the description of the proton structure, expressed in terms of parton distributions.

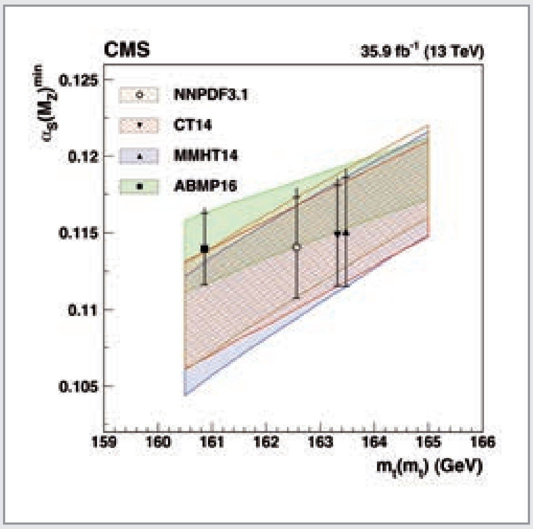

Figure 1
Correlation of the top-quark mass and the strong coupling constant assuming different parton distribution functions [1]

The mass of the top quark plays a key role in the description of the electroweak and strong interactions. Its value is closely related to the masses of the W and Higgs bosons. A significant deviation of the value of m_t from the expectation would provide a hint at new physics. In proton–proton collisions at the LHC, the extracted value of m_t depends on α_S and on the parton distributions, as shown in Fig. 1. The precision of the parton distributions and of α_S can be significantly improved by using precise measurements of the rates of energetic jet production at the LHC. However, further hints at new physics, for example the compositeness of quarks, might also appear in this process, requiring special care in the data interpretation.

With the large data set to be collected at the LHC in the next five years, the production rates of jets and top quark–antiquark pairs can be measured with improved accuracy. Furthermore, both processes can be investigated together, with the constraints on the couplings of possible new interactions imposed simultaneously with the improved description of the parton distributions. In a close collaboration of the ATLAS and CMS experiments, utmost precision in the measurements of the top-quark mass and of the strong coupling can be achieved, which would allow for less ambiguous interpretation. This in turn could provide hints at fundamentally new interactions, which would recast our understanding of matter.

Contact:
Katerina Lipka, katerina.lipka@desy.de

Reference:
[1] CMS Collaboration, Eur. Phys. J. C 79, 5 (2019)

Fingerprints of the vacuum

Pushing the precision frontier to resolve complex patterns of new Higgs bosons at the LHC

The vacuum of space is not empty. This was impressively demonstrated by the discovery of a Higgs boson in 2012, which showed that the vacuum is permeated by a Higgs field. There are, however, strong reasons to believe that the vacuum is more complex and that additional Higgs bosons exist. These may hold the key to some of the most fundamental questions of particle physics, such as the nature of dark matter. A new Helmholtz Young Investigator Group (YIG) at DESY searches for characteristic, but challengingly complex signatures of additional Higgs bosons that traditional data analyses would not have been able to resolve, in order to probe the vacuum structure in a previously almost inaccessible kinematic regime.

Additional Higgs bosons produced at the LHC will be short-lived and can only be identified through their decay products. The YIG targets decays of heavy neutral Higgs bosons into a pair of top quarks, which provide access to a particularly little explored kinematic regime of models with two Higgs fields (2HDMs). However, these decays are notoriously challenging to identify due to strong interference effects between the signal and the dominant background process, which distort the signal shape from a simple peak to a more complicated peak–dip structure (Fig. 1). While this structure is more difficult to distinguish from background fluctuations (noise), its shape, like a fingerprint, carries valuable information about the properties of the two Higgs fields, such as their possible interactions with dark matter.

The search conducted by the YIG requires a precise measurement of the interfering background process from gluon-induced top-quark pair production via Standard Model processes. It also necessitates the development of advanced statistical analysis tools to quantify the agreement between the observed data distributions and the predictions for the characteristic interference patterns in a range of different 2HDM-type models and their multidimensional parameter regions.

Furthermore, the YIG works towards preparing the ATLAS experiment for the high-luminosity phase of the LHC (HL-LHC) by working on fast, efficient algorithms for the reconstruction of particle trajectories in the new ATLAS tracking detector (ITk), which will partly be built at DESY. A particular focus lies on the dense environments encountered, for example, in the collimated decays of highly energetic top quarks or Higgs bosons, which are characterised by many overlapping particle trajectories that are challenging to reconstruct and identify unambiguously.

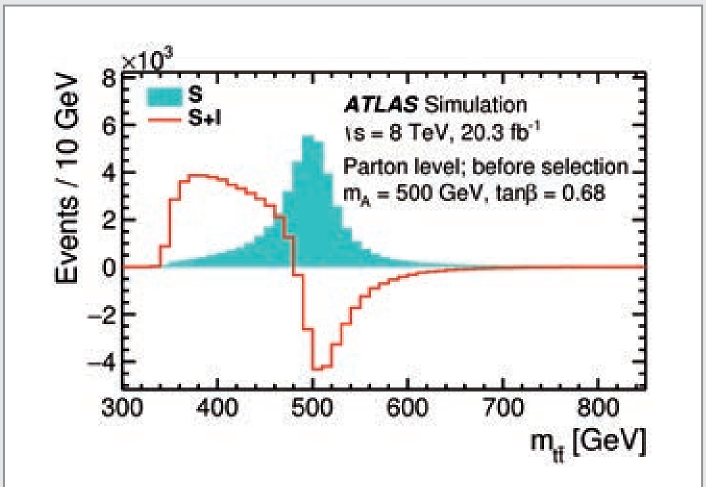

Figure 1

Signal shape of a heavy Higgs boson decaying into a top–antitop quark pair for one representative choice of 2HDM parameters with (red) and without (turquoise) interference [1]

Contact:
Katharina Behr, katharina.behr@desy.de

References:

[1] ATLAS Collaboration, Phys. Rev. Lett. 119, 191803 (2017)
[2] https://hgf.desy.de/ivf/projekte/vh_ng_1503/
[3] https://atlas.desy.de/e168372/e308361/

Flattening the field

FLASHForward reaches first milestone towards efficient and quality-preserving plasma accelerators

Beam-driven plasma accelerators may be key to the future of high-energy physics, promising to accelerate particle bunches with high quality and high efficiency, while taking up significantly less space than conventional accelerators. The FLASHForward facility at DESY aims to demonstrate all this in a single, self-consistent stage. Building on years of careful commissioning, 2020 brought numerous experimental successes, most striking of which was the demonstration of optimal beam loading: precisely shaping the accelerated bunch to destructively interfere with the plasma wakefield in such a way that all the particles are accelerated uniformly. This resulted in record-high energy transfer efficiency and the first-ever energy spread preservation in a plasma accelerator – an important milestone and the first step towards building the ultimate stage.

Need for beam quality and energy efficiency

What will high-energy physics look like in 30 years? In terms of great new discoveries, no one knows, of course. However, it is already clear that we will need bigger and better particle accelerators, delivering higher energies and higher luminosities. The esteemed Michael Peskin, a professor of theoretical physics at SLAC in the USA, is calling for 10 TeV lepton beams with a luminosity of 10^{36} cm^{-2} s^{-1} at least – far beyond what is currently available.

Plasma wakefield accelerators may be our best bet to reach these lofty goals, with the promise of multi-GV/m accelerating gradients and high beam quality – both crucial to building a next-generation collider. However, such accelerators will require an enormous amount of beam power and therefore very high wall-plug energy efficiency. If the plasma wakefield is driven by a particle beam (as opposed to a laser pulse, at least for now), the energy efficiency can be made sufficiently high, starting from highly efficient klystrons to accelerate the driver beam, then transferring this energy to the trailing beam efficiently and rapidly via a plasma (Fig. 1). This is one of the main goals of the FLASHForward facility at DESY: to demonstrate that plasma wakefields can accelerate particles not only with a high gradient, but also with a high overall efficiency, while maintaining a high beam quality (i.e. low energy spread and emittance).

Beam loading in a plasma wakefield

Simultaneously achieving high gradient, high efficiency and high beam quality is fundamentally very challenging. This is because plasma wakefields dissipate rapidly – within a few

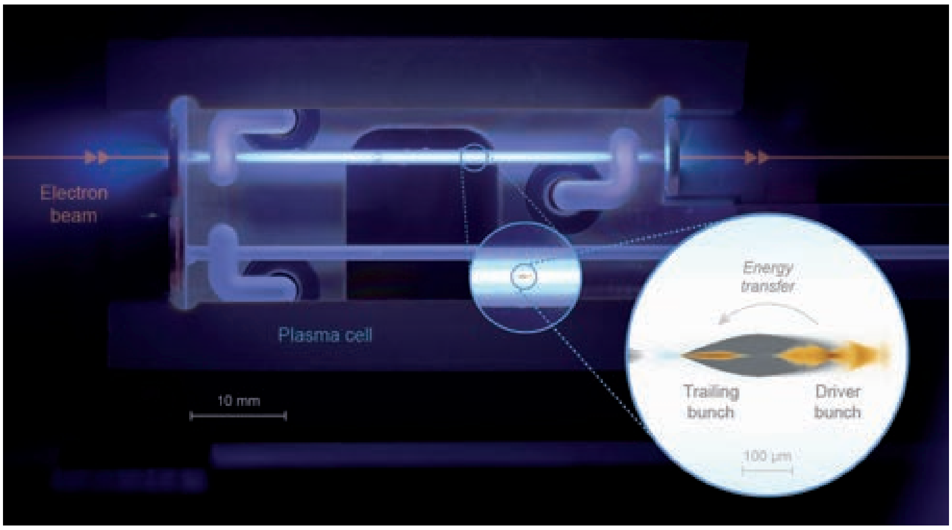

Figure 1

The 50 mm long plasma accelerator cell at FLASHForward during operation. The inset shows a simulation of a leading electron driver bunch (travelling towards the right) rapidly and efficiently accelerating a trailing electron bunch.

wakefield oscillations only, compared to upwards of 10^{10} in a superconducting radio frequency cavity – which means that all the energy in the wake must be extracted immediately, ideally within the first oscillation. This is possible through the use of strong beam loading, whereby the accelerated beam interferes destructively with the wakefield from the driver beam and extracts energy in the process. However, for maximum energy extraction, the accelerated bunch must occupy a large range of phases (up to 90 degrees or more) in the wakefield, which typically leads to very large energy spreads, thus significantly degrading the beam quality.

The solution, proposed shortly after the discovery of plasma wakefields in the 1980s [1] and later refined for more realistic non-linear wakes [2], is to shape the current profile of the accelerated bunch in exactly such a way as to flatten the wakefield – so-called "optimal" beam loading.

Precise shaping of beams at FLASHForward

Careful shaping of the current profile is possible thanks to the advanced capabilities of the FLASH linear accelerator, with its two magnetic compressor chicanes and a third-harmonic cavity, in combination with a precise energy collimator system at FLASHForward [3]. In addition, the newly commissioned PolariX transverse deflection cavity allows the longitudinal phase space to be measured with unprecedented resolution. Finally, the beams need to be precisely focused to micrometre-scale beam sizes and millimetre-scale beta functions [4].

First energy spread preservation

Using a large multidimensional parameter scan, enabled by the exquisite stability and tuneability of FLASH, the highly sensitive optimal-beam-loading operating point was reached experimentally in March 2020 [5]. A careful beam characterisation was performed (Fig. 2), demonstrating that the (permille) energy spread was the same before and after acceleration, with an energy transfer efficiency of (42 ± 4)%. Moreover, this was also the first demonstration of full charge coupling in a plasma accelerator: 100 pC in, 100 pC out. The bunch was accelerated by about 45 MeV with an accelerating gradient of 1.3 GV/m.

Measuring and simulating the wakefield

To directly demonstrate that the wakefield had been flattened, a newly developed wakefield-sampling technique [6] was used to measure the wakefield with femtosecond-scale resolution. Comparing this measurement with a particle-in-cell (PIC) simulation, accurately modelled based on a 6D reconstruction of the incoming electron beam, showed excellent agreement and indicated that the wakefield was indeed strongly beam-loaded by the presence of the accelerated bunch.

In short, FLASHForward is making great strides towards reaching its core objectives. We believe this result is only one of many yet to come.

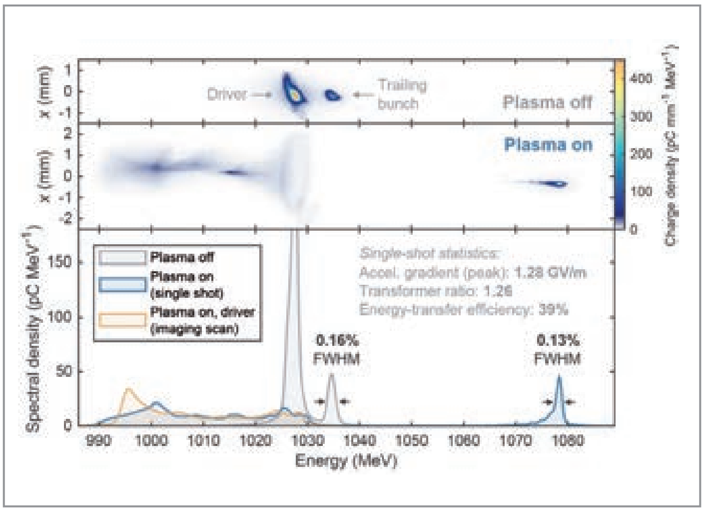

Figure 2

Single-shot spectrometer images, with and without plasma acceleration, show that the spread of the energy spectrum, quantified by the full width at half maximum (FWHM), is preserved during acceleration. From Ref. [5].

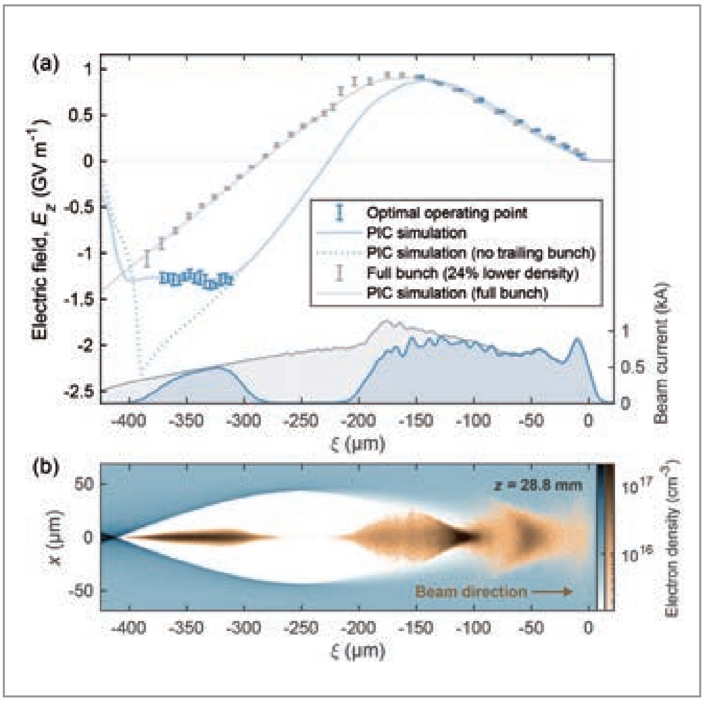

Figure 3

(a) Measurement of the longitudinally averaged wakefield using a novel wakefield-sampling technique [6], demonstrating field flattening by beam loading.

(b) PIC simulations accurately predict the shape of the wakefield. From Ref. [5].

Contact:

Carl A. Lindstrøm, carl.a.lindstroem@desy.de

References:

[1] S. van der Meer, CLIC Note No. 3 (1985)
[2] M. Tzoufras et al., Phys. Rev. Lett. 101, 145002 (2008)
[3] S. Schröder et al., J. Phys. Conf. Ser. 1596, 012002 (2020)
[4] C. A. Lindstrøm et al., Phys. Rev. Accel. Beams 23, 052802 (2020)
[5] C. A. Lindstrøm et al., Phys. Rev. Lett. 126, 014801 (2021)
[6] S. Schröder et al., Nat. Commun. 11, 5984 (2020)

Slower than light

Time-of-flight measurements for particle identification at future Higgs factories

The European Strategy for Particle Physics identifies an electron–positron "Higgs factory" as the highest-priority next collider. The basic requirements for experiments at such a facility are well established in terms of jet energy resolution, hermeticity as well as momentum and impact parameter resolutions for charged particles. More recently, it has been realised that the ability to distinguish different kinds of charged hadrons can add significant advantages. The mass and thereby the identity of a particle can be determined by measuring the specific energy loss in a gaseous main tracker – or, enabled by recent advanced in technology, by registering the arrival time of the particle in the outer tracker or inner calorimeter layers. This topic is one of the current research activities of the FTX group at DESY, which concentrates on research and technologies for future particle physics experiments.

Determining the mass of a particle

The mass of a particle relates its velocity and its momentum. Thus, if both can be measured independently of each other, the mass of the particle can be determined. The time difference between the production of the particle (i.e. the collision of the beams) and its arrival at a time-sensitive detector, combined with the path length, gives the velocity. The curvature radius of a charged-particle track in the magnetic field of the experiment yields the momentum. With a path length of about 2 m and time resolutions of 100 ps or better, typical charged hadrons, such as pions, kaons and protons, can be expected to be distinguishable.

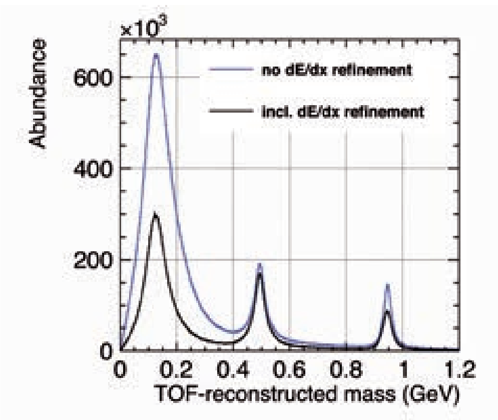

Figure 1

Masses of various particles as reconstructed from the time-of-flight measurement in a full simulation of the ILD detector concept, assuming a 50 ps resolution, based on various physics processes at a centre-of-mass energy of 500 GeV. Peaks around the nominal mass values for (from left to right) pions, kaons and protons can be clearly observed. Additional information, such as the specific energy loss d*E*/d*x*, can help to enrich a desired target species, in this example the kaons [1].

In a typical Higgs factory detector, there are two promising possibilities to incorporate fast timing: The outermost layer(s) of the tracking system could be equipped with low-gain avalanche diodes, or the inner layers of the electromagnetic calorimeter, read out by CMOS silicon sensors, could be pushed to deliver a few 10 ps resolution per hit. The evaluation of the performance and realism of each option is currently ongoing. In this context, an important aspect to be studied is the relation between the time resolution of individual hits and the resulting resolution of the reconstructed time-of-flight of a particle.

For the outer tracking (double-)layer, it is rather straightforward to combine the two hit times to one "particle time". In the calorimeter, this procedure is more involved: Once a shower starts to develop, there are potentially many hits to combine, improving the resolution beyond the single-hit resolution. On the other hand, not all shower particles travel at the speed of light. With increasing depth in the calorimeter, it thus becomes more and more challenging to relate the time of a hit to the arrival time of the primary particle. Last but not least, fast timing enhances the power dissipation in the detector – a possible conflict with the particle flow paradigm, which relies on low-power detectors without need for active cooling.

These aspects have been investigated in the full simulation of the ILD detector concept for the International Linear Collider (ILC). To this end, the first ten layers of the ILD electromagnetic calorimeter have been assumed to deliver

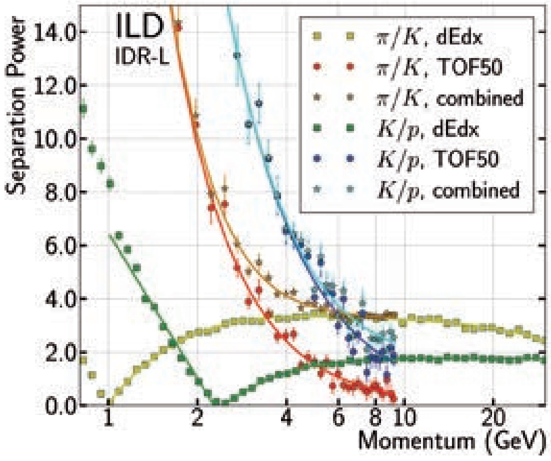

Figure 2

Separation power of pions vs. kaons and kaons vs. protons as a function of the momentum from the specific energy loss measurement in the ILD TPC (d*E*/d*x*) and from a time-of-flight measurement assuming a time resolution of 50 ps for hits in the electromagnetic calorimeter (TOF50). By combining both, the separation can be improved significantly up to momenta of 5–10 GeV [2].

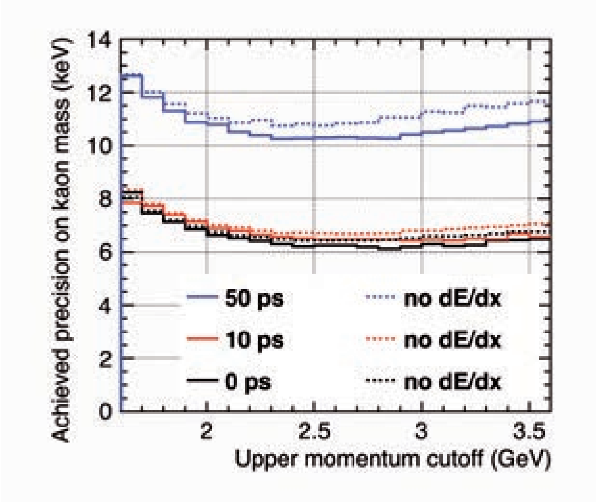

Figure 3

Expected statistical uncertainty on the kaon mass after about ten years of ILC operation at a centre-of-mass energy of 500 GeV, as a function of the highest particle momentum considered. With a time resolution of 50 ps per hit in the first ten layers of the ILD electromagnetic calorimeter, a statistical precision of about 10 keV could be reached [1].

time information with resolutions of 50, 10 and 0 ps, where "0 ps" refers to the true hit time. Figure 1 shows the mass distribution obtained from the time-of-flight measurement assuming 50 ps resolution. The mass peaks from pions, kaons and protons can be clearly distinguished.

Tell me your mass – I will tell you who you are!

The reconstructed mass value can be used to determine the type of particle, or its identity. The sensitivity of such identification methods can be expressed in terms of the statistical significance by which two neighbouring hypotheses can be distinguished. This separation power between the pion and kaon hypothesis and between the kaon and proton hypothesis is shown in Fig. 2 as a function of the particle momentum, in units of standard deviations.

Three different cases are displayed: The yellow and green squares show the separation power based on the measurement of the specific energy loss of the particles in the ILD time projection chamber (TPC) – a well-established technique, but with "blind spots" around momenta of 1 and 2 GeV. The red and blue circles show the separation power based on the mass measurement by means of the time-of-flight method, corresponding to Fig. 1. For momenta below 3 or 5 GeV, the particle identification by time-of-flight is superior to that by specific energy loss, as it effectively covers the "blind spots" of the latter. The orange and cyan stars, finally, show the combined separation power of both methods. With this combination, kaons and protons could be distinguished with at least three standard deviations up to a momentum of 8 GeV, while pions and kaons could be separated up to momenta of 20 GeV with the same significance.

The mass of the kaon

A simple physics application of the mass reconstruction from time-of-flight measurements is the determination of the mass of the charged kaon. The kaon mass has been measured in the past by spectroscopy of kaonic atoms, where a hull electron is replaced by a negatively charged kaon. The two most precise measurements of the kaon mass differ by many standard deviations. They are combined with data from other experiments to a world average with an uncertainty of 13 keV [3].

Figure 3 shows the expected statistical uncertainty on the kaon mass from about half of the amount of data assumed to be delivered by the ILC in 20 years of operation (here 4 fb^{-1} at a centre-of-mass energy of 500 GeV) as a function of the upper momentum cut-off. With a time resolution of 50 ps per ILD calorimeter hit, a statistical precision of about 10 keV is achievable, which could resolve the discrepancy between the two conflicting measurements from kaonic atoms. The evaluation of the achievable systematic uncertainty is currently in progress.

Contact:

Jenny List, jenny.list@desy.de

References:

[1] U. Einhaus, PhD Thesis, in preparation
[2] ILD Interim Design Report, arXiv:2003.01116 [physics.ins-det]
[3] Particle Data Group, The Review of Particle Physics, Prog. Theor. Exp. Phys. 2020, 083C01 (2020)

The topology of showers

A detailed look into how particles interact with matter

Calorimeters are a fundamental part of modern particle physics experiments. They measure the energy of particles by stopping them, so that the particles deposit their energy in the material of the calorimeter in a large shower. A highly granular calorimeter technology developed by the DESY FTX group allows not only a precise measurement of the particle energy, but also detailed studies of the shape and topology of the showers. This information can be used to distinguish between showers caused by various particle types and to improve the modelling of showers in simulation programs.

The power of granularity

An important information you would like to have about each particle produced in an event at a particle collider is its energy and type. While you can measure the energy of charged particles in tracking detectors, the energy of electrically neutral particles can only be determined by stopping them and measuring the shower of additional particles produced in this process. The devices designed to do that are called calorimeters, and originally accumulated the shower energies deposited in large spatial areas. With increasing requirements on the ability to distinguish between showers of close-by particles and with increasing particle densities, calorimeters are designed with much smaller cell sizes, providing a detailed look into the shape and structure of the showers.

Depending on the type of incoming particle, the showers can look very different: Particles like electrons or photons, which only interact electromagnetically, lead to compact and relatively homogenous showers, while most hadrons (particles consisting of quarks and antiquarks), like kaons or charged pions, produce longer and wider showers that can have a lot of substructure. In general, all electromagnetic showers look very similar, while hadron showers vary a lot. A fraction of the energy in a hadronic shower is also deposited by photons and electrons, leading to electromagnetic subshowers inside hadron showers. A special role is played by muons, which interact very little with the calorimeter material and only leave a track of small energy depositions. These differences between the shower types can be exploited to identify the type of particle that caused them. The finer the granularity of the calorimeter, the more information about the shower topology is available.

The CALICE collaboration is developing several concepts for high-granularity calorimeters. One of them, based on small scintillator tiles read out individually by silicon photomultipliers, is being devised at DESY in a strong international team with many partner institutes. The team has built a large calorimeter prototype consisting of about 22 000 channels of 3 x 3 cm^2 scintillator tiles, grouped in 38 layers within a steel absorber structure of about four interaction lengths. The prototype was tested in beams of electrons, muons and charged pions at DESY and CERN. The data of nearly 100 million events recorded in these tests are now used to study the shower shapes.

Shower shapes and subshowers

By studying the development of a hadron shower along the direction of the incoming particle (Fig. 1), the core containing electromagnetic subshowers within the hadron shower can be made visible: While moderate-energy depositions stretch over a long range deep into the calorimeter, the high-energy

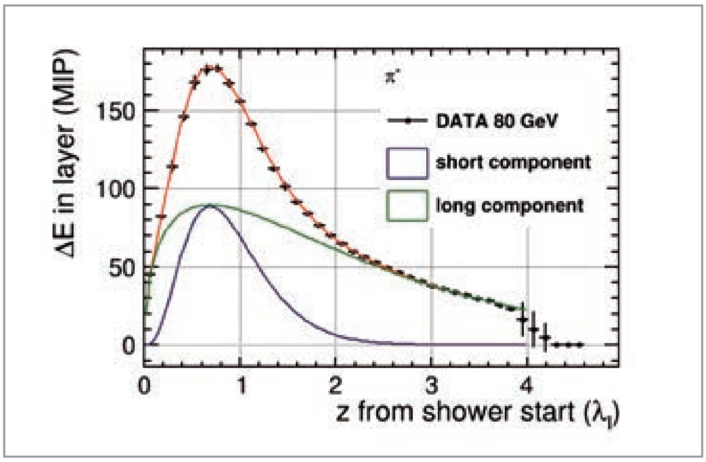

Figure 1

Longitudinal development of pion showers of 80 GeV. The long (green) and short (blue) components are determined by a fit.

depositions caused by the electromagnetic core are only observed in a short range close to the starting point of the shower.

The precise determination of the starting point and the detailed studies of the shower shape in longitudinal and transverse direction are only possible thanks to the high granularity of the prototype. Their comparison with simulations based on various models of the interaction of hadrons with the calorimeter material can help to improve these interaction models.

Particle identification

The differences between the various shower types were used to develop an algorithm to identify the type of the incident particle. Several variables related to the size, density and structure of the shower served as input to train a boosted decision tree (BDT). A very good separation of typically 99% efficiency of correctly identifying a charged pion was reached, with a mis-identification probability of 0.3% for electrons and 0.2% for muons. The results of this BDT were then used to identify contamination by non-wanted particle species in the beam tests and reject the corresponding events.

The distribution of the energy sum measured in an 80 GeV run enriched with electrons is shown in Fig. 2. As indicated by the coloured histograms, about 15% of the events are not caused by electrons, and their rejection is crucial to determine the energy resolution of the calorimeter for electrons.

Particle separation

In order to reach the best measurement of the energy of jets – bundles of close-by particles produced in high-energy particle collisions – the detector part with the best energy resolution should be used for each particle. For charged particles, this is typically a tracking detector, while electrically neutral particles can only be measured in a calorimeter. This means that, usually, the energy depositions in showers caused by charged particles in the calorimeter need to be identified and ignored, a task performed by particle flow algorithms (PFAs). This task becomes more difficult the closer the showers of charged and neutral particles are.

Events recorded in the beam tests of the calorimeter prototype have been overlaid and are used to test the ability of PandoraPFA [1] to correctly assign the energy depositions to the showers. An example of two overlaid showers is shown in Fig. 3.

What else?

The detailed information about the shower topologies offers a wide range of further applications. Energy depositions in the shower core can be taken into account with a different weight in the energy reconstruction of hadron showers to improve the resolution. Tracks within hadron showers can be used as abundant source of reference signals for detector calibration. In environments with large pile-up, like at the High-Luminosity LHC (HL-LHC), the energy depositions from pile-up particles can be identified and rejected already in the clustering algorithm used to reconstruct the showers. And, last but not least, the huge amount of information is an ideal field of application for machine learning algorithms to optimally exploit the available information for the extraction of physical quantities.

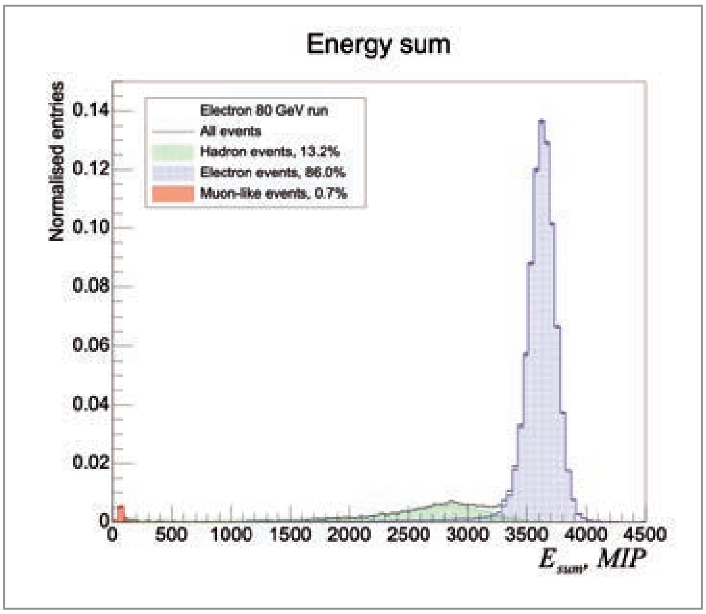

Figure 2

Energy deposition of events in an 80 GeV “electron run”. The distributions for the particle species determined by the BDT are indicated by the coloured histograms.

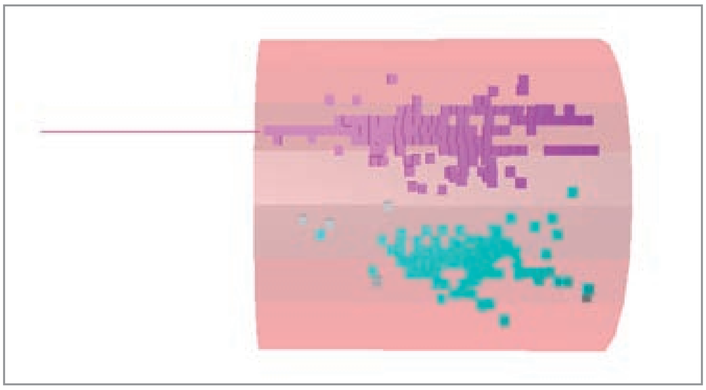

Figure 3

Event display of two overlaid showers and their assignment by PandoraPFA to the charged (magenta) and neutral (cyan) hadron shower

Contact:

Katja Krüger, katja.krueger@desy.de

Felix Sefkow, felix.sefkow@desy.de

Reference:

[1] M. Thomson, Particle Flow Calorimetry and the PandoraPFA Algorithm, Nucl. Instrum. Meth. A611, 25 (2009)

Record-breaking collisions

SuperKEKB collider achieves the world's highest luminosity

Despite the restrictions imposed by the COVID-19 pandemic, the operation of the SuperKEKB collider and the Belle II experiment at KEK in Japan in 2020 was very successful. In June, the team of SuperKEKB accelerator physicists achieved a new world record in instantaneous luminosity. By the end of the year, the Belle II collaboration had accumulated data corresponding to an integrated luminosity of almost 90 fb^{-1}. Thanks to the good performance of the detector, a number of very interesting physics results can be expected from this data set. Preliminary results based on part of these data were presented at the ICHEP2020 summer conference.

SuperKEKB operation

Since SuperKEKB produced its first electron–positron collisions in April 2018, KEK has been steadily improving the performance of its flagship collider. On 15 June 2020, SuperKEKB achieved the world's highest instantaneous luminosity for a colliding-beam accelerator, setting a record of 2.22×10^{34} $cm^{-2}s^{-1}$ (Fig. 1). Previously, the KEKB collider, SuperKEKB's predecessor, which was operated by KEK from 1999 to 2010, had already achieved the world's highest luminosity, reaching 2.11×10^{34} $cm^{-2}s^{-1}$. KEKB's record was surpassed in 2018, when the LHC proton–proton collider at CERN overtook the KEKB luminosity at 2.14×10^{34} $cm^{-2}s^{-1}$. The recent achievement returns the title of the world's highest-luminosity colliding-beam accelerator to KEK (the current record is 2.40×10^{34} $cm^{-2}s^{-1}$, obtained on 21 June 2020). It should be noted that the new luminosity record was achieved with a product of beam currents that was less than 25% that of KEKB, demonstrating the superiority and the potential of the SuperKEKB design.

Accelerator operation after the summer break was somewhat plagued by high background and low injection efficiency, the occurrence of beam instabilities due to high impedance of collimators as well as stronger than expected beam–beam effects at high bunch currents. As a result, the weekly integrated luminosity was noticeably lower than in the spring (Fig. 2). To alleviate the impedance problem, one of the collimators in the low-energy ring was replaced during the winter shutdown 2020/21.

Eventually, the ambitious goal of Belle II is to increase the integrated luminosity by a factor of 50 compared to the predecessor experiment Belle. This will require an even higher instantaneous luminosity, which is to be achieved mainly by further exploiting the potential of the beam collision method called the "nanobeam scheme". SuperKEKB is the first collider in the world at which this scheme, which promises a large increase in luminosity by squeezing the beams even harder, is realised. Currently, the vertical height of the beams at the collision point is about 220 nm, which will decrease to approximately 50 nm (about 1/1000 the width of a human hair) in the future.

However, the experience gained in the first years of SuperKEKB operation also revealed a number of challenges connected to this novel mode of operation. Accelerator experts at KEK are currently investigating ways to modify the very complicated final focus system so that the required peak luminosity can be achieved while maintaining tolerable beam lifetimes. The implementation of such modifications might require a longer shutdown in the second half of this decade.

Belle II data taking

Operating the experiment under the restrictions imposed by the COVID-19 pandemic was a particular challenge for the international Belle II collaboration. Protocols had to be

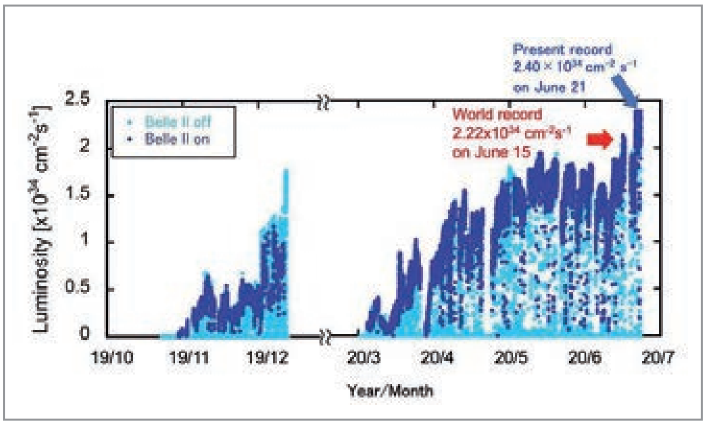

Figure 1

Development of the SuperKEKB peak luminosity in autumn 2019 and in the first half of 2020 developed to maximise safety and minimise the risk of infection. While safety-related activities inevitably had to be carried out by a relatively small pool of staff on site, a large part of the detector operations was conducted remotely by members of the collaboration from their home institutions. Despite these difficulties, the data taking efficiency of Belle II could be raised to about 89%, very close to the goal of 90% or more. By the end of 2020, Belle II had accumulated a total data sample corresponding to an integrated luminosity of almost 90 fb^{-1} (Fig. 2). The early part of these data formed the basis for a variety of results presented at the ICHEP2020 summer conference [2], including several “rediscoveries” of signals seen at previous B factories.

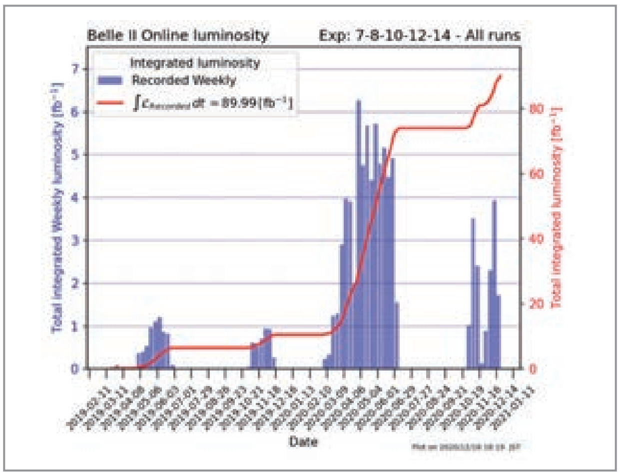

Figure 2

Total integrated weekly luminosity recorded by Belle II. By the end of 2020, the total integrated Belle II luminosity amounted to almost 90 fb^{-1}.

An example is given in Fig. 3, which shows a measurement of the D^0 lifetime reconstructed in the decay channel $D^* \rightarrow D^0 \pi_s$, $D^0 \rightarrow K\pi$ based on 9.6 fb^{-1} of the 2019 Belle II data set. The combined result from this and other decay channels is 412.3 ± 2.0 fs [3], which agrees very well with the world average of 410.1 ± 1.5 fs.

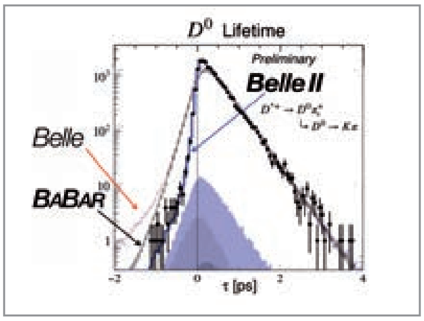

Figure 3

D^0 lifetime reconstructed in the decay $D^0 \rightarrow K\pi$ based on 9.6 fb^{-1} data collected by Belle II and compared to results obtained by the previous experiments Belle and BaBar

Correctly reconstructed decays should result in positive values of the measured lifetime ($\tau > 0$). Conversely, the width of the distribution for $\tau < 0$ is a measure of the resolution of the reconstructed vertex position. In Fig. 3, the Belle II results are compared to the corresponding distributions obtained by the previous experiments Belle and BaBar. The much steeper fall-off of the Belle II data for unphysical, negative lifetimes indicates that the vertex resolution of Belle II is approximately a factor of 2 better than at the previous experiments. This proves the successful concept of the Belle II vertex detector, with a greatly improved position resolution in the pixel vertex detector (PXD) in combination with a reduced beam pipe diameter.

It should be noted, however, that, in the presently operating PXD, only the inner of the foreseen two sensor layers is fully installed. This is expected to result in a degradation of the vertex resolution once luminosity and background levels increase towards the design values. This is the reason why, in parallel to operating and optimising the performance of the installed detector, the PXD collaboration is currently making significant efforts to construct a two-layered replacement detector (PXD2). The presently operating detector is scheduled to be replaced with the new PXD2 in a long shutdown in 2022.

Data processing and calibration

The anticipated rapid increase in the amount of recorded data calls for a modification of the data processing and calibration workflow. The Belle II computing model foresees the permanent storage of raw data and the initial processing for prompt calibration at KEK. A second copy of the raw data is then transferred outside KEK. Until 2020, Brookhaven National Laboratory (BNL) in the USA provided resources for the second data copy and for a half-yearly recalibration of all the data. For precision physics analyses, the latter step is essential in order to optimally profit from the improved level of detector understanding. From 2021 onward, this second data copy will be distributed to six so-called raw data centres worldwide. As one of them, DESY will store raw data in its tape library that will add up to 200 TB in 2021 and ramp up to 1.3 PB by 2024. Readiness and capacity for this large-scale data transfer were confirmed during a data challenge in 2020, in which the available bandwidth as well as tape migration and staging procedures were thoroughly tested and verified.

In 2021, the prompt calibration task will move from KEK to BNL, while DESY will take over the role as Belle II recalibration centre from BNL. This recalibration task, which requires 300 TB of disk space with a multiple-sized tape back-end, will have to be run every six months. The necessary computing power of ~20 kHS06 will be delivered by HTcondor-based batch farms. In fall 2020, DESY IT experts began to set up the system and performed first tests in order to be ready once data taking will resume at the beginning of 2021.

Contact:

Carsten Niebuhr, carsten.niebuhr@desy.de
Andreas Gellrich, andreas.gellrich@desy.de

References:

[1] https://www.kek.jp/en/newsroom/2020/06/26/1400/
[2] https://confluence.desy.de/display/BI/Belle+II+physics+results+presented+at+ICHEP+2020
[3] BELLE2-NOTE-PL-2020-008

Search for axion-like particles produced at Belle II

One of the first Belle II papers sets world-leading limits for ALPs

DESY scientists analysed the very first Belle II data, taken in 2018, to set world-leading limits on the coupling of axion-like particles to photons. The result, which is based on only 0.001% of the final Belle II data set, was published in 2020. The analysis was previously identified as a high-priority target for Belle II by a team including DESY theorists.

Axion-like particles at colliders

Axions and axion-like particles (ALPs) are predicted by many extensions of the Standard Model (SM). In 2017, a team of researchers including DESY theorists laid the groundwork for this analysis: They realised that a large parameter space for GeV ALPs with photon couplings is not constrained by any existing experiments, but can be studied with rather small data sets at *B* factories [1]. The search for ALPs also features as a high-priority target in the Belle II physics book [2].

Neutral final states at Belle II

The Belle II experiment is located at the asymmetric electron–positron collider SuperKEKB at KEK in Japan. The experiment started official physics data taking in 2019. However, for this analysis [3], the DESY Belle II group used a data set that was taken before, during a short calibration run at the Υ(4S) resonance (10.58 GeV) from April to July 2018. This data set corresponds to an integrated luminosity of only 0.45 fb^{-1}, less than 0.001% of the expected final data set of 50 ab^{-1}.

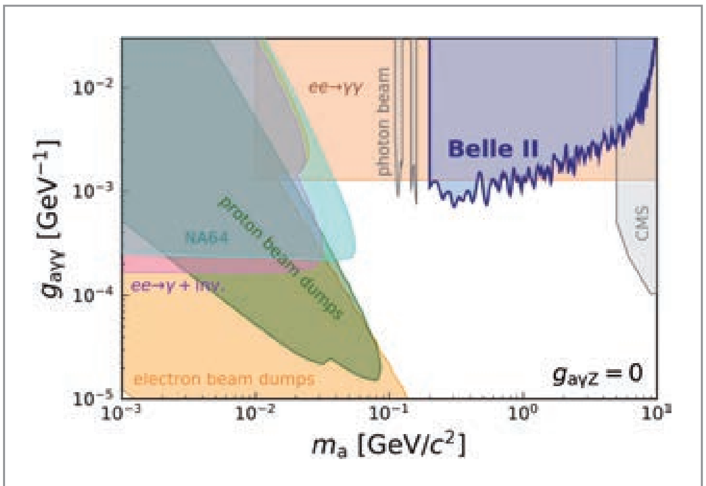

Figure 1

Upper limit (95% CL) on the ALP–photon coupling from this analysis and previous constraints from other experiments. Figure taken from [3].

The rather low background environment and the very efficient thallium-doped caesium iodide (CsI(Tl)) calorimeter with excellent energy and time resolution made it possible to search for the fully neutral final state $e^+e^- \to \gamma a$, $a \to \gamma\gamma$ in the ALP mass range $0.2 < m_a < 9.7$ GeV/c^2. The signature is a monoenergetic photon recoiling against the $a \to \gamma\gamma$ decay. Backgrounds for this analysis are dominated by the quantum electrodynamics (QED) process $e^+e^- \to \gamma\gamma\gamma$. Background contributions from SM pseudoscalars (e.g. η mesons) or $e^+e^- \to e^+e^-\gamma$ where both electron tracks are missed by the tracking system are much smaller.

The data are compatible with no excess over the locally smooth background in the whole probed mass range. The DESY team has set a world-leading upper limit on the ALP–photon coupling $g_{a\gamma\gamma}$ at the level of 10^{-3} GeV^{-1} (Fig. 1). In the future, with increased luminosity, Belle II is expected to improve the sensitivity to $g_{a\gamma\gamma}$ by at least one order of magnitude. The next step will be to search for even lighter ALPs at Belle II by improving the cluster separation at the hardware trigger level: The two decay photons from very light ALPs are highly boosted and only reconstructed as a single cluster in the calorimeter. This final state looks like the very high-rate SM process $e^+e^- \to \gamma\gamma$, which will typically be rejected by the Belle II trigger system.

Contact:

Torben Ferber, torben.ferber@desy.de
Michael De Nuccio, michael.de.nuccio@desy.de

References:

[1] M. Dolan, T. Ferber, C. Hearty, F. Kahlhoefer, K. Schmidt Hoberg, JHEP 12, 094 (2017)
[2] Belle II Collaboration and theory collaborators, Prog. Theor. Exp. Phys., 123C01 (2019)
[3] Belle II Collaboration, Phys. Rev. Lett. 125, 161806 (2020)

Any light particle searches

Magnets all over and more physics to find

Experiments at DESY looking for weakly interacting slim particles have advanced significantly, with ALPS II aiming for a first data run in 2021. Activities towards a cryo platform in the HERA North hall and studies for future experiments are gaining speed.

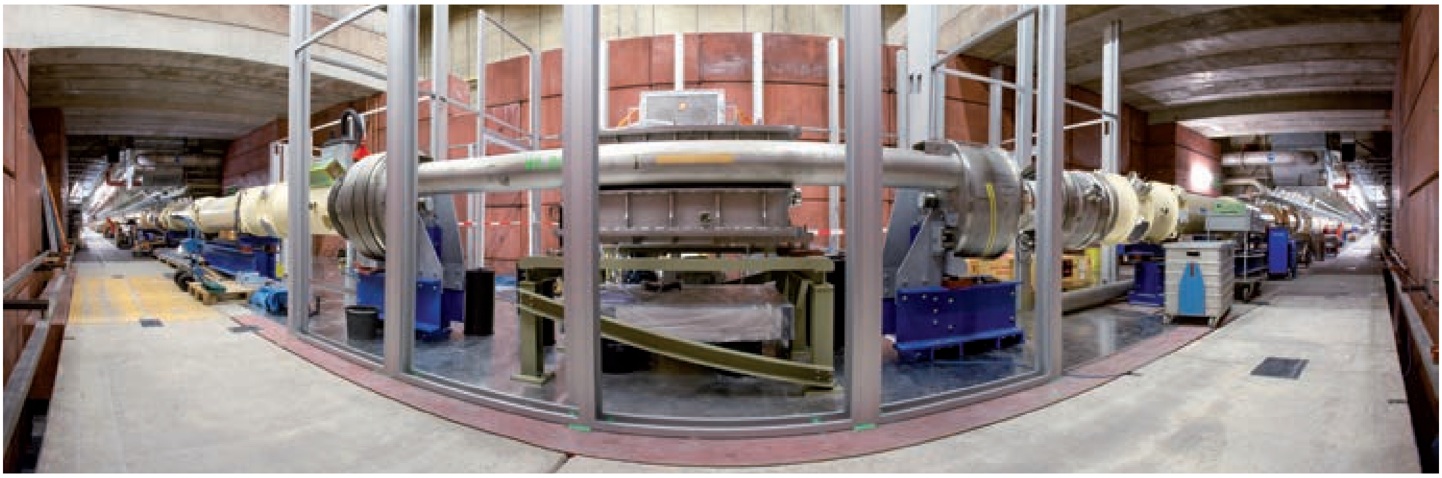

Figure 1

The panorama shows the central area of ALPS II with the big vacuum chamber for housing the light-tight wall and the complex optics to mode-match the optical cavities.

En route beyond the Standard Model

Weakly interacting slim particles (WISPs), with the axion as its most famous representative, may explain puzzling questions such as the conservation of CP symmetry in quantum chromodynamics, riddles concerning the evolution of stars and the dark components of our universe.

However, such WISPs are predicted to interact with the known constituents of nature only very feebly, so that experiments probing their existence cannot be performed at accelerators. Instead, the three WISP experiments under preparation at DESY by international collaborations will exploit the conversion of photons into WISPs and vice versa, which might take place in a magnetic field.

In 2020, significant progress of these experiments was achieved, especially regarding their magnets.

Any Light Particle Search II

The “light shining through the wall” experiment ALPS II is under construction in the North area of DESY’s former HERA accelerator complex. In the first part of this experiment, WISPs might be generated by light shining into a strong magnetic dipole field. The second compartment is shielded by a light-tight barrier, which does not pose any hindrance for WISPs, however. WISPs entering this area might convert back to photons, giving the impression of light shining through a wall. Thus, ALPS II will look for WISPs in a model-independent fashion.

Compared to previous similar experiments, ALPS II would improve the signal-to-noise ratio for a hypothetical WISP discovery by 12 orders of magnitude. This will be achieved by means of two mode-matched long-baseline and high-finesse optical cavities on both sides of the light-tight wall, dedicated extremely sensitive photon detection methods and a string of 24 modified superconducting HERA dipole magnets. Much progress was made in all these areas, with the completion of the magnet installation in the HERA tunnel being the most visible result in 2020 (Fig. 1).

The HERA dipole magnets were originally produced with a bent beam tube, as they guided the proton beam through the arcs of HERA. Unfortunately, the remaining horizontal aperture would have clipped the light mode resonating in the

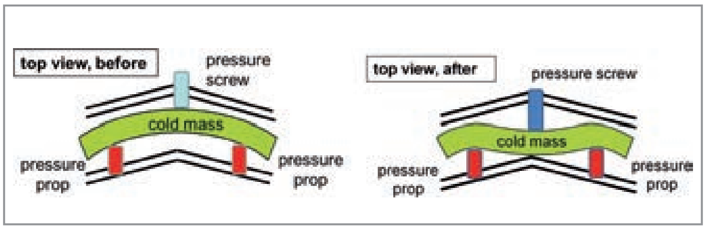

Figure 2

Scheme for straightening the beam tube of the HERA dipole magnets. The props were constructed so as to stay in place when cooling down the dipole; the screw will be replaced by a third prop. The suspensions for the cold mass (not shown) also had to be redesigned.

optical cavities and spoiled the sensitivity of ALPS II. Therefore, a brute-force straightening procedure was developed and successfully applied to 26 dipole magnets, enlarging the aperture from about 35 mm to 50 mm. The procedure and the results are summarised in [1]. Figure 2 gives an impression of the method.

In October 2019, the first of these modified magnets was installed in the HERA North hall. Twelve months later, the last magnet was put into place in the magnet string. Figure 1 shows the status of the experiment in late October 2020.

In addition, great progress was achieved on the other infrastructure items, such as cleanroom construction, installation of cryogenic piping, implementation of safety measures and cabling for the experiment. Installation of the optics was scheduled to start in early January 2021, but was delayed due to the pandemic-related shutdown of the DESY activities. If the shutdown ends in March 2021, it will still be feasible to finish the construction and commissioning of ALPS II by the end of 2021.

Encouraging progress was also made regarding the superconducting transition edge sensor (TES) detection system planned to be used for photon detection at ALPS II during a later data run. In contrast to the heterodyne detection scheme for the first science runs, the TES will allow for single-photon counting. In 2020, a very low intrinsic background rate of a few 10^{-6} counts per second could be demonstrated, fulfilling the ALPS II specifications. In future, these detector developments will be significantly strengthened with the help of funding by the STFC (UK) within the framework of a new project on "quantum-enhanced interferometry for new physics".

International Axion Observatory

The IAXO experiment is planned to search for axions and other WISPs emitted by the sun with a signal-to-noise ratio improvement by more than four orders of magnitude compared to previous similar helioscopes. It will consist of a purpose-built large-scale superconducting magnet, X-ray optics, beamlines and detectors, all mounted on a large support and drive structure in order to ensure precise pointing towards the sun.

A prototype, BabyIAXO, is presently in preparation. The conceptual design of BabyIAXO was recently published [2]. BabyIAXO will not only allow for testing of all crucial components for IAXO, but will also probe new WISP parameter regions with signal-to-noise ratios two orders of magnitude beyond present experiments. The magnet will consist of two instead of eight superconducting coils of 10 m length, 700 mm diameter bores and two sets of optics, beamlines and detectors. The project was approved by the DESY management to be hosted at DESY, which offers an ideal environment as part of its emerging axion experimental programme.

Significant progress was made in 2020. The positioner of the mid-sized telescope prototype for the CTA gamma-ray observatory in Berlin was disassembled and transported to DESY in Hamburg in February, to be reused for BabyIAXO (Fig. 3).

Figure 3

The positioner of the CTA mid-sized telescope prototype arrives In the HERA South hall.

Figure 4 shows the layout of BabyIAXO. The mechanical design of the large support frame as well as the required modifications are well advanced. The magnet design devised by the CERN ATLAS magnet group is close to being finished. A dedicated magnet review, organised by the DESY Physics Research Committee (PRC), was held in November 2020. Samples of the conductor, an in-kind contribution of the Institute of Nuclear Research in Russia, are being tested at the University of Twente in the Netherlands. One of the two X-ray optics is a flight spare module on the XMM-Newton satellite, lent to the collaboration by ESA. The second optics will be built by collaborating institutes. The baseline detector will be a small time projection chamber with Micromegas readout, already successfully used for the CAST helioscope at CERN. Several other detector types are being developed within the collaboration. The management structure was enhanced, including the project office and technical coordination located at DESY.

Magnetized Disk and Mirror Axion eXperiment

MADMAX is a complex haloscope to search for dark-matter axions in the mass range preferred by specific (likely) cosmological scenarios and not accessible by any experiment taking data or under construction at present. In preparation of the final setup with 80 disks of 1.25 m diameter, the planning for a smaller prototype was the main focus of the collaboration in 2020.

The prototype setup will be used to test critical components, such as piezo motors for disk positioning as well as the disk cooling system itself, in a cryogenic and magnetic environment. The procurement phase of the cryogenic prototype vessel, hosting the system of disks, mirror and antenna as the heart of the experiment, is well prepared and will start soon. The prototype might also be able to produce first competitive limits for WISPs in the mass range around 100 µeV by using the 1.6 T Morpurgo dipole magnet at CERN. The experiment was therefore presented to the CERN SPS and PS Experiments Committee (SPSC), which issued a strong recommendation for access to Morpurgo.

In parallel to activities on the prototype, work on the final experiment is ongoing. A MADMAX magnet test coil (called MACQU) for the investigation of cable quench behaviour, using a similar cable-in-conduit (CIC) conductor as proposed for the final magnet, was designed and built in 2020. It will be tested in early 2021. This test will significantly influence the specification for the final superconducting magnet cable design. Figure 5 shows the MACQU equipped with some sensors for the quench tests.

The progress of the final experiment was presented to the DESY PRC in November 2020, and the committee stated that "MADMAX will dominate the axion dark-matter field for more than a decade". A status report is available at [3].

MADMAX will be an experiment using the cryo platform in the HERA North hall, which is presently under construction as a Helmholtz contribution to the cluster of excellence "Quantum Universe" of Universität Hamburg and DESY.

Cryo platform in HERA North

The new cryo platform at DESY is an expansion of the cryogenic infrastructure for ALPS II in the HERA North hall, which is currently being developed with the goal to supply up to three experiments with cold helium. It will be a central building block for realising activities planned within the cluster of excellence "Quantum Universe", such as the MADMAX experiment and the development of cryogenic mirrors for future gravitational-wave detectors. At the heart of the cryo platform will be a new valve box with a built-in subcooler. Preparations to create a technical specification for this "distribution box" are currently under way.

Cryogenic mirrors are of prime importance for future gravitational-wave interferometers. The first detection of gravitational waves in 2015 has opened a new window onto the universe. To exploit this new resource for precision astronomy, a new generation of laser-interferometric gravitational-wave observatories with unprecedented sensitivity is currently being developed. The mirrors constituting the interferometers in future observatories will be cryogenically cooled to suppress their temperature-induced fluctuating motion. Cooling the mirrors to a target temperature of ~20 K, without introducing detrimental vibrations from the cooling apparatus, presents a major technological challenge.

As part of the cluster of excellence "Quantum Universe" and in collaboration with Universität Hamburg, novel concepts for the gas cooling of test mass mirrors for future gravitational-wave observatories are being developed. A corresponding proposal has been published [4].

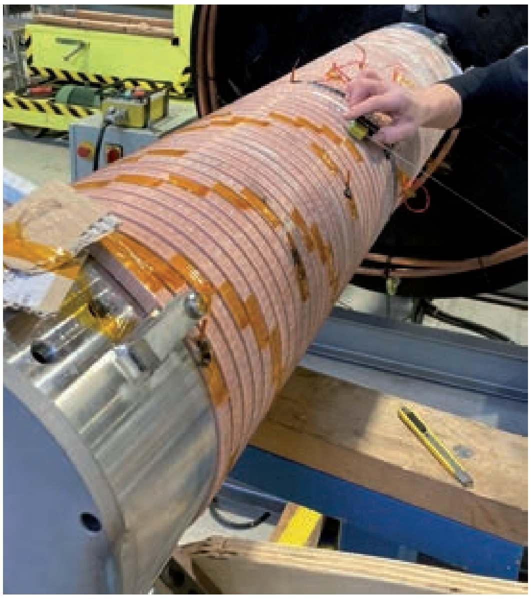

Figure 5
MACQU test setup for the MADMAX magnet cable at the company Bilfinger-Noell

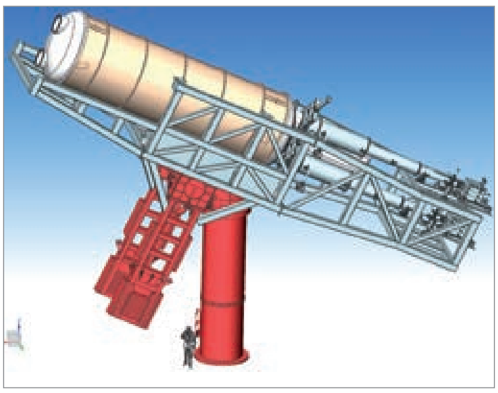

Figure 4
Design of the BabyIAXO experiment. The positioner (in red) was previously used for the CTA mid-sized telescope prototype in Berlin.

Contact:

Axel Lindner, axel.lindner@desy.de (ALPS II)
Uwe Schneekloth, uwe.schneekloth@desy.de (BabyIAXO)
Jörn Schaffran, joern.schaffran@desy.de (MADMAX)
Christoph Reinhardt, christoph.reinhardt@desy.de (cryo platform)

References:

[1] Straightening of superconducting HERA dipoles for the any-light-particle-search experiment ALPS II, EPJ Techn. Instrum. 8, 5 (2021)
[2] Conceptual Design of BabyIAXO, the intermediate stage towards the International Axion Observatory, arXiv:2010.12076 [physics.ins-det], submitted to JHEP
[3] MADMAX status report, arXiv:2003.10894 [physics.ins-det]
[4] Gas cooling of test masses for future gravitational-wave observatories, arXiv:2101.09164 [physics.ins-det], submitted to Class. Quantum Grav.

Theoretical particle physics

The DESY theory group covers a broad range of topics – from particle phenomenology and lattice gauge theory to cosmology and string theory. This scientific breadth is a unique asset of the group and of DESY, as it provides a setting for many fruitful interactions.

In particle phenomenology, results from the Large Hadron Collider (LHC) at CERN are at the centre of current activities. This includes a better understanding of the strong force (p. 50), which is indispensible for the interpretation of collider data. At DESY in Zeuthen, the lattice and particle phenomenology groups merged into the Zeuthen Particle Physics Theory group, sparking a new common research interest: quantum computing (p. 56).

Moreover, theoretical efforts in cosmology yielded much progress in our understanding of dark and visible matter. Recent developments underline the aspect of probing light dark matter with neutrino experiments (p. 54).

The third core activity of the group is string theory. The ultimate goal of these studies is to improve our understanding of the theories relevant for particle phenomenology, in particular theories at strong coupling. One promising avenue hereby is to constrain theories using so-called anomalies (p. 52).

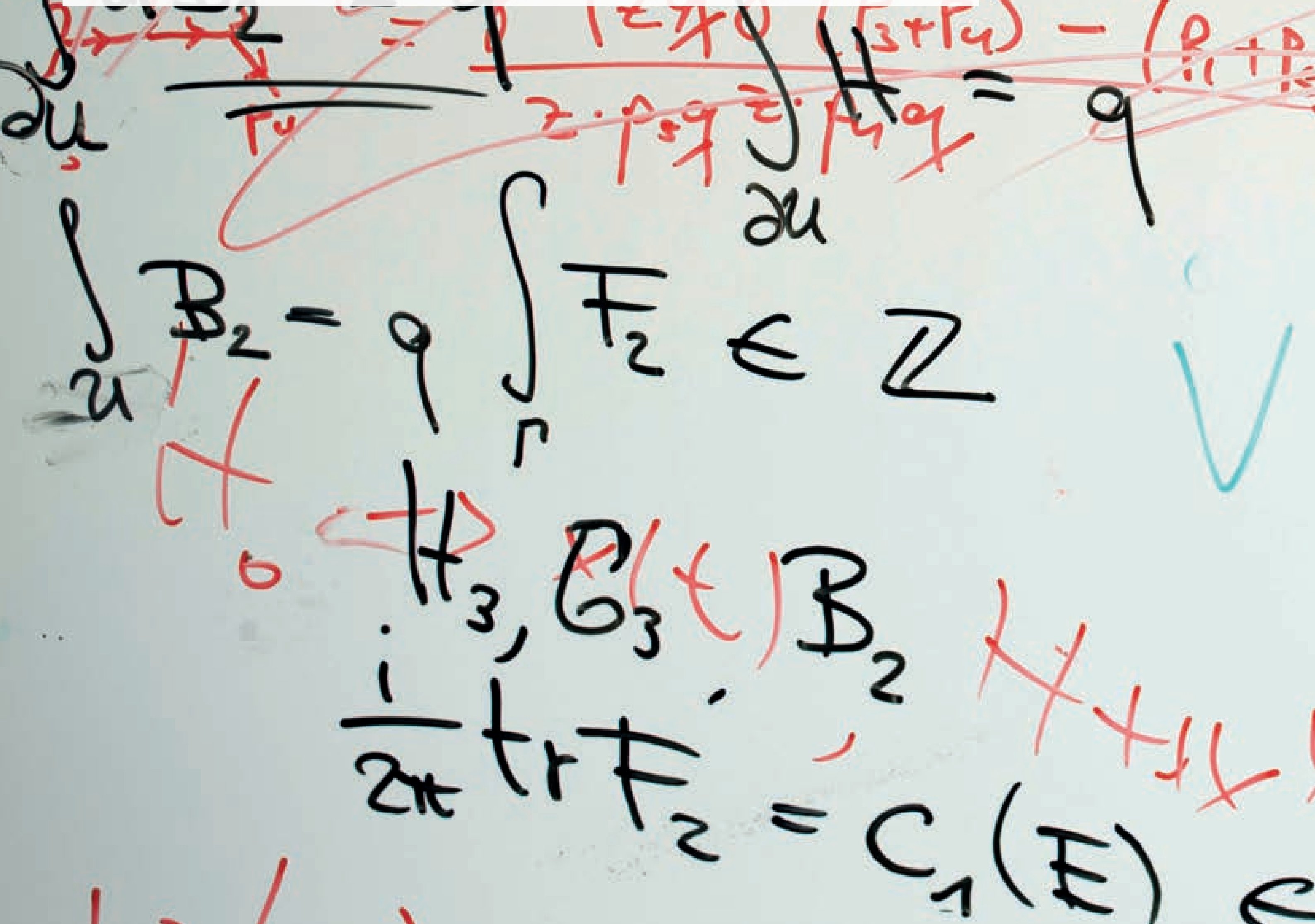


ISD
AISD

Simulating QCD with parton showers

Managing colours and large logarithms

The LHC collides hadrons, i.e. bound states of quarks and gluons. Therefore, every analysis, whether a measurement or a search for new physics, needs an understanding of quantum chromodynamics (QCD). Broadly speaking, there are three principal methods of making QCD predictions in the perturbative framework: approximating the interaction cross sections by summing large logarithms analytically, calculating at fixed-order level and using parton showers. The parton shower algorithms, which have been studied intensively at DESY in recent years, are an essential theoretical tool in any collider experiment. This raises the questions of how well we understand parton showers in the perturbative framework and how well the accuracy of their predictions can be controlled.

In the fixed-order calculation, the cross section is expanded in powers of the strong coupling and truncated at leading-, next-to-leading- or higher-order level. Every matrix element has to be calculated exactly, which is a tremendous work for amplitudes with many legs and loops. Since in these calculations hadronic jets are represented by one or two partons, the predictions are reliable only for very inclusive observables, where the typical resolution scale of the measurement is close to the scale of the hard process. Away from this safe region, we have to deal with large logarithms. The main advantage of the fixed-order calculations is that they can be implemented in an observable-independent way.

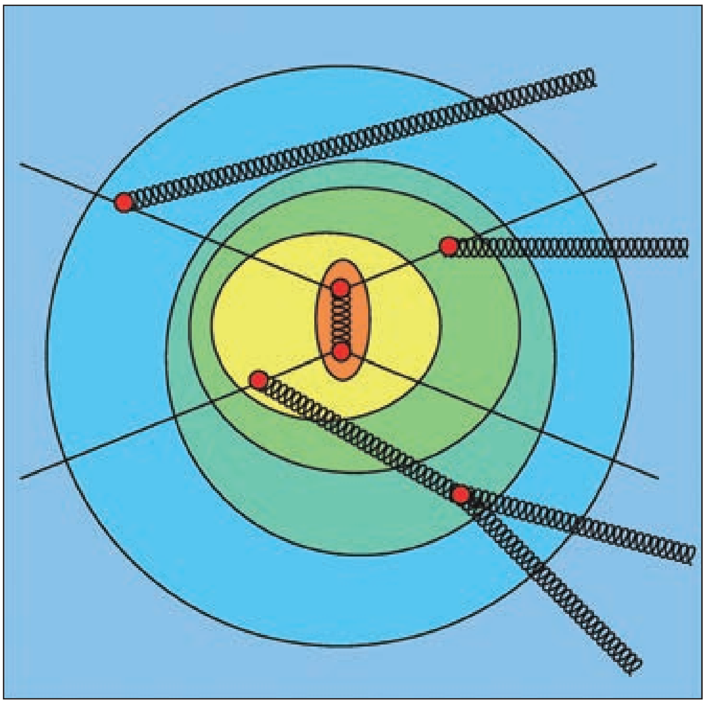

Figure 1

Sketch of parton shower evolution in real time. The interaction in the middle has the hardest scale (i.e. the largest momentum and energy transfer) and happens at short distance. Softer and more collinear emissions happen more and more "in the past" on the initial-state partons and more and more "in the future" on the final-state partons.

Fortunately, for simple and well-behaved observables, these logarithms can be summed up analytically at all perturbative orders. The procedure relies on the factorisation property of the cross section. The cross section factorises into a product of observable-dependent soft and collinear functions and a process-dependent hard function. Solving the corresponding renormalisation group equations (RGEs), we can sum up the soft and collinear logarithms.

The parton shower calculation tries to combine the strength of the fixed-order computation and the analytical summation. While, in the analytical calculation, we try to sum up the large logarithms of the observable at cross section level, in the parton shower calculation, we manage to sum up the real and virtual partonic emissions so as to produce final states containing many partons. To obtain the cross section, we apply the desired measurement to these final states. The algorithm is independent of the observable, just like in the fixed-order calculations.

The idea of parton shower algorithms as a phenomenological model of QCD cross section was invented in the mid-1980s. It was motivated by the factorisation property of the cross section, in which a single radiation becomes soft or collinear. This parton splitting picture was implemented in a classical probabilistic framework (Fig. 1). It has always been a question

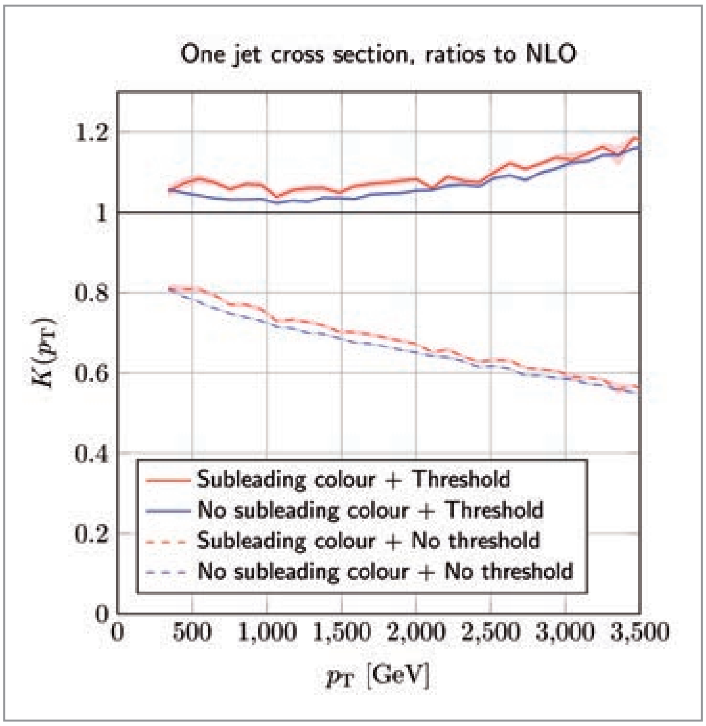

Figure 2

Transverse momentum distribution of single-jet production at the LHC. The difference between the red and blue lines shows the effect of the subleading colour contributions, and the differences between the corresponding solid and dashed lines demonstrate the effect of the threshold logarithms. The differences between the dashed lines and the $K(p_T) = 1$ line illustrate the effect of the visible logarithms (jet cone size in this example).

whether it is possible to give a first-principle definition of parton showers in QCD perturbation theory that leads to this probabilistic parton splitting picture after applying systematic approximations to the general theory. In recent years, members of the DESY theory group have developed such a theory [1] in collaboration with the University of Oregon in the USA.

Any partonic state is fully described by the QCD density operator. The QCD density operator also has a universal factorisation property when one or more, real or virtual, soft or collinear partons are emitted. This allows us to write an RGE for the density operator. Its solution leads to the parton shower evolution operator. The shower evolution operator is an exponential of an operator that acts on the linear space of the QCD density operators.

This is as difficult as it sounds. One source of complication is the QCD colour structure. A typical event at the LHC consists of 20–30 partons on average, which corresponds to a colour space with a dimension on the order of 10^{37}–10^{65}. Clearly, there is no way to diagonalise and exponentiate any operator on such a basis. The soft gluon emissions always introduce non-trivial colour interferences and correlations, while the operators of the collinear emissions are diagonal in colour space. Using the LC+ approximation, we can fully exponentiate the collinear part exactly and treat the wide-angle soft radiation perturbatively in the shower evolution [2]. The error that we make is suppressed by a factor of $1/N_c^2 = 1/9$ and one power of the relevant large logarithm. This algorithm has been implemented in the DESY-OREGON event generator, DEDUCTOR [3]. Figure 2 illustrates the effect of the subleading colour contributions for single-jet production.

From a strict theory point of view, the primary purpose of the parton shower is to sum up the real and virtual radiation systematically, but it is also capable of summing large logarithms consistently. The exponent of the shower evolution operator is still a perturbative series and a subject of truncation in the strong coupling. This obviously leads to an error and can severely damage the logarithmic accuracy of the predictions. Working to higher order, the logarithmic accuracy improves and the result is less sensitive to the shower scheme. At the moment, only leading-order shower implementations are available, thus the parton shower predictions are more sensitive to the choice of scheme. Nowadays, checking and validating different parton shower schemes against known analytical results is a very active field of research.

At the LHC, the cross sections can suffer from two types of large logarithms, the logarithms in the parameters of the observable (visible logarithms) and the so-called threshold logarithms (invisible logarithms). The effects of these logarithms are illustrated in Fig. 2. Even in such a simple process, we can see that both logarithms have a sizeable contribution and that their effects tend to cancel each other.

Contact:

Zoltán Nagy, zoltan.nagy@desy.de

References:

[1] Z. Nagy and D. E. Soper, Phys. Rev. D 98, 014034 (2018)
[2] Z. Nagy and D. E. Soper, Phys. Rev. D 99, 054009 (2019)
[3] https://www.desy.de/~znagy/deductor

Novel results on conformal anomalies

Deriving a matching criterion

Anomalies are well known to theoretical physicists as the simplest example of a non-perturbative result in quantum field theory (QFT). Following Noether's theorem, a classical symmetry leads to a classically conserved current $\partial_\mu J^\mu = 0$, which may be broken at the quantum level $\partial_\mu J^\mu = \mathcal{A}$ due to an anomaly $\mathcal{A}$. The most standard example is that of chiral anomalies, also known as Adler–Bell–Jackiw anomalies. They are known to match across different phases of matter due to 't Hooft's argument, and they have been an indispensable tool for charting the phase space of matter.

Following the modern renormalisation group (RG) approach to QFT, different theories can be obtained from an RG flow that begins at the ultraviolet (UV), where the theory is in a conformal phase (Fig. 1). This conformal field theory (CFT) is a point on the so-called conformal manifold, the moduli space of all possible exactly marginal couplings. Turning on relevant deformations (for example mass terms), we trigger an RG flow that brings us to some infrared (IR) theory, the precise physics of which depends on the UV CFT we started with as well as on the relevant deformation by which we deformed it.

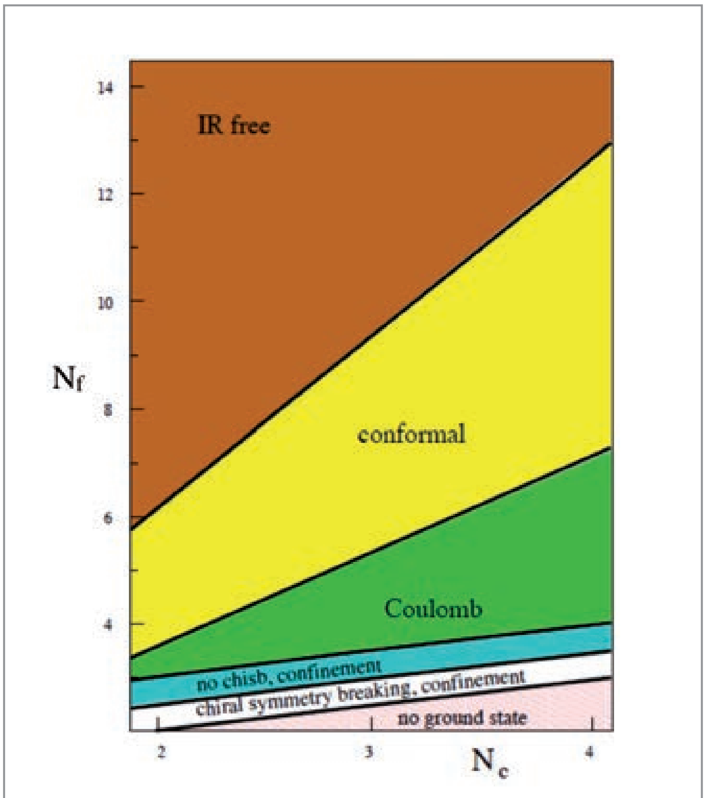

Figure 1

Phase space of supersymmetric QCD derived using chiral anomaly matching

Conformal anomalies

When CFTs are coupled to gravity, the gravitational effective action cannot simultaneously preserve Einstein's general coordinate transformations (diffeomorphisms) and Weyl transformations (local rescalings). There is an anomaly that is manifest in the clash between the conservation of the stress energy tensor $\partial_\mu T^{\mu\nu} = 0$ (due to diffeomorphisms) and its tracelessness $T^{\mu\mu} = 0$ (due to Weyl transformations).

The conservation of the stress energy tensor is usually kept intact at the price of tracelessness, leading to the famous Weyl anomaly [1]. In four dimensions, it contains two contributions, the coefficients of which are known as the *a* and *c* anomaly coefficients. The *a* coefficient is known to match across different phases of matter, with powerful implications for RG flows [2]. However, up to now, similar progress for the *c* coefficient has not been possible.

Conformal anomalies are classified into Type A and B. Type A conformal anomalies do not introduce a scale. They can be expressed in terms of topological invariants, thus they are very similar to the chiral anomalies, and they are known to match across different phases of matter. The *a* coefficient in the Weyl anomaly is an example. Type B conformal anomalies do introduce a scale. They generically depend non-trivially on all couplings, and there is no known reason why they should match in different phases. The c coefficient is an example.

A second class of examples of Type B conformal anomalies is the coefficient of two-point functions of operators with integer scaling dimensions $\Delta = 2 + n$ in the CFT phase

$$\langle \mathcal{O}_I(p)\bar{\mathcal{O}}_J(-p)\rangle \propto G_{I\bar{J}}\ p^{2n} \log\left(\frac{p^2}{\mu^2}\right) \quad .$$

The index I labels the different operators with the same scaling dimensions. Three-point functions of these operators with the stress energy tensor T in the CFT phase contain a term

$$\langle T(p_1)\mathcal{O}_I(p_2)\bar{\mathcal{O}}_J(p_3)\rangle \propto \ldots + G_{I\bar{J}}\ p_2^n\, p_3^n \ ,$$

the coefficient of which is precisely equal to the anomaly, in the CFT phase.

Here, we consider these anomalies in the CFT phase and in the Higgs phase in which the conformal symmetry is spontaneously broken (SSB). Should these Type B anomalies match? In Ref. [3, 4], we presented a comprehensive study using $\mathcal{N} = 2$ supersymmetric CFTs, for which powerful non-perturbative techniques are available.

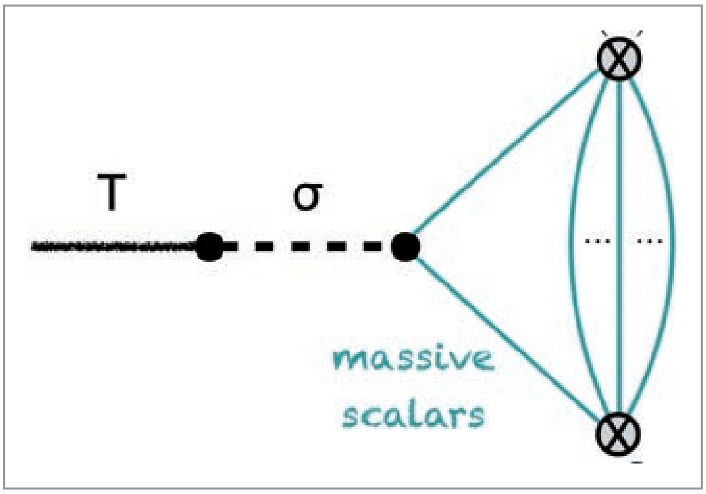

Figure 2

The stress energy tensor T coupling to the dilaton σ and then through the massive scalars to the operators $\mathcal{O}_I(p_2)\bar{\mathcal{O}}_J(p_3)$. The integral is proportional to the massive banana integral.

Type-B anomaly matching criterion

We derived the novel Ward identities $\nabla_k G_{I\bar{J}} = 0$, revealing that the anomaly is covariantly constant on the conformal manifold, both in the CFT and in the Higgsed (SSB) phases. These Ward identities imply that if and only if these anomalies match at one point on the conformal manifold, then they have to match at any point on the conformal manifold. Thus, a weak coupling computation, where perturbation theory is valid, is enough to show full non-perturbative matching!

Working out explicit examples with Feynman diagrams (Fig. 2), we were able to formulate novel conjectures concerning the matching of conformal anomalies.

- When the Higgs phase has no massless modes in the IR, Type B anomalies match along the Higgs-branch RG flow.
- When the Higgs phase has massless modes in the IR, anomalies associated with the IR chiral ring modes do match, but the rest of the Type B anomalies are not expected to match.

In the case of matching, the novel result is an otherwise unattainable non-perturbative result in the Higgs phase. On the other hand, mismatching leads to novel restrictions on the conformal manifold, in the form of indirect constraints stemming from the physics of the Higgs phase. Type B anomaly mismatch implies the existence of a second covariantly constant metric on the conformal manifold, which imposes restrictions on the holonomy group of the conformal manifold.

Contact:

Elli Pomoni, elli.pomoni@desy.de

References:

[1] M. J. Duff, "Twenty years of the Weyl anomaly", Class. Quant. Grav. 11, 1387–1404 (1994)
[2] Z. Komargodski and A. Schwimmer, "On Renormalization Group Flows in Four Dimensions", JHEP 12, 099 (2011)
[3] V. Niarchos, C. Papageorgakis and E. Pomoni, "Type-B Anomaly Matching and the 6D (2,0) Theory", JHEP 04 (2020)
[4] V. Niarchos, C. Papageorgakis, A. Pini and E. Pomoni, "(Mis-)Matching Type-B Anomalies on the Higgs Branch", JHEP 01, 106 (2021)

Light dark matter and neutrino experiments

Neutrino experiments as detectors of sub-GeV dark-matter particles upscattered by cosmic rays

Understanding the nature of dark matter is one of the biggest goals in particle physics and cosmology. An experimental technique called direct detection aims to detect scattering events between dark-matter and target particles inside detectors. This method is most sensitive if the dark-matter mass is on the order of the electroweak scale, while it loses sensitivity for lighter dark matter. Given this situation, a new idea to explore sub-GeV dark matter was proposed at DESY. If dark matter interacts with Standard Model particles, dark-matter particles are inevitably accelerated by cosmic rays, and neutrino experiments are sensitive to this high-energy component of dark matter.

Direct detection of dark matter

Evidence for dark matter (DM) is found in a wide range of scales, from galaxy rotation curves to the cosmic microwave background. Although there is a lot of evidence for DM, these findings are all based on gravitational effects, and the non-gravitational nature of DM is yet to be uncovered.

One conventional DM candidate, the weakly interacting massive particle (WIMP), is related to the hierarchy problem of the Higgs-boson mass, and hence the WIMP mass is typically assumed to be on the electroweak scale, on the order of 100 GeV to 1 TeV. Some information about interactions between DM and Standard Model (SM) particles is obtained by direct detection experiments, which aim at observing the scattering of DM particles off SM targets. This has resulted in a huge experimental effort that, however, has only set strong limits on the DM–SM interactions for DM masses above a few GeV, in the absence of any clear DM detection.

This situation is accompanied by the severe bounds that the LHC is putting on TeV-scale new physics, which cast some doubts on natural solutions to the hierarchy problem. Given this, in recent years the community has vigorously pursued the exploration of lighter DM candidates, in terms of both model building and phenomenological tests.

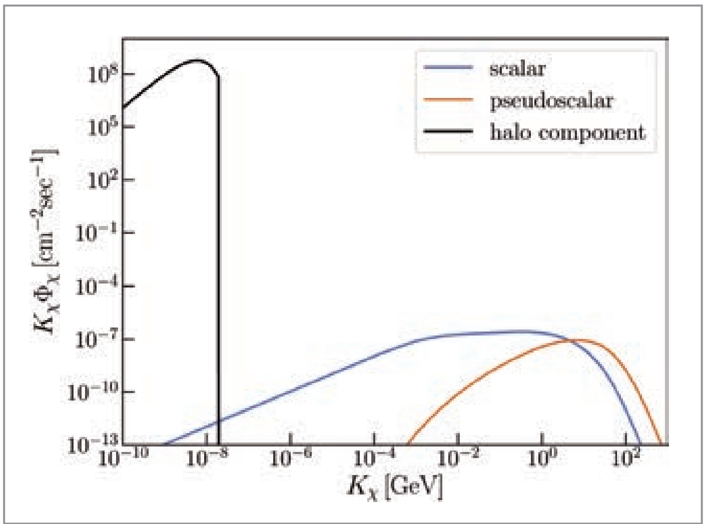

Figure 1

Expected dark-matter flux in the galaxy upscattered by cosmic rays, together with the standard halo component

Light dark matter upscattered by cosmic rays

The search for the interactions of sub-GeV DM candidates is challenged by the low energy thresholds required by direct detection experiments. As DM gets lighter, the recoil energy in direct detection experiments is suppressed both by the smaller DM kinetic energy and by the scattering kinematics (corresponding to the Thomson limit). Indeed, typical nuclear recoil energies lie below the keV scale, the threshold energy of "standard" experiments such as Xenon1T, as DM is lighter than the GeV scale.

In order to overcome this obstacle, a new detection strategy for sub-GeV DM was proposed at DESY [1] (the same idea was simultaneously put forward by a different group [2]). A crucial observation is that, if DM interacts with SM particles, a subdominant component of the DM flux with larger kinetic energy is unavoidably generated by cosmic rays that scatter off DM. Such upscattered light DM can induce visible recoils

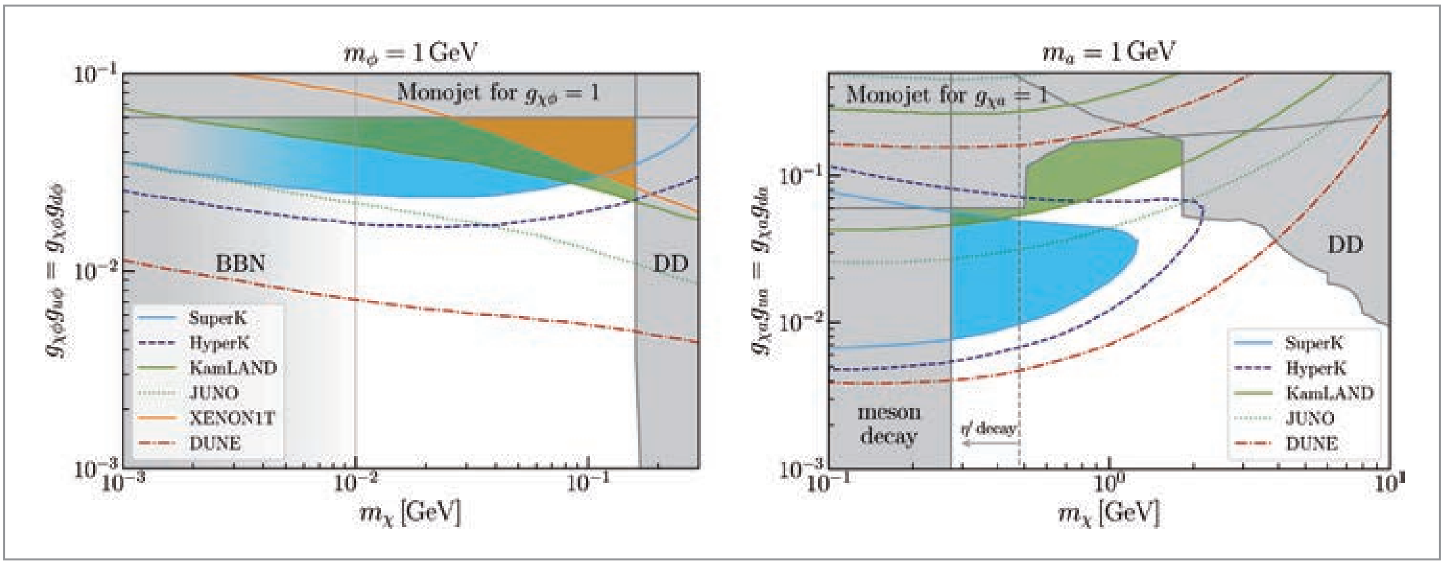

Figure 2

Parameter regions that are constrained by neutrino experiments. Constraints from other experiments are also shown (in grey).

in large-volume detectors, by means of the very same interactions that accelerated it.

An example of the expected DM flux upscattered by cosmic rays is depicted in Fig. 1. Although the overall flux of this high-energy component is quite small compared to the standard halo distribution, its higher kinetic energy makes it easier to probe this component of DM with terrestrial experiments. This is the case especially when DM is light, so that conventional direct detection is less sensitive.

Neutrino experiments as light dark matter detectors

Neutrino experiments such as Super-Kamiokande are usually not sensitive to the standard halo component of DM, since the threshold energy is on the order of MeV, i.e. higher than the typical recoil energy of the standard halo component of DM. Recoil events induced by the high-energy component of the DM flux generated by comic rays, on the other hand, can exceed the threshold energy of neutrino experiments thanks to the higher DM kinetic energy. Therefore, neutrino experiments can be used as a probe of light DM, and one can benefit from their large volumes and long exposure times.

As an example, the parameter regions that are constrained by neutrino experiments such as Super-Kamiokande and KamLAND are shown in Fig. 2 for two benchmark models, with scalar or pseudoscalar mediators that are coupled dominantly to quarks [3]. For comparison, the region constrained by Xenon1T is also shown for the scalar-mediator model. It is clear that this method is sensitive to the new parameter regions that are not yet probed by other experiments. A future prospect of this method is also shown, which demonstrates that future neutrino experiments such as Hyper-Kamiokande, DUNE and JUNO can cover an even larger portion of parameter regions that are yet to be explored.

A possibility of using this method not just to constrain, but to discover DM is discussed in [1] as well. In order to discover DM, one has to distinguish events induced by neutrinos from those due to DM particles. This may be enabled by using the directional information of events, as DM events are expected to originate dominantly from the direction of the galactic centre, while neutrino events are not correlated with the galactic centre.

In summary, sub-GeV DM is difficult to probe with the standard direct detection technique. An alternative way of exploring such light DM is to detect the high-energy component of the DM flux that would inevitably be generated by cosmic rays scattering off DM. Neutrino experiments are sensitive to this component and have the ability to be light DM detectors at the same time. Future developments of neutrino experiments will shed further light on the nature of DM, which is awaiting discovery.

Contact:

Yohei Ema, yohei.ema@desy.de

References:

[1] Y. Ema, F. Sala and R. Sato, Phys. Rev. Lett. 122, 181802 (2019)
[2] T. Bringmann and M. Pospelov, Phys. Rev. Lett. 122, 171801 (2019)
[3] Y. Ema, F. Sala and R. Sato, arXiv:2011.01939 [hep-ph]

Zeuthen Particle Physics Theory

Theoretical perturbative and non-perturbative particle physics at DESY in Zeuthen

The Lattice group and the Collider Phenomenology group at DESY in Zeuthen have merged to form the new Zeuthen Particle Physics Theory (ZPPT) group. This article presents an outlook on an interesting new field addressed by the ZPPT group, quantum computing, and shows how perturbative methods developed for the realm of particle physics have been used to advance the field of gravitational waves.

Zeuthen Particle Physics Theory

The newly founded ZPPT group merges the Collider Phenomenology group (CPG) and the Lattice group at DESY in Zeuthen, the latter also being a research group at the John von Neumann Institute for Computing (NIC). While the CPG performs high-loop perturbative calculations, the NIC group studies non-perturbative physics of the Standard Model. Both groups have the goal to reach high-precision results for the input and interpretation of ongoing and planned high-energy and nuclear-physics experiments worldwide. This concerns non-perturbative matrix elements in *B* physics and hadron structure on the lattice side, as well as multiloop calculations for observables within the Standard Model on the perturbative side. ZPPT also has a strong focus on algorithmic and methodological developments to improve the calculations, leading to even higher precision. In the following, we will concentrate on two particular research directions, namely quantum computing and gravitational waves.

Quantum computing

For a long time, quantum computers have been discussed as a means to perform numerical calculations much – in some cases even exponentially – faster than classical computers. The reason is that quantum computers can take advantage of the quantum mechanical principles of superposition and entanglement, which theoretically allows the simultaneous execution of many operations.

While realisations of quantum computers have been discussed within the research field of quantum information science for decades, usable quantum computing hardware that can furthermore be used by "normal" scientists has existed for only, say, the last three years. This development has led to a real change in the way quantum computing is viewed, since scientists can now code their application directly for the quantum device using specific libraries, written in Python and provided by companies such as IBM, Rigetti, Google or D-Wave. In addition, these companies have developed simulators of their quantum machines that run on your local classical computer, allowing you to develop and test the application codes that are to eventually be run on the quantum computer.

Instead of classical bits, a quantum computer utilises quantum bits, or qubits. A qubit is a quantum mechanical two-state system that can be brought into an arbitrary superposition. In addition, qubits can be entangled, meaning that the state of one qubit depends inherently on the state of the other qubit. Realisations of qubits are manyfold, e.g. through Josephson junctions, trapped ions, Rydberg atoms or photons, to name just a few.

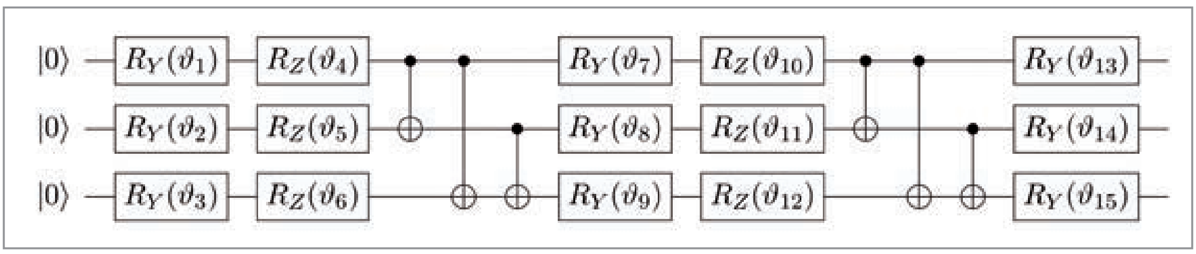

Figure 1
A quantum circuit. The various elements of the circuit are described in the text.

Quantum computing relies on the Hamiltonian formulation of a given problem. The goal is to compute the ground state and a few excited energies as well as the corresponding wave functions of such a Hamiltonian. This is in principle an exponentially hard problem. But here, quantum computing can help.

Instead of exploring the exponentially large Hilbert space, in the so-called variational quantum simulation approach, a quantum state is prepared through a quantum circuit (Fig. 1). In the figure, the states $|0\rangle$ denote the qubits, initialised in the state 0. These are followed by unitary gate operations $R_Y(\vartheta) = e^{i\vartheta\sigma_Y}$ ($R_Z(\vartheta) = e^{i\vartheta\sigma_Z}$) with σ_Y (σ_Z) Pauli matrices. These unitary operations are followed by entanglement gates (here CNOT gates), which connect two qubits and bring them into an entangled state.

Given the choice of the angles ϑ when executing this circuit, a state can be generated on the quantum computer and the problem Hamiltonian, i.e. the energy, can be measured for this state. The set of angles corresponding to this state and the measured energy can then be given to a classical computer on which a variational algorithm can be executed to find the minimal energy, i.e. the ground state. Excited states can then be computed by projecting the ground state obtained in this way out of the Hamiltonian. This hybrid approach – to calculate the very computing-intense cost function, here the energy, on the quantum computer and minimise this cost function on a classical computer – is called variational quantum simulation (VQS), an approach that is used in many applications in chemistry, biology and logistic problems.

The ZPPT group has used the VQS approach to develop a quantum simulation scheme for a U(1) gauge theory in two dimensions [1, 2] and plans to realise this protocol on an ion-trap-based experiment in the near future.

Gravitational waves

After the discovery of gravitational waves, precision calculations of the motion of a bound state of black holes or neutron stars have attracted much attention. Especially, in light of new proposed gravitational-wave experiments, improved predictions for the waveform of the signal are highly desirable. For the calculation of the waveform, the effective potential is required, which can be obtained as part of the corresponding Hamiltonian. The Hamiltonian can be derived using a variety of approaches depicted in Fig. 2. The figure also shows the region of validity in the plane depicting the mass ratio and the spatial separation of the two objects in the binary system.

The calculations are performed in the post-Newtonian framework, which is an expansion in both the inverse separation of the black holes and their relative velocities. As it turns out, in this framework, the problem can be mapped to the calculation of suitable Feynman diagrams in an effective field theory for gravity. This effective field theory, coined non-relativistic general relativity (NRGR), is conceptually very similar to non-relativistic quantum chromodynamics (NRQCD). The latter is well known in the context of particle physics and has been used to predict the properties of heavy-quark mesons and heavy-quark pair production at future electron–positron colliders.

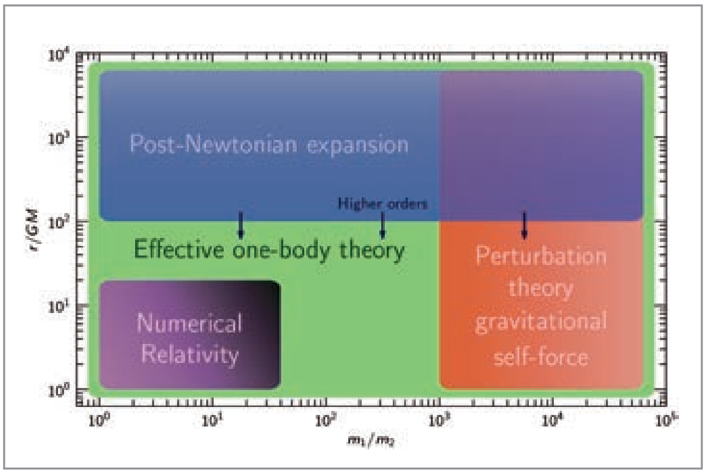

Figure 2

Various approaches for determining the motion of a binary system

Given the strong background of the ZPPT group in multiloop calculations and also in calculations in the framework of NRQCD, the techniques it uses for Standard Model calculations could easily be adapted to tackle problems within NRGR. In [3], the group calculated the complete corrections to the Hamiltonian, describing the motion of the binary system up to the fifth post-Newtonian order, which corresponds to the calculation of Feynman diagrams up to five loops.

This Hamiltonian, as in all problems of mechanics, is the starting point from which all observables, such as the bound state energy or the periastron advance, can be derived. Together with the luminosity function, which still remains unknown at this expansion order, the waveform of the signal can also be deduced. The results can be compared with partial results available in the literature that have been obtained using different methods, and perfect agreement is found in the overlap regions.

Contact:

Karl Jansen, karl.jansen@desy.de
Peter Marquard, peter.marquard@desy.de
Stefan Schäfer, stefan.schaefer@desy.de
Hubert Simma, hubert.simma@desy.de
Rainer Sommer, rainer.sommer@desy.de

References:

[1] J. F. Haase et.al, Quantum 5, 393 (2021)
[2] D. Paulson et al., arXiv:2008.09252
[3] J. Blümlein, A. Maier, P. Marquard, G. Schäfer, Nucl. Phys. B 965, 115352 (2021)

Projects and infrastructure

The experimental and theoretical research activities at DESY would not be possible without the contributions and support from numerous groups and people. One important service offered by DESY is its Test Beam Facility at the DESY II synchrotron. Scientists from all over the world are using the facility to subject newly developed detector components, e.g. for the LHC upgrades and other experiments, to tests with electron or positron beams (p. 60). In 2020, the group also successfully hosted the Beamline for Schools competition again (p. 62).

Just as essential are the DESY electronics groups, which design and manufacture important components for particle physics detectors. Important activities here are chip development (p. 64) and improvements in device production (p. 66).

Computing too is a crucial ingredient. The DESY IT group is constantly striving to improve its services for all users and needs, for example uniting the capabilities of the Helmholtz community (p. 68). These efforts led to the plan to unify access for all users and combine the provided services in a federated system (p. 70). Finally, scientific computing to help fight COVID-19 was and is a timely endeavour (p. 71).

Meanwhile, the DESY library group has been working to facilitate all processes related to publishing and to the management of publication databases (p. 74).

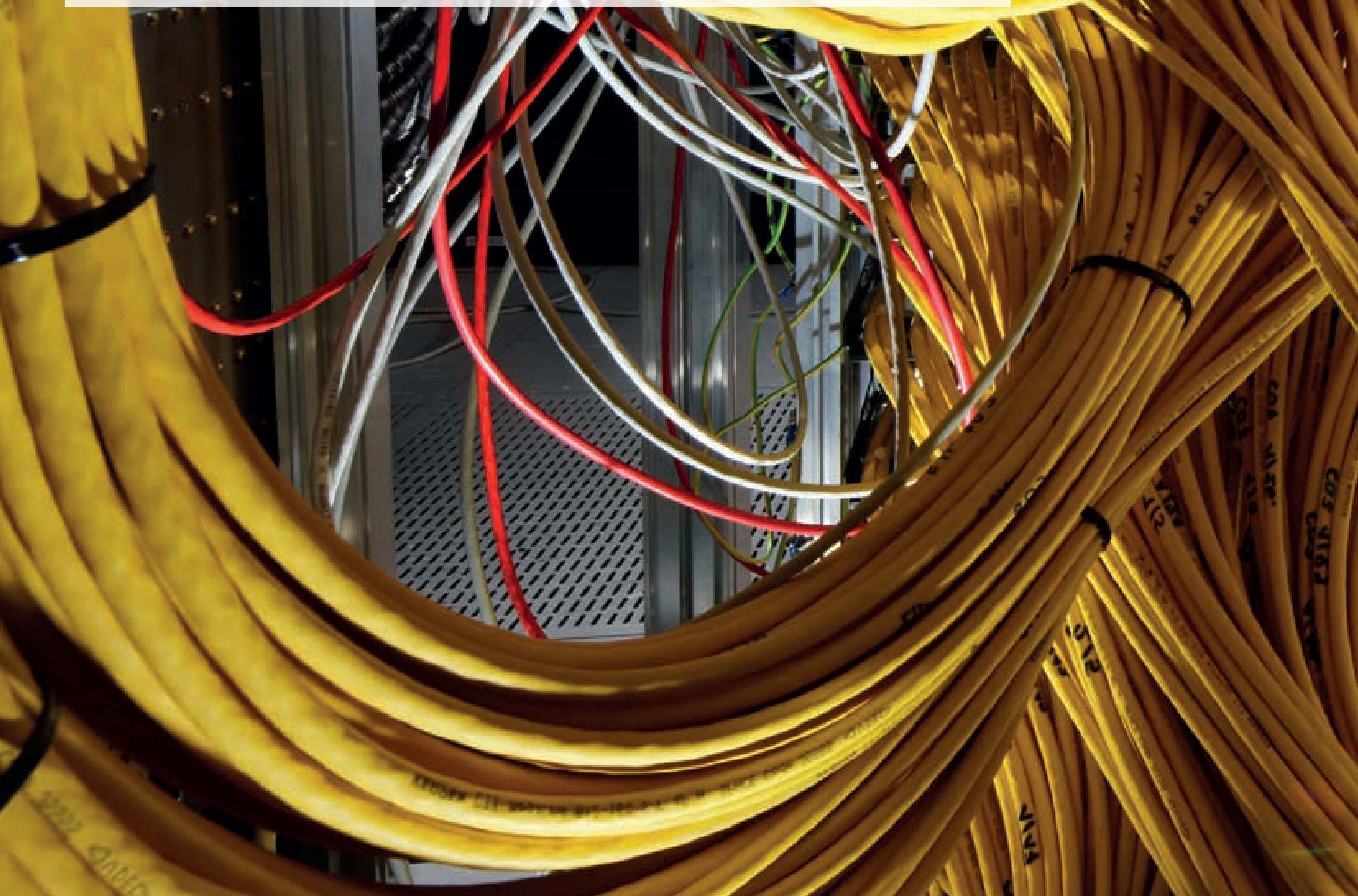

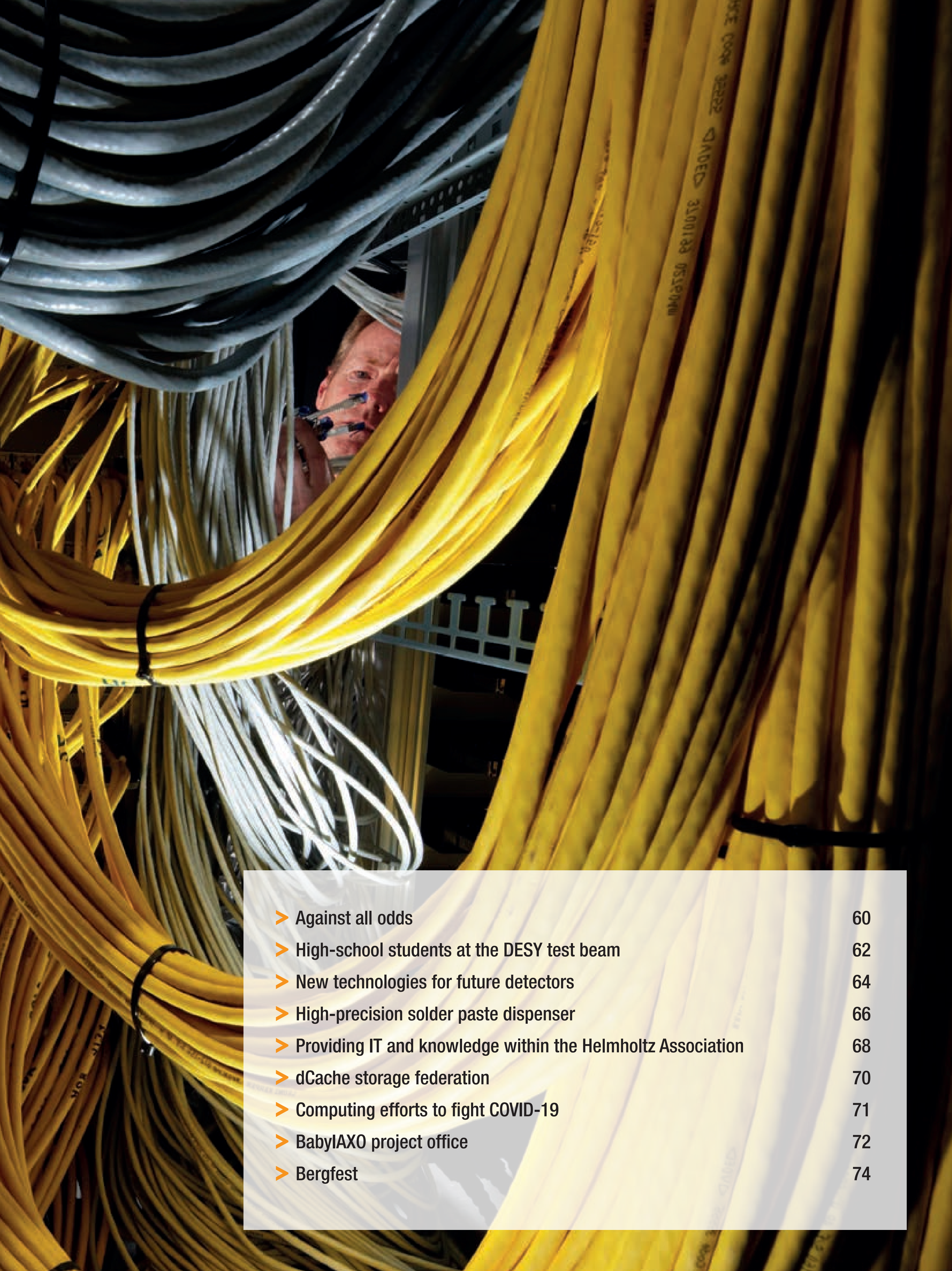

Against all odds

DESY II test beam keeps operating successfully despite the pandemic

DESY operates the DESY II Test Beam Facility for R&D projects from the global particle detector community. In 2020, the facility started running again in February. With the overall lockdown in Germany due to the COVID-19 pandemic, the facility was shut down in mid-March and reopened in June in a COVID-19-safe mode, running successfully until the December shutdown. The facility hosted the 2020 edition of the Beamline for Schools competition in close collaboration with CERN. The world-class infrastructures at DESY, such as the EUDET-type pixel beam telescopes or the large-bore magnets, continued to be in strong demand.

The DESY II Test Beam Facility

The DESY II Test Beam Facility uses the DESY II synchrotron for beam generation by means of micrometre-thin carbon fibre targets placed in the primary electron beam. It offers three beamlines located in Hall 2 on the DESY campus in Hamburg. The beamlines can be individually controlled by the user groups and provide electron or positron beams in the energy range from 1 to 6 GeV. The test beam team constantly adds improvements to the beamlines and strives to keep the facility a world-class venue for detector R&D.

2020 – a year full of challenges

During the winter shutdown 2019/20, the test beam team was busy as usual with general maintenance and preparations to get the facility ready for the 2020 run. All test beam slots but one were booked, and it looked like another record year would lie ahead. However, on 16 March, with the COVID-19 lockdown starting in Germany, the facility was closed and remained closed until the beginning of June.

Together with the DESY health and safety experts, a strategy was developed to allow COVID-19-safe user operation. This was adjusted a few times to react to the overall situation, but successfully enabled operation throughout the second half of the year. The main measure was to limit the number of users on site and in the huts, hence the size of teams was restricted to eight persons overall. In response to the more severe situation in fall, a compulsory negative PCR test was then required for all users, plus a quarantine for users entering from high-risk areas. Thanks to everyone's collaboration, the team made it work and safely provided many groups with much-needed test beam time. To simplify remote operations – particularly with the facility's workhorses, the beam telescopes – a TeamViewer-based remote-access solution was installed, allowing users to run the telescopes e.g. from their home institutes and thus reducing the number of people required on site.

Work in Hall 2 did not come to a complete stop, however, as this period of restricted activity was used to start renovating the hall, which was built shortly after the foundation of DESY. Fittingly coinciding with the 60th birthday of DESY, work started by tackling the old frosted glass window fronts and replacing them with modern transparent ones, making the hall much brighter. The next step included replacing the old lighting system of the hall with an all-LED-based solution and preparing for an overhaul of the overall power distribution. These activities were merely the start, and renovation will continue in the coming years.

Despite the COVID-19-induced difficulties, the 2020 run was very successful, with a total of 345 users from 27 countries conducting experiments at the facility. Mainly due to travel restrictions, this time over two thirds of the users came from Germany. Over 50% of the users again had an LHC background, but groups from Mu3e and Belle II also used the facility. Though outreach activities were heavily curtailed, it was possible to host the teacher education programme and the EDIT-2020 detector school in addition to the Beamline for Schools competition.

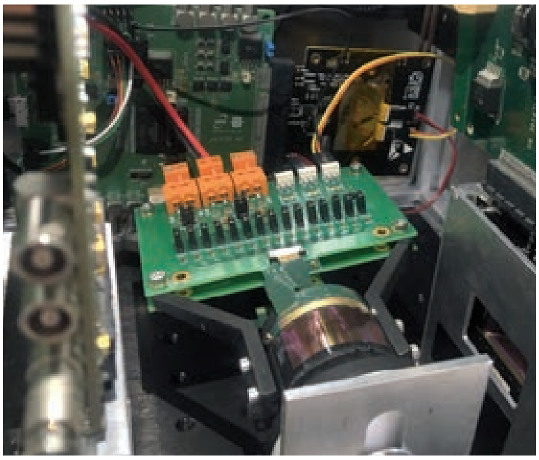

Figure 1
Prototype of a bent silicon sensor for the ALICE inner tracking system (courtesy of ALICE ITS3)

User highlights

ALICE ITS3

Using the DESY II Test Beam Facility, the ALICE ITS3 (Inner Tracking System upgrade for LHC LS3) R&D group successfully validated the feasibility of truly cylindrical tracking detectors based on bent monolithic active pixel sensors. For this purpose, silicon sensors were thinned down to 50 µm, thin enough to make them bendable to radii down to below 18 mm. The cylindrically shaped assemblies (Fig. 1) were characterised for efficiency using the test beam and found to maintain an excellent performance. With ample beam time (one week each in June, August and December), many important measurements were obtained. The group took advantage of the common software packages EUDAQ2 and Correyvreckan, the development of which is driven by DESY.

Along with the scientific experiment, given the worldwide travel restrictions, came the need to work partially remotely. A reduced team of German group members worked together on site with remote support – a second “experiment” that turned out so well it was repeated twice. In this context, the group highly acknowledged the local support provided by the DESY test beam team. The positive results obtained mark a major milestone of the project towards the integration of nearly massless detectors that can be “wrapped” around the beam pipe with little to no supporting material in their sensitive volumes. This class of next-generation detectors will allow for unprecedented low-material tracking layers for future experiments. The group is looking forward to future beam times at DESY with larger and more complex detector assemblies, which are planned for 2021.

Higgs factory tracking-detector studies

The silicon pixel detectors foreseen for the inner tracking layers of the various future Higgs factory proposals (CLIC, ILC, FCC-ee, CEPC) are subject to stringent requirements in terms of high measurement precision and low material content. A team from CERN, pursuing studies on such advanced pixel detectors within CERN’s strategic EP R&D programme and with collaborators from DESY, made extensive use of the DESY II beamlines and the available high-resolution beam telescopes. The 2020 test beam programme focused on comprehensive characterisations of hybrid assemblies with very small pixels with 25 µm pitch and of monolithic sensors produced with innovative pixel geometries and using adapted industry process technologies. Measurements under extreme operating conditions were performed to gain valuable insight into the complex structure of the different sensors (Fig. 2). The excellent performance of the DESY beam telescopes was instrumental in achieving the challenging precision measurement goals.

EDIT-2020

In February 2020, DESY hosted the EDIT-2020 school for the first time. The EDIT school, which is organised by the International Committee for Future Accelerators (ICFA), is targeted at young researchers in their graduate studies or their first postdoc year and aims to broaden their knowledge on detectors and instrumentation technologies for particle physics.

Figure 2

Test assembly with a CLICTD monolithic sensor above the cutout in the centre, mounted on a rotation stage inside the beam telescope (courtesy of CLICdp)

Besides the lecture programme, in which experts in the field give overview talks, the EDIT school has a unique emphasis on dedicated lab courses, including activities in the test beam. The 48 students from all over the world were able to take advantage of the beam telescopes, get hands-on experience with a calorimeter stack and perform exercises to reconstruct the data they had just acquired. Throughout the two weeks, there was a very vibrant atmosphere, and the school was praised as a big success by the participants. The school was just finished before the March 2020 lockdown took effect.

Outlook for 2021 and beyond

The winter shutdown 2020/21 will again be a busy time at the facility. New primary target stations will be installed in January to further increase availability and significantly decrease the effort for swapping a target. As a second major project, a direct extraction beamline from DESY II will be implemented and commissioned in 2021. This will add unique capabilities to the facility and, if test operation is concluded successfully, such a direct extraction beamline could later be added for user operation.

Summary

2020 was a difficult year for the DESY II Test Beam Facility, and we are looking forward to a more normal year 2021. Despite the difficulties during the pandemic, a lot of progress was made and the facility kept delivering beam to the users. The success of the DESY II Test Beam Facility would not have been possible without the support of many individuals and groups from the DESY particle physics and accelerator divisions. We would like to take this opportunity to thank everybody involved.

Contact:
testbeam-coor@desy.de
Ralf Diener, Norbert Meyners, Marcel Stanitzki

Reference:
http://testbeam.desy.de

High-school students at the DESY test beam

CERN's Beamline for Schools competition: successful second round at DESY during the pandemic

In autumn 2020, CERN's Beamline for Schools competition took place at the DESY II Test Beam Facility for the second time. For the very first time in the seven-year history of the competition, one of the two winning teams came from Germany. The second winning team originated from the birthplace of Beamline for Schools, Geneva in Switzerland, which was also a premiere. Another first time was the unusual realisation of the winning experiments, as the Swiss winning team could unfortunately not travel to DESY due to the COVID-19 pandemic and therefore took part remotely from CERN. Despite all the challenges to overcome, the seventh edition of the competition once again turned out to be a very successful event.

International science competition

In the Beamline for Schools (BL4S) competition, teams of high-school students are asked to phrase their own research questions and design fixed-target experiments to investigate them. The constraints: The experiment has to be devised in such a way that it can be performed at a test beam facility within one week of beam time, and it should make use of the detectors and equipment available to the project. The competition is open worldwide and has received contributions by teams from 91 countries over the past seven years. In 2020 alone, 198 experiment proposals were submitted, including first-time participations from Guatemala, Iraq, Kazakhstan, Nigeria, North Macedonia, Saudi Arabia, Taiwan and Tanzania. The first prize for two winning teams per year is a two-week visit to CERN or, in 2019, 2020 and 2021, to DESY to conduct their own proposed experiments guided by scientists.

The competition has been managed by CERN since 2014, where it started as a highlight of CERN's 60th anniversary activities. Until 2018, the experiments were performed at the PS test beams at CERN. Due to the long shutdown of the CERN accelerator complex, the competition had to evolve: DESY premiered as host in 2019 and committed to receive the winning teams and experiments again in 2020 and 2021, with great interest to continue this collaboration in the future.

Winning teams of BL4S 2020

In 2020, selecting the winning teams became even harder. With almost 200 submitted proposals from 47 countries and more than 1400 participating students, the selection committee took their time and evaluated all the proposals very carefully. After two challenging months, 23 teams were shortlisted and 10 teams received a special mention, all of them winning attractive prizes. For the two winning teams – the team ChDR-CHEESE from the Werner-von-Siemens-Gymnasium in Berlin and the team Nations' Flying Foxes from the International School of Geneva, Switzerland – the main prize was a trip to DESY.

The students' experiments

The students proposed two challenging, though exciting experiments for the 2020 edition of BL4S.

On the track of early particle physics experiments, the team Nations' Flying Foxes proposed to attempt an indirect measurement of Δ^+ baryons. To this end, electrons were to be directed at a thin metal target, while the consecutive tracking and analysis focused on the very few particles that leave the target at a large angle with respect to the initial path. Determining the energy of these particles should finally provide insight into the processes in the target and provide clues about the generation of the elusive baryon.

The team ChDR-CHEESE (Fig. 1) got interested in a certain kind of light: Cherenkov radiation, which is emitted by highly energetic particles passing through transparent matter.

Figure 1

German winners of the Beamline for Schools competition 2020 at DESY

However, the team was not content with "simply" measuring the light produced when particles pass through matter, but aimed to investigate what happens when a particle passes so close to a glass rod that the electric field reaches into the glass. The GeV electrons at the DESY II Test Beam Facility were to provide the answer.

Corona – and now?

During summer 2020, both winning teams prepared for their stay at DESY – almost all other plans for the summer had been cancelled anyway due to the COVID-19 pandemic. Up to two weeks before their departure, everything looked promising. Unfortunately, the second wave of the pandemic did not stop at the BL4S competition and, unlike the German team, the Swiss team was sadly unable to travel to DESY. The BL4S team reacted quickly and, with some last-minute changes, the programme was reorganised: One BL4S team member stayed at CERN, where the Swiss team took part in the experiments remotely, with the German team being their eyes and ears at DESY (Fig. 2).

When it became clear that the Swiss team would have to take part remotely, the German team made an even greater effort to get in touch with them and learn as much as possible about their experiment. In the daily morning meetings, where the status, problems and plan for the day were discussed, DESY and CERN connected by videoconference – as well as for all the lectures and even a virtual visit to the European XFEL. The data acquired at DESY was also transferred to CERN, so that both teams could analyse their experimental data with the help of volunteers at the two sites. In addition, the BL4S team organised a VIP/Sponsor Day and the final presentations by both teams in a virtual format. This came with the additional advantage that friends, families and schools could also participate in these events and gain insight into the students' lives as scientists.

All in all, 2020 was a challenging year also for BL4S. It was the first time in the history of the competition as well as for DESY that an experiment was performed remotely – but successfully in the end.

As the German team ChDR-CHEESE put it: "BL4S has shaped and will shape our lives. Since all the members of the team ChDR-CHEESE are currently studying a STEM subject, we believe we will greatly benefit from being exposed to research at an early age, gaining both first experience with experiments and data analysis skills and reporting the results in a presentation and maybe even a scientific publication."

BL4S 2021

The next round of the BL4S competition in 2021 will again be hosted at the DESY II Test Beam Facility – if the pandemic situation permits. Exceptionally, the deadline for the submission of proposals has been extended to 15 April 2021, with the winners to be announced in June.

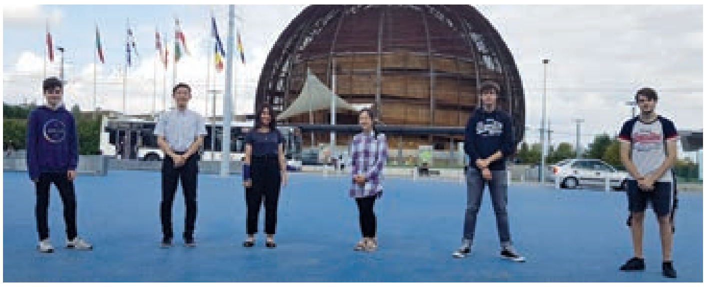

Figure 2

Students working on their experimental setup at DESY and remotely from CERN

Acknowledgements

BL4S is an education and outreach project funded by the CERN & Society Foundation and supported by individual donors, foundations and companies. In addition, BL4S at DESY is supported by a large number of local groups. We would like to take this opportunity to thank the volunteers, colleagues and groups involved for their invaluable support.

Authors:
Sarah Aretz, sarah.aretz@desy.de
Paul Schütze, paul.schuetze@desy.de

Contact:
Paul Schütze, paul.schuetze@desy.de
Marcel Stanitzki, marcel.stanitzki@desy.de
Barbara Warmbein, barbara.warmbein@desy.de

Reference:
https://beamlineforschools.cern

Documentary Beamline for Schools 2019:
https://videos.cern.ch/record/2710166

New technologies for future detectors

Benefiting from monolithic approaches and multiprocessor system-on-chips

The next generation of experiments for particle physics and photon science demands novel area array detectors with highest spatial and timing resolution, in the case of tracking detectors in particle physics along with ultralow mass. Following the strategic goals of the fourth programme-oriented funding (PoF IV) period of the Helmholtz research programme Matter and Technologies, these future needs will be addressed by means of state-of-the-art deep sub-micrometre CMOS processes for monolithic detectors and silicon photonics, with new methods for their ultra-compact packaging, as well as modern multiprocessor system-on-chip (MPSoC) hardware for off-detector terabit data transmission and preprocessing. These technologies significantly broaden DESY's competences in the development of hybrid detectors and pave the way for innovative detector designs and intelligent data acquisition concepts.

During the PoF III to PoF IV transition year 2020, new CMOS technologies for sensor and photonics applications were ramped up at DESY in order to extend the functionality and performance of previous hybrid development approaches. Design kits for two imaging processes (TPSCo at 65 nm and LFoundry at 150 nm) and a silicon photonics process (GF at 90 nm) were launched and applied for first concept and feasibility studies. In-house flip-chip mounting technologies were optimised accordingly to cope with smaller pitches, copper metallisation and pillar technology.

Both approaches, together with classical deep sub-micrometre CMOS technologies, allow more intelligence and data processing capacities to be integrated into the front-end. Modern MPSoCs with fast serial transceivers and powerful processors enable high-speed data throughput, the development and application of advanced methods for data processing, such as machine learning, and optimal use of modern high-performance hardware in combination with off-detector commercially available off-the-shelf (COTS) transceivers.

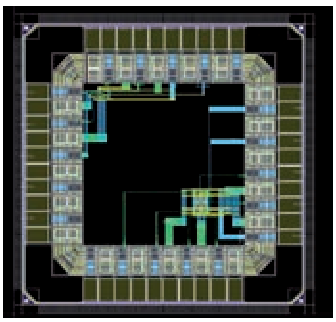

Figure 1

Layout of the first test chip with small sensor pixel array, pixel and front-end electronics in 65 nm CMOS technology

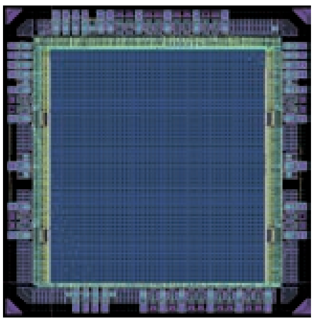

Figure 2

Layout of the digital SiPM prototype with 32 x 32 pixel matrix in 150 nm CMOS technology

Active pixel sensors

For particle and photon detection, first steps in using the new CMOS technologies were made by developing prototypes of monolithic active pixel sensors. The first prototype chip was designed using the 65 nm CMOS imaging sensor process and comprises a 2 x 2 matrix of particle-sensitive 16 x 16 μm^2 diodes. When hit by a particle, each pixel generates an electrical signal. This signal charge is collected and amplified by means of charge-sensitive amplifiers located within the sensor pixel. The test chip has a size of 1.5 x 1.5 mm^2 (Fig. 1) and has been submitted for fabrication in 2021.

The second prototype chip uses the 150 nm CMOS process and comprises 32 x 32 pixels at 70 µm pitch. Each pixel consists of four single-photon avalanche diodes (SPADs) biased above their breakdown voltage. A quenching circuit and an inverter in each pixel operate the silicon photomultiplier (SiPM) chip in the digital domain and enable a very fast event discrimination. The fully characterised SPAD cells are developed by the Bruno Kessler Foundation (FBK) in Italy. The prototype chip shown in Fig. 2 has a size of 3.2 x 3.2 mm^2 and enables full hit matrix readout at 3 MHz frame rate and timing measurements at 100 ps resolution. Submission for fabrication is scheduled for 2021.

Silicon photonics

Silicon photonics allows optical and electro-optical components to be embedded in CMOS chips. Figure 3 shows a preliminary layout of a single-channel 25 Gbit/s electronic–photonic integrated circuit (EPIC) in 90 nm silicon-on-insulator (SOI) CMOS technology. The transmitter converts high-speed electrical input data into an optical output data stream. A multistage driver (DRV in Fig. 3) generates a high-voltage swing required for an optical Mach–Zehnder modulator

(MZM), which outputs an optical signal modulated with the electrical input. The MZM accepts a continuous-wave optical signal and the amplified electrical input data from the on-chip driver. The optical fibres are coupled to the chip through edge couplers. On-chip waveguides guide the light to and from the MZM. In future, a receiver channel will be added to obtain full transceiver functionality. An optical waveguide steers the light to an on-chip photodetector, whose electrical output will be connected to amplifiers for further signal processing. A clock-and-data recovery circuit will be used to recover the clock needed for data regeneration, demultiplexing and off-chip data sending. The concept can be extended to handle a multiple of the 25 Gbit/s data channels, e.g. by utilising an advanced pulse amplitude modulation transceiver architecture.

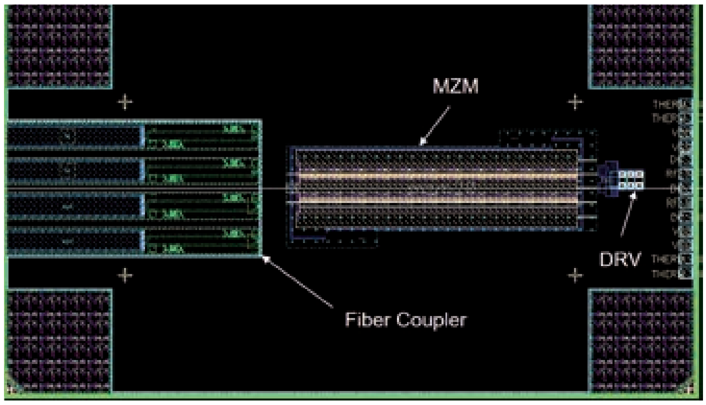

Figure 3

Layout of the EPIC in 90 nm SOI CMOS technology

Flip-chip interconnects

After working with nickel–gold as standard under-bump metallisation material for a while, the processes were extended and optimised to use copper instead. Copper enables low-loss signal redistribution as well as novel 3D integration technologies. The modified processes were successfully applied to thin and small pad contacts as well as to larger pillar-type contacts. Furthermore, pillars can also add a spacer functionality to the integration concept.

Figure 4 shows two bonded samples, where solder is sandwiched between copper contacts. The deposition of lead-free solder spheres with 30 µm diameter facilitates contact pitches down to 50 µm. In the case of the pillar-based interconnects, the solder completely converts into intermetallic phases with high melting point. In this way, subsequent assembly steps using the same solder can be performed without any impact. Furthermore, a low-force bonding approach was established, which is beneficial for the integration of sensitive components. With such capabilities and flexibilities in the processes, DESY is in the position to prototype the stacking of multiple chips with different functionalities in a single package.

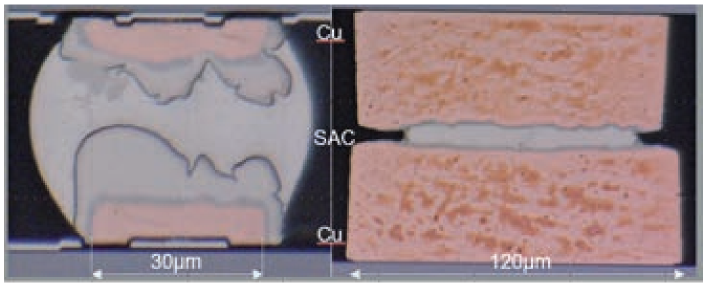

Figure 4

Flip-chip interconnect with copper pads (left) and pillars (right)

Data processing

To cope with the expected high data rates of future detectors, flexible and powerful readout systems are essential. These can be based on state-of-the-art MPSoCs, which are composed of a field-programmable gate array (FPGA) with multiple high-speed transceivers for data throughputs up to the terabit range and multiple processors for applications, real-time purposes and graphics manipulations. FPGA and processors can exchange data over a configurable high-speed bus system.

In order to gain experience with these new challenges for printed circuit board (PCB) design, DESY, together with the Institute for Data Processing and Electronics (IPE) at KIT in Karlsruhe, Germany, developed a stand-alone readout board (DTS100G) based on a Xilinx Zynq UltraScale+ ZU11EG FPGA. It offers 4 GB of on-board RAM, a SODIMM socket for up to 32 GB of DDR4 RAM and a wide range of interfaces to its processors, for example Gigabit Ethernet, USB 3.0, DisplayPort, µSD card and a SATA/PCIe M.2 slot. The FPGA's sixteen 32 Gb/s and thirty-two 16 Gb/s transceivers and more than 100 LVDS inputs and outputs are accessible through QSFP28, FireFly, FMC and FMC+ connectors. These can be equipped with commercial mezzanine cards, including fast SSD-based data storage, 100 Gb/s Ethernet adapters, ultrafast ADCs, etc., or with in-house developments as interfaces to data sources from detectors.

The FPGA, together with a four-core application-processing unit, a two-core real-time processing unit and an additional graphics-processing unit, allows for a versatile and efficient firmware and software design for the whole data acquisition chain. While the FPGA handles reception, preprocessing, buffering and packaging of the data, the processors can analyse data subsets with more sophisticated algorithms written in a high-level language and give feedback to the preprocessing logic with machine learning techniques. Using LINUX OS, the system can efficiently communicate through standard interfaces with the outside world for monitoring and control tasks. The board is currently in production, and first prototypes are expected for the second quarter of 2021.

Contact:
Karsten Hansen, karsten.hansen@desy.de
Manfred Zimmer, manfred.zimmer@desy.de

High-precision solder paste dispenser

Optimising printed circuit board production

The DESY Electronics Service Centre (ZE) has expanded the possibility of solder paste printing in surface-mounted device production by using an inline dispenser in the pick-and-place machine. This allows a flexible adjustment of the position and quantity of solder paste, even on partially assembled or warped printed circuit boards.

The increasing demands on the resolution and readout speed of detectors for particle physics and photon science experiments lead to an increase in the packing density and a reduction of the dimensions of the electronic components used in the assemblies for signal acquisition and processing. These demands can only be met with surface-mounted devices (SMDs). Before the actual placement process, in which the pick-and-place machine places the components to be soldered on the printed circuit board (PCB), solder paste must be applied to the PCB at the later soldering points. This process of applying solder paste has great influence on the functionality and reliability of the assembly. The amount of solder paste and the exact positioning of the application must be adjusted individually for each solder joint based on the component used and the PCB layout.

Errors at this point in the manufacturing process lead to short circuits or missing or bad-quality solder joints. The result is time-consuming troubleshooting and rework as well as unreliable assemblies. Failures of successfully tested assemblies may also occur after a shorter or longer period of operation of the assembly after installation. This is especially fatal for detector assemblies, since replacement is not possible for a long time after the start of the operating phase. In practice, two different methods of solder paste application are used:

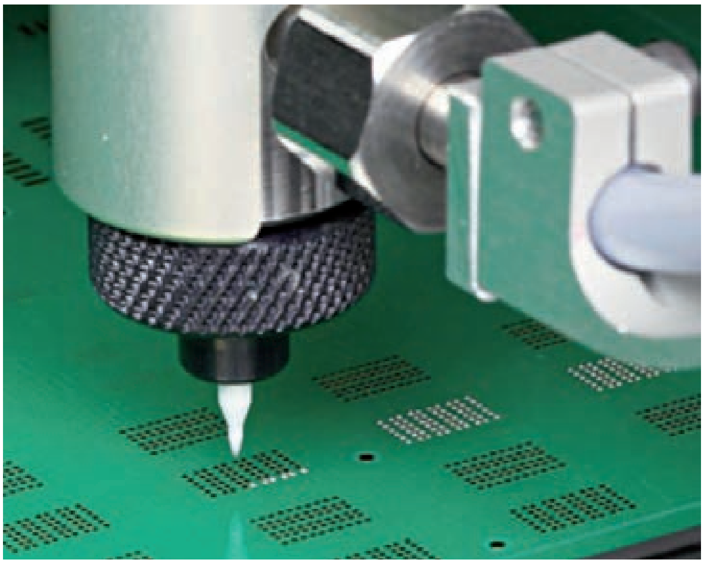

Figure 1

Dispenser head (courtesy of Yamaha Motor Corp. S10S20)

SMD stencil printer (squeegee method)

The PCB is clamped into the printer together with a lasered stainless-steel squeegee template. The solder paste is printed onto the PCB by the squeegee with programmed contact pressure and speed through the openings of the stencil. The stencil must be individually designed and manufactured for each PCB. To a limited extent, the amount of solder paste can be adjusted according to the diameter of the opening and in steps as required.

One advantage of this process is that even very small solder pad diameters below 300 µm can be safely applied. The prerequisite is that the hole pattern of the stencil exactly matches the real geometry of the PCB. This process has been used in SMD production at DESY ZE for many years.

Solder paste jetter

In the second process, a special printer is used, in which, similar to an inkjet printer, solder pellets are applied to the circuit board at preprogrammed points by a dispenser. The volume and position of the solder paste can be freely programmed.

The advantage of this process is that no template is required and that the solder paste volume and position can be adjusted subsequently. Particularly in prototype construction, this saves the expense of constantly reproducing the stencils. Devices of this type are very expensive and have a larger footprint. However, previously available devices were not capable of reproducibly realising the smallest solder pad geometries found at DESY. For this reason, DESY ZE has not used such a device so far.

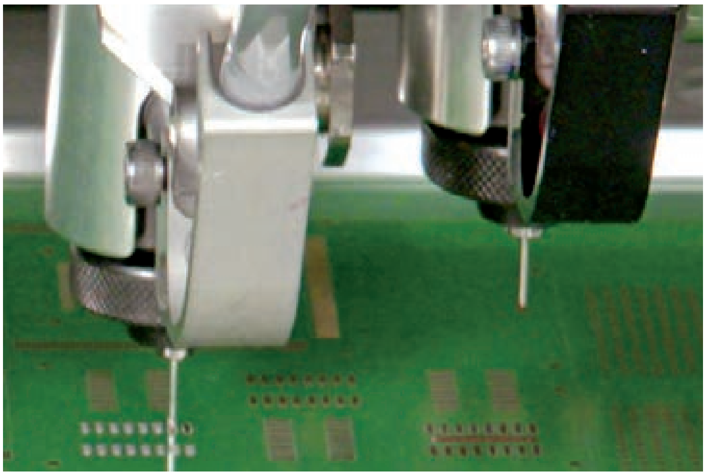

Figure 2

Dot station (courtesy of Yamaha Motor Corp. S10S20)

Upgrading a pick-and-place machine with a solder paste dispenser

The automatic pick-and-place machine used at DESY ZE in SMD production has six placement heads. However, there is the option to replace one or more of the placement heads, which are intended for placing electronic components, with dispenser modules. Depending on the type of dispenser module, it is possible to apply either adhesive or solder paste to the PCB.

This was first tested at DESY in the Detector Assembly Facility (DAF) for bonding scintillator tiles to assemblies of the HGCAL calorimeter for the CMS experiment at CERN. To this end, a machine from the same series (with a smaller number of placement heads) was equipped with a compressed-air dispenser optimised for gluing operations and with advanced control software, which controls the bonding processes and provides camera-guided quality control of the adhesive volume.

Based on this positive experience, the automatic pick-and-place machine in SMD production at DESY ZE was then equipped with a screw dispenser module (Fig. 1), which is especially suitable for dispensing solder paste.

One disadvantage of solder paste printing by means of stencil printing is that, once the stencil has been manufactured, it is no longer possible to make changes to the location and quantity of the solder paste print. This actually becomes problematic only when there are manufacturing tolerances in the PCB production. This danger exists especially with very large PCBs, where defects add up over the entire length of the PCB or where deviations can occur from batch to batch. In the case of ceramic circuit boards (LTCC), for example, the production process causes both shrinkage and partial twisting of the circuit board.

At DESY, there are indeed PCBs for which this is the case. Until now, attempts have been made to remedy this problem by means of time-consuming manual dispensing at critical points. A big advantage of the possibility of dispensing directly in the pick-and-place machine is that the PCB only has to be clamped once and that solder paste can also be precisely applied later for repairs on already assembled PCBs. In addition, it is now possible for the first time to implement chip-on-chip technology.

Since the dispensers can be easily exchanged in the pick-and-place machine, depending on the technology required, placement can be carried out with a full placement capacity of six heads as well as flexibly integrated adhesive and/or solder paste dispensing.

The dot station (Fig. 2) allows online control of the solder paste or adhesives.

Fact sheet of the i-PULSE Dispenser

The i-PULSE Dispenser has the outstanding feature of placing a dispense point within only 70 µs. The exceptional axis positioning capability of 0.3 µm in the *x*/*y* direction and 0.06 µm in the *z* direction is the best prerequisite for maintaining the assured manufacturing tolerance of ±50 µm even over decades of operation. Standard media, such as adhesive and solder paste, can be dispensed at a rate of up to 10 mg/s. Dot and line diameters from 0.3 to 1.2 mm are possible in the standard configuration, optionally also above and below this range.

Contact:

Otto-Christian Zeides, otto-christian.zeides@desy.de

Reinhard Schappeit, reinhard.schappeit@desy.de

Providing IT and knowledge within the Helmholtz Association

Federated IT services and imaging solutions for all research areas, fostered by DESY

The Helmholtz Association has established many overarching platforms and projects, organised in the Incubator framework. Their core purpose is to foster cross-institutional and cross-centre scientific collaboration within the association and to build a common Helmholtz knowledge base as well as an IT and research infrastructure. DESY coordinates two main pillar initiatives of this incubator process, the Helmholtz Federated IT Services (HIFIS) and the Helmholtz Imaging Platform (HIP). In 2020, to a large extent facilitated and even pushed by the COVID-19 pandemic, both platforms gained momentum. With the start of 2021, DESY provides significant support to all Helmholtz research communities, ranging from multiple services for the Helmholtz Cloud to scientific consulting services and a knowledge base for advanced methods for solving complex imaging tasks.

Federated IT services for Helmholtz

The HIFIS platform [1] was established to provide common access to IT resources within the Helmholtz Association as well as training and support for professional and sustainable scientific software development. The Helmholtz cloud services [2] offered by HIFIS include services for large data transfer, high-performance computing as well as documentation and collaboration tools of all kinds – the need for the latter has been forcefully demonstrated during the pandemic.

DESY coordinates the backbone services cluster, one of the three main clusters of HIFIS. Most significantly, the implementation of the authentication and authorisation infrastructure (Helmholtz AAI) – including the necessary infrastructure policies – was pursued in 2020. The establishment of such a Helmholtz-wide AAI service is an organisational and technological key component to allow common access to distributed IT services. Based on this infrastructure, cloud services, e.g. for data management, collaboration and scientific work, have already been used as prototypes for numerous research groups and more than 1000 individual users in 2020. The productive start of the Helmholtz Cloud is envisioned for 2021. The full establishment of such a federated IT infrastructure in the Helmholtz Association will allow closer partnering with European IT and research communities involved for example in the European Grid Infrastructure (EGI) and the European Open Science Cloud (EOSC).

DESY plays central roles in the HIFIS cloud cluster, as it is responsible for implementing and supplying the central access layer for all upcoming Helmholtz cloud services: the Helmholtz Cloud Portal. In addition, DESY has been offering many cloud services, of which several (dCache, Sync&Share, Docker in Kubernetes, Jupyter) are being included in the initial Helmholtz cloud service portfolio.

Led by DESY, HIFIS fostered a service agreement with the German National Research and Education Network (DFN) on operating a Helmholtz-wide virtual private network (Helmholtz backbone), covering the majority of Helmholtz centres. By the end of 2020, HIFIS backbone connections had been set up between four Helmholtz centres (DESY, HZDR, KIT and DKFZ). The other centres will be connected in 2021. An application scenario is currently being developed with HZDR to route the data transfers of the HZDR working group at the European XFEL through the new network infrastructure.

A further major aspect of the DESY contributions to the backbone framework is the implementation of core services. Unsurprisingly, managed data transfer is of high interest for researchers dealing with distributed data treasures and computation resources. Together with users from the Helmholtz AI Local Unit for Matter (HZDR), DESY has set up the HIFIS transfer service, based on previously implemented solutions for ESCAPE Data Lake and the Worldwide LHC Computing Grid (WLCG). The HIFIS transfer service is currently in pilot use and will be further developed in 2021.

Central access and research support

The Helmholtz Cloud Portal [3], provided by DESY, allows harmonised access to all Helmholtz cloud services. It contains all necessary information to access the available services and enables any user who has been identified using the AAI to obtain detailed information on service status and his/her access possibilities. The first version of the portal will be available by February 2021.

HIFIS further provides a central helpdesk system [4], allowing support for Helmholtz cloud services, as well as in-depth consulting for complex research software engineering (RSE)-related problems [5]. Coordinated by DESY, HZB and HZDR and based on the AAI technology, this system allows the distribution of tasks related to the different HIFIS clusters and external service providers. It can be reached by any user via mail [6] and topic-specific contact forms [7]. Automatic assignment of contact forms to specific helpdesk channels can be easily implemented.

The versatile architecture of this helpdesk system made it valuable for all other platforms. Hence, adaptations of the helpdesk service have been provided for the Helmholtz AI voucher system [8] and the HIP helpdesk [9] and are envisioned for the Helmholtz Metadata Collaboration (HMC) [10] helpdesk as well.

Imaging solutions for innovative research

The HIP [11] brings scientists and engineers in the Helmholtz Association together to promote and develop imaging science and foster synergies across imaging modalities and applications within the association.

A significant amount of research data produced within the Helmholtz Association is imaging data. To obtain such data, the association has a unique collection of imaging modalities at its disposal, ranging from nanoscale to global observations. Imaging science is an enabling technology used in all the research fields of the Helmholtz Association. Correspondingly, it has a rich portfolio of expertise covering research on novel imaging modalities, experimental work using large-scale research facilities, expertise in mathematics and imaging-related computer science as well as research in image analysis within specific fields of application.

The HIP coordinating management team and a service team are located at DESY. Further service teams were established at DKFZ in Heidelberg and MDC in Berlin. The management unit is under the roof of the DESY photon science division, while the service team is integrated in DESY IT. HIP is still in the ramp-up phase, and thus, establishing infrastructure, communication channels as well as a Scientific Advisory Committee and a Steering Board has been the main focus so far. The service team has started to implement a web platform called HIP modalities. HIP modalities is foreseen to form the core of the HIP network, interlinking imaging experts, instruments, modalities and corresponding algorithmic solutions at one site. It will thus provide means of increasing the visibility and findability of the impressive portfolio of Helmholtz imaging facilities and expertise.

Most notably, HIP mediates funding for imaging projects. For the first call, 25 project applications were submitted through the newly developed HIP project proposal management system. The evaluation found many promising and interesting proposals, so that the total budget was increased by the Helmholtz Initiative and Networking Fund (IVF) to over 4 million euros in order to fund 11 projects with a participation of 13 Helmholtz centres. HIP provides the unique possibility for the funded projects to request support from the service teams. Further activities of HIP involve a helpdesk (DKFZ) for all imaging-related issues (helpdesk@helmholtz-imaging.de) and the development of the HIP solutions framework (MDC), where software solutions for imaging developed at one of the Helmholtz centres can find a common framework.

The Hamburg HIP team is looking forward to being completed in 2021 with the appointment of the related research group (W3) in collaboration with Universität Hamburg.

HIP | HELMHOLTZ IMAGING PLATFORM

HIFIS | HELMHOLTZ FEDERATED IT SERVICES

Contact:

Uwe Jandt, uwe.jandt@desy.de
Philipp Heuser, philipp.heuser@desy.de

References:

[1] https://hifis.net
[2] https://hifis.net/news/2020/10/13/initial-service-portfolio
[3] https://cloud.helmholtz.de
[4] https://support.hifis.net
[5] https://software.hifis.net/services/consulting
[6] support@hifis.net
[7] https://hifis.net/contact
[8] https://www.helmholtz.ai/themenmenue/news-events/news/news/article/27682/index.html
[9] https://www.helmholtz-imaging.de/our_services/helpdesk/
[10] https://helmholtz-metadaten.de
[11] https://www.helmholtz-imaging.de

dCache storage federation

Large-scale data management on global scales

The dCache project is a DESY IT-led collaboration between DESY, Fermilab and the Nordic e-Infrastructure Collaboration (NeIC) that provides the eponymous open-source software. Many dCache instances are deployed internationally to satisfy the ever more demanding storage requirements of various scientific communities. dCache's multifaceted approach provides an integrated way of supporting different use cases with the same storage, from high-throughput data ingest to wide access and support for distributed and federated systems.

Distributed dCache instances

With dCache [1], different institutes can contribute to an aggregated storage system. dCache may be configured so that data is preferentially accepted using local storage when available, falling back to using more remote storage if all local storage is either full or offline. The NDGF Tier-1 groups four Nordic countries and Slovenia into a single distributed Tier-1 centre for the WLCG. For storage, there is a single dCache instance that has storage nodes in each of the member insti–tutes. Several institutes have tape libraries to which dCache has access. dCache ensures that the Tier-1 centre is always able to accept data from CERN, provided at least one site is up. As another example, the AGLT2 is a distributed Tier-2 site for the WLCG, formed from a collaboration between the University of Michigan and Michigan State University in the USA. It provides an excellent example of the dCache federation ability. Data ingested at any campus is written locally, using storage nodes located on the same campus. However, as this is a single dCache instance, the files are represented in a single namespace and may be accessed from any location.

Smart data handling in distributed clusters

Although the AGLT2 and NDGF sites have been operating for over a decade, such distributed setups are still exceptions. However, to reduce operational overhead and improve data availability, more and more small Tier-2 centres will come together to build a so-called data lake. A client requesting access to data stored on local campus resources will read the data from those resources. Attempts to read data only stored non-locally, however, will trigger automatic, dCache-internal replication of that data to the local campus resources. This and subsequent access will use the local resources. In addition to on-demand replication, dCache provides mechanisms for manual data placement. The replicas can be cached copies only, i.e. removed when space is needed, or have a guarantee on the remote site's availability window to support scheduled data-processing activities.

Caching and data placement have always been the foundation of the dCache design. To reduce the operation costs of a distributed deployment, the dCache developers introduced the concept of a "zone". A zone is a virtual container that collects multiple dCache services into a logical group. Those virtual groups are available in data placement and replication rules as well as for dCache intercomponent communication. In high-availability setups, where redundant copies of critical compo-nents are running at different zones, the local zone instance of a component is preferred in order to reduce performance penalties introduced by network latency. For data movement, the standard dCache internal pool-to-pool copy is used, and all data integrity mechanisms, such as check summing or transport layer security (TLS), are available for in-transit data protection. Such caching sites can be spawned on demand when the data processing is to be extended by external computing resources without managed storage. The dCache services, zones and caching nodes can be added and removed dynamically in the distributed deployment without configuration changes on other sites. This reduces the operational overhead of distributed deployments and provides a foundation for highly available dynamic storage federation. Moreover, in combination with a site-local read-only namespace replica, full access to the data can be provided even when the connection to the main site is lost, without compromising authorisation and data integrity.

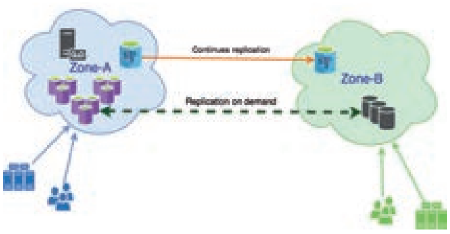

Figure 1
On-demand file replication in a distributed dCache instance spanned over geographically distant sites

Contact:
Tigran Mkrtchyan, tigran.mkrtchyan@desy.de; Christian Voss, christian.voss@desy.de

Reference:

[1] dCache – Keeping up With the Evolution of Science:
https://doi.org/10.1051/epjconf/202024504039

Computing efforts to fight COVID-19

Large-scale data management on global scales

The COVID-19 pandemic has not only challenged the DESY IT groups to enable an infrastructure for safe working at home. Administrators and scientists from the DESY ATLAS and CMS groups as well as photon scientists at PETRA III organised and reallocated significant computing resources within a short time to research aimed at combatting the SARS-CoV-2 virus. Data taken at PETRA III were analysed locally on the Maxwell high-performance computing (HPC) cluster, and molecule simulations were processed in a global effort of the high-energy physics community. In both endeavours, the DESY IT groups in Hamburg and Zeuthen provided significant computing resources and experience.

Data analysis on the Maxwell HPC cluster

DESY's Maxwell HPC cluster features large-scale parallel computing resources and fast storage systems directly connected to instruments at the synchrotron radiation source PETRA III, providing a central platform at DESY for data analysis, artificial-intelligence applications and many other compute-intense approaches. In 2020, the Maxwell cluster, which was temporarily configured to give highest priority to COVID-19-related work on all computing resources, was instrumental to many COVID-19 research activities [1]. The structural investigation of the SARS-CoV-2 main protease with a large library of potential inhibitors remains a particularly challenging endeavour. To support these activities, the DESY IT group dedicated massive computing resources on the Maxwell cluster – up to a quarter of the 38 000 computing cores and 170 GPU accelerator cards – to data analysis and molecular-dynamics simulations (Fig. 1).

Direct contributions to worldwide distributed computing

Some computing nodes from the Grid high-throughput clusters at DESY in Hamburg [2] and the PAX high-performance cluster at DESY in Zeuthen [3] were repurposed from running high-energy physics jobs to instead serve molecule simulations within the Rosetta@home initiative, in which DESY was among the top 1% of contributors. In cooperation with the University of Wuppertal in Germany, a container solution for easy deployment was developed.

Worldwide distributed computing through the WLCG

The DESY Grid sites were part of both the ATLAS and CMS efforts to distribute Folding@home protein structure simulations through the Worldwide LHC Computing Grid (WLCG). Within the "CERN and LHC Computing" team, DESY CPUs made a significant impact as part of the ATLAS and CMS donors, which were the main contributors to the team. As accelerator cards are particularly suitable for such molecule simulations, the powerful GPU nodes at DESY in Zeuthen were also employed for this purpose. Furthermore, a successful collaboration between ATLAS and DESY IT in Hamburg made it possible to opportunistically integrate the GPU resources of DESY's National Analysis Facility (NAF) [4] into the central submission of Folding@home jobs by ATLAS. With all these initiatives, DESY's overall contribution to the CERN and LHC Computing team's Folding@home effort was one of the most substantial.

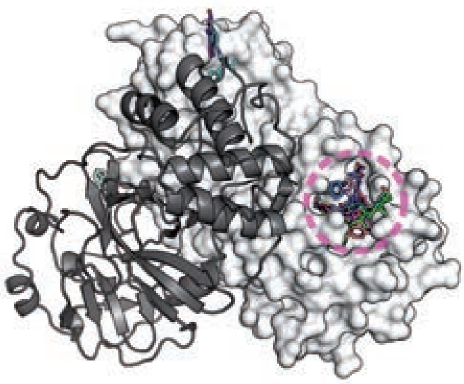

Figure 1
SARS-CoV-2 protein visualisation, computed on the Maxwell HPC cluster (courtesy of Sebastian Günther and Alke Meents)

Overall, between April and September 2020, about 6% of the available DESY computing resources were dedicated to activities concerning COVID-19 research. Since then, analysis of the data taken at PETRA III has been ongoing and integrated into the normal workflows. The COVID-19-related distributed computing activities have wound down by now, but should further computation efforts be required, the DESY IT groups are well prepared at different levels to rapidly ramp up the resources again for such studies.

Contact:

Thomas Hartmann, thomas.hartmann@desy.de
Yves Kemp, yves.kemp@desy.de
Götz Waschk, goetz.waschk@desy.de
Frank Schlünzen, frank.schluenzen@desy.de
David South, david.south@desy.de
Christoph Wissing, christoph.wissing@desy.de

References:

[1] https://confluence.desy.de/display/IS/Publications
[2] https://doi.org/10.1088/1742-6596/396/4/042026
[3] https://doi.org/10.1088/1742-6596/396/4/042007
[4] https://doi.org/10.1051/epjconf/202024507003

BabyIAXO project office

Realising interdisciplinary scientific projects

Leading science programmes persistently advance cutting-edge technology to realise their facilities. Building the right instruments is a major challenge, building the instruments right yet another. The BabyIAXO project office at DESY develops and demonstrates a coherent project management approach with particular emphasis on strengthening the ties between engineering and management.

BabyIAXO

BabyIAXO is a helioscope for searching for solar axions, which is currently in preparation at DESY (Fig. 1). Primarily a technology prototype for the International Axion Observatory (IAXO), BabyIAXO will also be a fully functional particle physics experiment aiming to find evidence for solar axions. Axions are particles that have been proposed to solve the strong charge–parity (CP) problem, and they are also dark-matter candidates. Axions would be emitted from the sun and converted into observable photons in BabyIAXO's superconducting magnet. BabyIAXO and IAXO are developed by the international IAXO collaboration [1]. DESY, with its experience from previous large-scale accelerator projects, contributes the project office as a service to the IAXO collaboration.

Specialties of scientific projects

Scientific projects have specific characteristics that make them complex. They require highly interdisciplinary engineering with contributions from many different fields, including mechanical, electrical and automation engineering, infrastructure and utilities engineering as well as civil, safety and environmental engineering. Projects have to integrate and coordinate the many contributions, and with them the diverse engineering methods and cultures.

Many contributions are delivered in kind, i.e. they are financed and readily delivered by the project partner. This in turn implies that many decisions regarding technologies and scheduling remain solely with the contributing partner, and the projects have to adapt accordingly. In addition, as development and optimisation of technological components continue throughout the project, management needs to be prepared to incorporate engineering changes also at very late stages to ensure the best possible solutions for the instruments.

Scientific projects are very long-term affairs. Development and operation of projects like BabyIAXO may last more than a decade, requiring the projects to preserve management and engineering decisions and expertise over several generations of scientists, technicians and engineers. This is particularly challenging as a lot of expertise is with young scientists who participate in the projects only for a limited time in the course of advancing their careers.

Project management objectives

Project management has to consider the specific needs of all stakeholders. Most prominently, it has to integrate the administrative and engineering efforts, which are both vital for project success. Management has to provide stable advance planning when directing the project to stay on budget and time. Engineering has to integrate the various technical contributions, quickly allocate and determine the impact of changes and, together with management, find ways to incorporate changes with minimum effect on the overall project planning. Both management and engineering need to systematically record decisions and carry forward project

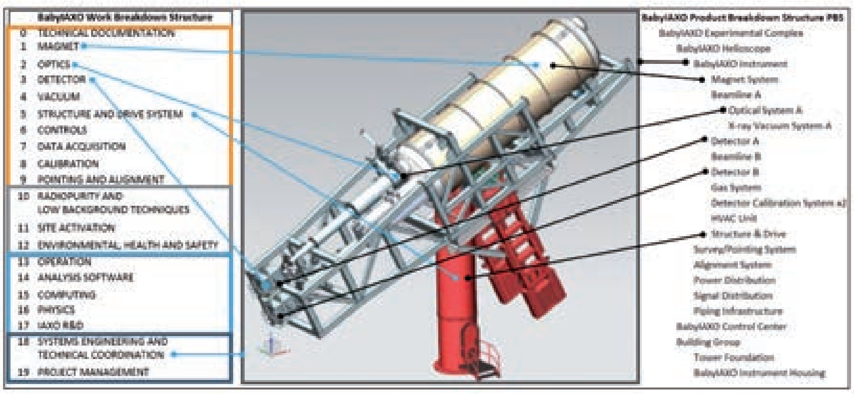

Figure 1

Management (left) and engineering (right) view of the BabyIAXO instrument. The work breakdown structure (WBS) summarises all project work, including work packages for producing the instrument components (orange), providing site and infrastructure (grey), conducting the scientific programme (blue) and integrating the instrument (black). The product breakdown structure (PBS) organises the components according to their functional and technical connections. WBS–PBS matching ensures that all components are taken care of in the project planning.

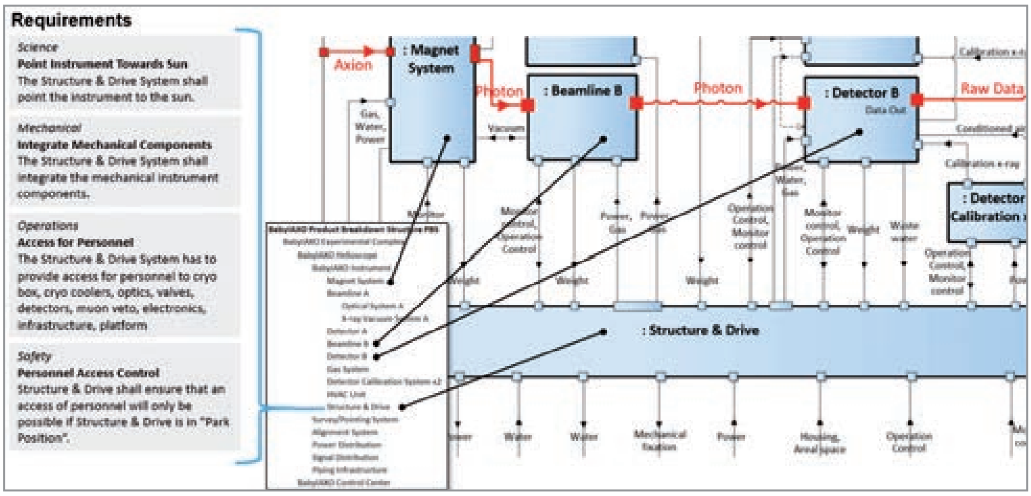

Figure 2

Example of PBS-based engineering of the structure and drive system of BabyIAXO. Requirements specify the system's role from different perspectives (left). Pointing functionality and personnel access are addressed in the mechanical design (Fig. 1, centre), while component integration and access control involve abundant mechanical connections, supply lines and signal flow, which are specified in the logical design (right, simplified example).

knowledge and experience. Moderating and aligning the management and engineering views lays the foundation for achieving all technical and administrative performance goals.

Making it work: the engineering view

The engineering view is expressed through the product breakdown structure (PBS), which defines and decomposes all subsystems and components according to their functional and technical dependencies (Fig. 1, right). The PBS is the foundation for engineering the project: Requirements outline the expected capabilities and properties of each PBS component. Logical models visualise component interactions and identify their interfaces and connections. Design models further detail the components' mechanical, electrical and automation properties.

Figure 2 illustrates PBS-driven engineering with a small example of the BabyIAXO structure and drive system, the central tower and platform that integrate and position the instrument. At the top, the diagram includes the instrument's functional principle, i.e. converting solar axions in the magnet and propagating the resulting photons through the beamline to the detector, putting engineering, operational and scientific aspects in context.

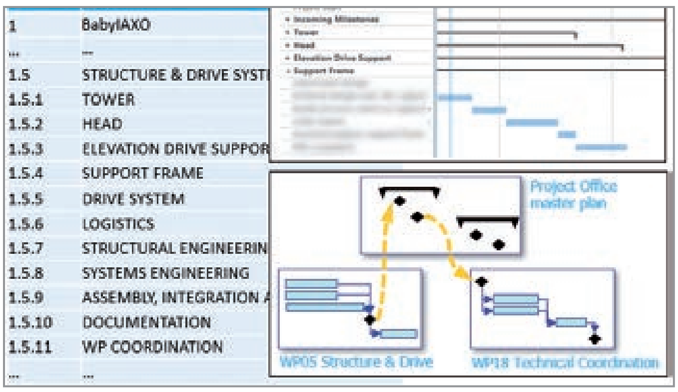

Figure 3

Example of WBS-based management of the structure and drive work package (WP). Level-2 WBS refines the WP contributions and organizes the schedule. Key milestones are propagated to the top-level project plan, which is used in the project office to manage dependencies across WPs.

Getting it done: the management view

The management view is expressed through the work breakdown structure (WBS), which lists all work packages (WP) and their agreed responsibilities (Fig. 1, left). The WBS is the foundation for managing the project: Scoping statements define the extent of each WP's responsibility. Level-2 WBS further refines WP activities, WP schedules determine which activities are performed when and by whom, and milestones track the production progress of the corresponding PBS components.

Coordinate, communicate, control: the project office

The project office (PO) aligns management and engineering activities. PO compiles and iterates the WBS with the WP teams and maintains the schedules. It drives the WBS–PBS mapping and ensures that all components are included in the project planning. PO is the project's central coordination and communication hub, making sure that all teams receive and access the same, latest information.

Conclusion

WBS- and PBS-based management and engineering views provide the project with a common vocabulary and better focus in communication. They help in vision sharing and generating a common understanding throughout all teams, which leads to better and faster decision-making. WBS and PBS are the foundation for systematic and efficient engineering and management processes as well as for organising and maintaining decisions, knowledge and project documentation. WBS–PBS matching is an important vehicle for establishing the consistency and completeness of both management and engineering views. The BabyIAXO project office approach integrates management and engineering views into a coherent project management method and provides a general reference for managing mid-range scientific projects.

Contact:

Lars Hagge, lars.hagge@desy.de

Reference:

[1] ALPS contribution, this report, p. 45

Bergfest

Information services during a global pandemic

Many aspects of the services provided by the DESY library and documentation group were already done virtually. The COVID-19 pandemic nevertheless forced the group to implement new workflows and introduce different ways of working together. Although many things remain to be done, the group celebrated “Bergfest” in several areas and is out of the woods by now.

News from the library

In 2018, the library group started to implement a new shelving scheme for the print collection that allows the ever growing diversification of research activities at DESY to be appropriately reflected [1]. Since then, all new acquisitions have received the new shelf marks according to the well-established, internationally used Dewey Decimal Classification (DDC) scheme. Alongside, the group started to resystematise all existing items (Fig. 1). This required them to fetch each item, check the contents, relabel it and, after creating some free space at the required spot, sort it back into the collection. On the virtual side, this work also allowed for some improvements, such as the interlinking of editions or of print and electronic editions.

Due to necessary construction works in Building 025F, the group evacuated the items there to shelve them temporarily in stacks in the basement of the central library. The construction work was planned to take a few months, meaning that all the items from Building 025F were actually located close to the library for some time. The group took the opportunity to process their resystematisation with priority. This work is finished by now, and all the items will be moved back with the new shelving in place.

As for the items in the central library, by the end of 2020, the group had finished all available items in the fields of computer sciences (004–006), mathematics (510–519), quantum mechanics (530.12), nuclear physics (539.x) and technology and engineering (600, 620–629, 670). Thus, a lot of “hardware” was moved around (Fig. 2). By the end of 2020, the group had treated around 12 000 titles or 13 500 individual items – equivalent, when stacked, to an approximately 500 m high pile of solid paper. Climbing this hill, about 50% of the DESY library holdings are done, and the group is now working downhill again.

As all this work cannot be done purely virtually, it came to a temporary stop because of the measures required to contain the COVID-19 pandemic. After some investigation, however, the group was able to implement a scheme to transport media very efficiently, so that a large part of the work can now be done from the home office.

During the pandemic-related lockdowns, the group had to limit some of its services, especially as soon as staff interaction was required. Still, at DESY in Hamburg and Zeuthen, most of the services could be kept up and running, such as the Hamburg–Zeuthen exchange, interlibrary loan, requests, access to the collection, etc. Much to the regret of the users, the guaranteed service hours could not be maintained at the usual level – a measure that was usually met with understanding, however. After discussions with the DESY health management, the group also had to close down most of its work spaces, especially the most popular “quiet corners”. Still, a few well-ventilated desks were provided. To improve safety, the group also installed a CO_2 measurement device. The well-used coffee corner also had to be closed, but it will be back.

Figure 1

New shelf marks with DDC and linking between ebook and print in catalogue display

Figure 2

Resystematisation work

Figure 3

New INSPIRE dashboard for back-end

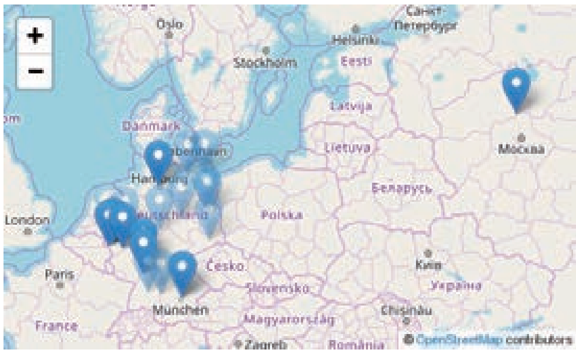

Figure 4

Geographic distribution of JOIN² instances

INSPIRE

In 2020, the INSPIRE publication database was in the final transition to the most recent version of the INVENIO open-source system built by CERN (Fig. 3). The old system now runs in a virtual environment for back-office purposes only and for a few tasks that have not yet been ported.

This sometimes frantic transition took place in a period of repeated lockdowns and home office. While the development of INVENIO is mainly done at CERN, it depends on specifications defined and tested by all partners, especially those working on content and curation. Usually, such a process requires close interaction between the developers and curators involved.

Astonishingly, this was barely affected by home office. Ten years ago, the workflow for the SPIRES back-end was driven by stacks of paper moved from one shelf to another. Thankfully, this changed years ago. One goal of the new INSPIRE platform was an integrated back-end, where cataloguers at all participating labs could use the same tools. With this all-electronic and mostly browser-based infrastructure in place, it was relatively easy for everyone involved to work from home. The main thing that had to be replaced was the office grapevine. However, with the heavy use of chat channels, it turned out that people at DESY were suddenly in the same “corridor” as people at CERN or Fermilab, who were working from home too. While, previously, one group could easily feel left out from the discussions of another group, now the challenge is to filter the amount of messages. All in all, forced by a virus, the INSPIRE collaboration has moved closer together.

JOIN² and PubDB

In 2020, library and documentation activities continued in the framework of the JOIN² project – an INVENIO-based repository used as central publication system at DESY and its project partners – together with DESY’s new partner, the Joint Institute for Nuclear Research (JINR) in Dubna, Russia. JOIN² repositories are now able to process records with media files (e.g. video lectures, seminars, tutorials), and the results were presented at the XXII International Conference on Data Analytics and Management in Data Intensive Domains [2].

Today, JOIN² repositories serve more than 20 000 staff members and over 5000 local visitors annually across all the partner institutions (Fig. 4). They provide more than 300 000 records as well as nearly 90 000 high-quality authority records freely on the Internet. This makes JOIN² one of the larger INVENIO users worldwide.

To ease the maintenance effort for the running instances and make it easier to install monthly updates, the JOIN² software is now available as a portable Docker container, a standard software unit that packages up code so the application runs quickly and reliably from one computing environment to another. At DESY, the production system was replaced by the Docker version in November 2020, running on a new virtual machine. The migration proceeded without problems. Data delivery to other systems (e.g. websites) was interrupted for a few minutes only, as advertised. Further updates can now be processed seamlessly and much easier. As a side effect, reliability has further improved as well.

The INSPIRE updates mentioned above required a major rework of the JOIN² INSPIRE imports. While this transition was basically invisible to users and was done gradually as more and more services moved to the new INSPIRE platform, the group also took the opportunity to improve the metadata import, which in turn improved overall data quality.

Contact:

library@desy.de
Martin Köhler, martin.koehler@desy.de

References:

[1] DESY Particle Physics 2018, Highlights and Annual Report, p. 87
[2] I. Filozova et al., JINR Open Access Repository based on the JOIN2 Platform, Data Analytics and Management in Data Intensive Domains 2020, 2790, 142–155 (2020)


NUCLEAR
SCIENCE
VOL. 12
1962
OF
NUCLEAR
SCIENCE
VOL. 13
K
K
K
K
Ann
15

References

Committees

DESY Foundation Council

Representatives of the Federal Republic of Germany

MinR Dr. **V. Dietz** (Chair)
(Federal Ministry of Education and Research)

RD'in **Dr. A. Fischer**
(Federal Ministry of Education and Research)

T. Stolzenberg
(Federal Foreign Office)

Representatives of the Free and Hanseatic City of Hamburg

N. Abend
(Ministry of Education and Research)

LRD Dr. **R. Greve** (Deputy Chair)
(Ministry of Education and Research)

Representatives of the Federal State of Brandenburg

MR **C. Feller**
(Ministry of Science, Research and Culture)

H. Roth
(Ministry of Finance)

Representatives from science and industry

Prof. Dr. **A. Brückner**
(Leibniz-Institut für Katalyse e.V.)

Prof. Dr. **D. Lenzen**
(President of Universität Hamburg)

Dr. **M. Kraas**
(Olympus Surgical Technologies)

Dr. **G. Mecke**
(AIRBUS)

Guests

Dr. **R. Abela**
(Chair of the DESY Scientific Council)

Prof. Dr. **I. Gregor**
(Chair of the DESY Scientific Committee)

Prof. Dr. **O. Wiestler**
(President of the Hermann von Helmholtz Association)

A.-C. Jauch
(DESY Equal Opportunity Officer)

C. Joithe
(Chair of the DESY Works Council)

DESY Board of Directors

Prof. Dr. **H. Dosch**
(Chairman of the DESY Board of Directors)

C. Harringa
(Administrative Division)

Dr. **W. Leemans**
(Accelerator Division)

Prof. Dr. **J. Mnich**
(Particle Physics Division)

Prof. Dr. **E. Weckert**
(Photon Science Division)

Prof. Dr. **C. Stegmann**
(Astroparticle Physics Division)

Dr. **A. Willner**
(Chief Technology Officer)

DESY Scientific Council

Dr. **R. Abela** (Chair)
PSI (CH)

Prof. Dr. **W. Barletta**
MIT (USA)

Prof. Dr. **J. Hill**
BNL (USA)

Prof. Dr. **Y.-K. Kim**
University of Chicago (USA)

Prof. Dr. **T. Lohse**
Humboldt University Berlin (DE)

Prof. Dr. **J. McEnery**
NASA (USA)

Dr. **B. Murphy**
Christian-Albrechts-University Kiel (DE)

Prof. **A. Olinto**
University of Chicago (USA)

Prof. Dr. **L. Rivkin**
PSI (CH)

Prof. **B. Roldán Cuenya**
Fritz Haber Institute (DE)

Prof. Dr. **T. Salditt**
University of Göttingen (DE)

Prof. Dr. **J. Ullrich**
Physikalisch-Technische Bundesanstalt (DE)

Prof. **C. Wahlström**
Lund University (SE)

Prof. Dr. **N. Wermes**
University of Bonn (DE)

and the chairpersons of

DESY APC:
Dr. **C. Weinheimer,** University of Münster (DE)

DESY MAC:
Dr. **O. Bruening,** CERN (CH)

DESY PSC:
Dr. **Ch. David,** PSI (CH)

DESY PRC:
Prof. **P. Burrows,** University of Oxford (UK)

DESY Scientific Committee:
Prof. Dr. **I. Gregor,** DESY

European XFEL:
Prof. Dr. **R. Feidenhans'l,** European XFEL (DE)

DESY Scientific Committee

Elected members from

FH Hamburg:
K. Büßer (DESY/FLC)
M. Diehl (DESY/ T)
V. Gülzow (DESY/ IT)
I.M. Gregor (DESY/ATLAS, Chair)
S. Heim (DESY/ATLAS)
H. Jansen (DESY/CMS)
I. Melzer-Pellmann (DESY/CMS)
A. Mußgiller (DESY/CMS)
C. Niebuhr (DESY/Belle)
A. Ringwald (DESY/ALPS)
T. Schörner-Sadenius (DESY/CMS)
P. van der Reest (DESY/ IT)

FS Division:
S. Bari (DESY/FS-SCS)
A. Burkhardt (DESY/FS-PE)
R. Döhrmann (DESY/FS-PE)
H. Graafsma (DESY/FS-DS)
T. Laarmann (DESY/FS-PS)
N. Müller (DESY/FSR)
E. Plönjes-Palm (DESY/FS-FL)
H. Schulte-Schrepping (DESY/FS-BT)
O. Seeck (DESY/FS-PE)
M. Tischer (DESY/FS-US)
R. Treusch (DESY/FS-FL)

M Division:
N. Baboi (DESY/MDI)
M. Bieler (DESY/MBB)
H.-J. Eckold (DESY/MKK)
K. Honkavaara (DESY/MPY)
R. Kammering (DESY/MCS)
G. Kube (DESY/MDI)
L. Lilje (DESY/MVS)
S. Schreiber (DESY/MFL)
M. Schmitz (DESY/MIN)
N. Walker (DESY/MPY)

V Division:
I. Mahns (DESY/ITT)
C. Porthun (DESY/D4)

Zeuthen Campus:
M. Ackermann (DESY/Z_ICE)
I. Bloch (DESY/Z_DLAB)
J. Knapp (DESY/Z_GA)
S. Ohm (DESY/Z_HESS)
W. Winter (DESY/AP_THAT)

Delegates from partner institutes and committees:
B. Atlay (HU Berlin)
F. Ellinghaus (KET)
S. Fiedler (EMBL)
C. Gutt (KfS)
J. Haller (U Hamburg)
D. Lott (HZG)
S. Molodtsov (European XFEL)
N.N. (KfB)
K. Sengstock (U Hamburg)
K. Valerius (KAT)

Leading Scientists:
R. Aßmann (DESY/MPY)
R. Bartolini (DESY/MPY)
D. Berge (DESY/AP-GA)
T. Behnke (DESY/FLC)
K. Borras (DESY/CMS)
R. Brinkmann (DESY/MPY)
F. Calegari (DESY/FS-CFEL)
H. Chapman (DESY/FS-CFEL)
E. Gallo (DESY/CMS)
C. Grojean (DESY/T)
G. Grübel (DESY/FS-CSX)
B. Heinemann (DESY/ATLAS)
Ç. İşsever (DESY/ATLAS)
F. Kärtner (DESY/FS-CFEL)
M. Kasemann (D ESY/CMS)
M. Kowalski (DESY/Z_ICE)
J. Küpper (DESY/FS-CFEL)
K. Mönig (DESY/ATLAS)
K. Peters (DESY/ATLAS)
M. Pohl (DESY/Z_THAT)
R. Porto (DESY/Z-THAT)
N. Rohringer (DESY/FS-TUX)
K. Rossnagel (DESY/FS-SXQM)
R. Santra (DESY/FS-CFEL)
M. Schnell-Küpper (DESY/FS-SMP)
V. Schomerus (DESY/T)
C. Schroer (DESY/FS-PETRA)
C. Schwanenberger (DESY/CMS)
G. Servant (DESY/T)
H. Sondermann (DESY/FS-CS)
A. Stierle (DESY/FS-NL)
K. Tackmann (DESY/ATLAS)
S. Techert (DESY/FS-SCS)
G. Weiglein (DESY/T)
H. Weise (DESY/MPY)
H. Yan (DESY/Z_THAT)

Physics Research Committee (PRC)

P. Burrows (U Oxford, UK, Chair)
L. Covi (U Göttingen, DE)
L. Feld (RWTH Aachen, DE)
J. Fuster Verdú (IFIC Valencia, SP)
N. Glover (IPPP Durham, UK)
U. Husemann (KIT, DE)
Y. Semertzidis (KAIST Seoul, KR)
S. Stapnes (CERN, CH)
J. Templon (NIKHEF, NL)

Ex-officio members PRC:
H. Dosch (DESY)
W. Leemans (DESY)
J. Mnich (DESY)
C. Stegmann (DESY)
E. Weckert (DESY)

German Committee for Particle Physics (KET)

M. Beneke (TU München)
V. Büscher (U Mainz)
A. Caldwell (MPP München)
K. Desch (U Bonn)
F. Ellinghaus (U Wuppertal)
M. Elsing (CERN)
E. Garutti (U Hamburg)
T. Hebbeker (RWTH Aachen)
M. Kobel (TU Dresden)
J. List (DESY)
J. Mnich (DESY)
P. Schleper (U Hamburg)
U. Uwer (U Heidelberg, Chair)
G. Weiglein (DESY)

Memberships

Accelerator Advisory Committee AAC Fermilab
Hans Weise

Accelerator Research and Innovation for European Science and Society (ARIES)
Ralph Aßmann (Deputy Chair)

ACHIP Consortium Advisory Board, Moore Foundation
Reinhard Brinkmann

ACOT – Advisory Committee of TRIUMF
Volker Gülzow

AIDA-2020
Katja Krüger, Felix Sefkow

Akademie der Wissenschaften Hamburg
Wilfried Buchmüller

arXiv Scientific Advisary Board
Martin Köhler

ATLAS Collaboration Board
Klaus Mönig

ATLAS Tracker Upgrade Management Board
Ingrid Gregor

Auswahlkommission der Carl-Zeiss-Stiftung
Joachim Mnich (Chair)

BELLE II Scrutiny Committee
Karsten Büßer (Chair)

BNL Programme Advisory Committee, Machine Advisory Committee
Ralph Aßmann

CALICE Steering Board
Felix Sefkow

CERN Scientific Policy Committee
Reinhard Brinkmann

CMS Collaboration Board
Kerstin Borras
Matthias Kasemann (Chair)

CMS Management Board
Kerstin Borras

CMS Tracker Institution Board
Günter Eckerlin

Deutsches Forschungsnetz DFN Verwaltungsrat
Joachim Mnich

DPG Beirat Fachverband Teilchenphysik
Ties Behnke

DPG National Prize Committee
Georg Weiglein

DPG Wissenschaftlicher Beirat des Physikzentrums
Georg Weiglein

DPHEP International Steering Committee
Volker Gülzow

ERC Panel Member
Georg Weiglein

EuPRAXIA
Jens Osterhoff (Chair of WP9), Ralph Aßmann (CB Member), Reinhard Brinkmann (CB Member)

European Committee for Future Accelerators (ECFA)
Joachim Mnich

European Particle Physics Communication Network
Thomas Zoufal

European Strategy Group (ESG)
Joachim Mnich

Future Circular Collider (FCC) Collaboration Board
Ralph Aßmann

Galileo Galilei Institute (INFN) Scientific Committee
Christophe Grojean

Gauß Allianz
Volker Gülzow

German Executive Outreach Group (GELOG)
Matthias Kasemann, Thomas Naumann, Barbara Warmbein, Thomas Zoufal

GridKa Overview Board
Volker Gülzow

Hamilton Mathematics Institute, Trinity College Dublin, Advisory Board
Volker Schomerus

Helmholtz Arbeitskreis Bibliotheks- und Informationsmanagement
Martin Köhler

Helmholtz Programme Matter and Technologies
Ties Behnke (Spokesperson)

Helmholtz Research Topic Elementary Particle Physics
Joachim Mnich (Spokesperson)

Helmholtz Alliance “Physics at the Terascale”
Ties Behnke (Scientific Coordinator)

IESC Scientific Committee
Géraldine Servant

INFN/LNF Scientific Commitee
Ralph Aßmann

INSPIRE Directorate
Kirsten Sachs

Interactions Collaboration Board
Christian Mrotzek

International Large Detector
Ties Behnke (Spokesperson)

IT-Koordinierungsausschuss (KoDa)
Volker Gülzow (Chair)

Jefferson Lab Programme Advisory Committee
Markus Diehl

John Adams Institute Advisory Board
Reinhard Brinkmann (Chair)

John von Neumann Institute for Computing (NIC)
Joachim Mnich (Director)

Joint Institute for Nuclear Research JINR, Programme Advisory Committee for Particle Physics
Joachim Mnich

Joint Institute for Nuclear Research JINR, Scientific Council
Joachim Mnich

Komitee für Beschleunigerphysik
Ralph Aßmann (Deputy Chair), Jens Osterhoff

Komitee für Elementarteilchenphysik (KET)
Kerstin Borras, Jenny List, Joachim Mnich, Georg Weiglein

LCC Physics and Detector Executive Board
Ties Behnke, Karsten Büßer, Frank Gaede (Chair), Jenny List

LHC Computing Resources Review Board
Volker Gülzow

LHC Computing Resources Scrutiny Group
Frank Gaede

LHC Resources Review Board
Manfred Fleischer

LHC Experiments Committee
Katja Krüger

Linear Collider Board (LCB)
Joachim Mnich

Long-Baseline Neutrino Committee Fermilab
Ties Behnke

NIC Scientific Council
Stefan Schäfer

NIKHEF Scientific Advisory Committee (SAC)
Joachim Mnich

NRC-ACOT Advisory Committee on TRIUMF
Hans Weise

PAC Center for Frontiers in Nuclear Science
Markus Diehl (Chair)

Particle Data Group
Brian Foster (Author), Klaus Mönig (Author), Andreas Ringwald (Author), Georg Weiglein (Author), Christian Spiering (Author)

Physics Preparatory Group of the European Strategy for Particle Physics
Beate Heinemann

Physics Review Panel, Academy of Finland
Christophe Grojean (Chair)

PIER Executive Board (Research field Particle & Astroparticle Physics)
Georg Weiglein

PIER Research Committee
Georg Weiglein

Royal Society Deputy
Brian Foster (Chair)

Scientific Advisory Committee Super TAU Charm Factory, BNP, Russia
Felix Sefkow

SCOAP^3 Executive Committee
Florian Schwennsen

SuperKEKB Machine Advisory Committee
Ralph Aßmann

TESLA Technology Collaboration
Hans Weise (Chair)

Wolfgang Pauli Centre
Volker Schomerus (Chair)

Publications

ALPS

Published

A. Andrianavalomahefa et al.
Search for dark photons as candidates for Dark Matter with FUNK.
36th International Cosmic Ray Conference, Madison (United States), 24 Jul 2019 - 1 Aug 2019.
Proceedings of Science / International School for Advanced Studies, vol. (ICRC2019):517, and PUBDB-2021-00020.
SISSA, Trieste.
doi: 10.3204/PUBDB-2021-00020.

A. Andrianavalomahefa et al.
Limits from the FUNK experiment on the mixing strength of hidden-photon dark matter in the visible and near-ultraviolet wavelength range.
Physical review / D, 102(4):042001, and PUBDB-2021-00005, arXiv:2003.13144.
doi: 10.1103/PhysRevD.102.042001.

J. Beacham et al.
Physics beyond colliders at CERN: beyond the Standard Model working group report.
Journal of physics / G, 47(1):010501, and PUBDB-2019-05237, CERN-PBC-REPORT-2018-007.
doi: 10.1088/1361-6471/ab4cd2.

J. H. Pold and A. D. Spector.
Demonstration of a length control system for ALPS II with a high finesse 9.2 m cavity.
EPJ Techniques and Instrumentation, 7:1, and PUBDB-2020-04523, arXiv:1710.06634. DESY 17-149.
doi: 10.1140/epjti/s40485-020-0054-8.

P. A. Zyla et al.
Review of Particle Physics.
Progress of theoretical and experimental physics, 2020(8):083C01, and PUBDB-2020-03047.
doi: 10.1093/ptep/ptaa104.

Ph.D. Thesis

R. C. G. Smith.
Digital Control Systems in the Regeneration Cavity of ALPS IIa.
Leibniz Universität Hannover, 2020.

ATLAS

Published

A. Alonso-Serrano, M. P. Dabrowski and T. Naumann.
Post-Editorial of “The Multiverse” Special Volume.
Universe, 6(1):17, and PUBDB-2021-00343.
doi: 10.3390/universe6010017.

ATLAS Collaboration.
A search for the $Z\gamma$ decay mode of the Higgs boson in pp collisions at $\sqrt{s}$ = 13 TeV with the ATLAS detector.
Physics letters / B, 809:135754 (1, and PUBDB-2020-03810, arXiv:2005.05382. CERN-EP-2020-052.
doi: 10.1016/j.physletb.2020.135754.

ATLAS Collaboration.
ATLAS data quality operations and performance for 2015-2018 data-taking.
Journal of Instrumentation, 15(04):P04003, and PUBDB-2020-02537, arXiv:1911.04632. CERN-EP-2019-207.
doi: 10.1088/1748-0221/15/04/P04003.

ATLAS Collaboration.
Combination of searches for Higgs boson pairs in pp collisions at $\sqrt{s}$ =13 TeV with the ATLAS detector.
Physics letters / B, 800:135103, and PUBDB-2019-04982, arXiv:1906.02025. CERN-EP-2019-099.
doi: 10.1016/j.physletb.2019.135103.

ATLAS Collaboration.
Combined measurements of Higgs boson production and decay using up to 80 fb^{-1} of proton-proton collision data at $\sqrt{s} = 13$ TeV collected with the ATLAS experiment.
Physical review / D D, 101(1):012002, and PUBDB-2020-02598, arXiv:1909.02845. CERN-EP-2019-097.
doi: 10.1103/PhysRevD.101.012002.

ATLAS Collaboration.
CP Properties of Higgs Boson Interactions with Top Quarks in the $t\bar{t}H$ and tH Processes Using $H \rightarrow \gamma\gamma$ with the ATLAS Detector.
Physical review letters, 125(6):061802: 1, and PUBDB-2020-03040, arXiv:2004.04545. CERN-EP-2020-046.
doi: 10.1103/PhysRevLett.125.061802.

ATLAS Collaboration.
Determination of jet calibration and energy resolution in proton–proton collisions at $\sqrt{s} = 8$ TeV using the ATLAS detector.
The European physical journal / C, 80(12):1104 (1, and PUBDB-2020-05248, arXiv:1910.04482. CERN-EP-2019-057.
doi: 10.1140/epjc/s10052-020-08477-8.

ATLAS Collaboration.
Dijet resonance search with weak supervision using $\sqrt{s} = 13$ TeV pp collisions in the ATLAS detector.
Physical review letters, 125(13):131801 (1, and PUBDB-2020-04590, arXiv:2005.02983. CERN-EP-2020-062.
doi: 10.1103/PhysRevLett.125.131801.

ATLAS Collaboration.
Erratum to: Measurement of differential cross sections and W^+/W^- cross-section ratios for W boson production in association with jets at $\sqrt{s}$ = 8 TeV with the ATLAS detector.
Journal of high energy physics, 2020(10):48, and PUBDB-2021-00441, arXiv:1711.03296. CERN-EP-2017-213.
doi: 10.1007/JHEP10(2020)048.

ATLAS Collaboration.
Erratum to: Measurement of differential cross sections for single diffractive dissociation in $\sqrt{s}$ = 8 TeV pp collisions using the ATLAS ALFA spectrometer.
Journal of high energy physics, 2020(10):182, and PUBDB-2021-00447, arXiv:1911.00453. CERN-EP-2019-190.
doi: 10.1007/JHEP10(2020)182.

ATLAS Collaboration.
Erratum to: Measurements of top-quark pair differential and double-differential cross-sections in the ℓ+jets channel with pp collisions at $\sqrt{s} = 13$ TeV using the ATLAS detector [Eur. Phys. J. C 79 (2019) 1028].
The European physical journal / C, 80(11):1092, and PUBDB-2021-00418, arXiv:1908.07305. CERN-EP-2019-149. arXiv:1908.07305. CERN-EP-2019-149.
doi: 10.1140/epjc/s10052-020-08541-3.

ATLAS Collaboration.
Evidence for electroweak production of two jets in association with a $Z\gamma$ pair in pp collisions at $\sqrt{s} = 13$ TeV with the ATLAS detector.
Physics letters / B, B803:135341, and PUBDB-2020-02549, arXiv:1910.09503. CERN-EP-2019-206.
doi: 10.1016/j.physletb.2020.135341.

ATLAS Collaboration.
Evidence for $t\bar{t}t\bar{t}$ production in the multilepton final state in proton–proton collisions at $\sqrt{s} = 13$ TeV with the ATLAS detector.
The European physical journal / C, 80(11):1085 (1, and PUBDB-2020-05096, arXiv:2007.14858. CERN-EP-2020-111.
doi: 10.1140/epjc/s10052-020-08509-3.

ATLAS Collaboration.
Fluctuations of anisotropic flow in Pb+Pb collisions at $\sqrt{s_{NN}}$ = 5.02 TeV with the ATLAS detector.
Journal of high energy physics, 01(1):051, and PUBDB-2020-04623, arXiv:1904.04808. CERN-EP-2019-023.
doi: 10.1007/JHEP01(2020)051.

ATLAS Collaboration.
Higgs boson production cross-section measurements and their EFT interpretation in the 4ℓ decay channel at $\sqrt{s}$ =13 TeV with the ATLAS detector.
The European physical journal / C, 80(10):957 (1, and PUBDB-2020-04620, arXiv:2004.03447. CERN-EP-2020-034.
doi: 10.1140/epjc/s10052-020-8227-9.

ATLAS Collaboration.
Measurement of azimuthal anisotropy of muons from charm and bottom hadrons in Pb+Pb collisions at $\sqrt{s_{NN}}$ =5.02 TeV with the ATLAS detector.
Physics letters / B, B807:135595, and PUBDB-2020-02960, arXiv:2003.03565. CERN-EP-2019-274.
doi: 10.1016/j.physletb.2020.135595.

ATLAS Collaboration.
Measurement of azimuthal anisotropy of muons from charm and bottom hadrons in pp collisions at $\sqrt{s} = 13$ TeV with the ATLAS detector.
Physical review letters, 124(8):082301, and PUBDB-2020-02599, arXiv:1909.01650. CERN-EP-2019-166.
doi: 10.1103/PhysRevLett.124.082301.

ATLAS Collaboration.
Measurement of differential cross sections for single diffractive dissociation in $\sqrt{s} = 8$ TeV pp collisions using the ATLAS ALFA spectrometer.
Journal of high energy physics, 2020(2):42, and PUBDB-2020-02542, arXiv:1911.00453. CERN-EP-2019-190.
doi: 10.1007/JHEP02(2020)042.

ATLAS Collaboration.
Measurement of isolated-photon plus two-jet production in pp collisions at $\sqrt{s} = 13$ TeV with the ATLAS detector.
Journal of high energy physics, 2020(3):179, and PUBDB-2020-02525, arXiv:1912.09866. CERN-EP-2019-210.
doi: 10.1007/JHEP03(2020)179.

ATLAS Collaboration.
Measurement of J/ψ production in association with a $W^\pm$ boson with pp data at 8 TeV.
Journal of high energy physics, 2020(1):95, and PUBDB-2020-02566, arXiv:1909.13626. CERN-EP-2018-352.
doi: 10.1007/JHEP01(2020)095.

ATLAS Collaboration.
Measurement of long-range two-particle azimuthal correlations in Z-boson tagged pp collisions at $\sqrt{s}$=8 and 13 TeV.
The European physical journal / C, 80(1):64, and PUBDB-2020-04624, arXiv:1906.08290. CERN-EP-2019-103.
doi: 10.1140/epjc/s10052-020-7606-6.

ATLAS Collaboration.
Measurement of soft-drop jet observables in pp collisions with the ATLAS detector at $\sqrt{s}$ =13 TeV.
Physical review / D D, 101(5):052007, and PUBDB-2020-02524, arXiv:1912.09837. CERN-EP-2019-269.
doi: 10.1103/PhysRevD.101.052007.

ATLAS Collaboration.
Measurement of the azimuthal anisotropy of charged-particle production in $Xe+Xe$ collisions at $\sqrt{s_{NN}} = 5.44$ TeV with the ATLAS detector.
Physical review / C covering nuclear physics, 101(2):024906, and PUBDB-2020-02536, arXiv:1911.04812. CERN-EP-2019-227.
doi: 10.1103/PhysRevC.101.024906.

ATLAS Collaboration.
Measurement of the Lund Jet Plane Using Charged Particles in 13 TeV Proton-Proton Collisions with the ATLAS Detector.
Physical review letters, 124(22):222002, and PUBDB-2020-02361, arXiv:2004.03540. arXiv:2004.03540. CERN-EP-2020-030.
doi: 10.1103/PhysRevLett.124.222002.

ATLAS Collaboration.
Measurement of the transverse momentum distribution of Drell–Yan lepton pairs in proton–proton collisions at $\sqrt{s} = 13$ TeV with the ATLAS detector.
The European physical journal / C Particles and fields,

C80(7):616, and PUBDB-2020-02963, arXiv:1912.02844. CERN-EP-2019-223.
doi: 10.1140/epjc/s10052-020-8001-z.

ATLAS Collaboration.
Measurement of the $t\bar{t}$ production cross-section and lepton differential distributions in $e\mu$ dilepton events from pp collisions at $\sqrt{s} = 13$ TeV with the ATLAS detector.
The European physical journal / C Particles and fields, 80(6):528, and PUBDB-2020-02552, arXiv:1910.08819. CERN-EP-2019-203.
doi: 10.1140/epjc/s10052-020-7907-9.

ATLAS Collaboration.
Measurement of the $t\bar{t}$ production cross-section in the lepton+jets channel at $\sqrt{s} = 13$ TeV with the ATLAS experiment.
Physics letters / B, 810:1, and PUBDB-2020-03601, arXiv:2006.13076. CERN-EP-2020-096.
doi: 10.1016/j.physletb.2020.135797.

ATLAS Collaboration.
Measurement of the $Z(\rightarrow \ell^+\ell^-)\gamma$ production cross-section in pp collisions at $\sqrt{s} = 13$ TeV with the ATLAS detector.
Journal of high energy physics, 2020(3):54, and PUBDB-2020-02534, arXiv:1911.04813. CERN-EP-2019-228.
doi: 10.1007/JHEP03(2020)054.

ATLAS Collaboration.
Measurements of inclusive and differential cross-sections of combined $t\bar{t}\gamma$ and $tW\gamma$ production in the $e\mu$ channel at 13 TeV with the ATLAS detector.
Journal of high energy physics, 2020(9):1, and PUBDB-2020-03604, arXiv:2007.06946. CERN-EP-2020-100.
doi: 10.1007/JHEP09(2020)049.

ATLAS Collaboration.
Measurements of the Higgs boson inclusive and differential fiducial cross sections in the 4ℓ decay channel at $\sqrt{s}$ = 13 TeV.
The European physical journal / C, 80(10):942, and PUBDB-2020-04622, arXiv:2004.03969. CERN-EP-2020-035.
doi: 10.1140/epjc/s10052-020-8223-0.

ATLAS Collaboration.
Measurements of the production cross-section for a Z boson in association with b-jets in proton-proton collisions at $\sqrt{s} = 13$ TeV with the ATLAS detector.
Journal of high energy physics, 2007(7):44, and PUBDB-2020-02961, arXiv:2003.11960. CERN-EP-2020-022.
doi: 10.1007/JHEP07(2020)044.

ATLAS Collaboration.
Measurements of top-quark pair spin correlations in the $e\mu$ channel at $\sqrt{s} = 13$ TeV using pp collisions in the ATLAS detector.
The European physical journal / C, 80(8):754 (1, and PUBDB-2020-05002, arXiv:1903.07570. CERN-EP-2019-034.
doi: 10.1140/epjc/s10052-020-8181-6.

ATLAS Collaboration.
Observation of the associated production of a top quark and a Z boson in pp collisions at $\sqrt{s} = 13$ TeV with the ATLAS detector.
Journal of high energy physics, 2020(7):124, and PUBDB-2020-02948, arXiv:2002.07546. CERN-EP-2019-273.
doi: 10.1007/JHEP07(2020)124.

ATLAS Collaboration.
Operation of the ATLAS trigger system in Run 2.
Journal of Instrumentation, 15(10):P10004 (1, and PUBDB-2020-04570, arXiv:2007.12539. CERN-EP-2020-109.
doi: 10.1088/1748-0221/15/10/P10004.

ATLAS Collaboration.
Performance of electron and photon triggers in ATLAS during LHC Run 2.
The European physical journal / C Particles and fields, 80(1):47, and PUBDB-2020-02637, arXiv:1909.00761. CERN-EP-2019-169.
doi: 10.1140/epjc/s10052-019-7500-2.

ATLAS Collaboration.
Performance of the ATLAS muon triggers in Run 2.
Journal of Instrumentation, 15(09):P09015 (1, and PUBDB-2020-04891, arXiv:2004.13447. CERN-EP-2020-031.
doi: 10.1088/1748-0221/15/09/p09015.

ATLAS Collaboration.
Performance of the missing transverse momentum triggers for the ATLAS detector during Run-2 data taking.
Journal of high energy physics, 2020(8):80 (1, and PUBDB-2020-03326, arXiv:2005.09554. CERN-EP-2020-050.
doi: 10.1007/JHEP08(2020)080.

ATLAS Collaboration.
Performance of the upgraded PreProcessor of the ATLAS Level-1 Calorimeter Trigger.
Journal of Instrumentation, 15(11):P11016, and PUBDB-2020-04638, arXiv:2005.04179. CERN-EP-2020-042.
doi: 10.1088/1748-0221/15/11/P11016.

ATLAS Collaboration.
Reconstruction and identification of boosted di-τ systems in a search for Higgs boson pairs using 13 TeV proton-proton collision data in ATLAS.
Journal of high energy physics, 11(11):163, and PUBDB-2020-05035, arXiv:2007.14811. CERN Preprint ID: CERN-EP-2020-118.
doi: 10.1007/JHEP11(2020)163.

ATLAS Collaboration.
Search for a scalar partner of the top quark in the all-hadronic $t\bar{t}$ plus missing transverse momentum final state at $\sqrt{s}$=13 TeV with the ATLAS detector.
The European physical journal / C Particles and fields, 80(8):737, and PUBDB-2020-03039, arXiv:2004.14060. CERN-EP-2020-044.
doi: 10.1140/epjc/s10052-020-8102-8.

ATLAS Collaboration.
Search for chargino-neutralino production with mass splittings near the electroweak scale in three-lepton final states in $\sqrt{s}$=13 TeV pp collisions with the ATLAS detector.
Physical review / D D, 101(7):072001, and PUBDB-2020-02526, arXiv:1912.08479. CERN-EP-2019-263.
doi: 10.1103/PhysRevD.101.072001.

ATLAS Collaboration.
Search for dijet resonances in events with an isolated charged lepton using $\sqrt{s} = 13$ TeV proton-proton collision data collected by the ATLAS detector.
Journal of high energy physics, 2020(6):151, and PUBDB-2020-02949, arXiv:2002.11325. CERN-EP-2019-276.
doi: 10.1007/JHEP06(2020)151.

ATLAS Collaboration.
Search for direct production of electroweakinos in final states with missing transverse momentum and a Higgs boson decaying into photons in pp collisions at $\sqrt{s}$ = 13 TeV with the ATLAS detector.
Journal of high energy physics, 10(10):005, and PUBDB-2020-04625, arXiv:2004.10894. CERN-EP-2019-204.
doi: 10.1007/JHEP10(2020)005.

ATLAS Collaboration.
Search for direct production of electroweakinos in final states with one lepton, missing transverse momentum and a Higgs boson decaying into two b-jets in pp collisions at $\sqrt{s} = 13$ TeV with the ATLAS detector.
The European physical journal / C, 80(8):691, and PUBDB-2020-04637, arXiv:1909.09226. CERN-EP-2019-188. arXiv:1909.09226. CERN-EP-2019-188.
doi: 10.1140/epjc/s10052-020-8050-3.

ATLAS Collaboration.
Search for direct stau production in events with two hadronic τ-leptons in $\sqrt{s} = 13$ TeV pp collisions with the ATLAS detector.
Physical review / D D, 101(3):032009, and PUBDB-2020-02533, arXiv:1911.06660. CERN-EP-2019-191.
doi: 10.1103/PhysRevD.101.032009.

ATLAS Collaboration.
Search for displaced vertices of oppositely charged leptons from decays of long-lived particles in pp collisions at $\sqrt{s}$ =13 TeV with the ATLAS detector.
Physics letters / B, 801:135114 (1, and PUBDB-2021-00375, arXiv:1907.10037. CERN-EP-2019-139.
doi: 10.1016/j.physletb.2019.135114.

ATLAS Collaboration.
Search for electroweak production of charginos and sleptons decaying into final states with two leptons and missing transverse momentum in $\sqrt{s} = 13$ TeV pp collisions using the ATLAS detector.
The European physical journal / C Particles and fields, 80(2):123, and PUBDB-2020-02638, arXiv:1908.08215. CERN-EP-2019-106.
doi: 10.1140/epjc/s10052-019-7594-6.

ATLAS Collaboration.
Search for flavour-changing neutral currents in processes with one top quark and a photon using 81 fb^{-1} of pp collisions at $\sqrt{s} = 13$ TeV with the ATLAS experiment.
Physics letters / B, 800:135082, and PUBDB-2019-05089, arXiv:1908.08461. CERN-EP-2019-155.
doi: 10.1016/j.physletb.2019.135082.

ATLAS Collaboration.
Search for heavy Higgs bosons decaying into two tau leptons with the ATLAS detector using pp collisions at $\sqrt{s} = 13$ TeV.
Physical review letters, 125(5):051801, and PUBDB-2020-02959, arXiv:2002.12223. CERN-EP-2020-014.
doi: 10.1103/PhysRevLett.125.051801.

ATLAS Collaboration.
Search for heavy neutral Higgs bosons produced in association with b-quarks and decaying into b-quarks at $\sqrt{s} = 13$ TeV with the ATLAS detector.
Physical review / D, 102(3):032004, and PUBDB-2020-04603, arXiv:1907.02749. CERN-EP-2019-092.
doi: 10.1103/PhysRevD.102.032004.

ATLAS Collaboration.
Search for Heavy Resonances Decaying into a Photon and a Hadronically Decaying Higgs Boson in pp Collisions at $\sqrt{s}$ = 13 TeV with the ATLAS Detector.
Physical review letters, 125(25):251802 (1, and PUBDB-2020-05247, arXiv:2008.05928. CERN-EP-2020-128. CERN preprint ID: CERN-EP-2020-128.
doi: 10.1103/PhysRevLett.125.251802.

ATLAS Collaboration.
Search for Higgs Boson Decays into a Z Boson and a Light Hadronically Decaying Resonance Using 13 TeV pp Collision Data from the ATLAS Detector.
Physical review letters, 125(22):221802 (1, and PUBDB-2020-05255, arXiv:2004.01678. CERN-EP-2020-033.
doi: 10.1103/PhysRevLett.125.221802.

ATLAS Collaboration.
Search for Higgs boson decays into two new low-mass spin-0 particles in the 4b channel with the ATLAS detector using pp collisions at $\sqrt{s} = 13$ TeV.
Physical review / D, 102(11):112006, and PUBDB-2020-05101, arXiv:2005.12236. CERN-EP-2020-067.
doi: 10.1103/PhysRevD.102.112006.

A. Basalaev.
Search for Higgs boson in the final state with two leptons and a photon produced in pp collisions at a center-of-mass energy of $\sqrt{s}$ = 13 TeV with the ATLAS detector.
40th International Conference on High Energy Physics, Prague(online) (Czech Republic), 28 Jul 2020 - 6 Aug 2020.
Proceedings of Science / International School for Advanced Studies, vol. (ICHEP2020):094, and PUBDB-2020-05032.
SISSA, Trieste.

ATLAS Collaboration.
Search for light long-lived neutral particles produced in pp collisions at $\sqrt{s}$ = 13 TeV and decaying into collimated leptons or light hadrons with the ATLAS detector.

The European physical journal / C Particles and fields, 80(5):450, and PUBDB-2020-02609, arXiv:1909.01246. CERN-EP-2019-140.
doi: 10.1140/epjc/s10052-020-7997-4.

ATLAS Collaboration.
Search for long-lived, massive particles in events with a displaced vertex and a muon with large impact parameter in pp collisions at $\sqrt{s} = 13$ TeV with the ATLAS detector.
Physical review / D, 102(3):032006, and PUBDB-2020-04629, arXiv:2003.11956. CERN-EP-2019-219.
doi: 10.1103/PhysRevD.102.032006.

ATLAS Collaboration.
Search for long-lived neutral particles produced in pp collisions at $\sqrt{s} = 13$ TeV decaying into displaced hadronic jets in the ATLAS inner detector and muon spectrometer.
Physical review / D D, 101(5):052013, and PUBDB-2020-02530, arXiv:1911.12575. CERN-EP-2019-240.
doi: 10.1103/PhysRevD.101.052013.

ATLAS Collaboration.
Search for Magnetic Monopoles and Stable High-Electric-Charge Objects in 13 Tev Proton-Proton Collisions with the ATLAS Detector.
Physical review letters, 124(3):031802, and PUBDB-2020-04586, arXiv:1905.10130. CERN-EP-2019-084.
doi: 10.1103/PhysRevLett.124.031802.

ATLAS Collaboration.
Search for new non-resonant phenomena in high-mass dilepton final states with the ATLAS detector.
Journal of high energy physics, 11(11):5, and PUBDB-2020-04588, arXiv:2006.12946. CERN-EP-2020-066.
doi: 10.1007/JHEP11(2020)005.

ATLAS Collaboration.
Search for new resonances in mass distributions of jet pairs using 139 fb^{-1} of pp collisions at $\sqrt{s} = 13$ TeV with the ATLAS detector.
Journal of high energy physics, 2020(3):145, and PUBDB-2020-02556, arXiv:1910.08447. CERN-EP-2019-162.
doi: 10.1007/JHEP03(2020)145.

ATLAS Collaboration.
Search for non-resonant Higgs boson pair production in the $bb\ell\nu\ell\nu$ final state with the ATLAS detector in pp collisions at $\sqrt{s} = 13$ TeV.
Physics letters / B, 801:135145, and PUBDB-2020-02639, arXiv:1908.06765. CERN-EP-2019-143.
doi: 10.1016/j.physletb.2019.135145.

ATLAS Collaboration.
Search for pairs of scalar leptoquarks decaying into quarks and electrons or muons in $\sqrt{s} = 13$ TeV pp collisions with the ATLAS detector.
Journal of high energy physics, 10(10):112 (1, and PUBDB-2020-04265, arXiv:2006.05872. CERN-EP-2020-084.
doi: 10.1007/JHEP10(2020)112.

ATLAS Collaboration.
Search for resonances decaying into a weak vector boson and a Higgs boson in the fully hadronic final state produced in proton−proton collisions at $\sqrt{s} = 13$ TeV with the ATLAS detector.
Physical review / D, 102(11):112008 (1, and PUBDB-2020-05098, arXiv:2007.05293. CERN-EP-2020-073.
doi: 10.1103/PhysRevD.102.112008.

ATLAS Collaboration.
Search for squarks and gluinos in final states with same-sign leptons and jets using 139 fb^{-1} of data collected with the ATLAS detector.
Journal of high energy physics, 2006(6):46, and PUBDB-2020-02572, arXiv:1909.08457. CERN-EP-2019-161.
doi: 10.1007/JHEP06(2020)046.

ATLAS Collaboration.
Search for the $HH \rightarrow b\bar{b}b\bar{b}$ process via vector-boson fusion production using proton-proton collisions at $\sqrt{s} = 13$ TeV with the ATLAS detector.
Journal of high energy physics, 2020(7):108, and PUBDB-2020-02947, arXiv:2001.05178. CERN-EP-2019-267.
doi: 10.1007/JHEP07(2020)108.

ATLAS Collaboration.
Search for the Higgs boson decays $H \rightarrow ee$ and $H \rightarrow e\mu$ in pp collisions at $\sqrt{s} = 13$ TeV with the ATLAS detector.
Physics letters / B, 801:135148, and PUBDB-2020-02568, arXiv:1909.10235. CERN-EP-2019-184.
doi: 10.1016/j.physletb.2019.135148.

ATLAS Collaboration.
Search for top squarks in events with a Higgs or Z boson using 139 fb^{-1} of pp collision data at $\sqrt{s} = 13$ TeV with the ATLAS detector.
The European physical journal / C, 80(11):1080 (1, and PUBDB-2020-05100, arXiv:2006.05880. CERN-EP-2020-074.
doi: 10.1140/epjc/s10052-020-08469-8.

ATLAS Collaboration.
Search for $t\bar{t}$ resonances in fully hadronic final states in pp collisions at $\sqrt{s} = 13$ TeV with the ATLAS detector.
Journal of high energy physics, 10(10):61 (1, and PUBDB-2020-04587, arXiv:2005.05138. CERN-EP-2020-055.
doi: 10.1007/JHEP10(2020)061.

ATLAS Collaboration.
Searches for electroweak production of supersymmetric particles with compressed mass spectra in $\sqrt{s} = 13$ TeV pp collisions with the ATLAS detector.
Physical review / D D, 101(5):052005, and PUBDB-2020-02527, arXiv:1911.12606. CERN-EP-2019-242.
doi: 10.1103/PhysRevD.101.052005.

ATLAS Collaboration.
Searches for lepton-flavour-violating decays of the Higgs boson in $\sqrt{s} = 13$ TeV pp collisions with the ATLAS detector.
Physics letters / B, 800:135069, and PUBDB-2019-05057, arXiv:1907.06131. CERN-EP-2019-126.
doi: 10.1016/j.physletb.2019.135069.

ATLAS Collaboration.
The ABC130 barrel module prototyping programme for the ATLAS strip tracker.
Journal of Instrumentation, 15(09):P09004, and PUBDB-2021-00611, arXiv:2009.03197.
doi: 10.1088/1748-0221/15/09/P09004.

ATLAS Collaboration.
The ATLAS ITk strip detector system for the High Luminosity LHC upgrade.
Nuclear instruments & methods in physics research / A, 958:162053, and PUBDB-2021-00413.
doi: 10.1016/j.nima.2019.04.007.

ATLAS Collaboration.
Transverse momentum and process dependent azimuthal anisotropies in $\sqrt{s_{\mathrm{NN}}} = 8.16$ TeV p+Pb collisions with the ATLAS detector.
The European physical journal / C Particles and fields, 80(1):73, and PUBDB-2020-02543, arXiv:1910.13978. CERN-EP-2019-217.
doi: 10.1140/epjc/s10052-020-7624-4.

ATLAS Collaboration.
Z boson production in Pb+Pb collisions at $\sqrt{s_{\mathrm{NN}}}$= 5.02 TeV measured by the ATLAS experiment.
Physics letters / B, B802:135262, and PUBDB-2020-02546, arXiv:1910.13396. CERN-EP-2019-182.
doi: 10.1016/j.physletb.2020.135262.

I. Melzer-Pellmann.
Searches for Supersymmetry.
1831205. European Physical Society Conference on High Energy Physics, Ghent (Belgium), 10 Jul 2019 - 17 Jul 2019.
Proceedings of Science / International School for Advanced Studies, vol. (EPS-HEP2019):710, and PUBDB-2020-05249. SISSA, Trieste.
doi: 10.22323/1.364.0710.

G. Balbi et al.
Measurements of Single Event Upset in ATLAS IBL.
Journal of Instrumentation, 15(06):P06023, and PUBDB-2020-02513, arXiv:2004.14116.
doi: 10.1088/1748-0221/15/06/P06023.

C. Bierlich et al.
Robust Independent Validation of Experiment and Theory: Rivet version 3.
SciPost physics, 8(2):026 (1, and PUBDB-2021-00487, arXiv:1912.05451. MCnet-19-26.
doi: 10.21468/SciPostPhys.8.2.026.

T. Bisanz et al.
EUTelescope: A modular reconstruction framework for beam telescope data.
Journal of Instrumentation, 15(09):P09020, and PUBDB-2020-04555, arXiv:2011.10356.
doi: 10.1088/1748-0221/15/09/P09020.

L. Brenner et al.
Comparison of unfolding methods using RooFitUnfold.
International journal of modern physics / A, 35(24):2050145, and PUBDB-2021-00464, arXiv:1910.14654.
doi: 10.1142/S0217751X20501456.

M. Defranchis.
Probing QCD using top quark pair production at $\sqrt{s}$ = 13TeV in CMS.
1781734. European Physical Society Conference on High Energy Physics, Ghent (Belgium), 10 Jul 2019 - 17 Jul 2019.
Proceedings of Science / International School for Advanced Studies, vol. (EPS-HEP2019):679, and PUBDB-2020-05250, arXiv:2002.09288.
SISSA, Trieste.
doi: 10.22323/1.364.0679.

J. C. Hönig et al.
Investigation of nitrogen enriched silicon for particle detectors.
Journal of Instrumentation, 15(05):P05006, and PUBDB-2021-00446.
doi: 10.1088/1748-0221/15/05/P05006.

S. Jaster-Merz et al.
Development of a Beam Profile Monitor based on Silicon Strip Sensors for Low-Charge Electron Beams.
1. 4th European Advanced Accelerator Concepts Workshop, Elba (Italy), 15 Sep 2019 - 20 Sep 2019.
Journal of physics / Conference Series, vol. 15961:012047, and PUBDB-2020-04285.
IOP Publ., Bristol.
doi: 10.1088/1742-6596/1596/1/012047.

I. Kremastiotis et al.
Design and Characterization of the CLICTD Pixelated Monolithic Sensor Chip.
IEEE transactions on nuclear science, 67(10):2263, and PUBDB-2021-00520.
doi: 10.1109/TNS.2020.3019887.

A. Luszczak and H. Kowalski.
Investigation of High Energy Behaviour of HERA Data.
Physics letters / B, 802:135199, and PUBDB-2020-05112, arXiv:1903.09719.
doi: 10.1016/j.physletb.2020.135199.

L. Nozka et al.
Performance studies of new optics for the time-of-flight detector of the AFP project.
Optics express, 28(13):19783, and PUBDB-2020-03243.
doi: 10.1364/OE.394582.

P. Pani et al.
Characterization of monolithic GAGG:Ce coupled to both PMT and SiPM array for gamma imaging in Nuclear Medicine.
Journal of Instrumentation, 15(05):C05011 (1, and PUBDB-2021-00251.
doi: 10.1088/1748-0221/15/05/C05011.

F. Rühr et al.
Testbeam studies of barrel and end-cap modules for the ATLAS ITk strip detector before and after irradiation.
Nuclear instruments & methods in physics research / A, 979:164430 (1, and PUBDB-2021-00252.
doi: 10.1016/j.nima.2020.164430.

T. Sykora and ATLAS Collaboration.
ATLAS Forward Proton Time-of-Flight Detector: LHC Run2 performance and experiences.
10. International Conference on Instrumentation for Colliding Beam Physics, Novosibirsk (Russian Federation), 24 Feb 2020 - 28 Feb 2020.
Journal of Instrumentation, vol. 1510:C10004 (1, and PUBDB-2021-00538, ATL-FWD-PROC-2020-001.
Inst. of Physics, London.
doi: 10.1088/1748-0221/15/10/C10004.

Y. C. Yap.
Recent observation and measurements of diboson processes from the ATLAS experiment.
Modern physics letters / A, 35(28):2030013, and PUBDB-2021-00346, arXiv:2006.08285.
doi: 10.1142/S021773232030013X.

Ph.D. Thesis

J.-H. Arling.
Detection and Identification of Electrons and Photons - Applications in the ATLAS Experiment, for the ATLAS ITk Detector and at the DESY II Test Beam.
Technical University of Dortmund, Hamburg, 2020.

F. Braren.
Measurement and Interpretation of Higgs Boson Differential Cross Sections in the Diphoton Decay Channel and Measurement of the Photon Identification Efficiency in the ATLAS Experiment.
University of Hamburg, 2020.

V. Kitali.
Search for invisible decays of the Higgs boson produced invector-boson fusion in final states with jets and large missingtransverse energy with the ATLAS detector.
University of Hamburg, 2020.

X. Lou.
Search for Dark Matter Produced in Association with Heavy Standard Model Particles at s√=13 TeV with the ATLAS Detector at the LHC.
University of Hamburg, 2020.

D. Rauch.
Aspects of Rare Production and Decay Processes of the Higgs Boson.
University of Hamburg, 2020.

E. Rossi.
Characterization of Silicon Modules and Sensors for the ATLAS Inner Tracker Strip Detector.
Universität Hamburg, Hamburg, 2020.

Belle II

Published

F. Abudinén et al.
Search for Axionlike Particles Produced in e^+e^- Collisions at Belle II.
Physical review letters, 125(16):161806, and PUBDB-2020-03957, arXiv:2007.13071. Belle II Preprint 2020-001. KEK Preprint 2020-10. arXiv:2007.13071.
doi: 10.1103/PhysRevLett.125.161806.

Belle Collaboration.
Dalitz analysis of $D^0 \to K^-\pi^+\eta$ decays at Belle.
Physical review / D D, 102(1):1, and PUBDB-2020-03128, arXiv:2003.07759. KEK Preprint 2019-60. Belle Preprint 2020-04. KEK Preprint 2020-04. UCHEP-20-01.
doi: 10.1103/PhysRevD.102.012002.

Belle Collaboration.
Evidence for a vector charmonium-like state in $e^+e^- \to D_s^+ D_{s2}^*(2573)^-$+c.c.
Physical review / D D, 101(9):091101: 1, and PUBDB-2020-03054, arXiv:2004.02404. arXiv:2004.02404.
doi: 10.1103/PhysRevD.101.091101.

Belle Collaboration.
Measurement of $R(D)$ and $R(D^*)$ with a Semileptonic Tagging Method.
Physical review letters, 124(16):161803, and PUBDB-2020-02372, arXiv:1910.05864. Belle-2019-18. KEK-2019-40. arXiv:1910.05864. Belle-2019-18. KEK-2019-40.
doi: 10.1103/PhysRevLett.124.161803.

Belle Collaboration.
Measurement of the charm-mixing parameter y_{CP} in $D^0 \to K_S^0\omega$ decays at Belle.
Physical review / D, 102(7):071102, and PUBDB-2020-03954, arXiv:1912.10912. Belle Preprint 2019-22. KEK Preprint 2019-52.
doi: 10.1103/PhysRevD.102.071102.

Belle Collaboration.
Observation of the Radiative Decays of $(1S)$ to χ_{c1}.
Physical review letters, 124(12):122001, and PUBDB-2020-02371, arXiv:1910.10915. Belle preprint 2019-21.
doi: 10.1103/PhysRevLett.124.122001.

Belle Collaboration.
Search for a doubly charged DDK bound state in $(1S, 2S)$ inclusive decays and via direct production in e^+e^- collisions at $\sqrt{s}$ = 10.520, 10.580, and 10.867 GeV.
Physical review / D, 102(11):112001 (1, and PUBDB-2020-04747, arXiv:2008.13341. Belle Preprint 2020-10. KEK Preprint 2020-11. arXiv:2008.13341. Belle Preprint 2020-10. KEK Preprint 2020-11.
doi: 10.1103/PhysRevD.102.112001.

Belle Collaboration.
Search for $B^+ \to \mu^+\nu_\mu$ and $B^+ \to \mu^+ N$ with inclusive tagging.
Physical review / D, 101(3):032007, and PUBDB-2021-00557, arXiv:1911.03186. Belle Preprint 2019-17. KEK Preprint 2019-39.
doi: 10.1103/PhysRevD.101.032007.

Belle Collaboration.
Search for B^0 decays to invisible final states $(+\gamma)$ at Belle.
Physical review / D D, 102(1):1, and PUBDB-2020-03125, arXiv:2004.03826.
doi: 10.1103/PhysRevD.102.012003.

Belle Collaboration.
Search for lepton-number- and baryon-number-violating tau decays at Belle.
Physical review / D, 102(11):111101, and PUBDB-2021-00014, arXiv:2010.15361. Belle Preprint 2020-16. KEK Preprint 2020-33.
doi: 10.1103/PhysRevD.102.111101.

Belle Collaboration.
Search for transitions from $\Upsilon(4S)$ and $\Upsilon(5S)$ to $\eta_b(1S)$ and $\eta_b(2S)$ with emission of an ω meson.
Physical review / D, 102(9):092011 (1, and PUBDB-2020-04928, arXiv:2009.11720. Belle Preprint 2020-15. KEK Preprint 2020-17.
doi: 10.1103/PhysRevD.102.092011.

Belle Collaboration.
Study of $B \to p\bar{p}\pi\pi$.
Physical review / D D, 101(5):052012, and PUBDB-2020-03050, arXiv:1912.05999. Belle Preprint 2019-16. KEK Preprint 2019-23.
doi: 10.1103/PhysRevD.101.052012.

Belle Collaboration.
Study of electromagnetic decays of orbitally excited Ξ_c baryons.
Physical review / D, 102(7):071103 (1, and PUBDB-2020-04249, arXiv:2009.03951. Belle Preprint 2019-07 KEK Prepint 2020-6.
doi: 10.1103/PhysRevD.102.071103.

Belle Collaboration.
Update of inclusive cross sections of single and pairs of identified light charged hadrons.
Physical review / D D, 101(9):092004, and PUBDB-2020-03037, arXiv:2001.10194. Belle Preprint 2020-01. KEK Preprint 2019-56.
doi: 10.1103/PhysRevD.101.092004.

Belle II Collaboration.
Global decay chain vertex fitting at Belle II.
Nuclear instruments & methods in physics research / A, 976:164269, and PUBDB-2021-00550, arXiv:1901.11198.
doi: 10.1016/j.nima.2020.164269.

B. Spruck.
Belle II Pixel Detector Commissioning and Operational Experience.
1816956. The 28th International Workshop on Vertex Detectors, Lopud (Croatia), 13 Oct 2019 - 18 Oct 2019.
Proceedings of Science / International School for Advanced Studies,1, and PUBDB-2020-04800.
SISSA, Trieste.
doi: 10.22323/1.373.0015.

Belle-II Collaboration.
Measurement of the integrated luminosity of the Phase 2 data of the Belle II experiment.
Chinese physics / C High energy physics and nuclear physics C, 44(2):021001, and PUBDB-2020-00005, arXiv:1910.05365.
doi: 10.1088/1674-1137/44/2/021001.

Belle-II Collaboration.
The Belle II Physics Book.
Progress of theoretical and experimental physics, 2020(2):029201, and PUBDB-2021-00641, arXiv:1808.10567. KEK Preprint 2018-27. BELLE2-PUB-PH-2018-001. FERMILAB-PUB-18-398-T. JLAB-THY-18-2780. INT-PUB-18-047. UWThPh 2018-26.
doi: 10.1093/ptep/ptaa008.

Belle-II Collaboration and DEPFET Collaboration and PXD Collaboration.
Belle II pixel detector: Performance of final DEPFET modules.
Nuclear instruments & methods in physics research / A, 958:162222, and PUBDB-2021-00501.
doi: 10.1016/j.nima.2019.05.063.

S. Camarda et al.
DYTurbo: fast predictions for Drell–Yan processes.
The European physical journal / C, 80(5):251, and PUBDB-2021-00642, arXiv:1910.07049.
doi: 10.1140/epjc/s10052-020-7757-5.

S. Camarda et al.
Erratum to: DYTurbo: fast predictions for Drell–Yan processes.
The European physical journal / C, 80(5):440, and PUBDB-2021-00643, arXiv:1910.07049.
doi: 10.1140/epjc/s10052-020-7972-0.

R. Cheaib.
Towards First Results on V_{ub} and V_{cb} with the Belle II experiment.
40th International Conference on High Energy physics, Prague (Czech Republic), 28 Jul 2020 - 6 Aug 2020.
Proceedings of Science / International School for Advanced Studies, vol. (ICHEP2020):390, and PUBDB-2020-04996.
SISSA, Trieste.
doi: 10.3204/PUBDB-2020-04996.

K. Chilikin et al.
First search for the η_{c2}(1D) in B decays at Belle.
Journal of high energy physics, 2020(5):34, and PUBDB-2020-03043, arXiv:2003.08335. Belle Preprint 2020-02. KEK Preprint 2019-58.
doi: 10.1007/JHEP05(2020)034.

S. T. Cunliffe.
Dark sector physics with Belle II.
European Physical Society Conference on High Energy Physics, Ghent (Belgium), 10 Jul 2019 - 17 Jul 2019.
Proceedings of Science / International School for Advanced Studies,1, and PUBDB-2020-03889.
SISSA, Trieste.

M. Duerr et al.
Invisible and displaced dark matter signatures at Belle II.
Journal of high energy physics, 2020(2):39, and PUBDB-2020-00738, DESY-19-141. OUTP-19-10P. TTK-19-46. arXiv:1911.03176.
doi: 10.1007/JHEP02(2020)039.

A. Gellrich, T. Kuhr and D. Knittel.
Operating the Belle II Collaborative Services and Tools.
9. 24th International Conference on Computing in High Energy and Nuclear Physics, Adelaide (Australia), 4 Nov 2019 - 8 Nov 2019.
The European physical journal / Web of Conferences, vol. 2459:08009, and PUBDB-2020-04785.
EDP Sciences, Les Ulis.
doi: 10.1051/epjconf/202024508009.

A. Glazov.
Defiducialization: providing experimental measurements for accurate fixed-order predictions.
The European physical journal / C, 80(9):1, and PUBDB-2020-03608, arXiv:2001.02933. DESY-20-001.
doi: 10.1140/epjc/s10052-020-08435-4.

Group, Belle II Tracking.
Track finding at Belle II.
Computer physics communications, 259:107610, and PUBDB-2020-05261, arXiv:2003.12466. arXiv:2003.12466.
doi: 10.1016/j.cpc.2020.107610.

II, Belle.
Search for an Invisibly Decaying Z' Boson at Belle II in $e^+e^- \to \mu^+\mu^-(e^\pm\mu^\mp)$ Plus Missing Energy Final States.
Physical review letters, 124(14):141801 (1, and PUBDB-2020-03705, arXiv:1912.11276. Belle II Preprint 2019-002. KEK Preprint 2019-55.
doi: 10.1103/PhysRevLett.124.141801.

Y. T. Lai et al.
Development of the Level-1 track trigger with Central Drift Chamber detector in Belle II experiment and its performance in SuperKEKB 2019 Phase 3 operation.
Journal of Instrumentation, 15(06):C06063, and PUBDB-2021-00440.
doi: 10.1088/1748-0221/15/06/C06063.

LHCb Collaboration.
First branching fraction measurement of the suppressed decay $\Xi_c^0 \to \pi^-\Lambda_c^+$.
Physical review / D, 102(7):071101 (1, and PUBDB-2021-00415, arXiv:2007.12096. CERN-EP-2020-129. LHCb-PAPER-2020-016.
doi: 10.1103/PhysRevD.102.071101.

LHCb Collaboration.
Measurement of $\psi(2S)$ production cross-sections in proton-proton collisions at $\sqrt{s}$ = 7 and 13 TeV.
The European physical journal / C, 80(3):185, and PUBDB-2021-00354, arXiv:1908.03099. CERN-EP-2019-150. LHCb-PAPER-2018-049.
doi: 10.1140/epjc/s10052-020-7638-y.

LHCb Collaboration.
Measurement of CP violation in $B^0 \to D^{*\pm}D^\mp$ decays.
Journal of high energy physics, 03(3):147 (1, and PUBDB-2021-00173, arXiv:1912.03723. LHCb-PAPER-2019-036. CERN-EP-2019-264.
doi: 10.1007/JHEP03(2020)147.

LHCb Collaboration.
Measurement of the $\eta_c(1S)$ production cross-section in pp collisions at $\sqrt{s} = 13$ TeV.
The European physical journal / C, 80(3):191 (1, and PUBDB-2021-00436, arXiv:1911.03326. LHCb-PAPER-2019-024. CERN-EP-2019-214.
doi: 10.1140/epjc/s10052-020-7733-0.

LHCb Collaboration.
Measurement of the relative branching fractions of $B^+ \to h^+h'^+h'^-$ decays.
Physical review / D, 102(11):112010 (1, and PUBDB-2021-00426, arXiv:2010.11802. CERN-EP-2020-189. LHCb-PAPER-2020-031.
doi: 10.1103/PhysRevD.102.112010.

LHCb Collaboration.
Observation of a new baryon state in the $\Lambda_b^0\pi^+\pi^-$ mass spectrum.
Journal of high energy physics, 06(6):136, and PUBDB-2021-00445, arXiv:2002.05112. CERN-EP-2020-013. LHCb-PAPER-2019-045.
doi: 10.1007/JHEP06(2020)136.

LHCb Collaboration.
Observation of Enhanced Double Parton Scattering in Proton-Lead Collisions at $\sqrt{s_{NN}}$ =8.16 TeV.
Physical review letters, 125(21):212001 (1, and PUBDB-2021-00379, arXiv:2007.06945. LHCb-PAPER-2020-010. CERN-EP-2020-119.
doi: 10.1103/PhysRevLett.125.212001.

LHCb Collaboration.
Observation of the semileptonic decay $B^+ \to p\bar{p}\mu^+\nu_\mu$.
Journal of high energy physics, 03(3):146 (1, and PUBDB-2021-00176, arXiv:1911.08187. LHCb-PAPER-2019-034. CERN-EP-2019-236.
doi: 10.1007/JHEP03(2020)146.

LHCb Collaboration.
Search for $A' \to \mu^+\mu^-$ Decays.
Physical review letters, 124(4):041801 (1, and PUBDB-2021-00400, arXiv:1910.06926. LHCb-PAPER-2019-031. CERN-EP-2019-212.
doi: 10.1103/PhysRevLett.124.041801.

LHCb Collaboration.
Search for CP violation in $Xi_c^+ \to pK^-\pi^+$ decays using model-independent techniques.
The European physical journal / C, 80(10):986 (1, and PUBDB-2021-00437, arXiv:2006.03145. CERN-EP-2020-069. LHCb-PAPER-2019-026.
doi: 10.1140/epjc/s10052-020-8365-0.

LHCb Collaboration.
Search for the Rare Decays $B_s^0 \to e^+e^-$ and $B^0 \to e^+e^-$.
Physical review letters, 124(21):211802 (1, and PUBDB-2021-00399, arXiv:2003.03999. LHCb-PAPER-2020-001. CERN-EP-2020-023.
doi: 10.1103/PhysRevLett.124.211802.

LHCb Collaboration.
Strong constraints on the $b \to s\gamma$ photon polarisation from $B^0 \to K^{*0}e^+e^-$ decays.
Journal of high energy physics, 12(12):81 (1, and PUBDB-2021-00431, arXiv:2010.06011. LHCb-PAPER-2020-020. CERN-EP-2020-176.
doi: 10.1007/JHEP12(2020)081.

LHCb Collaboration.
Study of the $\psi_2(3823)$ and $\chi_{c1}(3872)$ states in $B^+ \to \left(J\psi\pi^+\pi^-\right)K^+$ decays.
Journal of high energy physics, 08(8):123, and PUBDB-2021-00358, arXiv:2005.13422. CERN-EP-2020-071. LHCb-PAPER-2020-009.
doi: 10.1007/JHEP08(2020)123.

S. Longo et al.
CsI(Tl) pulse shape discrimination with the Belle II electromagnetic calorimeter as a novel method to improve particle identification at electron–positron colliders.
Nuclear instruments & methods in physics research / A, 982:164562, and PUBDB-2021-00498, arXiv:2007.09642.
doi: 10.1016/j.nima.2020.164562.

F. Tenchini.
Performance of High-Level Reconstruction at Belle II.
Proceedings of Science / International School for Advanced Studies, 377:1, and PUBDB-2020-04395.
doi: 10.22323/1.377.0054.

Master Thesis

S. Stengel.
Optimization of the π^0 reconstruction selections for the Belle II experiment.
Johannes Gutenberg University, Institute of Nuclear Physics Mainz, Mainz, 2020.

CMS

Published

I. Melzer-Pellmann.
Searches for Supersymmetry.
1831205. European Physical Society Conference on High Energy Physics, Ghent (Belgium), 10 Jul 2019 - 17 Jul 2019.
Proceedings of Science / International School for Advanced Studies, vol. (EPS-HEP2019):710, and PUBDB-2020-05249. SISSA, Trieste.
doi: 10.22323/1.364.0710.

L. Benato et al.
Teaching machine learning with an application in collider particle physics.
09. 5th International Summer School on INtelligent Signal Processing for FrontIEr Research and Industry, Huazhong (China), 12 May 2019 - 26 May 2019.
Journal of Instrumentation, vol. 1509:C09011 (1, and PUBDB-2020-04507.
Inst. of Physics, London.
doi: 10.1088/1748-0221/15/09/C09011.

A. Bermudez Martinez et al.
The transverse momentum spectrum of low mass Drell-Yan production at next-to-leading order in the parton branching methodThe transverse momentum spectrum of low mass Drell–Yan production at next-to-leading order in the parton branching method.
The European physical journal / C Particles and fields, C80(7):598, and PUBDB-2020-02792, arXiv:2001.06488. DESY-20-006.
doi: 10.1140/epjc/s10052-020-8136-y.

T. Bisanz et al.
EUTelescope: A modular reconstruction framework for beam telescope data.
Journal of Instrumentation, 15(09):P09020, and PUBDB-2020-04555, arXiv:2011.10356.
doi: 10.1088/1748-0221/15/09/P09020.

CMS Collaboration.
A measurement of the Higgs boson mass in the diphoton decay channel.
Physics letters / B B, 805:135425, and PUBDB-2020-01716, arXiv:2002.06398. CMS-HIG-19-004. CERN-EP-2020-004.
doi: 10.1016/j.physletb.2020.135425.

CMS Collaboration.
A multi-dimensional search for new heavy resonances decaying to boosted WW, WZ, or ZZ boson pairs in the dijet final state at 13 TeV.
The European physical journal / C Particles and fields C, 80(3):237, and PUBDB-2020-01597, arXiv:1906.05977. CMS-B2G-18-002. CERN-EP-2019-107.
doi: 10.1140/epjc/s10052-020-7773-5.

CMS Collaboration.
A multi-dimensional search for new heavy resonances decaying to boosted WW, WZ, or ZZ boson pairs in the dijet final state at 13 TeV.
The European physical journal / C Particles and fields C, 80(3):237, and PUBDB-2020-01598, arXiv:1906.05977. CMS-B2G-18-002. CERN-EP-2019-107.
doi: 10.1140/epjc/s10052-020-7773-5.

CMS Collaboration.
A search for bottom-type, vector-like quark pair production in a fully hadronic final state in proton-proton collisions at $\sqrt{s} =$ 13 TeV.
Physical review / D, 102(11):112004, and PUBDB-2021-00709, arXiv:2008.09835. CMS-B2G-19-005. CERN-EP-2020-154.
doi: 10.1103/PhysRevD.102.112004.

CMS Collaboration.
A search for the standard model Higgs boson decaying to charm quarks.
Journal of high energy physics, 2003(3):131, and PUBDB-2020-01711, arXiv:1912.01662. CMS-HIG-18-031. CERN-EP-2019-257.
doi: 10.1007/JHEP03(2020)131.

CMS Collaboration.
Beam test performance of prototype silicon detectors for the Outer Tracker for the Phase-2 Upgrade of CMS.
Journal of Instrumentation, 15(03):P03014, and PUBDB-2021-00560.
doi: 10.1088/1748-0221/15/03/P03014.

CMS Collaboration.
Bose-Einstein correlations of charged hadrons in proton-proton collisions at $\sqrt{s} = 13$ Tev.
Journal of high energy physics, 2020(3):14, and PUBDB-2020-01700, arXiv:1910.08815. CMS-FSQ-15-009. CERN-EP-2019-151.
doi: 10.1007/JHEP03(2020)014.

CMS Collaboration.
Calibration of the CMS hadron calorimeters using proton-proton collision data at $\sqrt{s} = 13$ TeV.
Journal of Instrumentation, 15(05):P05002, and PUBDB-2020-02262, arXiv:1910.00079. CMS-PRF-18-001. CERN-EP-2019-179.
doi: 10.1088/1748-0221/15/05/P05002.

CMS Collaboration.
Combined search for supersymmetry with photons in proton-proton collisions at $\sqrt{s} = 13$ TeV.
Physics letters / B, B801:135183, and PUBDB-2020-00481, arXiv:1907.00857. CMS-SUS-18-005. CERN-EP-2019-114.
doi: 10.1016/j.physletb.2019.135183.

CMS Collaboration.
Dependence of inclusive jet production on the anti-k_T distance parameter in pp collisions at $\sqrt{s} = 13$ TeV.
Journal of high energy physics, 12(12):82 (1, and PUBDB-2020-05199, arXiv:2005.05159. CMS-SMP-19-003. CERN-EP-2020-040.
doi: 10.1007/JHEP12(2020)082.

CMS Collaboration.
Determination of the strong coupling constant $\alpha_S(m_Z)$ from measurements of inclusive $W^{\pm}$ and Z boson production cross sections in proton-proton collisions at $\sqrt{s} = 7$ and 8 TeV.
Journal of high energy physics, 2020(6):18, and PUBDB-2020-02640, arXiv:1912.04387. CMS-SMP-18-005. CERN-EP-2019-259.
doi: 10.1007/JHEP06(2020)018.

CMS Collaboration.
Evidence for Top Quark Production in Nucleus-Nucleus Collisions.
Physical review letters, 125(22):222001 (1, and PUBDB-2021-00589, arXiv:2006.11110. CMS-HIN-19-001. CERN-EP-2020-101.
doi: 10.1103/PhysRevLett.125.222001.

CMS Collaboration.
Evidence for WW production from double-parton interactions in proton-proton collisions at $\sqrt{s} = 13$ TeV.
The European physical journal / C, 80(1):41, and PUBDB-2020-00797, arXiv:1909.06265.
doi: 10.1140/epjc/s10052-019-7541-6.

CMS Collaboration.
Extraction and validation of a new set of CMS PYTHIA8 tunes from underlying-event measurements.
The European physical journal / C, 80(1):4, and PUBDB-2020-00479, arXiv:1903.12179. CMS-GEN-17-001. CERN-EP-2019-007.
doi: 10.1140/epjc/s10052-019-7499-4.

CMS Collaboration.
Identification of heavy, energetic, hadronically decaying particles using machine-learning techniques.
Journal of Instrumentation, 15(06):P06005, and PUBDB-2020-02644, arXiv:2004.08262. FERMILAB-PUB-20-191-CMS. CMS-JME-18-002. CERN-EP-2020-037.
doi: 10.1088/1748-0221/15/06/P06005.

CMS Collaboration.
Inclusive search for highly boosted Higgs bosons decaying to bottom quark-antiquark pairs in proton-proton collisions at $\sqrt{s} = 13$ TeV.
Journal of high energy physics, 12(12):85 (1, and PUBDB-2020-05200, arXiv:2006.13251. CMS-HIG-19-003. CERN-EP-2020-107.
doi: 10.1007/JHEP12(2020)085.

CMS Collaboration.
Investigation into the event-activity dependence of Υ(nS) relative production in proton-proton collisions at $\sqrt{s} = 7$ TeV.
Journal of high energy physics, 2020(11):1, and PUBDB-2020-05203, arXiv:2007.04277. CMS-BPH-14-009. CERN-EP-2020-075.
doi: 10.1007/JHEP11(2020)001.

CMS Collaboration.
Measurement of $B_c(2S)^+$ and $B_c^*(2S)^+$ cross section ratios in proton-proton collisions at $\sqrt{s} = 13$ TeV.
Physical review / D, 102(9):092007, and PUBDB-2021-00496, arXiv:2008.08629. CMS-BPH-19-001. CERN-EP-2020-146.
doi: 10.1103/PhysRevD.102.092007.

CMS Collaboration.
Measurement of CKM matrix elements in single top quark t-channel production in proton-proton collisions at $\sqrt{s} = 13$ TeV.
Physics letters / B, 808:135609, and PUBDB-2020-02833, arXiv:2004.12181. FERMILAB-PUB-20-190-CMS. CMS-TOP-17-012. CERN-EP-2020-047.
doi: 10.1016/j.physletb.2020.135609.

CMS Collaboration.
Measurement of differential cross sections and charge ratios for t-channel single top quark production in proton-proton collisions at $\sqrt{s} = 13$ TeV.
The European physical journal / C Particles and fields, 80(5):370, and PUBDB-2020-02261, DFF-10-96. hep-

th/9610092. arXiv:1907.08330. CMS-TOP-17-023. CERN-EP-2019-138.
doi: 10.1140/epjc/s10052-020-7858-1.

CMS Collaboration.
Measurement of electroweak production of a Wboson in association with two jets in proton–proton collisions at s√=13TeV.
The European physical journal / C, 80(1):43, and PUBDB-2020-00792, arXiv:1903.04040.
doi: 10.1140/epjc/s10052-019-7585-7.

CMS Collaboration.
Measurement of properties of $B^0_s \to \mu^+\mu^-$ decays and search for $B^0 \to \mu^+\mu^-$ with the CMS experiment.
JHEP reports, 04(4):188, and PUBDB-2020-01697, arXiv:1910.12127. CMS-BPH-16-004. CERN-EP-2019-215.
doi: 10.1007/JHEP04(2020)188.

CMS Collaboration.
Measurement of quark- and gluon-like jet fractions using jet charge in PbPb and pp collisions at 5.02 TeV.
Journal of high energy physics, 2020(7):1, and PUBDB-2020-03492, arXiv:2004.00602. CMS-HIN-18-018. CERN-EP-2020-019.
doi: 10.1007/JHEP07(2020)115.

CMS Collaboration.
Measurement of $t\bar{t}$ normalised multi-differential cross sections in pp collisions at $\sqrt{s} = 13$ TeV, and simultaneous determination of the strong coupling strength, top quark pole mass, and parton distribution functions.
The European physical journal / C, 80(7):658, and PUBDB-2020-04207, arXiv:1904.05237. CMS-TOP-18-004. CERN-EP-2019-028. arXiv:1904.05237. CMS-TOP-18-004. CERN-EP-2019-028.
doi: 10.1140/epjc/s10052-020-7917-7.

CMS Collaboration.
Measurement of the Υ(1S) pair production cross section and search for resonances decaying to $\Upsilon(1S)\mu^+\mu^-$ in proton-proton collisions at $\sqrt{s} = 13$ TeV.
Physics letters / B, 808:135578, and PUBDB-2020-02831, arXiv:2002.06393. CMS-BPH-18-002. CERN-EP-2020-003. arXiv:2002.06393. CMS-BPH-18-002. CERN-EP-2020-003.
doi: 10.1016/j.physletb.2020.135578.

CMS Collaboration.
Measurement of the associated production of a Z boson with charm or bottom quark jets in proton-proton collisions at $\sqrt{s}$=13 TeV.
Physical review / D, D102(3):032007, and PUBDB-2020-03469, arXiv:2001.06899. CMS-SMP-19-004. CERN-EP-2019-262. arXiv:2001.06899. CMS-SMP-19-004. CERN-EP-2019-262.
doi: 10.1103/PhysRevD.102.032007.

CMS Collaboration.
Measurement of the χ_{c1} and χ_{c2} polarizations in proton-proton collisions at $\sqrt{s} = 8$ TeV.
Physical review letters, 124(16):162002, and PUBDB-2020-01713, arXiv:1912.07706. CMS-BPH-13-001. CERN-EP-2019-279.
doi: 10.1103/PhysRevLett.124.162002.

CMS Collaboration.
Measurement of the χ_{c1} and χ_{c2} polarizations in proton-proton collisions at $\sqrt{s} = 8$ TeV.
Physical review letters, 124(16):162002, and PUBDB-2020-01714, arXiv:1912.07706. CMS-BPH-13-001. CERN-EP-2019-279.
doi: 10.1103/PhysRevLett.124.162002.

CMS Collaboration.
Measurement of the cross section for electroweak production of a Z boson, a photon and two jets in proton-proton collisions at $\sqrt{s} = 13$ TeV and constraints on anomalous quartic couplings.
Journal of high energy physics, 2020(6):76, and PUBDB-2020-02642, arXiv:2002.09902. CMS-SMP-18-007. CERN-EP-2020-007. arXiv:2002.09902. CMS-SMP-18-007. CERN-EP-2020-007.
doi: 10.1007/JHEP06(2020)076.

CMS Collaboration.
Measurement of the cross section for $t\bar{t}$ production with additional jets and b jets in pp collisions at $\sqrt{s} = 13$ TeV.
Journal of high energy physics, 2020(7):1, and PUBDB-2020-03489, arXiv:2003.06467. CMS-TOP-18-002. CERN-EP-2020-011. FERMILAB-PUB-20-129-CMS.
doi: 10.1007/JHEP07(2020)125.

CMS Collaboration.
Measurement of the jet mass distribution and top quark mass in hadronic decays of boosted top quarks in pp collisions at $\sqrt{s} =$ 13 Te.
Physical review letters, 124(20):202001, and PUBDB-2020-02263, arXiv:1911.03800. CMS-TOP-19-005. CERN-EP-2019-226.
doi: 10.1103/PhysRevLett.124.202001.

CMS Collaboration.
Measurement of the single top quark and antiquark production cross sections in the t channel and their ratio in proton-proton collisions at $\sqrt{s} = 13$ TeV.
Physics letters / B, 800:135042, and PUBDB-2019-05187, arXiv:1812.10514. CMS-TOP-17-011. CERN-EP-2018-321.
doi: 10.1016/j.physletb.2019.135042.

CMS Collaboration.
Measurement of the top quark forward-backward production asymmetry and the anomalous chromoelectric and chromomagnetic moments in pp collisions at $\sqrt{s} = 13$ TeV.
Journal of high energy physics, 2020(6):146, and PUBDB-2020-02641, arXiv:1912.09540. CMS-TOP-15-018. CERN-EP-2019-270.
doi: 10.1007/JHEP06(2020)146.

CMS Collaboration.
Measurement of the top quark Yukawa coupling from $t\bar{t}$ kinematic distributions in the dilepton final state in proton-proton collisions at $\sqrt{s} = 13$ TeV.
Physical review / D, 102(9):092013 (1, and PUBDB-2020-05204, arXiv:2009.07123. CMS-TOP-19-008. CERN-

EP-2020-152.
doi: 10.1103/PhysRevD.102.092013.

CMS Collaboration.
Measurement of the $t\bar{t}b\bar{b}$ production cross section in the all-jet final state in pp collisions at $\sqrt{s} = 13$ TeV.
Physics letters / B B, B803:135285, and PUBDB-2020-01696, arXiv:1909.05306. CMS-TOP-18-011. CERN-EP-2019-183.
doi: 10.1016/j.physletb.2020.135285.

CMS Collaboration.
Measurement of top quark pair production in association with a Z boson in proton-proton collisions at $\sqrt{s} = 13$ TeV.
Journal of high energy physics, 2020(3):56, and PUBDB-2020-01694, arXiv:1907.11270. CNS-TOP-18-009. CERN-EP-2019-124.
doi: 10.1007/JHEP03(2020)056.

CMS Collaboration.
Measurements of production cross sections of WZ and same-sign WW boson pairs in association with two jets in proton-proton collisions at $\sqrt{s} = 13$ TeV.
Physics letters / B, 809:1, and PUBDB-2020-03546, arXiv:2005.01173. CMS-SMP-19-012. CERN-EP-2020-064. FERMILAB-PUB-20-189-CMS.
doi: 10.1016/j.physletb.2020.135710.

J. Knolle.
Measurements of top quark properties with the CMS experiment.
LHCP2020: The Eighth Annual Conference on Large Hadron Collider Physics, Online (Online), 25 May 2020 - 30 May 2020.
Proceedings of Science / International School for Advanced Studies, vol. (LHCP2020):072, and PUBDB-2020-05301. SISSA, Trieste.
doi: 10.3204/PUBDB-2020-05301.

CMS Collaboration.
Measurements of $t\bar{t}H$ production and the CP structure of the Yukawa interaction between the Higgs boson and top quark in the diphoton decay channel.
Physical review letters, 125(6):061801 (1, and PUBDB-2020-03490, arXiv:2003.10866. CMS-HIG-19-013. CERN-EP-2020-028.
doi: 10.1103/PhysRevLett.125.061801.

CMS Collaboration.
Measurements with silicon photomultipliers of dose-rate effects in the radiation damage of plastic scintillator tiles in the CMS hadron endcap calorimeter.
Journal of Instrumentation, 15(06):P06009, and PUBDB-2020-02643, arXiv:2001.06553. CMS-PRF-18-003. CERN-EP-2019-266. arXiv:2001.06553. CMS-PRF-18-003. CERN-EP-2019-266.
doi: 10.1088/1748-0221/15/06/P06009.

CMS Collaboration.
Mixed higher-order anisotropic flow and nonlinear response coefficients of charged particles in PbPb collisions at $\sqrt{s_{NN}} = 2.76$ and 5.02 TeV.
The European physical journal / C Particles and fields, C80(6):534, and PUBDB-2020-02635, arXiv:1910.08789. CMS-HIN-17-005. CERN-EP-2019-211.
doi: 10.1140/epjc/s10052-020-7834-9.

CMS Collaboration.
Multiparticle correlation studies in p Pb collisions at s N N = 8.16 TeV.
Physical review / C, 101(1):014912, and PUBDB-2020-00791, arXiv:1904.11519.
doi: 10.1103/PhysRevC.101.014912.

CMS Collaboration.
Observation of electroweak production of Wγ with two jets in proton-proton collisions at $\sqrt{s} = 13$ TeV.
Physics letters / B, 811:135988 (1, and PUBDB-2020-05206, arXiv:2008.10521. CMS-SMP-19-008. CERN-EP-2020-143.
doi: 10.1016/j.physletb.2020.135988.

CMS Collaboration.
Observation of the $B_s^0 \rightarrow X(3872)\phi$ decay.
Physical review letters, 125(15):152001, and PUBDB-2020-04210, arXiv:2005.04764. CMS-BPH-17-005. CERN-EP-2020-070. arXiv:2005.04764. CMS-BPH-17-005. CERN-EP-2020-070.
doi: 10.1103/PhysRevLett.125.152001.

CMS Collaboration.
Observation of the Production of Three Massive Gauge Bosons at $\sqrt{s}$ =13 TeV.
Physical review letters, 125(15):151802 (1, and PUBDB-2020-04213, arXiv:2006.11191. CMS-SMP-19-014. CERN-EP-2020-076.
doi: 10.1103/PhysRevLett.125.151802.

CMS Collaboration.
Observation of the Λ b 0 → J / ψ Λ decay in proton-proton collisions at s = 13 TeV.
Physics letters / B, 802:135203, and PUBDB-2020-00802, arXiv:1911.03789. CMS-BPH-19-002. CERN-EP-2019-224.
doi: 10.1016/j.physletb.2020.135203.

CMS Collaboration.
Performance of the CMS Level-1 trigger in proton-proton collisions at $\sqrt{s} = 13$ TeV.
Journal of Instrumentation, 15(10):P10017, and PUBDB-2020-04214, arXiv:2006.10165. CMS-TRG-17-001. CERN-EP-2020-065.
doi: 10.1088/1748-0221/15/10/P10017.

CMS Collaboration.
Performance of the reconstruction and identification of high-momentum muons in proton-proton collisions at $\sqrt{s} = 13$ TeV.
Journal of Instrumentation, 15(02):P02027, and PUBDB-2020-01710, arXiv:1912.03516. CMS-MUO-17-001. CERN-EP-2019-238.
doi: 10.1088/1748-0221/15/02/P02027.

CMS Collaboration.
Pileup mitigation at CMS in 13 TeV data.
Journal of Instrumentation, 15(09):1, and PUBDB-2020-03487, arXiv:2003.00503. CMS-JME-18-001. CERN-EP-2020-017.
doi: 10.1088/1748-0221/15/09/P09018.

CMS Collaboration.
Production of Λ_c^+ baryons in proton-proton and lead-lead collisions at $\sqrt{s_{NN}} = 5.02$ TeV.
Physics letters / B B, B803:135328, and PUBDB-2020-01600, arXiv:1906.03322. CMS-HIN-18-009. CERN-EP-2019-102.
doi: 10.1016/j.physletb.2020.135328.

CMS Collaboration.
Reconstruction of signal amplitudes in the CMS electromagnetic calorimeter in the presence of overlapping proton-proton interactions.
Journal of Instrumentation, 15(10):P10002 (1, and PUBDB-2020-04212, arXiv:2006.14359. CERN-EGM-18-001. CERN-EP-2020-105.
doi: 10.1088/1748-0221/15/10/P10002.

CMS Collaboration.
Running of the top quark mass from proton-proton collisions at $\sqrt{s} = 13$TeV.
Physics letters / B B, B803:135263, and PUBDB-2020-01702, arXiv:1909.09193. CMS-TOP-19-007. CERN-EP-2019-189.
doi: 10.1016/j.physletb.2020.135263.

CMS Collaboration.
Search for a charged Higgs boson decaying into top and bottom quarks in events with electrons or muons in proton-proton collisions at s√= 13 TeV.
Journal of high energy physics, 2020(1):96, and PUBDB-2020-00794, arXiv:1908.09206. CMS-HIG-18-004. CERN-EP-2019-164.
doi: 10.1007/JHEP01(2020)096.

CMS Collaboration.
Search for a heavy Higgs boson decaying to a pair of W bosons in proton-proton collisions at $\sqrt{s} = 13$ TeV.
Journal of high energy physics, 2003(3):34, and PUBDB-2020-01712, arXiv:1912.01594. CMS-HIG-17-033. CERN-EP-2019-230.
doi: 10.1007/JHEP03(2020)034.

CMS Collaboration.
Search for a heavy pseudoscalar Higgs boson decaying into a 125 GeV Higgs boson and a Z boson in final states with two tau and two light leptons at $\sqrt{s} = 13$ TeV.
Journal of high energy physics, 2003(3):65, and PUBDB-2020-01699, arXiv:1910.11634. CMS-HIG-18-023. CERN-EP-2019-231.
doi: 10.1007/JHEP03(2020)065.

CMS Collaboration.
Search for a light charged Higgs boson in the $H^\pm \to$ cs channel in proton-proton collisions at $\sqrt{s} = 13$ TeV.
Physical review / D, 102(7):072001, and PUBDB-2020-04211, arXiv:2005.08900. CMS-HIG-18-021. CERN-EP-2020-057. arXiv:2005.08900. CMS-HIG-18-021. CERN-EP-2020-057.
doi: 10.1103/PhysRevD.102.072001.

CMS Collaboration.
Search for a light pseudoscalar Higgs boson in the boosted $\mu\mu\tau\tau$ final state in proton-proton collisions at $\sqrt{s} = 13$ TeV.
Journal of high energy physics, 2020(8):1, and PUBDB-2020-03547, arXiv:2005.08694. CMS-HIG-18-024. CERN-EP-2020-061.
doi: 10.1007/JHEP08(2020)139.

CMS Collaboration.
Search for a narrow resonance lighter than 200 GeV decaying to a pair of muons in proton-proton collisions at $\sqrt{s} = 13$ TeV.
Physical review letters, 124(13):131802, and PUBDB-2020-01715, arXiv:1912.04776. CMS-EXO-19-018. CERN-EP-2019-265.
doi: 10.1103/PhysRevLett.124.131802.

CMS Collaboration.
Search for an excited lepton that decays via a contact interaction to a lepton and two jets in proton-proton collisions at $\sqrt{s} =$ 13 TeV.
Journal of high energy physics, 2020(5):52, and PUBDB-2020-02321, arXiv:2001.04521. CMS-EXO-18-013. CERN-EP-2019-280.
doi: 10.1007/JHEP05(2020)052.

CMS Collaboration.
Search for charged Higgs bosons decaying into a top and a bottom quark in the all-jet final state of pp collisions at $\sqrt{s}$ = 13 TeV.
Journal of high energy physics, 2007(7):126, and PUBDB-2020-03470, arXiv:2001.07763. CMS-HIG-18-015. CERN-EP-2019-277. arXiv:2001.07763. CMS-HIG-18-015. CERN-EP-2019-277.
doi: 10.1007/JHEP07(2020)126.

CMS Collaboration.
Search for dark matter particles produced in association with a Higgs boson in proton-proton collisions at $\sqrt{s}$ = 13 TeV.
Journal of high energy physics, 2020(3):25, and PUBDB-2020-01602, arXiv:1908.01713. CMS-EXO-18-011. CERN-EP-2019-141.
doi: 10.1007/JHEP03(2020)025.

CMS Collaboration.
Search for dark matter particles produced in association with a Higgs boson in proton-proton collisions at $\sqrt{s}$ = 13 TeV.
Journal of high energy physics, 2020(3):25, and PUBDB-2020-01603, arXiv:1908.01713. CMS-EXO-18-011. CERN-EP-2019-141.
doi: 10.1007/JHEP03(2020)025.

CMS Collaboration.
Search for decays of the 125 GeV Higgs boson into a Z boson and a ρ or ϕ meson.
Journal of high energy physics, 11(11):39 (1, and PUBDB-2020-05202, arXiv:2007.05122. CMS-HIG-19-012. CERN-EP-2020-120. FERMILAB-PUB-20-340-CMS.
doi: 10.1007/JHEP11(2020)039.

CMS Collaboration.
Search for dijet resonances using events with three jets in proton-proton collisions at $\sqrt{s} = 13$ TeV.
Physics letters / B B, 805:135448, and PUBDB-2020-01709, arXiv:1911.03761. CMS-EXO-19-004. CERN-EP-2019-229.
doi: 10.1016/j.physletb.2020.135448.

CMS Collaboration.
Search for direct pair production of supersymmetric partners to the τ lepton in proton-proton collisions at $\sqrt{s} = 13$ TeV.
The European physical journal / C, 80(3):189, and PUBDB-2021-00505, arXiv:1907.13179. CMS-SUS-18-006. CERN-EP-2019-154.
doi: 10.1140/epjc/s10052-020-7739-7.

CMS Collaboration.
Search for direct top squark pair production in events with one lepton, jets, and missing transverse momentum at 13 TeV with the CMS experiment.
Journal of high energy physics, 2005(5):32, and PUBDB-2020-02320, arXiv:1912.08887. CMS-SUS-19-005. CMS-SUS-19-009. CERN-EP-2019-233.
doi: 10.1007/JHEP05(2020)032.

CMS Collaboration.
Search for disappearing tracks in proton-proton collisions at $\sqrt{s} = 13$ TeV.
Physics letters / B, 806:135502, and PUBDB-2020-02645, arXiv:2004.05153. FERMILAB-PUB-20-192-CMS. CMS-EXO-19-010. CERN-EP-2020-043.
doi: 10.1016/j.physletb.2020.135502.

CMS Collaboration.
Search for electroweak production of a vector-like T quark using fully hadronic final states.
Journal of high energy physics, 2020(1):36, and PUBDB-2020-00796, arXiv:1909.04721.
doi: 10.1007/JHEP01(2020)036.

CMS Collaboration.
Search for heavy Higgs bosons decaying to a top quark pair in proton-proton collisions at $\sqrt{s} = 13$ TeV.
Journal of high energy physics, 2020(4):171, and PUBDB-2020-01691, arXiv:1908.01115. CMS-HIG-17-027. CERN-EP-2019-147.
doi: 10.1007/JHEP04(2020)171.

CMS Collaboration.
Search for high mass dijet resonances with a new background prediction method in proton-proton collisions at $\sqrt{s} = 13$ TeV.
Journal of high energy physics, 2020(5):33, and PUBDB-2020-02265, arXiv:1911.03947. CMS-EXO-19-012. CERN-EP-2019-222.
doi: 10.1007/JHEP05(2020)033.

CMS Collaboration.
Search for lepton flavour violating decays of a neutral heavy Higgs boson to $\mu\tau$ and eτ in proton-proton collisions at $\sqrt{s} = 13$ TeV.
Journal of high energy physics, 2020(3):103, and PUBDB-2020-01704, arXiv:1911.10267. CMS-HIG-18-017. CERN-EP-2019-170.
doi: 10.1007/JHEP03(2020)103.

CMS Collaboration.
Search for light pseudoscalar boson pairs produced from decays of the 125 GeV Higgs boson in final states with two muons and two nearby tracks in pp collisions at $\sqrt{s} = 13$ TeV.
Physics letters / B, 800:135087, and PUBDB-2019-05193, arXiv:1907.07235. CMS-HIG-18-006. CERN-EP-2019-105.
doi: 10.1016/j.physletb.2019.135087.

CMS Collaboration.
Search for new neutral Higgs bosons through the H→ ZA → $\ell^+\ell^-$b$\bar{\text{b}}$ process in pp collisions at $\sqrt{s} = 13$ TeV.
Journal of high energy physics, 2003(3):55, and PUBDB-2020-01708, arXiv:1911.03781. CMS-HIG-18-012. CERN-EP-2019-254.
doi: 10.1007/JHEP03(2020)055.

CMS Collaboration.
Search for physics beyond the standard model in events with jets and two same-sign or at least three charged leptons in proton-proton collisions at $\sqrt{s} = 13$ TeV.
The European physical journal / C, 80(8):752, and PUBDB-2020-03471, arXiv:2001.10086. CMS-SUS-19-008. CERN-EP-2020-001. arXiv:2001.10086. CMS-SUS-19-008. CERN-EP-2020-001.
doi: 10.1140/epjc/s10052-020-8168-3.

CMS Collaboration.
Search for physics beyond the standard model in multilepton final states in proton-proton collisions at $\sqrt{s} = 13$ TeV.
Journal of high energy physics, 2003(3):51, and PUBDB-2020-01707, arXiv:1911.04968. CMS-EXO-19-002. CERN-EP-2019-237.
doi: 10.1007/JHEP03(2020)051.

CMS Collaboration.
Search for production of four top quarks in final states with same-sign or multiple leptons in proton–proton collisions at s√=13 TeV.
The European physical journal / C, 80(2):75, and PUBDB-2020-00793, arXiv:1908.06463. CMS-TOP-18-003. CERN-EP-2019-163.
doi: 10.1140/epjc/s10052-019-7593-7.

CMS Collaboration.
Search for resonant pair production of Higgs bosons in the $bbZZ$ channel in proton-proton collisions at $\sqrt{s} = 13$ TeV.
Physical review / D, 102(3):032003 (1, and PUBDB-2020-03549, arXiv:2006.06391. CMS-HIG-18-013. CERN-EP-2020-079.
doi: 10.1103/PhysRevD.102.032003.

CMS Collaboration.
Search for supersymmetry in pp collisions at $\sqrt{s} = 13$ TeV with 137 fb^{-1} in final states with a single lepton using the sum of masses of large-radius jets.
Physical review / D D, D101(5):052010, and PUBDB-2020-01706, arXiv:1911.07558. CMS-SUS-19-007. CERN-EP-2019-213.
doi: 10.1103/PhysRevD.101.052010.

CMS Collaboration.
Search for supersymmetry in proton-proton collisions at $\sqrt{s} = 13$ TeV in events with high-momentum Z bosons and missing transverse momentum.
Journal of high energy physics, 2020(9):149, and PUBDB-2020-04215, arXiv:2008.04422. CMS-SUS-19-013. CERN-EP-2020-149. arXiv:2008.04422. CMS-SUS-19-013. CERN-

EP-2020-149.
doi: 10.1007/JHEP09(2020)149.

CMS Collaboration.
Search for supersymmetry with a compressed mass spectrum in events with a soft τ lepton, a highly energetic jet, and large missing transverse momentum in proton-proton collisions at s√= 13 TeV.
Physical review letters, 124(4):041803, and PUBDB-2020-00800, arXiv:1910.01185.
doi: 10.1103/PhysRevLett.124.041803.

CMS Collaboration.
Search for top squark pair production in a final state with two tau leptons in proton-proton collisions at $\sqrt{s} = 13$ TeV.
Journal of high energy physics, 2020(2):15, and PUBDB-2020-00801, CMS-PAS-SUS-19-003. arXiv:1910.12932.
doi: 10.1007/JHEP02(2020)015.

CMS Collaboration.
Searches for physics beyond the standard model with the M_{T2} variable in hadronic final states with and without disappearing tracks in proton-proton collisions at $\sqrt{s} = 13$ TeV.
The European physical journal / C, 80(1):3, and PUBDB-2020-00483, arXiv:1909.03460. CMS-SUS-19-005. CERN-EP-2019-180.
doi: 10.1140/epjc/s10052-019-7493-x.

CMS Collaboration.
Strange hadron production in pp and pPb collisions at $\sqrt{s_{NN}} =$ 5.02 TeV.
Physical review / C covering nuclear physics, 101(6):064906, and PUBDB-2020-02636, arXiv:1910.04812. CMS-HIN-16-013. CERN-EP-2018-213.
doi: 10.1103/PhysRevC.101.064906.

CMS Collaboration.
Studies of charm quark diffusion inside jets using PbPb and pp collisions at $\sqrt{s_{NN}} = 5.02$ TeV.
Physical review letters, 125(10):102001 (1, and PUBDB-2020-03468, arXiv:1911.01461. CMS-HIN-18-007. CERN-EP-2019-247.
doi: 10.1103/PhysRevLett.125.102001.

CMS Collaboration.
Study of central exclusive $\pi^+\pi^-$ production in proton-proton collisions at $\sqrt{s} = 5.02$ and 13 TeV.
The European physical journal / C, 80(8):1, and PUBDB-2020-03488, arXiv:2003.02811. CMS-FSQ-16-006. CERN-EP-2020-005.
doi: 10.1140/epjc/s10052-020-8166-5.

CMS Collaboration.
Study of excited Λ_b^0 states decaying to $\Lambda_b^0\pi^+\pi^-$ in proton-proton collisions at $\sqrt{s} = 13$ TeV.
Physics letters / B B, 803:135345, and PUBDB-2020-01719, arXiv:2001.06533. CMS-BPH-19-003. CERN-EP-2019-288.
doi: 10.1016/j.physletb.2020.135345.

CMS Collaboration.
Study of J/ψ meson production inside jets in pp collisions at $\sqrt{s} = 8$ TeV.
Physics letters / B B, 804:135409, and PUBDB-2020-01701, arXiv:1910.01686. CMS-BPH-15-003. CERN-EP-2019-186.
doi: 10.1016/j.physletb.2020.135409.

CMS Collaboration.
The production of isolated photons in PbPb and pp collisions at $\sqrt{s_{NN}} = 5.02$ TeV.
Journal of high energy physics, 2020(7):116, and PUBDB-2020-02832, arXiv:2003.12797. FERMILAB-PUB-20-194-CMS. CMS-HIN-18-016. CERN-EP-2020-032.
doi: 10.1007/JHEP07(2020)116.

CMS Collaboration.
W^+W^- boson pair production in proton-proton collisions at $\sqrt{s} = 13$ TeV.
Physical review / D, 102(9):092001 (1, and PUBDB-2020-05205, arXiv:2009.00119. CMS-SMP-18-004. CERN-EP-2020-144.
doi: 10.1103/PhysRevD.102.092001.

CMS Collaboration and TOTEM Collaboration.
Measurement of single-diffractive dijet production in proton-proton collisions at $s = \sqrt{s}$ =s= 8 TeV with the CMS and TOTEM experiments.
The European physical journal / C, 80(12):1164, and PUBDB-2021-00704, arXiv:2002.12146. CMS-FSQ-12-033. TOTEM-2020-001. CERN-EP-2019-260.
doi: 10.1140/epjc/s10052-020-08562-y.

CMS Collaboration and TOTEM Collaboration.
The CMS Precision Proton Spectrometer timing system: performance in Run 2, future upgrades and sensor radiation hardness studies.
Journal of Instrumentation, 15(05):C05054, and PUBDB-2021-00459, arXiv:2004.11068.
doi: 10.1088/1748-0221/15/05/C05054.

D0 Collaboration.
Studies of $X(3872)$ and $\psi(2S)$ production in $p\bar{p}$ collisions at 1.96 TeV.
Physical review / D, 102(7):072005 (1, and PUBDB-2021-00159, arXiv:2007.13420. FERMILAB-PUB-20-363-E.
doi: 10.1103/PhysRevD.102.072005.

M. Defranchis.
Probing QCD using top quark pair production at $\sqrt{s}$ = 13TeV in CMS.
1781734. European Physical Society Conference on High Energy Physics, Ghent (Belgium), 10 Jul 2019 - 17 Jul 2019.
Proceedings of Science / International School for Advanced Studies, vol. (EPS-HEP2019):679, and PUBDB-2020-05250, arXiv:2002.09288.
SISSA, Trieste.
doi: 10.22323/1.364.0679.

A. Elwood, D. Krücker and M. Shchedrolosiev.
Direct optimization of the discovery significance in machine learning for new physics searches in particle colliders.
Journal of physics / Conference Series, 1525:012110, and

PUBDB-2020-04526.
doi: 10.1088/1742-6596/1525/1/012110.

A. V. Lipatov, M. A. Malyshev and H. Jung.
On relation between Parton Branching Approach and CCFM evolution.
Physical review / D, 101(3):034022, and PUBDB-2020-00915, arXiv:1910.11224. DESY-19-183. DESY 19-183.
doi: 10.1103/PhysRevD.101.034022.

M. Meschini et al.
Radiation resistant innovative 3D pixel sensors for the CMS upgrade at the High Luminosity LHC.
Nuclear instruments & methods in physics research / A, 978:164429, and PUBDB-2021-00510, CMS-CR-2020-039.
doi: 10.1016/j.nima.2020.164429.

PROSA Collaboration.
Improved constraints on parton distributions using LHCb, ALICE and HERA heavy-flavour measurements and implications for the predictions for prompt atmospheric-neutrino fluxes.
Journal of high energy physics, 2004(4):118, and PUBDB-2020-01631, arXiv:1911.13164. DESY-19-211.
doi: 10.1007/JHEP04(2020)118.

C. Schwanenberger and O. Fischer.
Beyond the Standard Model physics at the LHeC and the FCC-he.
1831163. European Physical Society Conference on High Energy Physics, Ghent (Belgium), 10 Jul 2019 - 17 Jul 2019.
Proceedings of Science / International School for Advanced Studies, vol. (EPS-HEP2019):563, and PUBDB-2020-05252. SISSA, Trieste.
doi: 10.22323/1.364.0563.

Master Thesis

F. C. Colombina.
Search for tZq in dilepton final states with Machine Learning techniques.
Universit'a degli Studi di Milano - Bicocca, 2020.

T. Wening.
Transverse Momentum Dependent Parton Density Function for the Photon.
University of Hamburg, 2020.

Ph.D. Thesis

S. Consuegra Rodriguez.
Search for light bosons in the final state with muons and tau leptons with CMS Run II data.
Universität Hamburg, Hamburg, 2020.

V. Danilov.
The measurement of W± boson charge asymmetry at $\sqrt{s} = 13$ TeV with the CMS detector using the 2015 data set and a global QCD analysis on this asymmetry.
University of Hamburg, 2020.

M. Defranchis.
First measurement of the running of the top quark mass.
Universität Hamburg, Hamburg, 2020.

D. Dominguez Damiani.
Cross Section measurements of $t\bar{t}$ pair production in the boosted regime in proton-proton collisions at $\sqrt{s} = 13$ TeV with the CMS experiment at the Large Hadron Collider.
Universität Hamburg, Hamburg, 2020.

M. Haranko.
Development of a test DAQ system for the CMS Phase-2 outer tracker upgrade.
Universität Hamburg, Hamburg, 2020.

J. Knolle.
Measuring luminosity and the $\mathrm{t\bar{t}Z}$ production cross section with the CMS experiment.
Universität Hamburg, Hamburg, 2020.

J. Lange.
Measurement of the top quark mass in the all-jets final state at $\sqrt{s} = 13$ TeV and combination with the lepton+jets channel.
Universität Hamburg, Hamburg, 2020.

D. Perez Adan.
Search for Light Bosons in Exotic Decays of the 125 GeV Higgs Boson.
Universität Hamburg, Hamburg, 2020.

A. Singh.
Search for supersymmetric particles in gluino-gluino pair production events at CMS.
Universität Hamburg, Hamburg, 2020.

A. Vagnerini.
Search for Higgs bosons in the final state with b-quarks in the semi-leptonic channel with the CMS 2017 data.
Universität Hamburg, Hamburg, 2020.

A. Velyka.
Concept and Development of Enhanced Lateral Drift (ELAD) Sensors.
Universität Hamburg, Hamburg, 2020.

Electronics Development

Master Thesis

A. Ashim.
Design of a driver circuit for Mach-Zehnder modulators with data rates up to 20 Gbps implemented in a 90 nm SOI CMOS process.
TU Hamburg-Harburg, 2020.

H1

Published

R. Zlebcik.
Diffractive PDF determination from HERA inclusive and jet data at NNLO QCD.
1831245. XXVII International Workshop on Deep Inelastic Scattering and Related Subjects, Turin (Italy), 8 Jul 2019 - 12 Jul 2019.
Proceedings of Science / International School for Advanced Studies, vol. (EPS-HEP2019):500, and PUBDB-2020-05019.
SISSA, Trieste.
doi: 10.22323/1.364.0500.

H1 Collaboration.
Measurement of Exclusive $\pi^+\pi^-$ and ρ^0 Meson Photoproduction at HERA.
The European physical journal / C, 80(12):1189, and PUBDB-2021-00100, arXiv:2005.14471. DESY-20-080.
doi: 10.1140/epjc/s10052-020-08587-3.

HERMES

Published

A. Airapetian et al.
Azimuthal single- and double-spin asymmetries in semi-inclusive deep-inelastic lepton scattering by transversely polarized protons.
Journal of high energy physics, 2020(12):010, and PUBDB-2020-05309, arXiv:2007.07755. DESY-20-119.
doi: 10.1007/JHEP12(2020)010.

H. Marukyan.
Overview of recent HERMES results.
1. XVIII Workshop on High Energy Spin Physics, Dubna (Russia), 2 Sep 2019 - 6 Sep 2019.
Journal of physics / Conference Series, vol. 14351:012041, and PUBDB-2020-01607, HERMES-19-002.
IOP Publ.20382, Bristol.
doi: 10.1088/1742-6596/1435/1/012041.

IT

Published

C. Beyer et al.
Beyond HEP: Photon and accelerator science computing infrastructure at DESY.
24th International Conference on Computing in High Energy and Nuclear Physics (CHEP 2019), Adelaide (Australia), 4 Nov 2019 - 8 Nov 2019.
The European physical journal / Web of Conferences, vol. 245:07036, and PUBDB-2020-04519.
EDP Sciences, Les Ulis.
doi: 10.1051/epjconf/202024507036.

C. Beyer et al.
Consolidating the interactive analysis and Grid infrastructure at DESY.
24th International Conference on Computing in High Energy and Nuclear Physics, Adelaide (Australia), 4 Nov 2019 - 8 Nov 2019.
The European physical journal / Web of Conferences, vol. 245:07003, and PUBDB-2020-04518.
EDP Sciences, Les Ulis.
doi: 10.1051/epjconf/202024507003.

A. Gellrich, T. Kuhr and D. Knittel.
Operating the Belle II Collaborative Services and Tools.
9. 24th International Conference on Computing in High Energy and Nuclear Physics, Adelaide (Australia), 4 Nov 2019 - 8 Nov 2019.
The European physical journal / Web of Conferences, vol. 2459:08009, and PUBDB-2020-04785.
EDP Sciences, Les Ulis.
doi: 10.1051/epjconf/202024508009.

T. Mkrtchyan et al.
dCache - Keeping up With the Evolution of Science.
The European physical journal / Web of Conferences, 245:9, and PUBDB-2020-05110.
doi: 10.1051/epjconf/202024504039.

L. Morschel et al.
dCache – Efficient Message Encoding For Inter-Service Communication in dCache: Evaluation of Existing Serialization Protocols as a Replacement for Java Object Serialization.
24th International Conference on Computing in High Energy and Nuclear Physics, Adelaide (Australia), 4 Nov 2019 - 8 Nov 2019.
The European physical journal / Web of Conferences, vol. 245:05017, and PUBDB-2020-04903.
EDP Sciences, Les Ulis.
doi: 10.1051/epjconf/202024505017.

L

Published

I. Filozova et al.
JINR Open Access Repository based on the JOIN² Platform.
Data Analytics and Management in Data Intensive Domains 2020, Voronezh (Russia), 13 Oct 2020 - 16 Oct 2020.
CEUR workshop proceedings, vol. 2790:142, and PUBDB-2021-00818.
RWTH Aachen, Aachen, Germany.
doi: 10.3204/PUBDB-2021-00818.

Linear Collider

Published

H. Baer et al.
The ILC as a natural SUSY discovery machine and precision microscope: from light higgsinos to tests of unification.
Physical review / D D, 101(9):095026, and PUBDB-2020-02739, arXiv:1912.06643. ILD-PHYS-2019-001. DESY-19-227. KEK Preprint 2019-53.
doi: 10.1103/PhysRevD.101.095026.

T. Brümmer et al.
Design study for a compact laser-driven source for medical x-ray fluorescence imaging.
Physical review accelerators and beams, 23(3):031601 (1, and PUBDB-2020-05317.
doi: 10.1103/PhysRevAccelBeams.23.031601.

Y. Chen et al.
Frequency-Detuning Dependent Transient Coaxial RF Coupler Kick in an L -Band Long-Pulse High-Gradient RF Photogun.
Physical review accelerators and beams, 23(1):010101, and PUBDB-2020-00656.
doi: 10.1103/PhysRevAccelBeams.23.010101.

CLICdp Collaboration.
Conformal tracking for all-silicon trackers at future electron–positron colliders.
Nuclear instruments & methods in physics research / A, 956:163304, and PUBDB-2021-00541, arXiv:1908.00256. CLICdp-Pub-2019-003.
doi: 10.1016/j.nima.2019.163304.

P. Craievich et al.
Novel X-band transverse deflection structure with variable polarization.
Physical review accelerators and beams, 23(11):112001 (1, and PUBDB-2020-04482.
doi: 10.1103/PhysRevAccelBeams.23.112001.

P. Drechsel, G. Moortgat-Pick and G. Weiglein.
Prospects for direct searches for light Higgs bosons at the ILCwith 250 GeV.
The European physical journal / C, 80(10):922, and PUBDB-2020-03907, DESY-20-083. arXiv:1801.09662.
doi: 10.1140/epjc/s10052-020-08438-1.

R. Ete et al.
MarlinMT - parallelising the Marlin framework.
24th International Conferene on Computing in High Energy and Nuclear Physics, Adelaide (Australia), 4 Nov 2019 - 8 Nov 2019.
The European physical journal / Web of Conferences, vol. 245:05022, and PUBDB-2020-04876.
EDP Sciences, Les Ulis.
doi: 10.1051/epjconf/202024505022.

P. Faccioli, C. Lourenco and T. Madlener.
From prompt to direct J/ψ production: new insights on the χ_{c1} and χ_{c2} polarizations and feed-down contributions from a global-fit analysis of mid-rapidity LHC data.
The European physical journal / C, 80(7):623, and PUBDB-2020-04856, arXiv:2006.15446.
doi: 10.1140/epjc/s10052-020-8201-6.

F. Gaede, B. Hegner and G. A. Stewart.
PODIO: recent developments in the Plain Old Data EDM toolkit.
24th International Conferene on Computing in High Energy and Nuclear Physics, Adelaide (Australia), 4 Nov 2019 - 8 Nov 2019.
The European physical journal / Web of Conferences, vol. 245:05024 (1, and PUBDB-2020-04987.
EDP Sciences, Les Ulis.
doi: 10.1051/epjconf/202024505024.

F. Gaede et al.
DD4hep a community driven detector description for HEP.
24th International Conferene on Computing in High Energy and Nuclear Physics, Adelaide (Australia), 4 Nov 2019 - 8 Nov 2019.
The European physical journal / Web of Conferences, vol. 245:02004, and PUBDB-2020-04875.
EDP Sciences, Les Ulis.
doi: 10.1051/epjconf/202024502004.

M. Habermehl, C. M. Berggren and J. List.
WIMP dark matter at the International Linear Collider.
Physical review / D, 101(7):075053 (1, and PUBDB-2020-04905, 2001.03011. arXiv:2001.03011. DESY-19-237. ILD-PHYS-2020-001.
doi: 10.1103/PhysRevD.101.075053.

S.-i. Kawada, J. List and C. M. Berggren.
Prospects of measuring the branching fraction of the Higgs boson decaying into muon pairs at the International Linear Collider.
The European physical journal / C, 80(12):1186, and PUBDB-2020-05273, arXiv:2009.04340. ILD-PHYS-2020-002.
doi: 10.1140/epjc/s10052-020-08729-7.

M. Kobayashi et al.
Electron and ion transmission of the gating foil for the TPC in the ILC experiment.
1. Micro-Pattern Gaseous Detectors Conference 2019, La Rochelle (France), 5 May 2019 - 10 May 2019.
Journal of physics / Conference Series, vol. 14981:012020, and PUBDB-2020-04813.
IOP Publ., Bristol.
doi: 10.1088/1742-6596/1498/1/012020.

C. A. Lindstroem et al.
Matching small beta functions using centroid jitter and two beam position monitors.
Physical review accelerators and beams, 23(5):052802, and PUBDB-2020-02357, arXiv:2002.06022. DESY-20-038.
doi: 10.1103/PhysRevAccelBeams.23.052802.

N. M. Lockmann et al.
Noninvasive THz spectroscopy for bunch current profile reconstructions at MHz repetition rates.
Physical review accelerators and beams, 23(11):112801, and PUBDB-2020-04551.
doi: 10.1103/PhysRevAccelBeams.23.112801.

B. Schmidt et al.
Benchmarking Coherent Radiation Spectroscopy as a Tool for High-Resolution Bunch Shape Reconstruction at Free-Electron Lasers.
Physical review accelerators and beams, 23(6):062801, and PUBDB-2020-01429.
doi: 10.1103/PhysRevAccelBeams.23.062801.

S. Schröder et al.
Tunable and precise two-bunch generation at FLASHForward.
1. 4th European Advanced Accelerator Concepts Workshop 15-20 September 2019, Isola d'Elba (Italy), 15 Sep 2019 - 21 Sep 2019.
Journal of physics / Conference Series, vol. 15961:012002 (1, and PUBDB-2020-04017, arXiv:2005.12071. DESY-20-039. IOP Publ., Bristol.
doi: 10.1088/1742-6596/1596/1/012002.

S. Schröder et al.
High-resolution sampling of beam-driven plasma wakefields.
Nature Communications, 11(1):5984 (1, and PUBDB-2020-04652.
doi: 10.1038/s41467-020-19811-9.

The DUNE Collaboration.
Volume I. Introduction to DUNE.
Journal of Instrumentation, 15(08):T08008 (1, and PUBDB-2020-05216, 1. arXiv:2002.02967. FERMILAB-PUB-20-024-ND. FERMILAB-DESIGN-2020-01.
doi: 10.1088/1748-0221/15/08/T08008.

S. V. Trofymenko et al.
Formation Region eEfects in X-ray Transition Radiation from 1 to 6 GeV Electrons in Multilayer Targets.
Nuclear instruments & methods in physics research / B Beam interactions with materials and atoms, 476:44, and PUBDB-2020-02481.
doi: 10.1016/j.nimb.2020.04.033.

M. Wenskat et al.
Vacancy-Hydrogen Interaction in Niobium during Low-Temperature Baking.
Scientific reports, 10(1):8300, and PUBDB-2020-02437, arXiv:2004.13450. DESY-20-074.
doi: 10.1038/s41598-020-65083-0.

M. Zeng et al.
Plasma eyepieces for petawatt class lasers.
Physics of plasmas, 27(2):023109 (1, and PUBDB-2020-05315, arXiv:1901.07974.
doi: 10.1063/1.5116416.

Master Thesis

R. Brabants.
Longitudinal Bunch Profile Diagnostics at a Laser-Driven Plasma Wakefield Acceleration Experiment.
University of Hamburg, 2020.

J. L. Dresselhaus.
Paving the way of high repetition rate laser wakefield acceleration by solving heat induced grating deformation issues.
University of Hamburg, 2020.

Ph.D. Thesis

J.-H. Röckemann.
Experimental and theoretical studies on electron-beam focusing using active plasma lenses.
University of Hamburg, 2020.

P. V. Winkler.
Emittance Measurements at Laser-Wakefield Accelerators.
University of Hamburg, 2020.

Theory

Published

J. Ablinger et al.
Subleading logarithmic QED initial state corrections to $e^+e^- \to \gamma / Z^0$ to $O(\alpha^6L^5)$.
Nuclear physics / B Particle physics, 955:115045, and PUBDB-2020-02240, arXiv:2004.04287. DESY-19-231. DO-TH 19/32. TTP20–012. SAGEX 19–36.
doi: 10.1016/j.nuclphysb.2020.115045.

J. Ablinger et al.
The three-loop polarized pure singlet operator matrix element with two different masses.
Nuclear physics / B Particle physics, B952:114916, and PUBDB-2020-02282, DESY-19-163. arXiv:1911.11630. DO-TH 19/19. TTP 19-038. SAGEX-19-23-E.
doi: 10.1016/j.nuclphysb.2020.114916.

J. Ablinger et al.
The three-loop single mass polarized pure singlet operator matrix element.
Nuclear physics / B Particle physics, B953:114945, and PUBDB-2020-02434, DESY-19-216. arXiv:1912.02536. DO-TH 19/02. TTP 19-043. MSUHEP-19-026. SAGEX 19-30.
doi: 10.1016/j.nuclphysb.2020.114945.

J. Ablinger et al.
The Two-mass Contribution to the Three-Loop Polarized Operator Matrix Element $A_{gg,Q}^{(3)}$.
Nuclear physics / B Particle physics, 955:115059, and PUBDB-2020-02245, DESY-20-051. DO–TH 20/03. TTP 20–013. SAGEX–20–07–E. 2004.08916 [hep-ph].
doi: 10.1016/j.nuclphysb.2020.115059.

J. Ablinger et al.
Three loop QCD corrections to heavy quark form factors.
1. 19th International Workshop on Advanced Computing and Analysis Techniques in Physics Research, Saas-Fee (Switzerland), 11 Mar 2019 - 15 Mar 2019.
Journal of physics / Conference Series, vol. 15251:012018 (1, and PUBDB-2020-05323, arXiv:1905.03728. DESY-19-078. DO-TH 19/06.
IOP Publ., Bristol.
doi: 10.1088/1742-6596/1525/1/012018.

A. Achúcarro et al.
Origin of ultra-light fields during inflation and their suppressed non-Gaussianity.
Journal of cosmology and astroparticle physics, 2010(10):018 (1, and PUBDB-2020-03809, arXiv:1908.06956. DESY-19-121.
doi: 10.1088/1475-7516/2020/10/018.

A. Achúcarro et al.
Shift-symmetric orbital inflation: Single field or multifield?
Physical review / D D, 102(2):021302, and PUBDB-2020-03009, arXiv:1901.03657. DESY-19-015.
doi: 10.1103/PhysRevD.102.021302.

A. H. Ajjath et al.
Resummed Drell-Yan cross-section at N^3LL.
Journal of high energy physics, 10(10):153 (1, and PUBDB-2020-04577, arXiv:2001.11377. IMSc/2019/12/16. DESY-19-191. SI-HEP-2019-23.
doi: 10.1007/JHEP10(2020)153.

M. Akhond et al.
Five-brane webs, Higgs branches and unitary/orthosymplectic magnetic quivers.
Journal of high energy physics, 2020(12):164, and PUBDB-2021-00111, arXiv:2008.01027. CTP-SCU/2020026. DESY-20-128.
doi: 10.1007/JHEP12(2020)164.

L. Alasfar et al.
B anomalies under the lens of electroweak precision.
Journal of high energy physics, 2020(12):016, and PUBDB-2020-05282, DESY-20-091. HU-EP-20/12-RTG. SISSA 16/2020/FISI. UCI-TR 2020-10. arXiv:2007.04400.
doi: 10.1007/JHEP12(2020)016.

S. Alekhin, J. Bluemlein and S. Moch.
Heavy-flavor PDF evolution and variable-flavor number scheme uncertainties in deep-inelastic scattering.
Physical review / D, 102(5):054014, and PUBDB-2020-04060, arXiv:2006.07032. DESY-20-061. DO-TH 20/05. SAGEX-20-09.
doi: 10.1103/PhysRevD.102.054014.

C. Alexandrou et al.
Comparison of topological charge definitions in Lattice QCD.
The European physical journal / C Particles and fields, 80(5):424, and PUBDB-2020-02186, DESY-17-115. arXiv:1708.00696.
doi: 10.1140/epjc/s10052-020-7984-9.

C. Alexandrou et al.
Parton distribution functions from lattice QCD using Bayes-Gauss-Fourier transforms.
Physical review / D, 102(9):094508, and PUBDB-2020-04539, arXiv:2007.13800.
doi: 10.1103/PhysRevD.102.094508.

C. Alexandrou et al.
Ruling Out the Massless Up-Quark Solution to the Strong C P Problem by Computing the Topological Mass Contribution with Lattice QCD.
Physical review letters, 125(23):232001, and PUBDB-2020-05260, arXiv:2002.07802.
doi: 10.1103/PhysRevLett.125.232001.

C. Alexandrou et al.
The nucleon axial, tensor and scalar charges and σ-terms in lattice QCD.
Physical review / D, 102(5):054517 (1, and PUBDB-2020-04179.
doi: 10.1103/PhysRevD.102.054517.

C. Alexandrou et al.
Unpolarized and helicity generalized parton distributions of the proton within lattice QCD.
Physical review letters, 125(26):262001, and PUBDB-2021-00148, arXiv:2008.10573.
doi: 10.1103/PhysRevLett.125.262001.

C. Alexandrou et al.
Complete flavor decomposition of the spin and momentum fraction of the proton using lattice QCD simulations at physical pion mass.
Physical review / D D, D101(9):094513, and PUBDB-2020-02369, arXiv:2003.08486.
doi: 10.1103/PhysRevD.101.094513.

C. Alexandrou et al.
Moments of nucleon generalized parton distributions from lattice QCD simulations at physical pion mass.
Physical review / D D, 101(3):034519, and PUBDB-2020-01424, arXiv:1908.10706.
doi: 10.1103/PhysRevD.101.034519.

C. Alexandrou et al.
Nucleon strange electromagnetic form factors.
Physical review / D D, 101(3):031501, and PUBDB-2020-02140, arXiv:1909.10744.
doi: 10.1103/PhysRevD.101.031501.

S. Ali et al.
Continuum extrapolation of Ward identities in $\mathcal{N} = 1$ supersymmetric SU(3) Yang–Mills theory.
The European physical journal / C, 80(6):548 (1, and PUBDB-2021-00590, arXiv:2003.04110. MS-TP-20-17.
doi: 10.1140/epjc/s10052-020-8113-5.

J. R. Andersen et al.
A Positive Resampler for Monte Carlo Events with Negative Weights.
The European physical journal / C, 80(11):1007, and PUBDB-2021-00010, arXiv:2005.09375. DCPT/20/30. DESY-20-090. IPPP/20/15. LU-TP-20-21. MCNET-20-14. SAGEX-20-12.
doi: 10.1140/epjc/s10052-020-08548-w.

N. Andrei et al.
Boundary and Defect CFT: Open Problems and Applications.
Journal of physics / A, 53(45):453002, and PUBDB-2021-00500, arXiv:1810.05697.
doi: 10.1088/1751-8121/abb0fe.

C. Angelantonj et al.
String Defects, Supersymmetry and the Swampland.
Journal of high energy physics, 11(11):125, and PUBDB-2020-04699, arXiv:2007.12722. CPHT-RR046.072020. DESY-20-123.
doi: 10.1007/JHEP11(2020)125.

S. Aoki et al.
FLAG Review 2019.
The European physical journal / C, 80(2):113, and PUBDB-2020-04064, arXiv:1902.08191.
doi: 10.1140/epjc/s10052-019-7354-7.

M. Ardu et al.
Axion quality from the (anti)symmetric of SU(N).
Journal of high energy physics, 11(11):90, and PUBDB-2020-04601, arXiv:2007.12663. DESY 20-124.
doi: 10.1007/JHEP11(2020)090.

K. J. Bae et al.
Fingerprint matching of beyond-WIMP dark matter: neural network approach.
Journal of cosmology and astroparticle physics, 2020(03):042, and PUBDB-2020-01564, DESY-19-109.
doi: 10.1088/1475-7516/2020/03/042.

H. Bahl, I. Sobolev and G. Weiglein.
Precise prediction for the mass of the light MSSM Higgs boson for the case of a heavy gluino.
Physics letters / B, 808:135644 (1, and PUBDB-2020-03824, arXiv:1912.10002. DESY-19-235.
doi: 10.1016/j.physletb.2020.135644.

H. Bahl, I. Sobolev and G. Weiglein.
The light MSSM Higgs boson mass for large $\tan\beta$ and complex input parameters.
The European physical journal / C, 80(11):1063 (1, and PUBDB-2020-04597, arXiv:2009.07572. DESY-20-085.
doi: 10.1140/epjc/s10052-020-08637-w.

H. Bahl et al.
Indirect $\mathcal{CP}$probes of the Higgs-top-quark interaction: current LHC constraints and future opportunities.
Journal of high energy physics, 2020(11):127, and PUBDB-2020-05000, arXiv:2007.08542.
doi: 10.1007/JHEP11(2020)127.

H. Bahl et al.
Theoretical uncertainties in the MSSM Higgs boson mass calculation.
The European physical journal / C Particles and fields, C80(6):497, and PUBDB-2020-02402, arXiv:1912.04199. DESY-19-083. IFT-UAM/CSIC-19-076. MPP-2019-242. arXiv:1912.04199.
doi: 10.1140/epjc/s10052-020-8079-3.

H. Bahl et al.
HL-LHC and ILC sensitivities in the hunt for heavy Higgs bosons.
The European physical journal / C, C80(10):916 (1, and PUBDB-2020-03807, arXiv:2005.14536. BONN-TH 2019-04. DESY-19-093. KA-TP-09-2019. IFT-UAM/CSIC-19-075.
doi: 10.1140/epjc/s10052-020-08472-z.

H. Bahl et al.
Precision calculations in the MSSM Higgs-boson sector with FeynHiggs 2.14.
Computer physics communications, 249:107099, and PUBDB-2020-05246, arXiv:1811.09073. DESY-18-179. CP3-Origins-2018-035. DNRF90. IFT-UAM-CSIC-18-095. MPP–2018–229.
doi: 10.1016/j.cpc.2019.107099.

M. C. Bañuls et al.
Simulating Lattice Gauge Theories within Quantum Technologies.
The European physical journal / D, 74(8):165, and PUBDB-2020-04018.
doi: 10.1140/epjd/e2020-100571-8.

T. Bargheer, V. Chestnov and V. Schomerus.
The Multi-Regge Limit from the Wilson Loop OPE.
Journal of high energy physics, 2005(5):2, and PUBDB-2020-01807, arXiv:1906.00990. DESY-19-099.
doi: 10.1007/JHEP05(2020)002.

B. Basso, L. J. Dixon and G. Papathanasiou.
The Origin of the Six-Gluon Amplitude in Planar $\mathcal{N}=4$ SYM.
Physical review letters, 124(16):161603, and PUBDB-2020-01802, arXiv:2001.05460. SLAC-PUB-17501. DESY 20-002. DESY-20-002.
doi: 10.1103/PhysRevLett.124.161603.

G. Bell, R. Rahn and J. Talbert.
Generic dijet soft functions at two-loop order: uncorrelated emissions.
Journal of high energy physics, 2020(9):15 (1, and PUBDB-2020-03812, arXiv:2004.08396. SI-HEP-2020-11. QFET-2020-01. Nikhef 2020-007. DESY-19-157.
doi: 10.1007/JHEP09(2020)015.

M. Benayoun, L. DelBuono and F. Jegerlehner.
$BHLS_2$, a New Breaking of the HLS Model and its Phenomenology.
The European physical journal / C, 80(2):81 (1, and PUBDB-2020-04177, arXiv:1903.11034. arXiv:1903.11034.
doi: 10.1140/epjc/s10052-020-7611-9.

M. Benayoun, L. DelBuono and F. Jegerlehner.
Erratum to: $BHLS_2$, a new breaking of the HLS model and its phenomenology.
The European physical journal / C, 80(3):244 (1), and PUBDB-2020-04178, arXiv:1903.11034.
doi: 10.1140/epjc/s10052-020-7724-1.

J. Bernigaud, I. de Medeiros Varzielas and J. Talbert.
Finite family groups for fermionic and leptoquark mixing patterns.
Journal of high energy physics, 2020(1):194, and PUBDB-

2020-00736, DESY-19-091.
doi: 10.1007/JHEP01(2020)194.

T. Biekoetter, M. Chakraborti and S. Heinemeyer.
A 96 GeV Higgs boson in the N2HDM.
The European physical journal / C, 80(1):2 (1, and PUBDB-2021-00592, arXiv:1903.11661. IFT-UAM/CSIC-19-034.
doi: 10.1140/epjc/s10052-019-7561-2.

G. Billis, F. J. Tackmann and J. Talbert.
Higher-order Sudakov resummation in coupled gauge theories.
Journal of high energy physics, 2020(3):182, and PUBDB-2020-01565, DESY-19-128.
doi: 10.1007/JHEP03(2020)182.

T. Binder, K. Mukaida and K. Petraki.
Rapid bound-state formation of Dark Matter in the Early Universe.
Physical review letters, 124(16):161102, and PUBDB-2020-01811, arXiv:1910.11288. DESY-19-181. IPMU19-0148.
doi: 10.1103/PhysRevLett.124.161102.

T. Binder et al.
Dark matter bound-state formation at higher order: a non-equilibrium quantum field theory approach.
Journal of high energy physics, 2020(9):86 (1, and PUBDB-2020-03827, arXiv:2002.07145. 20-022.
doi: 10.1007/JHEP09(2020)086.

F. A. Bishara et al.
Renormalization group effects in dark matter interactions.
Journal of high energy physics, 2020(3):89, and PUBDB-2021-00569.
doi: 10.1007/JHEP03(2020)089.

F. Bishara et al.
A New Precision Process at FCC-hh: the diphoton leptonic Wh channel.
Journal of high energy physics, 2007(7):75, and PUBDB-2020-02805, arXiv:2004.06122. DESY-20-054. ZU-TH 09/20.
doi: 10.1007/JHEP07(2020)075.

F. Björkeroth et al.
Axion-electron decoupling in nucleophobic axion models.
Physical review / D D, 101(3):035027, and PUBDB-2020-01571, DESY 19-194.
doi: 10.1103/PhysRevD.101.035027.

F. Björkeroth et al.
Covert symmetries in the neutrino mass matrix.
Journal of high energy physics, 2002(2):66, and PUBDB-2020-01809, arXiv:1910.00576.
doi: 10.1007/JHEP02(2020)066.

J. de Blas et al.
Higgs Boson studies at future particle colliders.
Journal of high energy physics, 2020(1):139, and PUBDB-2020-01300, DESY-19-079.
doi: 10.1007/JHEP01(2020)139.

J. Blümlein et al.
From Momentum Expansions to Post-Minkowskian Hamiltonians by Computer Algebra Algorithms.
Physics letters / B, 801:135157, and PUBDB-2020-00175, DESY-19-185. DO-TH 19/21. SAGEX-19-25.
doi: 10.1016/j.physletb.2019.135157.

J. Blümlein et al.
Fourth post-Newtonian Hamiltonian dynamics of two-body systems from an effective field theory approach.
Nuclear physics / B Particle physics, 955:115041, and PUBDB-2020-02247, DESY 20–025. DO–TH 20/01. SAGEX-20–03. 2003.01692 [gr-qc].
doi: 10.1016/j.nuclphysb.2020.115041.

J. Blümlein et al.
Testing binary dynamics in gravity at the sixth post-Newtonian level.
Physics letters / B, 807:135496, and PUBDB-2020-02440, arXiv:2003.07145. DESY-20-044. DO-TH 20/02. SAGEX-20-06.
doi: 10.1016/j.physletb.2020.135496.

J. Blümlein et al.
The $O(\alpha^2)$ Initial State QED Corrections to $e^+e^- \to \gamma^*/Z_0^*$.
Nuclear physics / B Particle physics, 956:115055, and PUBDB-2020-02260, arXiv:2003.14289. DESY-18-196. DO-TH 19/31. TTP 19-045. SAGEX 19-34.
doi: 10.1016/j.nuclphysb.2020.115055.

K. Bondarenko et al.
Direct detection and complementary constraints for sub-GeV dark matter.
Journal of high energy physics, 2020(3):118, and PUBDB-2020-01343, DESY-19-140.
doi: 10.1007/JHEP03(2020)118.

Q. R. C. Bonnefoy, E. Dudas and S. Pokorski.
Chiral Froggatt-Nielsen models, gauge anomalies and flavourful axions.
Journal of high energy physics, 2020(1):191, and PUBDB-2020-00739, DESY-19-154.
doi: 10.1007/JHEP01(2020)191.

Q. Bonnefoy et al.
Infinite Black Hole Entropies at Infinite Distances and Tower of States.
Nuclear physics / B Particle physics, 958:115112, and PUBDB-2020-03012, arXiv:1912.07453. IPhT-T19/163. CPHT096.122019. MPP-2019-257. DESY-19-226. LMU–ASC 54/19.
doi: 10.1016/j.nuclphysb.2020.115112.

T. Bourton and E. Pomoni.
Instanton counting in class $\mathcal{S}_k$.
Journal of physics / A, 53(16):39, and PUBDB-2021-00544, arXiv:1712.01288. DESY-17-189.
doi: 10.1088/1751-8121/ab6a6d.

M. D. Brida et al.
Non-perturbative renormalization by decoupling.
Physics letters / B, 807:135571, and PUBDB-2020-02878, WUB/19-05. DESY-19-224.
doi: 10.1016/j.physletb.2020.135571.

W. Buchmuller, V. Domcke and K. Schmitz.
From NANOGrav to LIGO with metastable cosmic strings.
Physics letters / B, 811:135914 (1, and PUBDB-2020-04632, arXiv:2009.10649. CERN-TH-2020-157. DESY-20-154.
doi: 10.1016/j.physletb.2020.135914.

W. Buchmuller et al.
Probing the scale of grand unification with gravitational waves.
Physics letters / B, B809:1, and PUBDB-2020-03575, arXiv:1912.03695. CERN-TH-2019-215. DESY-19-210. IPMU 19-0179.
doi: 10.1016/j.physletb.2020.135764.

I. Burić, V. Schomerus and M. Isachenkov.
Conformal Group Theory of Tensor Structures.
Journal of high energy physics, 2020(10):1, and PUBDB-2020-03813, arXiv:1910.08099. 19-172. DESY-19-172.
doi: 10.1007/JHEP10(2020)004.

I. Burić, V. Schomerus and E. Sobko.
Superconformal blocks: general theory.
Journal of high energy physics, 2020(1):159, and PUBDB-2020-00734, DESY-19-057. arXiv:1904.04852. NORDITA 2019-032.
doi: 10.1007/JHEP01(2020)159.

I. Burić, V. Schomerus and E. Sobko.
The superconformal X-ing equation.
Journal of high energy physics, 10(10):147, and PUBDB-2021-00112, arXiv:2005.13547.
doi: 10.1007/JHEP10(2020)147.

D. Buttazzo et al.
Scalar gauge dynamics and Dark Matter.
Journal of high energy physics, 2020(1):130, and PUBDB-2020-00620, DESY-19-197.
doi: 10.1007/JHEP01(2020)130.

C. Caprini et al.
Detecting gravitational waves from cosmological phase transitions with LISA: an update.
Journal of cosmology and astroparticle physics, 2020(03):024, and PUBDB-2020-01346, DESY-19-159.
doi: 10.1088/1475-7516/2020/03/024.

S. Caron-Huot et al.
The Steinmann Cluster Bootstrap for $\mathcal{N} = 4$ Super Yang-Mills Amplitudes.
Proceedings of Science / International School for Advanced Studies, (CORFU2019):003, and PUBDB-2020-04191, arXiv:2005.06735. DESY-20-087.
doi: 10.22323/1.376.0003.

F. Carta and A. Mininno.
No go for a flow.
Journal of high energy physics, 05(5):108 (1, and PUBDB-2020-04592, arXiv:2002.07816. DESY-20-021. IFT-UAM/CSIC-20-24.
doi: 10.1007/JHEP05(2020)108.

F. Carta, J. Moritz and A. Westphal.
A landscape of orientifold vacua.
Journal of high energy physics, 2005(5):107 (1, and PUBDB-2020-03839, arXiv:2003.04902. DESY-20-046.
doi: 10.1007/JHEP05(2020)107.

F. Carta et al.
Harmonic Hybrid Inflation.
Journal of high energy physics, 12(12):161, and PUBDB-2021-00110, arXiv:2007.04322. DESY-20-117.
doi: 10.1007/JHEP12(2020)161.

F. Carta et al.
The geometry of SUSY enhancement.
Journal of high energy physics, 2020(2):106, and PUBDB-2020-01348, DESY-19-177.
doi: 10.1007/JHEP02(2020)106.

Y. Chai et al.
Parton distribution functions of Δ^+ on the lattice.
Physical review / D D, 102(1):014508, and PUBDB-2020-02979, arXiv:2002.12044.
doi: 10.1103/PhysRevD.102.014508.

X. Chu, C. Garcia Cely and H. Murayama.
A Practical and Consistent Parametrization of Dark Matter Self-Interactions.
Journal of cosmology and astroparticle physics, 2006(06):043, and PUBDB-2020-02779, arXiv:1908.06067. DESY-19-137.
doi: 10.1088/1475-7516/2020/06/043.

X. Chu, C. Garcia Cely and H. Murayama.
Finite-Size Dark Matter and its Effect on Small-Scale Structure.
Physical review letters, 124(4):041101, and PUBDB-2020-00763, DESY-18-225. arXiv:1901.00075. IPMU18-0207.
doi: 10.1103/PhysRevLett.124.041101.

X. Cid Vidal et al.
Erratum to: New axion searches at flavor factories.
Journal of high energy physics, 2020(6):141, and PUBDB-2021-00402, arXiv:1810.09452. DESY-18-183.
doi: 10.1007/JHEP06(2020)141.

I. Coman, E. Pomoni and J. Teschner.
Trinion Conformal Blocks from Topological strings.
Journal of high energy physics, 2020(9):78 (1, and PUBDB-2020-03808, arXiv:1906.06351. DESY-19-106.
doi: 10.1007/JHEP09(2020)078.

M. L. Czakon et al.
Top quark pair production at complete NLO accuracy with NNLO+NNLL′ corrections in QCD.
Chinese physics / C, 44(8):083104 (1, and PUBDB-2020-03828, arXiv:1901.08281. 20-024.
doi: 10.1088/1674-1137/44/8/083104.

G. Das, M. C. Kumar and K. Samanta.
Resummed inclusive cross-section in ADD model at N^3LL.
Journal of high energy physics, 10(10):161 (1, and PUBDB-2020-04591, arXiv:1912.13039. DESY-19-171.
doi: 10.1007/JHEP10(2020)161.

G. Das, S.-O. Moch and A. Vogt.
Soft corrections to inclusive deep-inelastic scattering at four loops and beyond.
Journal of high energy physics, 2020(3):116, and PUBDB-2020-01298, arXiv:1912.12920. SI-HEP-2019-21. DESY 19-088. LTH 1205. DESY-19-088.
doi: 10.1007/JHEP03(2020)116.

J. De Blas et al.
HEPfit: a Code for the Combination of Indirect and Direct Constraints on High Energy Physics Models.
The European physical journal / C Particles and fields, C80(5):456, and PUBDB-2020-02403, arXiv:1910.14012. CERN-TH-2019-178. CPHT-RR060.102019. DESY-19-184.

FTUV/19-1031. IFIC/19-44. KEK-TH-2163. LPT-Orsay-19-36. PSI-PR-19-22. UCI-TR-2019-26.
doi: 10.1140/epjc/s10052-020-7904-z.

V. Del Duca et al.
All-order amplitudes at any multiplicity in the multi-Regge limit.
Physical review letters, 124(16):161602, and PUBDB-2020-01808, arXiv:1912.00188. DESY-19-180. CERN-TH-2019-204. IPPP/19/86. UUITP-48/19. SLAC-PUB-17491.
doi: 10.1103/PhysRevLett.124.161602.

F. Depta, M. Hufnagel and K. Schmidt-Hoberg.
Robust cosmological constraints on axion-like particles.
Journal of cosmology and astroparticle physics, 2005(05):009, and PUBDB-2020-01803, arXiv:2002.08370. DESY-20-003.
doi: 10.1088/1475-7516/2020/05/009.

P. F. Depta et al.
Complete leading-order standard model corrections to quantum leptogenesis.
Journal of high energy physics, 09(9):36, and PUBDB-2020-04596, arXiv:2005.01728. DESY-20-065.
doi: 10.1007/JHEP09(2020)036.

L. Di Luzio.
Accidental SO(10) axion from gauged flavour.
Journal of high energy physics, 11(11):074, and PUBDB-2020-04602, arXiv:2008.09119. DESY 20-133.
doi: 10.1007/JHEP11(2020)074.

L. Di Luzio.
Pati-Salam axion.
Journal of high energy physics, 2020(7):71 (1, and PUBDB-2020-04204, DESY-20-071. arXiv:2005.00012.
doi: 10.1007/JHEP07(2020)071.

L. Di Luzio et al.
Solar Axions Cannot Explain the XENON1T Excess.
Physical review letters, 125(13):131804 (1, and PUBDB-2020-04203, DESY-20-106. arXiv:2006.12487.
doi: 10.1103/PhysRevLett.125.131804.

L. Di Luzio et al.
The landscape of QCD axion models.
Physics reports, 870:1, and PUBDB-2020-03829, arXiv:2003.01100. DESY-20-036.
doi: 10.1016/j.physrep.2020.06.002.

M. Diehl, A. Manashov and A. Schafer.
Erratum to: Chiral perturbation theory for nucleon generalized parton distributions.
The European physical journal / A, 56(8):220, and PUBDB-2021-00484, hep-ph/0608113. DESY-06-123.
doi: 10.1140/epja/s10050-020-00193-x.

M. Diehl and P. Stienemeier.
Gluons and sea quarks in the proton at low scales.
The European physical journal / Plus Plus, 135(2):211, and PUBDB-2020-00735, DESY-19-068. arXiv:1904.10722.
doi: 10.1140/epjp/s13360-020-00200-6.

M. Diehl et al.
Sum rule improved double parton distributions in position space.
The European physical journal / C Particles and fields, 80(5):468, and PUBDB-2020-02353, DESY-20-011. arXiv:2001.10428. CERN-TH-2020-014.
doi: 10.1140/epjc/s10052-020-8038-z.

V. F. Domcke, R. Jinno and H. Rubira.
Deformation of the gravitational wave spectrum by density perturbations.
Journal of cosmology and astroparticle physics, 2006(06):046, and PUBDB-2020-03179, arXiv:2002.11083. DESY-20-029.
doi: 10.1088/1475-7516/2020/06/046.

V. F. Domcke et al.
Measuring the net circular polarization of the stochastic gravitational wave background with interferometers.
Journal of cosmology and astroparticle physics, 2005(05):1, and PUBDB-2020-03805, arXiv:1910.08052. DESY-19-161.
doi: 10.1088/1475-7516/2020/05/028.

V. F. Domcke et al.
Resonant backreaction in axion inflation.
Journal of cosmology and astroparticle physics, 2009(09):009 (1, and PUBDB-2020-03826, arXiv:2002.02952. DESY-20-017.
doi: 10.1088/1475-7516/2020/09/009.

V. F. Domcke et al.
Spontaneous Baryogenesis from Axions with Generic Couplings.
Journal of high energy physics, 08(8):096, and PUBDB-2020-04599, arXiv:2006.03148. DESY-20-100. CERN-TH-2020-088. TU-1102.
doi: 10.1007/JHEP08(2020)096.

V. Domcke, Y. Ema and K. Mukaida.
Chiral anomaly, Schwinger effect, Euler-Heisenberg Lagrangian and application to axion inflation.
Journal of high energy physics, 2020(2):55, and PUBDB-2020-01347, DESY-19-166.
doi: 10.1007/JHEP02(2020)055.

P. Drechsel, G. Moortgat-Pick and G. Weiglein.
Prospects for direct searches for light Higgs bosons at the ILCwith 250 GeV.
The European physical journal / C, 80(10):922, and PUBDB-2020-03907, DESY-20-083. arXiv:1801.09662.
doi: 10.1140/epjc/s10052-020-08438-1.

J. A. Dror et al.
Testing the Seesaw Mechanism and Leptogenesis with Gravitational Waves.
Physical review letters, 124(4):041804, and PUBDB-2020-00737, DESY-19-138.
doi: 10.1103/PhysRevLett.124.041804.

M. Duerr et al.
Invisible and displaced dark matter signatures at Belle II.
Journal of high energy physics, 2020(2):39, and PUBDB-2020-00738, DESY-19-141. OUTP-19-10P. TTK-19-46.

arXiv:1911.03176.
doi: 10.1007/JHEP02(2020)039.

M. A. Ebert and F. J. Tackmann.
Impact of isolation and fiducial cuts on q_T and N-jettiness subtractions.
Journal of high energy physics, 2020(3):158, and PUBDB-2020-01355, arXiv:1911.08486. DESY-19-199. MIT-CTP/5158.
doi: 10.1007/JHEP03(2020)158.

Y. Ema, R. Jinno and K. Nakayama.
High-frequency Graviton from Inflaton Oscillation.
Journal of cosmology and astroparticle physics, 09(09):015, and PUBDB-2020-04600, arXiv:2006.09972. DESY-20-104.
doi: 10.1088/1475-7516/2020/09/015.

Y. Ema, K. Mukaida and J. M. v. d. Vis.
Higgs inflation as nonlinear sigma model and scalaron as its σ-meson.
Journal of high energy physics, 11(11):11 (1, and PUBDB-2020-04593, arXiv:2002.11739. DESY-20-031.
doi: 10.1007/JHEP11(2020)011.

F. Erben et al.
Rho resonance, timelike pion form factor, and implications for lattice studies of the hadronic vacuum polarization.
Physical review / D D, 101(5):054504, and PUBDB-2020-01787, arXiv:1910.01083. MITP/19-062. DESY-19-165. MITP/19-062 DESY 19-165.
doi: 10.1103/PhysRevD.101.054504.

C. Eröncel, J. Hubisz and G. Rigo.
Radion-activated Higgs mechanism.
Physical review / D D, 101(5):055041, and PUBDB-2020-01843, arXiv:1912.11053. DESY 19-236. DESY-19-236.
doi: 10.1103/PhysRevD.101.055041.

N. Fonseca de Sa et al.
Axion fragmentation.
Journal of high energy physics, 2020(4):10, and PUBDB-2020-01572, DESY-19-202.
doi: 10.1007/JHEP04(2020)010.

N. Fonseca et al.
Relaxion Fluctuations (Self-stopping Relaxion) and Overview of Relaxion Stopping Mechanisms.
Journal of high energy physics, 2005(5):80, and PUBDB-2020-02404, arXiv:1911.08473. DESY-19-203.
doi: 10.1007/JHEP05(2020)080.

H. Fukaya et al.
Atiyah-Patodi-Singer index on a lattice.
Progress of theoretical and experimental physics, 2020(4):043B04, and PUBDB-2020-02367, arXiv:1910.09675. OU-HET-1027.
doi: 10.1093/ptep/ptaa031.

L. Funcke, K. Jansen and S. Kühn.
Topological vacuum structure of the Schwinger model with matrix product states.
Physical review / D D, 101(5):054507, and PUBDB-2020-02139, arXiv:1908.00551.
doi: 10.1103/PhysRevD.101.054507.

S. Gangal et al.
Higgs Production at NNLL$'$+NNLO using Rapidity Dependent Jet Vetoes.
Journal of high energy physics, 2020(5):54, and PUBDB-2020-02405, arXiv:2003.04323. CERN-TH-2020-036. DESY-20-035. TIFR/TH/20-7.
doi: 10.1007/JHEP05(2020)054.

M. Garny, T. Konstandin and H. Rubira.
The Schrödinger-Poisson method for Large-Scale Structure.
Journal of cosmology and astroparticle physics, 2020(04):003, and PUBDB-2020-01567, DESY-19-176.
doi: 10.1088/1475-7516/2020/04/003.

F. Giese, T. Konstandin and J. van de Vis.
Model-independent energy budget of cosmological first-order phase transitions—A sound argument to go beyond the bag model.
Journal of cosmology and astroparticle physics, 07:057, and PUBDB-2020-03913, arXiv:2004.06995.
doi: 10.1088/1475-7516/2020/07/057.

A. Gimenez Grau and P. Liendo.
Bootstrapping line defects in $\mathcal{N} = 2$ theories.
Journal of high energy physics, 2020(3):121, and PUBDB-2020-01342, DESY-19-126.
doi: 10.1007/JHEP03(2020)121.

A. Gimenez Grau et al.
A quantum framework for AdS/dCFT through fuzzy spherical harmonics on S^4.
Journal of high energy physics, 2004(4):132, and PUBDB-2020-01842, arXiv:1912.02468. DESY-19-220.
doi: 10.1007/JHEP04(2020)132.

Y. Gouttenoire, G. Servant and P. Simakachorn.
Beyond the Standard Models with Cosmic Strings.
Journal of cosmology and astroparticle physics, 2007(07):032, and PUBDB-2020-03011, arXiv:1912.02569. DESY-19-204.
doi: 10.1088/1475-7516/2020/07/032.

Y. Gouttenoire, G. Servant and P. Simakachorn.
BSM with Cosmic Strings: Heavy, up to EeV mass, Unstable Particles.
Journal of cosmology and astroparticle physics, 2007(07):016, and PUBDB-2020-02780, arXiv:1912.03245. DESY-19-206.
doi: 10.1088/1475-7516/2020/07/016.

J. R. Green, K. Jansen and F. Steffens.
Improvement, generalization, and scheme conversion of Wilson-line operators on the lattice in the auxiliary field approach.
Physical review / D D, 101(7):074509, and PUBDB-2020-01528, arXiv:2002.09408. CERN-TH-2020-028.
doi: 10.1103/PhysRevD.101.074509.

E. Hall et al.
Baryogenesis from a dark first-order phase transition.
Journal of high energy physics, 2020(4):42, and PUBDB-2020-01566, DESY-19-175.
doi: 10.1007/JHEP04(2020)042.

B. Heinemann, T. Heinzl and A. Ringwald.
LUXE: Combining high energy and intensity to spark the vacuum.
Europhysics news, 51(4):14, and PUBDB-2020-03385.
doi: 10.1051/epn/2020401.

N. Henke and G. Papathanasiou.
How tropical are seven- and eight-particle amplitudes?
Journal of high energy physics, 2008(8):5, and PUBDB-2020-03013, arXiv:1912.08254. DESY-19-229.
doi: 10.1007/JHEP08(2020)005.

N. Husung, P. Marquard and R. Sommer.
Asymptotic behavior of cutoff effects in Yang-Mills theory and in Wilson's lattice QCD.
The European physical journal / C Particles and fields C, 80(3):200, and PUBDB-2020-01470, DESY-19-188.
doi: 10.1140/epjc/s10052-020-7685-4.

K. Inomata et al.
Gravitational Wave Production right after a Primordial Black Hole Evaporation.
Physical review / D, 101(12):123533 (1, and PUBDB-2020-03838, arXiv:2003.10455. IPMU 20-0029. DESY-20-042. CTPU-PTC-20-05.
doi: 10.1103/PhysRevD.101.123533.

T. Ishikawa, K. Nakayama and K. Suzuki.
Casimir effect for lattice fermions.
Physics letters / B, 809:135713, and PUBDB-2020-03318, arXiv:2005.10758. DESY-20-094. KEK-TH-2220.
doi: 10.1016/j.physletb.2020.135713.

K. Jansen, E. H. Müller and R. Scheichl.
Multilevel Monte Carlo for quantum mechanics on a lattice.
Physical review / D, 102(11):114512, and PUBDB-2021-00141, arXiv:2008.03090.
doi: 10.1103/PhysRevD.102.114512.

R. Jinno et al.
Higgs inflation in metric and Palatini formalisms: required suppression of higher dimensional operators.
Journal of cosmology and astroparticle physics, 2020(03):063, and PUBDB-2020-01563, DESY-19-058.
doi: 10.1088/1475-7516/2020/03/063.

G. W. Kaelin, Z. Liu and R. A. Porto.
Conservative Dynamics of Binary Systems to Third Post-Minkowskian Order from the Effective Field Theory Approach.
Physical review letters, 125(26):261103, and PUBDB-2021-00109, arXiv:2007.04977. DESY-20-114. SLAC-PUB-17545.
doi: 10.1103/PhysRevLett.125.261103.

G. Kälin, Z. Liu and R. A. Porto.
Conservative Tidal Effects in Compact Binary Systems to Next-to-Leading Post-Minkowskian Order.
Physical review / D, 102(12):124025, and PUBDB-2020-05050, arXiv:2008.06047. DESY-20-131. SLAC-PUB-17555.
doi: 10.1103/PhysRevD.102.124025.

N. Kaloper and A. Westphal.
A Goldilocks Higgs.
Physics letters / B, B808:1, and PUBDB-2020-03010, arXiv:1907.05837. DESY-19-130.
doi: 10.1016/j.physletb.2020.135616.

Z. R. Kordov et al.
Electromagnetic contribution to Σ - Λ mixing using lattice QCD + QED.
Physical review / D D, 101(3):034517, and PUBDB-2020-01354, DESY-19-190.
doi: 10.1103/PhysRevD.101.034517.

G. A. Kotousov and S. L. Lukyanov.
Spectrum of the reflection operators in different integrable structures.
Journal of high energy physics, 2020(2):29, and PUBDB-2020-00741, DESY-19-168.
doi: 10.1007/JHEP02(2020)029.

LHC Reinterpretation Forum Collaboration.
Reinterpretation of LHC Results for New Physics: Status and Recommendations after Run 2.
SciPost physics, 9(2):022 (1, and PUBDB-2021-00016, arXiv:2003.07868. CERN-LPCC-2020-001. FERMILAB-FN-1098-CMS-T. Imperial/HEP/2020/RIF/01.
doi: 10.21468/SciPostPhys.9.2.022.

P. Liendo, Y. Linke and V. Schomerus.
A Lorentzian inversion formula for defect CFT.
Journal of high energy physics, 2008(8):1, and PUBDB-2020-03806, DESY-19-039. arXiv:1903.05222.
doi: 10.1007/JHEP08(2020)163.

P. Marquard et al.
Matching the heavy-quark fields in QCD and HQET at four loops.
Physical review / D, 102(5):054008 (1, and PUBDB-2020-03588, arXiv:2005.14047. DESY-20-092. P3H-20-023. SAGEX-20-14. TTP20-024.
doi: 10.1103/PhysRevD.102.054008.

O. Matsedonskyi and G. Servant.
High-Temperature Electroweak Symmetry Non-Restoration from New Fermions and Implications for Baryogenesis.
Journal of high energy physics, 2020(9):12 (1, and PUBDB-2020-03822, arXiv:2002.05174. arXiv:2002.05174 DESY-19-207.
doi: 10.1007/JHEP09(2020)012.

A. J. McLeod et al.
A Novel Algorithm for Nested Summation and Hypergeometric Expansions.
Journal of high energy physics, 11(11):122, and PUBDB-2021-00546, arXiv:2005.05612.
doi: 10.1007/JHEP11(2020)122.

I. de Medeiros Varzielas and J. Talbert Jr.
FCNC-free multi-Higgs-doublet models from broken family symmetries.
Physics letters / B, 800:135091, and PUBDB-2019-05052, arXiv:1908.10979. DESY-19-147.
doi: 10.1016/j.physletb.2019.135091.

D. Mohler and S. Schaefer.
Remarks on strange-quark simulations with Wilson fermions.
Physical review / D, 102(7):074506 (1, and PUBDB-2020-05163, arXiv:2003.13359. DESY-20-041. MITP/20-010.
doi: 10.1103/PhysRevD.102.074506.

Z. Nagy and D. E. Soper.
Evolution of parton showers and parton distribution functions.
Physical review / D, 102(1):014025, and PUBDB-2020-03007, arXiv:2002.04125. DESY-20-015.
doi: 10.1103/PhysRevD.102.014025.

V. Niarchos, C. Papageorgakis and E. Pomoni.
Type-B anomaly matching and the 6D (2,0) theory.
Journal of high energy physics, 2020(4):48, and PUBDB-2020-01569, DESY-19-189.
doi: 10.1007/JHEP04(2020)048.

F. Nieri and Y. Zenkevich.
Quiver $W_{\epsilon_1,\epsilon_2}$ algebras of 4d $\mathcal{N}=2$ gauge theories.
Journal of physics / A Mathematical and theoretical, A53(27):275401, and PUBDB-2020-02782, arXiv:1912.09969. DESY-19-233. ITEP-36/19.
doi: 10.1088/1751-8121/ab9275.

I. Novikov et al.
Parton Distribution Functions of the Charged Pion Within The xFitter Framework.
Physical review / D, 102(1):014040 (1, and PUBDB-2020-03740, arXiv:2002.02902. DESY-20-013.
doi: 10.1103/PhysRevD.102.014040.

M. A. Nozdrin et al.
Design of the New Control System for Linac-200.
Physics of particles and nuclei letters, 17(4):600, and PUBDB-2021-00499.
doi: 10.1134/S1547477120040342.

D. Pagani, H.-S. Shao and M. Zaro.
RIP $Hb\bar{b}$: How other Higgs production modes conspire to kill a rare signal at the LHC.
Journal of high energy physics, 11:036, and PUBDB-2020-04598, arXiv:2005.10277. DESY-20-089. TIF-UNIMI-2020-16.
doi: 10.1007/JHEP11(2020)036.

D. Pagani, I. Tsinikos and E. Vryonidou.
NLO QCD+EW predictions for tHj and tZj production at the LHC.
Journal of high energy physics, 08(8):082, and PUBDB-2021-00523, arXiv:2006.10086. DESY-20-101. LU-TP 20-33. CERN-TH-2020-090.
doi: 10.1007/JHEP08(2020)082.

F. G. Pedro and A. Westphal.
Flattened axion monodromy beyond two derivatives.
Physical review / D, 101(4):043501, and PUBDB-2020-00740, DESY-19-160.
doi: 10.1103/PhysRevD.101.043501.

E. Pomoni.
4D $\mathcal{N}=2$ SCFTs and spin chains.
Journal of physics / A Mathematical and theoretical, A53(28):283005, and PUBDB-2020-02781, arXiv:1912.00870. DESY-19-212.
doi: 10.1088/1751-8121/ab7f66.

M. Postma and J. M. v. d. Vis.
Source terms for electroweak baryogenesis in the vev-insertion approximation beyond leading order.
Journal of high energy physics, 2020(2):90, and PUBDB-2020-01349, DESY-19-182.
doi: 10.1007/JHEP02(2020)090.

T. Robens, T. Stefaniak and J. Wittbrodt.
Two-real-scalar-singlet extension of the SM: LHC phenomenology and benchmark scenarios.
The European physical journal / C Particles and fields C, 80(2):151, and PUBDB-2020-01252, DESY-19-142.
doi: 10.1140/epjc/s10052-020-7655-x.

J. Rong and J. Zhu.
On the ϕ^3 theory above six dimensions.
Journal of high energy physics, 04(4):151, and PUBDB-2020-04626, arXiv:2001.10864.
doi: 10.1007/JHEP04(2020)151.

M. Sakamoto, M. Takeuchi and Y. Tatsuta.
Zero-mode counting formula and zeros in orbifold compactifications.
Physical review / D, 102(2):025008, and PUBDB-2020-04595, KOBE-TH-20-03. DESY-20-063. arXiv:2004.05570.
doi: 10.1103/PhysRevD.102.025008.

R. Sato.
Simple gradient flow equation for the bounce solution.
Physical review / D, 101(1):016012, and PUBDB-2020-00617, DESY-19-122.
doi: 10.1103/PhysRevD.101.016012.

A. Sokolov.
Generic energy transport solutions to the solar abundance problem—a hint of new physics.
Journal of cosmology and astroparticle physics, 03(03):013, and PUBDB-2021-00625, arXiv:1907.06928.
doi: 10.1088/1475-7516/2020/03/013.

J. van de Vis et al.
Time-Scales for Nonlinear Processes in Preheating after Multifield Inflation with Nonminimal Couplings.
Physical review / D, 102(4):043528 (1, and PUBDB-2020-03320, arXiv:2005.00433. DESY-20-076. Nikhef 2020-014. MIT-CTP/5202.
doi: 10.1103/PhysRevD.102.043528.

Y. M. Welling.
Simple, exact model of quasisingle field inflation.
Physical review / D, 101(6):063535, and PUBDB-2020-01338, DESY-19-120.
doi: 10.1103/PhysRevD.101.063535.

N. Zerf et al.
Critical properties of the valence-bond-solid transition in lattice quantum electrodynamics.
Physical review / D D, 101(9):094505, and PUBDB-2020-02567, arXiv:2003.09226. DESY-20-045. HU-EP-20/05. LTH 1231.
doi: 10.1103/PhysRevD.101.094505.

P. A. Zyla et al.
Review of Particle Physics.
Progress of theoretical and experimental physics, 2020(8):083C01, and PUBDB-2020-03047.
doi: 10.1093/ptep/ptaa104.

Ph.D. Thesis

J. P. Carstensen.
Integrability in N = 1 Gauge Theories.
Universität Hamburg, Hamburg, 2020.

Y. Gouttenoire.
Heavy Dark Matter, Models and Methods of Detection beyond the Standard Paradigm.
University of Hamburg, 2020.

M. Hufnagel.
Primordial Nucleosynthesis in the Presence of MeV-scale Dark Sectors.
Universität Hamburg, Hamburg, 2020.

J. Michel.
Factorization and Resummation for Precision Physics at the LHC.
University of Hamburg, 2020.

J. Schütte-Engel.
Axion direct detection in particle and condensed matter physics.
Universität Hamburg, Hamburg, 2020.

I. Sobolev.
Precise predictions for Higgs physics in supersymmetric models.
Universität Hamburg, Hamburg, 2020.

ZEUS

Published

ZEUS Collaboration.
Study of proton parton distribution functions at high x using ZEUS data.
Physical review / D D, D101(11):112009, and PUBDB-2020-02877, arXiv:2003.08742. DESY-20-048.
doi: 10.1103/PhysRevD.101.112009.

ZEUS Collaboration.
Two-particle azimuthal correlations as a probe of collective behaviour in deep inelastic ep scattering at HERA.
Journal of high energy physics, 2004(4):70, and PUBDB-2020-01625, arXiv:1912.07431. DESY-19-174.
doi: 10.1007/JHEP04(2020)070.

Photographs and graphics
Claudia Höhne, DESY
Heiner Müller-Elsner, DESY
Ayan Paul, DESY
UiO/Jarli&Jordan
Valery Rubakov

Spengler Wiescholek Architekten Stadtplaner, WES GmbH Landschaftsarchitekten, Urban Catalyst GmbH; Visualisation: Moka-studio; Aerial image: Matthias Friedel

Belle II / KEK
Zachary Duer, Tanner Upthegrove, Leo Piilonen, George Glasson, W. Jesse Barber, Samantha Spytek, Christopher Dobson (Virginia Tech Institute for Creativity, Arts and Technology, Virginia Tech Department of Physics, Virginia Tech School of Education)
DESY

The figures were reproduced by permission of authors or journals.

Acknowledgement

We would like to thank all authors and everyone who helped in the creation of this annual report.

Imprint

Publishing and contact
Deutsches Elektronen-Synchrotron DESY
A Research Centre of the Helmholtz Association

Hamburg location:
Notkestr. 85, 22607 Hamburg, Germany
Tel.: +49 40 8998-0, Fax: +49 40 8998-3282
desyinfo@desy.de

Zeuthen location:
Platanenallee 6, 15738 Zeuthen, Germany
Tel.: +49 33762 7-70, Fax: +49 33762 7-7413
desyinfo.zeuthen@desy.de

www.desy.de
ISBN ISBN 978-3-945931-35-6
doi 10.3204/PUBDB-2020-04947

Editing
Ilka Flegel, Manfred Fleischer, Thomas Konstandin

Layout
Sabine Kuhls-Dawideit, Büro für Grafik und Design, Halstenbek

Production
Britta Liebaug

Printing
EHS Druck GmbH, Schenefeld

Editorial deadline
15 February 2021

Editorial note
The authors of the individual scientific contributions published in this report are fully responsible for the contents.

HELMHOLTZ
RESEARCH FOR GRAND CHALLENGES

Deutsches Elektronen-Synchrotron DESY
A Research Centre of the Helmholtz Association

The Helmholtz Association is a community of 18 scientific-technical and biological-medical research centres. These centres have been commissioned with pursuing long-term research goals on behalf of the state and society. The Association strives to gain insights and knowledge so that it can help to preserve and improve the foundations of human life. It does this by identifying and working on the grand challenges faced by society, science and industry. Helmholtz Centres perform top-class research in strategic programmes in six core fields: Energy, Earth & Environment, Health, Aeronautics, Space and Transport, Matter, and Key Technologies.

www.helmholtz.de